Non-Neuroleptic Antitubercular and Anticancer Therapeutics through Rational Drug Remodelling of Phenothiazines and Related Antipsychotics

Manare Molahlegi Dorothy Semenya

UNIVERSITY OF CAPE TOWN

March 2016

Non-Neuroleptic Antitubercular and Anticancer Therapeutics through Rational Drug Remodelling of Phenothiazines and Related Antipsychotics

Manare Molahlegi Dorothy Semenya

Thesis presented for the degree of Doctor of Philosophy

in the Department of Chemistry

University of Cape Town

Supervisor: Dr Anwar Jardine

Department of Chemistry, University of Cape Town

March 2016

Declaration

I declare that the thesis titled "**Non-Neuroleptic Antitubercular and Anticancer Therapeutics through Rational Drug Remodelling of Phenothiazines and Related Antipsychotics**" is my own work and has not been previously submitted for any degree or examination at this or any other university. All the relevant sources of information and support have been fully referenced and acknowledged.

Manare Molahlegi Dorothy Semenya

Signature: Signed by candidate Date: 15/03/2016

Dedication

To my parents Makgabo Jane Semenya (mom) and Kgabo Michael Patrick Semenya (dad)

In loving memory of Kgabo Michael Patrick Semenya

Dad, you were the voice of encouragement at the very beginning of this journey, I wish you were here to share this moment…

Mom, thank you for walking this journey with me. Your phone calls kept me going. I am grateful beyond words for your unconditional support and love.

Acknowledgements

"When you learn, teach. When you get, give" Maya Angelou

My esteemed gratitude goes to everyone that contributed to making this thesis possible. I'm forever grateful.

I wish to extend my sincere gratitude and appreciation to my supervisor, Dr Anwar Jardine, for his support, infinite patience and invaluable training throughout the course of this journey.

I would also like to acknowledge all the collaborators and service providers for their contribution to this thesis: Prof Muazzam Jacobs, Sumayah Salie, Dr Nai-Jen Hsu, Associate Prof Digby Warner, Ronnette Seldon, (Institute of Molecular Medicine and Infectious Diseases, UCT); Prof Sharon Prince (Division of Cell Biology, UCT); Sylvester Omoruyi, Dr Okobi Ekpo (Department of Medical Bioscience, University of the Western Cape); Nina Lawrence (Division of Clinical Pharmacology, UCT); Raban Masuka, Prof Kelly Chibale (Department of Chemistry, UCT); Perkin Elmer (formerly Caliper Life Sciences) MA USA.

Thank you Pete Roberts for running my NMR experiments, also for the training to use Bruker (400 MHz) and Varian (300 MHz) NMR spectrometers. For LCMS, I wish to acknowledge: Mass Spectroscopy Unit, Department of Molecular and Cell Biology (UCT), and Central Analytical Facilities (University of Stellenbosch). The assistance from the Department of Chemistry (UCT) administrative staff is also duly acknowledged, a special thanks to Deirdre Brooks.

I would also like to gratefully acknowledge the financial support from the South African National Research Foundation (NRF SANHARP), Technology Innovation Agency (TIA), Research Contracts & Intellectual Property Services (RCIPS) and the UCT Postgraduate Funding Office (International Travel Grant).

I sincerely thank all of my colleagues, past and present research group members in the Department of Chemistry, and my dear friends for their constant encouragement and companionship. A special thanks to: Anita Gulwa, Antonina Wasuna, Vernita Reid, Shakeela Sayed, Lutete Khonde, Marwaan Rylands, Dr Malkeet Kumar, Dr Kalwajit Singh, Gurminder Kaur, Dr Claire Le Manach and Dr Taigh Anderson.

For bearing with my extended absences from home, my heartfelt appreciation goes to my amazing family: Makgabo Jane Semenya (mom), Kgabo Michael Patrick Semenya (dad) Siblings (Phuti Semenya, Elsie Selolo and Mogobo Semenya), Salome Setati (aunt), Puleng Selolo (brother-in-law), Rosina Mathatho (grandma), Matlou Mathatho (aunt) and my bundles of joy Keamogetswe Selolo (niece) and Mokaba Selolo (nephew). Words cannot express how much I appreciate your unconditional love and support. I'm grateful to everyone who was part of this journey… your unwavering support didn't go unnoticed.

Praise and glory unto God, His grace carried me through the course of this unforgettable journey.

Abstract

In light of shrinking pharmaceutical drug pipelines and drug resistance, innovative drug discovery strategies are of imperative need. Drug repurposing and related strategies such as drug rescue and drug remodelling have garnered significant research interest. Various clinically approved non-antibiotics including phenothiazines hold promise as novel classes of therapeutics in other indications. However, in addition to inherent neuroleptic properties, phenothiazines and related antipsychotics elicit adverse side effects at clinically relevant doses thus precluding their extensive clinical application.

Herein, it was postulated that the selectivity of phenothiazines and related drugs for non-neuroleptic indications could be enhanced through rationalized structural remodelling. Phenothiazine and related neuroleptics are known to obey a lipophilic chromophore/basic side chain paradigm. Deviation from this paradigm is expected to decrease potential for neuroleptic effects. Therefore, the remodelling strategies involved introduction of novel functionalities that are dissimilar to native phenothiazine structures.

Prior to chemical synthesis, drug metabolism and pharmacokinetic related properties were predicted *in silico* to assess drug-likeness of the new chemical entities derived from phenothiazines and related antipsychotics. The *in silico* profiling also included prediction of blood/brain partition coefficients and CNS activity to determine their likelihood of exhibiting neuroleptic effects. The new chemical entities were then evaluated against drug-susceptible *Mycobacterium tuberculosis*-H37Rv. Furthermore, a selected series was screened for binding to dopamine and serotonin receptors to corroborate *in silico* CNS activity predictions.

Moreover, pharmacokinetic studies were conducted with the selected series to determine *in vitro* microsomal stability, kinetic solubility and *in vivo* toxicity profiles. Another objective of this study was to evaluate the new chemical entities for their potential as anticancer agents.

The key findings herein demonstrated that it is possible to abolish neuroleptic effects through rationalized structural manipulation and still retain bio-activities of interest. Several new chemical entities including *N*-alkylsulfonates (**DS0031**, **DS0032**, **DS0034**, **DS0035**, **DS00366**) and nitrobenzenesulfonamides (**DS00325**, **DS00326**, **DS00329**) of phenothiazines, displayed notable antitubercular (GAST/Fe MIC_{90} range: 9.9-125 µM; 7H9 MIC range 12.5-25 µg/mL) and anticancer (IC_{50} range 4.51-12.43 µM) activities in comparison to native phenothiazine drugs. Furthermore, *in vitro* and *in vivo* preclinical evaluation revealed favourable pharmacokinetic profiles. Overall, this study presents novel subclasses of phenothiazines that hold promise for further development as non-neuroleptic agents in either tuberculosis or cancer treatment regimens.

List of Abbreviations

ADMET	Absorption, Distribution, Metabolism, Excretion and Toxicity
AMPK	Adenosine monophosphate-activated protein kinase
ATP	Adenosine triphosphate
APT	Attached Proton Test
BBB	Blood-brain barrier
BH_3.THF	Borane-tetrahydrofuran complex
CH_3CN	Acetonitrile
CNS	Central nervous system
conc	Concentrated
CSC	Cancer stem cell
CuI	Copper iodide
δ	Chemical shift
d	Doublet
Da	Daltons
DCM	Dichloromethane
dd	Doublet of doublets
DNA	Deoxyribonucleic acid
D_2O	Deuterated water
DMF	Dimethylformamide
DMF-DMA	*N,N*-Dimethylformamide dimethyl acetal
DMSO	Dimethylsulfoxide
DR	Drug-resistant
EC_{50}	Half maximal effective concentration
eq	Equivalent (s)
ESI	Electronspray ionization

Et_2O	Diethyl ether
EtOAc	Ethyl acetate
EtOH	Ethanol
FASSIF	Fasted state simulated intestinal fluid
FGI	Functional group interconversion
GAST	Glycerol-alanine-salts
GFPMA	Green Fluorescent Protein Microplate Assay
h	Hour (s)
HBA	Hydrogen Bond Acceptor
HBD	Hydrogen Bond Donor
hERG	Human Ether-á-go-go-Related Gene
HCl	Hydrochloric acid
HIV	Human immunodeficiency virus
HRMS	High resolution mass spectroscopy
Hz	Hertz
H_2SO_4	Sulfuric acid
IC_{50}	Half maximal inhibitory concentration
IR	Infrared spectroscopy
IIDMM	Institute of Infectious Diseases and Molecular Medicine
J	Coupling constant
K_2CO_3	Potassium carbonate
K_i	Inhibition constant
LCMS	Liquid chromatography-mass spectroscopy
lit	Literature
m	Unresolved multiplet
MDCK	Madin-Darby canine kidney
MDR	Multidrug-resitant

MeOH	Methanol
MHz	Megahertz
MIC	Minimum Inhibitory Concentration
MIC_{90}	Concentration that inhibits 90% of bacterial isolates
MIC_{99}	Concentration that inhibits 99% of bacterial isolates
Min	Minutes
Mp	Melting point
MRI	Magnetic resonance imaging
MS	Mass spectroscopy
M.*tb*	*Mycobacterium tuberculosis*
MTT	3-(4,5dimethylthiazol-2-yl)-2,5-diphenyltetrazolium bromide
MW	Molecular weight
m/z	Mass to charge ratio
$NaBH_4$	Sodium borohydride
NADH	Nicotinamide adenine dinucleotide hydride
NaH	Sodium hydride
NaN_3	Sodium azide
NaO-*t*-Bu	Sodium *tert*-butoxide
Na_2CO_3	Sodium carbonate
n-BuLi	*n*-Butyl lithium
NCE	New Chemical Entity
NH_4Cl	Ammonium chloride
$NH_2NH_2.HCl$	Hydrazine hydrochloride
NH_2OH	Hydroxylamine
NH_2OAc	Ammonium acetate
NMR	Nuclear magnetic resonance spectroscopy
N_2	Nitrogen gas

$Pd_2(dba)_3$	Tris(dibenzylideneacetone)palladium(0)
P(*t*-Bu)$_3$	Tri-*tert*-butylphosphine
ppm	Parts per million
q	Quartet
QP	QikProp
qt	quintet
R_f	Retention factor
RO5	Lipinski's rule of five
Rt	Room temperature
s	Singlet
SAR	Structure-Activity Relationship
$SnCl_2.2H_2O$	Tin(II) chloride dihydrate
t	Triplet
TB	Tuberculosis
td	Triplet of doublets
TDR	Totally drug-resistant
THF	Tetrahydrofuran
TLC	Thin layer chromatography
UV	Ultraviolet
XDR	Extensively drug-resistant
WHO	World Health Organization

Table of Contents

List of Figures

List of Tables

Chapter 1

Drug repurposing and repositioning as a means to expedite drug discovery and development

Preface

The containment of the rising tide of resistance to existing drugs is a global priority. In this chapter, drug repurposing and related concepts are introduced as alternative strategies for the management of communicable and non-communicable diseases. In so doing, the utilization of non-antibiotics is reviewed as an unconventional approach for antimicrobial chemotherapy. Moreover, a discussion on the biological background of neuroleptic drugs as the non-antibiotics of interest is provided. Non-antibiotics are referred to as drugs that are originally employed to treat diseases of non-infectious aetiology and also possess antimicrobial activity, this definition was adopted herein. Furthermore, they either exhibit direct antimicrobial activity or act as adjuvants in combination with conventional antibiotics thus showing great potential for curbing drug resistance.

1.1 Drug Resistance

1.1.1 Drug Resistance: A hurdle in chemotherapeutic interventions

Drug resistance remains a major setback in the management of communicable diseases and also non-communicable diseases. For centuries infectious diseases of bacterial, fungal, parasitic and viral origins have been a threat to global public health. Various factors contribute to the spread of antimicrobial resistance including genetic, therapeutic and socio-economic factors. For instance, overuse of existing antibiotics has propagated resistance and efforts to eradicate the Tuberculosis (TB) scourge have become futile. An evidential example

of antimicrobial resistance is the evolution of *Mycobacterium tuberculosis* (M.*tb*), the causative agent of TB, from multidrug-resistant (MDR) to extensively drug-resistant (XDR) and more recently totally drug-resistant bacterium.[1,2] Antimicrobial resistance is also attributable to other factors such as the lack of disease prevention/ monitoring programmes and shrinking pharmaceutical drug pipelines.[3,4] Apart from antimicrobial resistance, resistance to chemotherapeutics employed in the management of non-communicable diseases such as cancer chemotherapeutics is also a grave concern.

Over the years, the World Health Organization (WHO) has continued to introduce policies and strategic plans to tackle antimicrobial resistance. Resource inadequacy and lack of regulatory authorities are amongst other pressing issues faced by low- to middle-income regions such as Africa. Antimicrobial resistance in these regions is further exacerbated by counterfeit and / or poor-quality antimicrobial medicines. Effective surveillance programmes are essential for tracking and controlling antimicrobial resistance. In 2011 on World Health Day, the WHO launched a policy package comprising strategies for the containment of antimicrobial resistance. The key strategies contained in the policy package include strengthening surveillance and laboratory capacity, regulation and promotion of rational use of medicines, accessibility to essential medicines that are of assured quality, fostering innovative research, enhancement of infection prevention and control programmes.[3]

1.2 Antimicrobial Chemotherapy: Historical background

Over the past few decades, antibiotics have been the panacea for microbial infections. Early in the 20th century, Paul Ehrlich introduced chemotherapy as a medical speciality. His research between 1854 and 1915 led to the discovery of methylene blue.[5] This cationic phenothiazinium dye displayed efficacy against Malaria. Alexander Fleming is also one of

the pioneers of antibiotic drug discovery owing to his serendipitous discovery of penicillin in 1928.[6,7,8] Within a short span of time, more antibiotics flooded the drug market, dubbing the period between 1950 and 1970's the 'golden age of antibiotics'.[5,9] Following the 'golden age' era, antibiotic drug pipelines began to dry up partly due to lengthy periods of drug discovery and development as well as the emergence of antimicrobial drug resistance. Table 1.1 highlights antimicrobial resistance events that occurred over the years.[10,11]

Table 1.1: Examples of antibiotic drug classes, their year of discovery and the years in which resistance was observed[10,11] DR: Drug-resistant; MDR: Multidrug-resistant; XDR: Extensively drug-resistant; TB: Tuberculosis

Class of antibiotics	Example	Year of discovery	Year of introduction	Antimicrobial resistance identified (year and pathogen)
Sulfonamides	**Prontosil**	1932	1936	**1942** *(Streptococcus)*
Beta-lactams	**Penicillin**	1928	1938	**1943** *(Staphylococcus aureus)*
				1965 *(Pneumococcus)*
Quinolines	**Chloroquine**	1934	1947	**1957** *(Plasmodium falciparum)*
Aminoglycosides	**Streptomycin**	1943	1946	**1980s** *(DR Tuberculosis)*
Macrolides	**Erythromycin**	1948	1951	**1968** *(Streptococcus)*
Tetracyclines	**Chlortetracycline**	1944	1952	**1959** *(Shigella)*
Rifamycins	**Rifampicin**	1957	1958	**1990s** *(MDR Tuberculosis)*
Glycopeptides	**Vancomycin**	1953	1958	**1988** *(Enterococcus)*
Oxazolidinones	**Linezolid**	1955	2000	**2001** *(Staphylococcus aureus)*
			2006	**2013** *(XDR Tuberculosis)*[12]
Lipopeptides	**Daptomycin**	1986	2003	**2013** *(Staphylococcus aureus)*[13]
Cephalosporins	**Ceftaroline**	2000	2010	**2011** *(Staphylococcus aureus)*
Macrolides	**Fidaxomicin** (*Clostridium difficile*)	1948	2011	-
Diarylquinolines	**Bedaquiline** (*MDR-TB)*	1997	2012	-

Curbing antimicrobial resistance is a multi-faceted problem and development of additional antibiotics has not provided much relief in treatment and/ or eradication of infectious diseases. This necessitates a search for alternative approaches including novel therapeutic drug classes that avoid current resistance mechanisms and/or therapeutics that target biological systems such as multidrug efflux pumps which confer resistance to antimicrobials.

In efforts to avert resistance, research interest is shifting toward discovery of unconventional therapeutics for the treatment of infectious diseases. On-going research reveals utilization of non-antibiotics as an alternative approach for antimicrobial chemotherapy.[5,6,14,15] Drug resistance reversal properties of some non-antibiotics such as neuroleptic phenothiazines hold promise for curbing the rise of antimicrobial resistance.[7,16]

1.2 Drug Repurposing: Use of existing drugs for new indications

1.2.1 Overview of drug repurposing and drug repositioning

De novo drug discovery and development *via* traditional approaches is an exhaustive and time-consuming process. This multi-stage process from basic research to a marketed drug could cost millions of dollars and development stages might take longer than a decade to complete (Figure 1.1).[17,18] Furthermore, the complexity associated with the drug development process renders it a financially risky endeavour as failures could arise at any point.

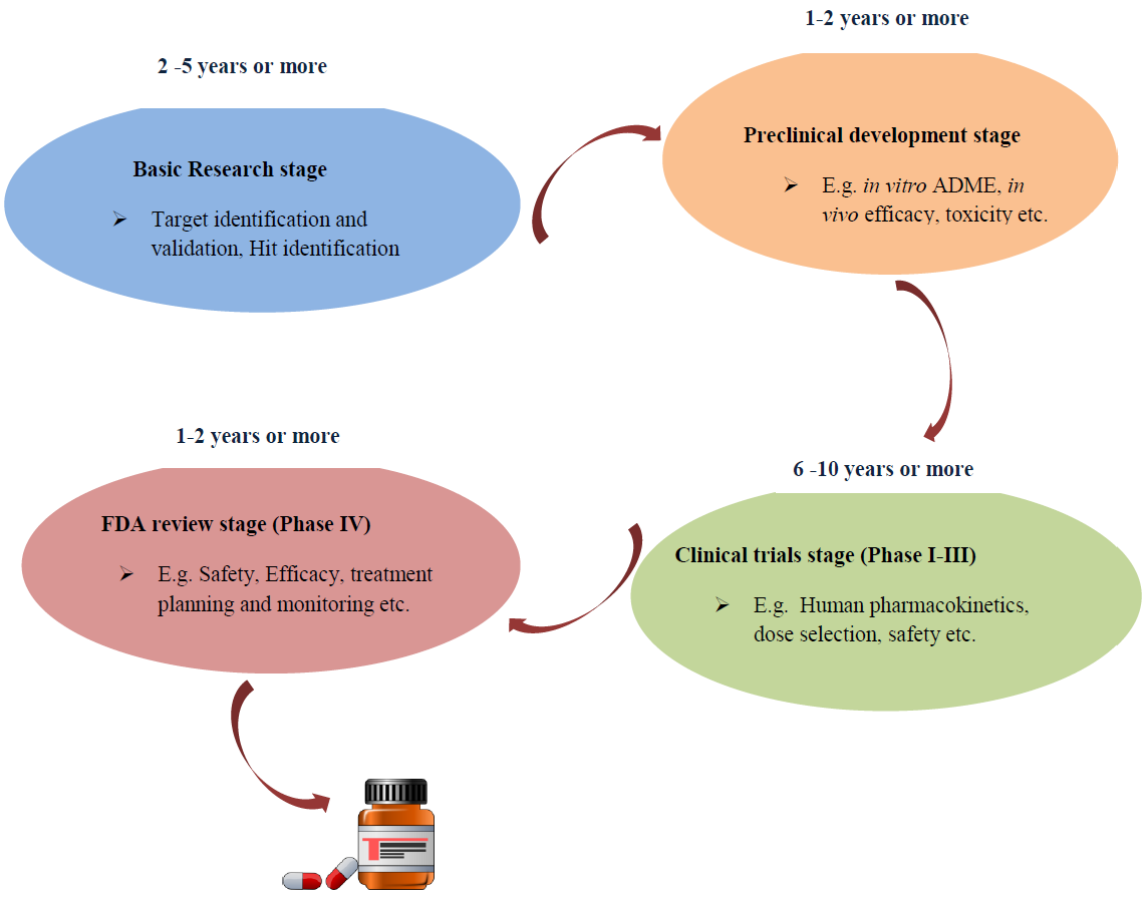

Figure 1.1: A simplified depiction of the drug discovery and development process from basic research to clinical trials and ultimately approval by regulatory authorities e.g. the Food and drug Administration (FDA).

In light of a consistent decline in antibiotics production and the emergence of resistance, novel and faster production routes are desperately sought. The use of clinically approved drugs for new indications, generically referred to as drug repurposing, has become an increasingly attractive strategy in drug discovery and development.[19,20] Drug repurposing is often used interchangeably with the term drug repositioning. Some authors define drug repositioning as the derivatization (drug remodelling) of an existing drug as a potential therapeutic in another disease, this definition is adopted herein. These strategies are closely associated with other concepts such as drug rescue whereby drugs that are abandoned or candidates that have failed in development stages are investigated for other indications.[21,22,23]

Clinically approved drugs have validated pharmacokinetic properties and toxicological profiles therefore their repurposing could potentially avoid high research costs and lengthy timelines. Moreover, technological advances in virtual screening methodologies present an opportunity for rapid screening of libraries of clinically approved drugs for therapeutic activities against new biomolecular targets in a manner that is both efficient and cost-effective.[20,24,25] Numerous clinically approved drugs have been successfully repurposed or are being investigated for other indications in efforts to rejuvenate pharmaceutical drug pipelines. Examples of clinically developed drugs that have been repurposed or being investigated for bio-activity in other diseases are tabulated below (Table 1.2).[22,26,27]

Table 1.2: Selected examples of drugs repurposed and/ or being investigated for new indications

Drug	Original Indication	New / Investigational Use	Reference
Thalidomide	**Sedative**	Multiple myeloma; Leprosy	Rajkumar *et al.*, 2000[28]
Thioridazine	**Antipsychotic**	(MDR-TB & XDR-TB)	Ordway *et al.*, 2003;[29] Amaral *et al.*, 2012;[1] Singh *et al.*, 2014[30]
Pyramithamine	**Antimalarial**	Toxoplasmosis	Montoya J G and Liensenfeld O, 2004[31]
Nifurtimox	**Chagas Disease**	Cancer (neuroblastoma)	Saulnier Sholler *et al*, 2006[32]
Statins	**Cholesterol-Lowering drugs**	*Staphylococcus Pneumonia*	Rosch *et al.*, 2010[33]
Doxycycline	**Antibacterial**	Malaria	Tan *et al.*, 2011[34]
Quinine	**Antimalarial**	Arthritis; Lupus	Bird *et al.*, 1995;[35] Murphy *et al.*, 2013[36]
Metformin	**Diabetes**	Gyneacologic Cancer	Febbraro *et al.*, 2014[37]
Mebendazole	**Anti-helminthic**	Cancer	Pantziarka *et al.*, 2014[38]
Linezolid	**Antibacterial**	Tuberculosis (MDR & XDR)	Lee *et al.*, 2012;[39] Ambrosio *et al.*, 2015[40]
Artemisinin	**Antimalarial**	Candidiasis	Bhattacharya *et al.*, 2015[41]
Auranofin	**Anti-inflammatory**	Hodgkin Lymphoma	Celegato *et al.*, 2015[42]

1.2.2 Non-antibiotics as alternative antimicrobial agents

The rise of antimicrobial resistance has nullified the effects of many conventional antibiotics. Over the years, non-antibiotics have been reported to augment the activity of classical antibiotics as 'helper compounds' or exhibit direct antimicrobial activity.[5] Several drug classes of non-antibiotics including neuroleptics, anti-inflammatory agents, antihypertensives and local anaesthetics possess antimicrobial properties (Table 1.3).[1,6,43,44]

Table 1.3: Examples of non-antibiotic drug classes that exhibit antimicrobial activity as per literature reports

Class of non-antibiotics	Example	Pathogen	MIC or IC_{50}	Reference
Antihistamines	**Mequitazine** 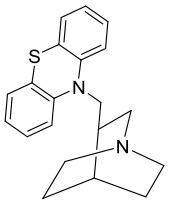	*Enterococcus faecium* 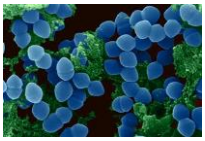	62.5 mg/mL	El-Nakeeb *et al.*, 2011[45]
Antihypertensives	**Amlodipine** 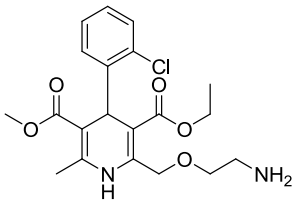	*Staphylococcus aureus* 	10 mg/mL	Mazumdar *et al*, 2010[5]
Analgesics	**Acetylsalicylic acid** 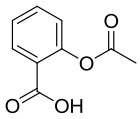	*Influenza virus* 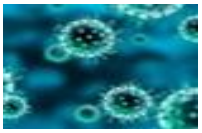	7 mg/mL	Mazur *et al*, 2007[46]
Analgesics	**Acetaminophen** 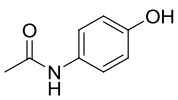	*Staphyloccocus aureus* 	1.25 mg/mL	Al Janabi *et al*, 2010[47]
Anti-inflammatory	**Diclofenac** 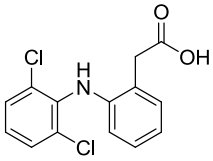	*Enterococcus faecium* 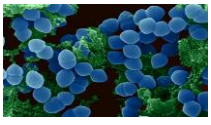	0.05 mg/mL	Salem-Milani *et al*, 2013[48]

Table 1.3 continued…

Class of non-antibiotics	Example	Pathogen	MIC or IC_{50}	Reference
Anaesthetics	**Proxymetacaine** 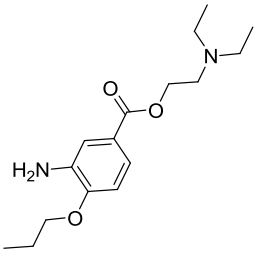	*Staphylococcus epidermidis* 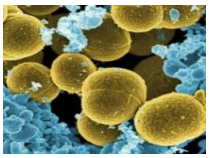	2.50 mg/mL	Pelosini *et al*, 2009[49]
Antidepressants	**Amitriptyline** 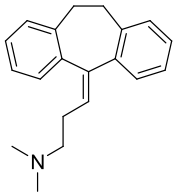	MS-*Staphylococcus aureus* 	128 mg/mL	Hendricks *et al*, 2003[50]
Antipsychotics	**Chlorpromazine** 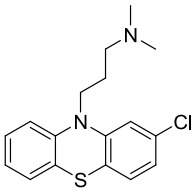	*Plasmodium falciparum* 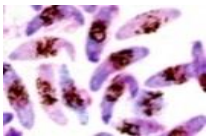	10 µM	Basco *et al*, 1992[51]
Diuretics	**Amiloride** 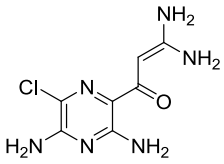	*Pseudomonas aeruginosa* 	0.80 mg/mL	Cohn *et al*, 1988[52]
Calcium channel blockers	**Verapamil** 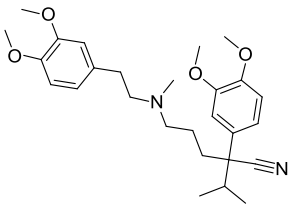	*E coli* 	3 mg/mL	Andersen *et al*, 2006[53]
Antipsychotics	**Chlorpromazine** 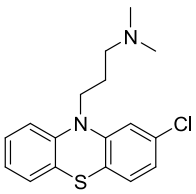	*Mycobacterium tuberculosis* 	0.010 mg/mL	Ordway *et al*, 2003[29]

Of note, neuroleptics, phenothiazine derivatives in particular, are appealing to researchers due to their wide spectrum of bio-activities including antibacterial, antimalarial, antiemetic, anticancer, antihistaminic and many more. More importantly, their multidrug-resistance reversal properties warrants further investigation for their use in the management of resistance.[1,43]

1.3 Multiple biological properties of neuroleptics

1.3.1 Historical overview

Clinical observations from the use of methylene blue for treatment of psychosis opened doors for the development of other phenothiazine-derived neuroleptics (Figure 1.2).[8,9]

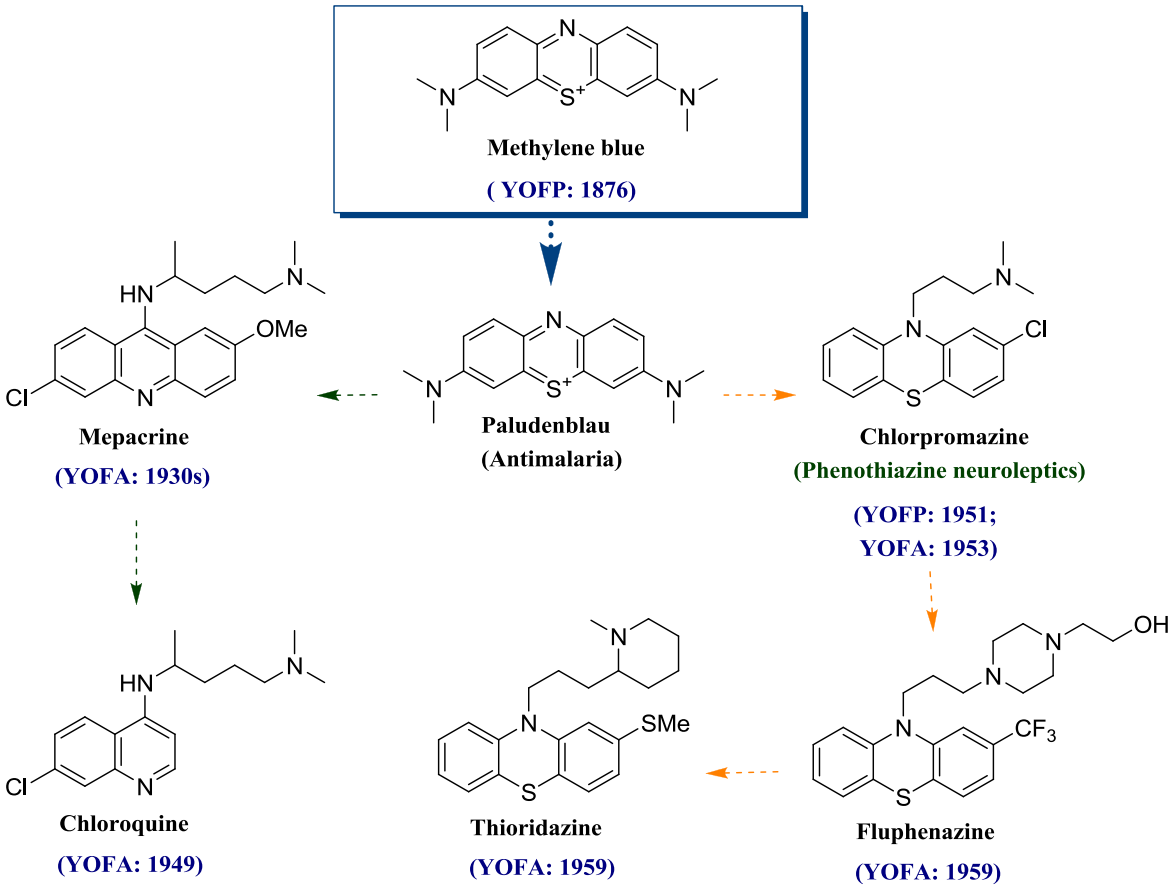

Figure 1.2: Structural evolution from the precursor structure, methylene blue, to phenothiazine neuroleptic thioridazine, and to antimalarial chloroquine. YOFP-Year of first preparation; YOFA-Year of FDA approval.

Chlorpromazine, a phenothiazine derivative, was first synthesized in 1951 by a French chemist, Paul Charpentier. Its use for treatment of psychosis revealed a plethora of negative side effects such as tardive dyskinesia, memory loss and hypotension.[6] However, favourable effects were also discovered when it was introduced in TB chemotherapy. Patients displayed alleviation of TB symptoms and in some cases an almost complete cure.[6,8] This observation was noted during the reign of rifampicin and isoniazid as potent anti-TB drugs, therefore novel anti-TB agents were not of imperative research interest. Nevertheless, research interest in chlorpromazine was not entirely weakened. Thioridazine, another phenothiazine derivative, was later developed and was found to be the least potent phenothiazine neuroleptic with much milder side effects including drowsiness. Severe side effects of thioridazine are much less frequent and may include QT interval prolongation and episodes of 'torsade de pointes' which could lead to sudden death.[6,8]

1.3.2 Neuroleptic action of phenothiazines by blockade of CNS receptors

The neuroleptic action of phenothiazines and related drugs has been linked to the blockade of serotonergic and dopaminergic receptors. They also inhibit other central nervous system (CNS) receptors including muscarinic, GABA-ergic, α-adrenergic and histamine receptors. Their affinity for CNS receptors is attributable to their structural resemblance to monoamine neurotransmitters such as dopamine (Figure 1.3).[54,55]

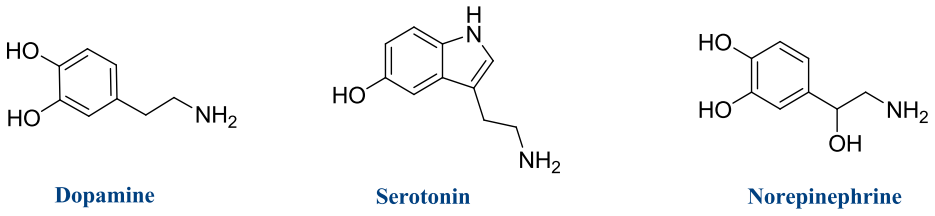

Figure 1.3: Examples of monoamine neurotransmitters.

The dopamine receptors are categorized into two primary groups, D_1-like receptors (D_1 & D_5) as well as D_2-like receptors (D_2, D_3 & D_5). Both receptor families are G-protein-coupled receptors that are associated with the activation of adenylate cyclase. Phenothiazines are known to be potent D_2 receptor antagonists. Their high affinity for dopamine receptors is evident in the inhibition constants (K_i) (Figure 1.4).[56,57]

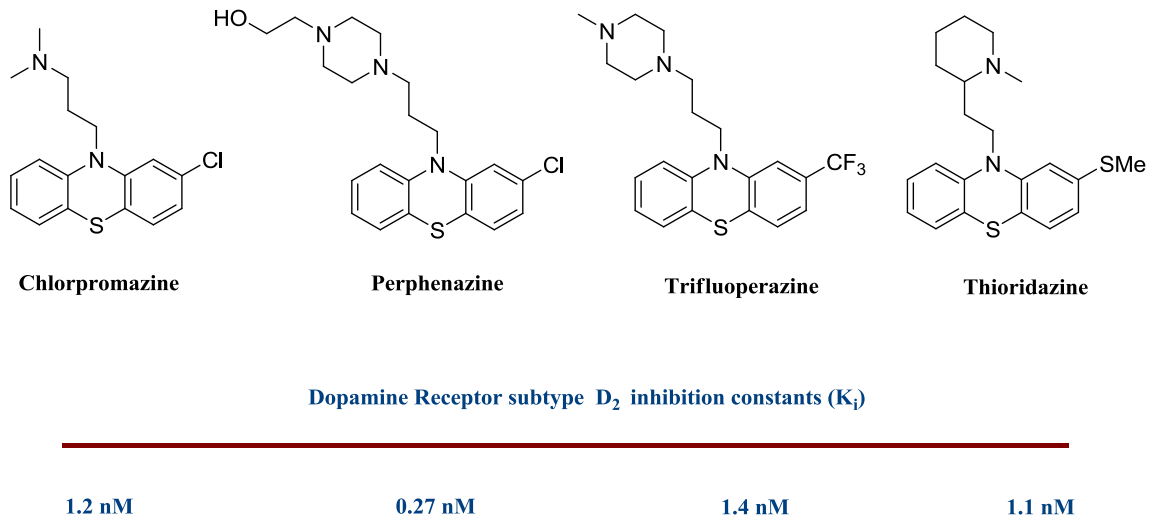

Figure 1.4: Examples of phenothiazine antipsychotics along with dopamine subtype 2 receptor (D_2) inhibition constants (K_i).

1.3.3 Repurposing of neuroleptic phenothiazines and related drugs

The repurposing of phenothiazines and their structural relatives has been investigated extensively. As previously mentioned, these drugs have been reported to possess a broad spectrum of non-neuroleptic biological activities including antimycobacterial, antiparasitic, anticancer, antiviral activities and many more.[6,55,58] Of the phenothiazines investigated for antimicrobial bio-activities, thioridazine has attracted the most research interest owing to its milder side effects. It also shows great potential as an adjuvant in treatment of antibiotic-resistant TB infections.[1,59] Most recently, thioridazine has been investigated as an adjuvant in

clinical trials against XDR-TB in combination with other drugs such as linezolid and moxifloxacin (Figure 1.5).[60,61,62] Other recent reports include its antitrypanosomal activity and reduction of tumor growth in a murine breast cancer model.[63,64] Imipramine, a phenothiazine structural relative, has also been repurposed for various indications including malaria, bacterial infections and cancer (Figure 1.5).[50,65,66,67]

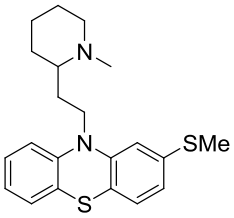

Thioridazine

MDR-Tuberculosis	(*in vivo* dose 32 & 70 mg/kg/day; synergistic effects observed when added to a regimen comprising isoniazid, rifampicin & pyrazinamide)	**van Soolingen *et al*., 2010[59]**
XDR-Tuberculosis	(Cured 10 of 12 XDR-TB patients in Buenos Aires, Argentina; Used as a salvage drug for XDR-TB patients in Mumbai India)	**Amaral *et al*., 2010[61]** **Udwadia *et al*., 2011[62]**
TDR-Tuberculosis	(Recommended for treatment of TDR-TB; inhibits bacterial efflux pumps)	**Amaral L, 2012[1]**
Breast Cancer	(reduces tumor growth, inhibits angiogenesis & proliferation; induces apoptosis)	**Yin *et al*., 2015[64]**
Chagas disease	(*in vivo* dose 80 mg/kg/day; inhibits trypanothione reductase)	**Lo Presti *et al*., 2015[63]**

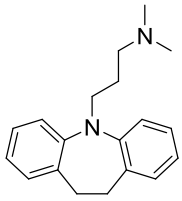

Imipramine

Malaria	(IC_{50} 56 uM; enhanced hemolysis induced by ferriprotoporphyrin IX)	**Dutta *et al*., 1990[65]**
Staph Infections	(*in vitro* MIC 128-256 mg/L; against drug-resitant strains of *Staphyloccocus aureus*)	**Hendricks *et al*., 2003[50]**
Brain Tumor	(Induces autophagic cell death in U-87MG human glioma cells)	**Jeon *et al*., 2011[66]**
Tuberculosis	(Inhibits *Mycobacterium tuberculosis* topoisomerase I)	**Godbole *et al*., 2015[67]**

Figure 1.5: Examples of bioactivities exhibited by repurposed neuroleptics.

1.3.4 Repositioning of phenothiazines

The phenothiazine core structure is a privileged scaffold that serves as a pharmacophoric subunit for the design of novel structures with a wide range of biological applications. Structures of these antipsychotics have been remodelled for a variety of indications including infectious and non-infectious diseases.[14,55]

1.3.4.1 Antimycobacterial activity of remodelled phenothiazines

Phenothiazines and their structural relatives have long been known for their antimycobacterial activity. Literature reports have revealed libraries of remodelled phenothiazines that display promising antimycobacterial activities.[68,69,70] In most cases the investigation of neuroleptic properties of the remodelled structures is rarely conducted. Selected examples of remodelled phenothiazines with antitubercular activity at MICs ranging from 0.5-25 µg/mL are given in Table 1.4.

Table 1.4: Selected examples of remodelled phenothiazines that show *in vitro* antitubercular activity

Phenothiazine Derivative	Antitubercular Activity	Investigation of CNS receptor binding	Reference
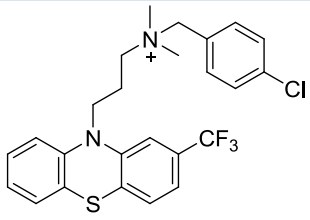	MIC **4 µM**	Not Reported	Bate *et al*.,2007[71]
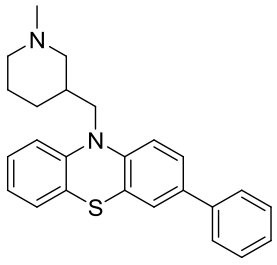	MIC **2.1 µg/mL**	Displayed notable dopamine and serotonin receptor binding activity; % inhibition of dopamine and serotonin receptor subtypes ranged from 0% (5-HT_{2A}) to 97% (D_3)	Madrid *et al*., 2007[72]

Table 1.4 continued…

Phenothiazine Derivative	Antitubercular Activity	Investigation of CNS receptor binding	Reference
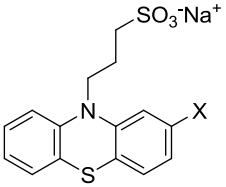 X= CF_3, SMe, Cl or H	MIC **12.5-25 µg/mL**	Displayed no dopamine and serotonin activity. Only one derivative (X = CF_3) displayed marginal serotoninergic binding activity.	Salie *et al*., 2014[73]
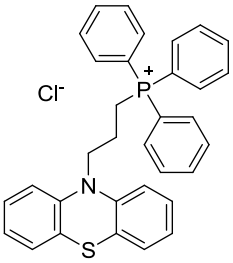	MIC **0.5 µg/mL**	Not Reported	Dunn *et al*., 2014[74]
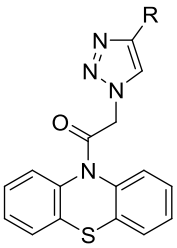 **R = Aliphatic or Aromatic**	MIC **6.25 µg/mL** .	Not Reported	Addla *et al*., 2014[69]
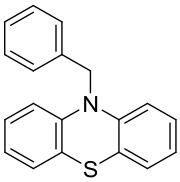	MIC **4 µg/mL**	Not Reported	He *et al*., 2015[68]

MIC- Minimum inhibitory concentration; Structures shown are the most active compounds as per reports.

1.3.4.2 Antifungal and antiparasitic properties of remodelled phenothiazines

Remodelled phenothiazines have also been reported to show antifungal and antiparasitic activities (Table 1.5). They have exhibited activity against various types of fungi including *Candida albicans*, *Aspergillus flavus*, and *Exophiala xenobiotica*.[70,75] Their antiparasitic acitivities have been demonstrated in various indications including malaria and Chagas disease.[76,77]

Table 1.5: Selected examples of remodelled phenothiazines that show *in vitro* antifungal and antiparasitic activities

Phenothiazine Derivative	Antifungal/ Antiparasitic Activity	Investigation of CNS Receptor Binding	Reference
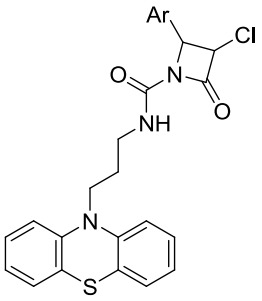	(antifungal) MIC **12.25-13.75 µg/mL**	Not Reported	Sharma *et al.*, 2012[70]
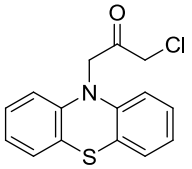	(antifungal) MIC **2-32 µg/mL**	Not Reported	Sarmiento *et al.*, 2011[75]
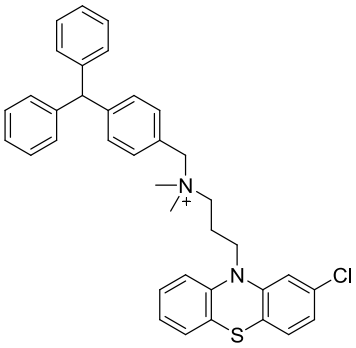	(antitrypanosomal) EC_{50} **0.062 µM**	Not Reported	Khan *et al.*, 2000[76]
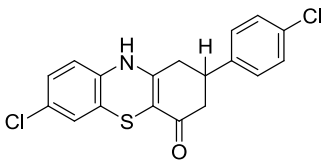	(antiplasmodial) IC_{50} **6 µM**	Not Reported	Dominquez *et al.*, 1997[77]

MIC-Minimum inhibitory concentration; EC_{50}-half maximal effective concentration; IC_{50}- half maximal inhibitory concentration; Structures shown are the most active compounds as per reports.

1.3.4.3 Anticancer activity of remodelled phenothiazines

Apart from remodelled phenothiazines showing great potential as antimicrobial agents, sporadic reports have shown their potential in non-communicable diseases such as cancer.

Phenothiazine derivatives have shown anticancer activity against a variety of cancer cell types including leukaemia, melanoma and CNS cancer (Table 1.6).[78,79,80] In other reports, remodelled structures displayed significant antiproliferative activity as well as activity against tubulin polymerization comparable to phenstatin.[78]

Table 1. 6: Selected examples of remodelled phenothiazines that show anticancer activity

Phenothiazine Derivative	**Anticancer Activity**	**Investigation of CNS Receptor Binding**	**Reference**
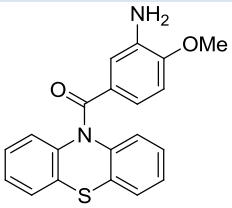	ITP IC_{50} :**11.82 µM** GI_{50} : **0.030 µM** (Leukemia SR Cell line)	Not Reported	Abuhaie *et al*., 2013[78]
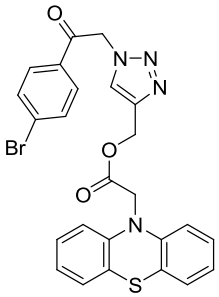	IC_{50} **1.3 ± 0.3 µM**	Not Reported	Belei *et al.*, 2012[79]
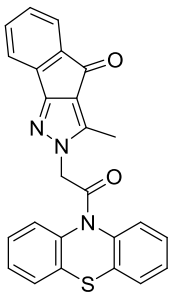	IC_{50} **3.35 ± 0.28 µM**	Not Reported	Baciu-Atudosie *et al*., 2012[81]
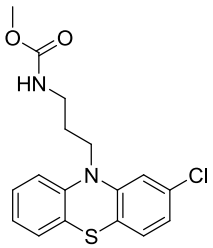	GI_{50} **> 40 µM**	Binding to dopamine receptor subtypes (D_1-D_5) was less than 10% at 0.1 mM, and greater at 1.0 mM ligand concentration	Kastrinsky *et al.*, 2015[80]

ITP-Inhibition of tubulin polymerization; IC_{50}- half maximal inhibitory concentration; GI_{50}- molar concentration indicating 50% growth inhibition of cancer cells; Structures shown are the most active compounds as per reports.

1.4 Documented non-neuroleptic modes of action of phenothiazines

Phenothiazines interfere with a number of metabolic pathways that are crucial for survival of pathogenic microorganisms. Reports reveal that they inhibit type II NADH:menaquinone odixoreductase, an essential enzyme involved in the respiratory chain.[82,83] More recently, Warman *et al.* provided further validation that type II NADH: menaquinone oxidoreductase is a molecular target of phenothiazines in M.*tb*.[84] Phenothiazines are also reported to have the propensity to concentrate in macrophages, an attribute that augments their antitubercular activity.[7]

Phenothiazines also inhibit calcium (Ca^{2+}) transportation consequently preventing its binding to Ca^{2+}-binding proteins such as calmodulin. This in turn inhibits Ca^{2+}-dependent enzyme systems such as ATP hydrolysis for cellular energy.[9] Their drug resistance reversal properties are conferred by their ability to inhibit Ca-calmodulin binding in synergistic combination with other antibiotics. Moreover, they interfere with bacterial efflux pump mechanisms which give rise to MDR strains when overexpressed.[85]

In various studies, phenothiazine analogs exhibited inhibition against P-glycoprotein efflux pumps in *Staphylococcus aureus*, which confer resistance to fluoroquinolone drugs and also activity against efflux pumps present in *Escherichia coli*.[86] Other reports reveal that due to increased permeability resulting from efflux pump inhibition, phenothiazines interfere with DNA-based processes thereby inhibiting replication.[9]

Abuhaie and co-workers reported novel phenothiazine-bearing compounds with significant activities against cell proliferation and tubulin polymerization.[78] Another study by Belei *et al.* demonstrated that phenothiazine derivatives containing a 1,2,3-triazole motif could be

potential inhibitors of farnesyltransferase, an enzyme involved the membrane localization of G-protein-Ras.[79] Thioridazine was found to induce autophagy in glioblastoma and also upregulated the activity of Adenosine monophosphate-activated protein kinase (AMPK), an enzyme that plays a crucial role in cellular energy homeostasis.[87] Moreover, thioridazine has also been reported to inhibit trypanothione reductase, an enzyme that is essential for the survival of *Trypanosoma cruzi* which causes Chagas disease.[63]

1.5 Adverse side effects of phenothiazines preclude their use in other indications

As discussed earlier, the neuroleptic action of phenothiazines is associated with a blockade of CNS dopaminergic receptors. Phenothiazines are also associated with adverse side effects including extrapyramidal symptoms such as tardive dyskinesia and bradykinesia.[56,88] At clinically relevant doses, inherent neuroleptic effects along with potential side effects preclude their extensive use in other indications. Many studies have reported on structural remodelling of phenothiazines for non-neuroleptic bio-activities.[70,74,78,79] However, investigation of their inherent neuroleptic properties is seldom reported and could potentially present hurdles at late-stage drug development.

Novel functionalities that are dissimilar to typical structures of phenothiazine drugs could be introduced through drug remodelling. However, it is important to fully probe and understand minimal structural requirements for neuroleptic activity. Deviation from these requirements could abrogate unwanted neuroleptic effects and improve selectivity for bio-activities of interest.

References

(1) Amaral, L.; Viveiros, M. Why Thioridazine in Combination with Antibiotics Cures Extensively Drug-Resistant Mycobacterium Tuberculosis Infections. *Int. J. Antimicrob. Agents* **2012**, *39* (5), 376–380.

(2) Amaral, L. Totally Drug Resistant Tuberculosis Can Be Treated with Thioridazine in Combination with Antibiotics to Which the Patient Was Initially Resistant. *Biochem. Pharmacol. Open Access* **2012**, *01* (01), 1–2.

(3) WHO. http://www.who.int/drugresistance/documents/situationanalysis/en/ *(accessed 07/10/2015)* Worldwide Country Situation Analysis : Response to Antimicrobial Resistance; 2015.

(4) WHO. http://www.who.int/tb/publications/global_report/en/ *(accessed 30/05/2015)*, Global Tuberculosis Report; 2014.

(5) Mazumdar, K.; Asok Kumar, K.; Dutta, N. K. Potential Role of the Cardiovascular Non-Antibiotic (Helper Compound) Amlodipine in the Treatment of Microbial Infections: Scope and Hope for the Future. *Int. J. Antimicrob. Agents* **2010**, *36* (4), 295–302.

(6) Wainwright, M. The Evolution of Antimycobacterial Agents from Non- Antibiotics. *Open J. Pharmacol.* **2012**, 2–1.

(7) Kristiansen, J. E.; Hendricks, O.; Delvin, T.; Butterworth, T. S.; Aagaard, L.; Christensen, J. B.; Flores, V. C.; Keyzer, H. Reversal of Resistance in Microorganisms by Help of Non-Antibiotics. *J. Antimicrob. Chemother.* **2007**, *59*, 1271–1279.

(8) Wainwright, M.; Amaral, L. The Phenothiazinium Chromophore and the Evolution of Antimalarial Drugs. *Trop. Med. Int. Heal.* **2005**, *10* (6), 501–511.

(9) Martins, M.; Dastidar, S. G.; Fanning, S.; Kristiansen, J. E.; Molnar, J.; Pag, J.; Schelz, Z.; Spengler, G.; Viveiros, M.; Amaral, L. Potential Role of Non-Antibiotics (Helper Compounds) in the Treatment of Multidrug-Resistant Gram-Negative Infections: Mechanisms for Their Direct and Indirect Activities. *Int. J. Antimicrob. Agents* **2008**, *31*, 198–208.

(10) Lewis K. Platforms for Antibiotic Discovery. *Nat. Rev. Drug Discov.* **2013**, *12*, 371–387.

(11) Ventola, C. L. The Antibiotic Resistance Crisis Part 1: Causes and Threats. *P T* **2015**, *40* (4), 277–283.

(12) Jaramillo Ernesto; Weyer Karin; Raviglione Mario. Linezolid for Extensively Drug-Resistant Tuberculosis. *N Engl J Med* **2013**, *368* (3), 290–291.

(13) Bayer A.S.; Schneider T; Sahl H.G. Mechanisms of Daptomycin Resistance in Staphylococcus Aureus: Role of the Cell Membrane and Cell Wall. *Ann N Y Acad Sci* **2013**, *1277*, 139–158.

(14) Pluta, K.; Morak-Młodawska, B.; Jeleń, M. Recent Progress in Biological Activities of Synthesized Phenothiazines. *Eur. J. Med. Chem.* **2011**, *46* (8), 3179–3189.

(15) Tan, Y. T.; Tillett, D. J.; McKay, I. A. Molecular Strategies for Overcoming Antibiotic Resistance in Bacteria. *Mol. Med. Today* **2000**, *6* (8), 309–314.

(16) Kristiansen, J. E.; Thomsen, V. F.; Martins, A.; Viveiros, M.; Amaral, L. Non-Antibiotics Reverse Resistance of Bacteria to Antibiotics. *In Vivo (Brooklyn).* **2010**, *24* (5), 751–754.

(17) Sarkar, S.; Suresh, M. R. An Overview of Tuberculosis Chemotherapy - A Literature Review. *J. Pharm. Pharm. Sci.* **2011**, *14* (2), 148–161.

(18) Hughes, J. P.; Rees, S. S.; Kalindjian, S. B.; Philpott, K. L. Principles of Early Drug Discovery. *Br. J. Pharmacol.* **2011**, *162* (6), 1239–1249.

(19) Kharkar, P. S. Drugs Acting on Central Nervous System (CNS) Targets as Leads for Non-CNS Targets. *F1000Research* **2014**, *3* (40), 1–7.

(20) Persaud-Sharma V; Zhou S. Drug Repositioning: A Faster Path to Drug Discovery. *Adv. Pharmacoepidemiol. Drug Saf.* **2012**, *1* (6), 1–3.

(21) Oprea, T. I.; Mestres, J. Drug Repurposing: Far Beyond New Targets for Old Drugs. *Am. Assoc. Pharm. Sci.* **2012**, *14* (4), 759–763.

(22) Allarakhia, M. Open-Source Approaches for the Repurposing of Existing or Failed Candidate Drugs: Learning from and Applying the Lessons across Diseases. *Drug Des. , Dev. Ther.* **2013**, *7*, 753–766.

(23) Njoroge, M.; Njuguna, N. M.; Mutai, P.; Ongarora, D. S. B.; Smith, P. W.; Chibale, K. Recent Approaches to Chemical Discovery and Development Against Malaria and the Neglected Tropical Diseases Human African Trypanosomiasis and Schistosomiasis. *Chem. Rev.* **2014**, *114*, 11138–11163.

(24) Ma D; Chan D; Leung C. Drug Repositioning by Structure-Based Virtual Screening. *Chem. Soc. Rev.* **2013**, *42*, 2130–2141.

(25) Shim, J. S.; Liu, J. O. Recent Advances in Drug Repositioning for the Discovery of New Anticancer Drugs. *Int. J. Biol. Sci.* **2014**, *10* (7), 654–663.

(26) Rangel-Vega, A.; Bernstein, L. R.; Mandujano-tinoco, E. A.; Debabov, D.; Visca, P. Drug Repurposing as an Alternative for the Treatment of Recalcitrant Bacterial Infections. *Front. Microbiol.* **2015**, *6* (282), 1–8.

(27) Andrews, K. T.; Fisher, G.; Skinner-adams, T. S. International Journal for Parasitology : Drugs and Drug Resistance Drug Repurposing and Human Parasitic Protozoan Diseases. *Int. J. Parasitol. Drugs Drug Resist.* **2014**, *4* (2), 95–111.

(28) Rajkumar, S. V.; Fonseca, R.; Dispenzieri, A.; Lacy, M. Q.; Lust, J. A.; Kyle, R. A.; Gertz, M. A.; Griepp, P. R. Thalidomide in the Treatment of in the Treatment of Relapsed Multiple Myeloma. *Mayo Clin Proc* **2000**, *75* (9), 897–901.

(29) Ordway, D.; Viveiros, M.; Leandro, C.; Almeida, J.; Martins, M.; Jette, E.; Molnar, J.; Amaral, L.; Kristiansen, J. E. Clinical Concentrations of Thioridazine Kill Intracellular Multidrug-Resistant Mycobacterium Tuberculosis. *Antimicrob. Agents Chemother.* **2003**, *47* (3), 917–922.

(30) Singh, A.; Sharma, S. Chemotherapeutic Efficacy of Thioridazine as an Adjunct Drug in a Murine Model of Latent Tuberculosis. *Tuberculosis* **2014**, *94* (6), 695–700.

(31) Montoya, J. G.; Liesenfeld, O. Toxoplamosis. *Lancet* **2004**, *363* (9425), 1965–1976.

(32) Saulnier Sholler, G. L.; Kalkunte, S.; Greenlaw, C.; McCarten, K.; Forman, E. Antitumor Activity of Nifurtimox Observed in a Patient with Neuroblastoma. *J. Pediatr. Heamtol. Oncol.* **2006**, *28* (10), 693–695.

(33) Rosch, J. W.; Boyd, A. R.; Hinojosa, E.; Pestina, T.; Hu, Y.; Persons, D. A.; Orihuela C.J.; Toumanen E. I. Statins Protect against Fulminant Pneumococcal Infection and Cytolysin Toxicity in a Mouse Model of Sickle Cell Disease. *J. Clin. Invest.* **2010**, *120* (2), 627–635.

(34) Tan, K. R.; Magill, A. J.; Parise, M. E.; Arguin, P. M. Doxycycline for Malaria Chemoprophylaxis and Treatment: Report from the CDC Expert Meeting on Malaria Chemoprophylaxis. *Am. J. Trop. Med.* **2011**, *84* (4), 517–531.

(35) Bird, M. R.; O'Neill, A. I.; Buchanan, R. R.; Ibrahim, K. M.; Des Parkin, J. Lupus Anticoagulant in the Elderly May Be Associated with Both Quinine and Quinidine Usage. *Pathology* **1995**, *27* (2), 136–139.

(36) Murphy, G., Lisnevskaia, L., Isenberg, D. Systemic Lupus Erythematosus and Other Autoimmune Rheumatic Diseases: Challenges to Treatment. *Lancet* **2013**, *382* (9894), 809–818.

(37) Febbraro, T.; Lengyel, E.; Romero, I. L. Old Drug, New Trick: Repurposing Metformin for Gynecologic Cancers. *Gynecol OnCol* **2014**, *135* (3), 614–621.

(38) Pantziarka, P.; Bouche, G.; Meheus, L.; Sukhatme, V.; Sukhatme, V. P. Repurposing Drugs in Oncology (ReDO)— Mebendazole as an Anti-Cancer Agent. *ecancer Med. Sci.* **2014**, *8* (443), 1–16.

(39) Lee M; Lee J; Carroll MW; Min S; Song T; Via LE; Goldfeder LC; Kang E; Jin B; Park H; Kwak H; Kim H; Jeon HS; Jeong I; Joh JS; Chen RY; Olivier KN; Shaw PA; Follmann D; Song SD; Lee JK; Lee D; Kim CT; Dartois V; Park SK; Cho SN; Barry CE 3rd. Linezolid for Treatment of Chronic Extensively Drug-Resistant Tuberculosis. *N Engl J Med* **2012**, *367* (16), 1508–1518.

(40) Ambrosio, L. D.; Centis, R.; Sotgiu, G.; Pontali, E.; Spanevello, A.; Migliori, G. B. New Anti-Tuberculosis Drugs and Regimens: 2015 Update. *ERJ Open Res.* **2015**, *1*, 1–15.

(41) Bhattacharya, A.; Kaur, H.; Kumar Lal, N.; Bharti, N. Repurposing Antimalarial Artemisinin against Candidiasis. *Int. J. Pharm. Sci. Rev. Res.* **2015**, *32* (1), 143–147.

(42) Celegato, M.; Borghese, C.; Casagrande, N.; Mongiat, M.; Kahle, X. U.; Paulitti, A.; Michele Spina; Alfonso Colombatti; Aldinucci, D. Preclinical Activity of Repurposed Drug Auranofin in Classical Hodgkin Lymphoma. *Blood* **2015**, *126* (11), 1394–1397.

(43) Koul, A.; Arnoult, E.; Lounis, N.; Guillemont, J.; Andries, K. The Challenge of New Drug Discovery for Tuberculosis. *Nature* **2011**, *469* (7331), 483–490.

(44) Kristiansen, J. E.; Amaral, L. The Potential Management of Resistant Infections with Non-Antibiotics. *J. Antimicrob. Chemother.* **1997**, *40* (3), 319–327.

(45) El-Nakeeb, M. A.; Abou-Shleib, H. M.; Khalil, A. M.; Omar, H. G.; El-Halfawy, O. M. In Vitro Antibacterial Activity of Some Antihistamines Belonging to Different Groups against Multi-Drug Resistant Clinical Isolates. *Brazilian J. Microbiol.* **2011**, *42*, 980–991.

(46) Mazur, I.; Wurzer, W. J.; Ehrhardt, C.; Pleschka, S.; Puthavathana, P.; Silverzahn, T.; Wolff, T.; Planz, O.; Ludwig, S. Acetylsalicylic Acid (ASA) Blocks Influenza Virus Propagation via Its NF-kB-Inhibiting Activity. *Cell Microbiol.* **2007**, *9* (7), 1683–1694.

(47) Al-Janabi, A. A. H. S. In Vitro Antibacterial Activity of Ibuprofen and Acetaminophen. *J. Glob. Infect. Dis.* **2010**, *2* (2), 105–108.

(48) Salem-Milani, A.; Balaei-Gajan, E.; Rahimi, S.; Moosavi, Z.; Abdollahi, A.; Zakeri-Milani, P.; Bolourian, M. Antibacterial Effect of Diclofenac Sodium on Enterococcus Faecalis. *J Dent* **2013**, *10* (1), 16–22.

(49) Pelosini L; Treffene S; Hollick EJ. Antibacterial Activity of Preservative-Free Topical Anesthetic Drops in Current Use in Ophthalmology Departments. *Cornea* **2009**, *28* (1), 58–61.

(50) Hendricks, O.; Butterworth, T. S.; Kristiansen, J. E. The in- v Itro Antimicrobial Effect of Non-Antibiotics and Putative Inhibitors of Efflux Pumps on Pseudomonas Aeruginosa and Staphylococcus Aureus. *Int. J. Antimicrob. Agents* **2003**, *22*, 262–264.

(51) Basco LK; Le Bras J. In Vitro Activities of Chloroquine in Combination with Chlorpromazine or Perchlorperazine against Isolates of Plasmodium Falciparum. *Antimicrob. Agents Chemother. Agents Chemother* **1992**, *36*, 209–213.

(52) Cohn, R. C.; Jacobs, M.; Aronoffl, S. C. In Vitro Activity of Amiloride Combined with Tobramycin against Pseudomonas Isolates from Patients with Cystic Fibrosis. *Antimicrob. Agents Chemother.* **1988**, *32* (3), 395–396.

(53) Andersen, C.; Holland, I.; Jacq, A. Verapamil, A Ca^{2+} Channel Inhibitor Acts as a Local Anaesthetic and Induces the Sigma E Dependent Extra-Cytoplasmic Stress Response in E. Coli. *Biochim Biophys Acta* **2006**, *1758* (10), 1587–1595.

(54) Feinberg, A. P.; Snyder, S. H. Phenothiazine Drugs: Structure-Activity Relationships Explained by a Conformation That Mimics Dopamine. *Proc. Nat. Acad. Sci.* **1975**, *72* (5), 1899–1903.

(55) Jaszczyszyn, A.; Gąsiorowski, K.; Świątek, P.; Malinka, W.; Cieślik-Boczula, K.; Petrus, J.; Czarnik-Matusewicz, B. Chemical Structure of Phenothiazines and Their Biological Activity. *Pharmacol. Reports* **2012**, *64* (1), 16–23.

(56) Jafari, S.; Fernandez-Enright, F.; Huang, X. F. Structural Contributions of Antipsychotic Drugs to Their Therapeutic Profiles and Metabolic Side Effects. *J. Neurochem.* **2012**, *120* (3), 371–384.

(57) Seeman, P. Dopamine D2 Receptors as Treatment Targets in Schizophrenia. *Clin. Schizophr. Relat. Psychoses* **2010**, *4* (1), 56–73.

(58) Sudeshna, G.; Parimal, K. Multiple Non-Psychiatric Effects of Phenothiazines: A Review. *Eur. J. Pharmacol.* **2010**, *648* (1-3), 6–14.

(59) Van Soolingen, D.; Hernandez-Pando, R.; Orozco, H.; Aguilar, D.; Magis-Escurra, C.; Amaral, L.; Van Ingen, J.; Boeree, M. J. The Antipsychotic Thioridazine Shows Promising Therapeutic Activity in a Mouse Model of Multidrug-Resistant Tuberculosis. *PLoS One* **2010**, *5* (9), 1–6.

(60) Alsaad, N.; Wilffert, B.; van Altena, R.; de Lange, W. C. M.; van der Werf, T. S.; Kosterink, J. G. W.; Alffenaar, J.-W. C. Potential Antimicrobial Agents for the Treatment of Multidrug-Resistant Tuberculosis. *Eur. Respir. J.* **2014**, *43* (3), 884–897.

(61) Amaral, L.; Boeree, M.; Gillespie, S.; Udwadia, Z.; van Soolingen, D. Thioridazine Cures Extensively Drug-Resistant Tuberculosis (XDR-TB) and the Need for Global Trials Is Now! *Int. J. Antimicrob. Agents* **2010**, *35* (6), 524–526.

(62) Udwadia, Z. F.; Sen, T.; Pinto, L. M. Safety and Efficacy of Thioridazine as Salvage Therapy in Indian Patients with XDR-TB. *Recent Pat Antiinfect Drug Discov* **2011**, *6*, 88–91.

(63) Lo Presti, M. S.; Bazán, P. C.; Strauss, M.; Báez, A. L.; Rivarola, H. W.; Paglini-Oliva, P. a. Trypanothione Reductase Inhibitors: Overview of the Action of Thioridazine in Different Stages of Chagas Disease. *Acta Trop.* **2015**, *145*, 79–87.

(64) Yin T; He S; Shen G; Ye T; Guo F; Wang Y. Dopamine Receptor Antagonist Thioridazine Inhibits Tumor Growth in a Murine Breast Cancer Model. *Mol. Med. Rep.* **2015**, *12* (3), 4103–4108.

(65) Dutta P; Pinto J; Rivlin R. Antimalarial Properties of Imipramine and Amitriptyline. *J Protozool* **1990**, *37* (1), 54–58.

(66) Jeon, S.; Kim, S.; Kim, Y.; Kim, Y.; Lim, Y.; Lee, Y.; Shin, S. The Tricyclic Antidepressant Imipramine Induces Autophagic Cell Death in U-87MG Glioma Cells. *Biochem Biophys Res Commun* **2011**, *413* (2), 311–317.

(67) Godbole, A. A.; Ahmed, W.; Bhat, R. S.; Bradley, E. K.; Ekins, S.; Nagaraja, V. Targeting Mycobacterium Tuberculosis Topoisomerase I by Small-Molecule Inhibitors. *Antimicrob. Agents Chemother.* **2015**, *59* (3), 1549–1547.

(68) He, C.-X.; Meng, H.; Zhang, X.; Cui, H.-Q.; Yin, D.-L. Synthesis and Bioevaluation of Phenothiazine Derivatives as New Antituberculosis Agents. *Chinese Chem. Lett.* **2015**, *26* (08), 951–954.

(69) Addla, D.; Jallapally, A.; Gurram, D.; Yogeeswari, P.; Sriram, D.; Kantevari, S. Rational Design, Synthesis and Antitubercular Evaluation of Novel 2-(trifluoromethyl)phenothiazine[1,2,3]triazole Hybrids. *Bioorg. Med. Chem. Lett.* **2014**, *24* (1), 233–236.

(70) Sharma, R.; Samadhiya, P.; Srivastava, S. D.; Srivastava, S. K. Synthesis and Pharmaceutical Importance of 2-Azetidinone Derivatives of Phenothiazine. *J. Chem. Sci.* **2012**, *124* (3), 633–637.

(71) Bate, A. B.; Kalin, J. H.; Fooksman, E. M.; Amorose, E. L.; Price, C. M.; Williams, H. M.; Rodig, M. J.; Mitchell, M. O.; Cho, S. H.; Wang, Y.; Franzblau, S. G. Synthesis and Antitubercular Activity of Quaternized Promazine and Promethazine Derivatives. *Bioorg. Med. Chem. Lett.* **2007**, *17* (5), 1346–1348.

(72) Madrid, P. B.; Polgar, W. E.; Tanga, M. J. Synthesis and Antitubercular Activity of Phenothiazines with Reduced Binding to Dopamine and Serotonin Receptors. *Bioorg. Med. Chem. Lett.* **2007**, *17*, 3014–3017.

(73) Salie, S.; Hsu, N.; Semenya, D.; Jardine, A.; Jacobs, M. Novel Non-Neuroleptic Phenothiazines Inhibit Mycobacterium Tuberculosis Replication. *J. Antimicrob. Chemother.* **2014**, *69* (6), 1551–1558.

(74) Dunn, E. A.; Roxburgh, M.; Larsen, L.; Smith, R. A. J.; McLellan, A. D.; Heikal, A.; Murphy, M. P.; Cook, G. M. Incorporation of Triphenylphosphonium Functionality Improves the Inhibitory Properties of Phenothiazine Derivatives in Mycobacterium Tuberculosis. *Bioorg. Med. Chem.* **2014**, *22* (19), 5320–5328.

(75) Sarmiento, G. P.; Vitale, R. G.; Afeltra, J.; Moltrasio, G. Y.; Moglioni, A. G. Synthesis and Antifungal Activity of Some Substituted Phenothiazines and Related Compounds. *Eur. J. Med. Chem.* **2011**, *46* (1), 101–105.

(76) Khan, M.; Austin, S.; Chan, C.; Yin, H.; Marks, D.; Vaghjiani, S.; Kendrick, H.; Yardley, V.; Croft, S.; Douglas, K. Use of an Additional Hydrophobic Binding Site, the Z Site, in the Rational Drug Design of a New Class of Stronger Trypanothione Reductase Inhibitor, Quaternary Alkylammonium Phenothiazines. *J. Med. Chem.* **2000**, *43*, 3148–3156.

(77) Dominquez, J.; Lopez, S.; Charris, J.; Iarruso, L.; Lobo, G.; Semenov, A.; Olson, J.; Rosenthal, P. Synthesis and Antimalarial Effects of Phenothiazine Inhibitors of a Plasmodium Falciparum Cysteine Protease. *J. Med. Chem.* **1997**, *40*, 2726–2732.

(78) Abuhaie, C.-M.; Bîcu, E.; Rigo, B.; Gautret, P.; Belei, D.; Farce, A.; Dubois, J.; Ghinet, A. Synthesis and Anticancer Activity of Analogues of Phenstatin , with a Phenothiazine A-Ring , as a New Class of Microtubule-Targeting Agents. *Bioorg. Med. Chem. Lett.* **2013**, *23* (1), 147–152.

(79) Belei, D.; Dumea, C.; Samson, A.; Farce, A.; Dubois, J.; Bîcu, E.; Ghinet, A. New Farnesyltransferase Inhibitors in the Phenothiazine Series. *Bioorganic Med. Chem. Lett.* **2012**, *22* (14), 4517–4522.

(80) Kastrinsky, D. B.; Sangodkar, J.; Zawarea, N.; Izadmehr, S.; Dhawanb, N. S.; Goutham, N.; Ohlmeyer, M. Reengineered Tricyclic Anti-Cancer Agents. *Bioorg. Med. Chem.* **2015**, *23* (19), 6528–6534.

(81) Baciu-Atudosie, L.; Ghinet, A.; Farce, A.; Dubois, J.; Belei, D.; Bîcu, E. Synthesis and Biological Evaluation of New Phenothiazine Derivatives Bearing a Pyrazole Unit as Protein Farnesyltransferase Inhibitors. *Bioorg. Med. Chem. Lett.* **2012**, *22* (22), 6896–6902.

(82) Weinstein, E. A.; Yano, T.; Li, L.; Avarbock, D.; Avarbock, A.; Helm, D.; Mccolm, A. A.; Duncan, K.; Lonsdale, J. T.; Rubin, H. Inhibitors of Type II NADH : Menaquinone Oxidoreductase Represent a Class of Antitubercular Drugs. **2005**.

(83) Teh, J. S.; Yano, T.; Rubin, H. Type II NADH: Menaquinone Oxidoreductase of Mycobacterium Tuberculosis. *Infect. Disord. Drug Targets* **2007**, *7* (2), 169–181.

(84) Warman, A. J.; Rito, T. S.; Fisher, N. E.; Moss, D. M.; Berry, N. G.; O'Neill, P. M.; Ward, S. A.; Biagini, G. A. Antitubercular Pharmacodynamics of Phenothiazines. *J. Antimicrob. Chemother.* **2013**, *68* (4), 869–880.

(85) Amaral, L.; Viveiros, M.; Molnar, J. Antimicrobial Activity of Phenothiazines. *In Vivo.* **2004**, *18*, 725–731.

(86) Kaatz, G. W.; Moudgal, V. V; Seo, S. M.; Kristiansen, E.; Kristiansen, J. E. Phenothiazines and Thioxanthenes Inhibit Multidrug Efflux Pump Activity in Staphylococcus Aureus. *Antimicrob. Agents Chemother.* **2003**, *47* (2), 719–726.

(87) Cheng, H.; Liang, Y.; Kuo, Y.; Chuu, C.; Lin, C.; Lee, M.; Wu, A. T. H.; Yeh, C.; Chen, E.; Su, C. Identification of Thioridazine , an Antipsychotic Drug , as an Antiglioblastoma and Anticancer Stem Cell Agent Using Public Gene Expression Data. *Cell Death Dis.* **2015**, *6*, 1–13.

(88) Field, S. K.; Fisher, D.; Jarand, J. M.; Cowie, R. L. New Treatment Options for Multidrug-Resistant Tuberculosis. *Ther. Adv. Respir. Dis.* **2012**, *6* (5), 255–268.

Chapter 2

Drug remodelling of neuroleptics and incorporation of *in silico* techniques for drug-likeness assessment

Preface

Implementation of innovative drug discovery strategies is a global priority for rejuvenation of shrinking pharmaceutical drug pipelines. The evolution of antimicrobials from non-antibiotics was reviewed in great detail in chapter 1. Drug repurposing is considered an appealing strategy in drug discovery thus exploiting clinically approved drugs for their validated pharmacokinetic and toxicological profiles. Second best to drug repurposing, drug remodelling is useful for creating New Chemical Entities (NCEs) with novel functionalities. Moreover, neuroleptic drugs were introduced as the non-antibiotics of interest for structural remodelling.

In this chapter, the structural background of neuroleptic drugs including the minimum structural requirements for their neuroleptic activity is under review. The understanding of pharmacokinetics of drugs including ADMET (A: Absorption; D: Distribution; M: Metabolism: E: Excretion and T: Toxicity) is crucial in drug discovery and development, a discussion is provided herein. Also, herein, the rationale behind this research study as well as specific aims and objectives are outlined. Furthermore, a discussion of the rationally selected strategies for remodelling central nervous system (CNS) drugs for non-neuroleptic bio-activities is provided. Lastly, the integration of *in silico* prediction tools in the remodelling for assessing drug-likeness of the NCEs is described. This includes prediction of CNS activity to generate NCEs that are less likely to exhibit neuroleptic effects.

2.1 The chemistry background of neuroleptics

Structural diversity of neuroleptics brings about their wide spectrum of neuropharmacological properties and various therapeutic effects. Neuroleptic drugs exert their neuroleptic action by a blockade of CNS receptors including dopaminergic (D_{1-5}), serotonergic (5-HT), muscarinic (M_{1-5}), adrenergic (α_{1-2}) and histamine (H_{1-4}) receptors.[1,2]

These drugs are generally categorized into two major classes i.e. first generation and second generation agents. The former is commonly referred to as 'typical' antipsychotics and the latter as 'atypical' antipsychotics. The distinction between the two classes is primarily based on their likelihood to produce undesirable extrapyramidal side effects. Atypical antipsychotics are known to produce a minimal of these effects at clinically effective doses.[1]

The two main classes consist of various heterocycles including tricyclic and tetracyclic ring systems such as phenothiazines, butyrophenones, thioxanthenes and dibenzodiazepines. Binding affinity for CNS receptors varies depending on the nature of these heterocyclic drugs.[1,3,4] Examples of clinically approved typical and atypical antipsychotic drugs, their chemical classification along with the types of CNS receptors they inhibit have been tabulated (Table 2.1).

Table 2.1: Chemical classification of typical and atypical antipsychotics and examples of CNS receptor subtypes exhibiting strong binding affinity. (Neurotransmitter: NT; Receptor subtype: RS)

Typical antipsychotics			**Atypical antipsychotics**	
Phenothiazines			***Dibenzodiazepine***	***Thienobenzodiazepine***
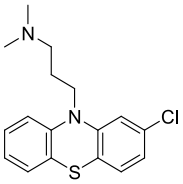	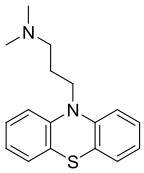	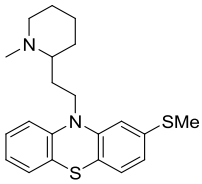	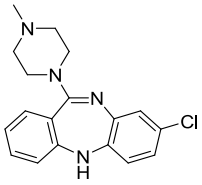	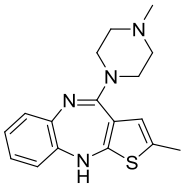
Chlorpromazine	Promazine	Thioridazine	Clozapine	Olanzepine
NT / **RS**			**NT** / **RS**	**NT** / **RS**
Dopamine / D_2, D_1, D_3			**Acetylcholine** / M_1	**Acetylcholine** / M_1
Serotonin / $5\text{-}HT_{2A}$, $5\text{-}HT_{2C}$			**Adrenaline** / α_1	**Histamine** / H_1
Adrenaline / α_1			**Histamine** / H_1	**Serotonin** / $5\text{-}HT_{2A}$
Histamine / H_1			**Serotonin** / $5\text{-}HT_{2C}$	
Butyrophenones			***Dibenzothiazepine***	***Benzisoxazole***
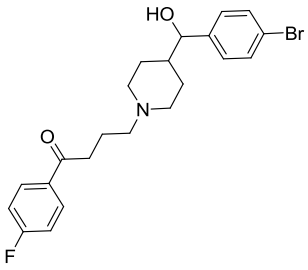	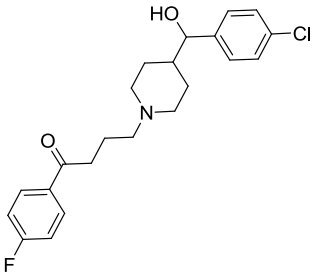		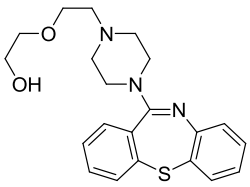	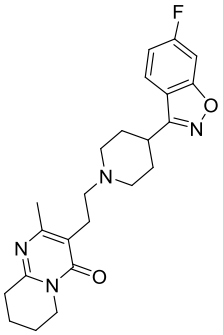
Bromperidol	Haloperidol		Quetiapine	Risperidone
NT / **RS**			**NT** / **RS**	**NT** / **RS**
Dopamine / D_2			**Histamine** / H_1	**Adrenaline** / α_1
Adrenaline / α_1			**Adrenaline** / α_1	**Serotonin** / $5\text{-}HT_{2A}$
Serotonin / $5\text{-}HT_{2A}$				**Dopamine** / D_2
Thioxanthenes			***Indole***	
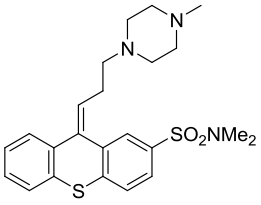	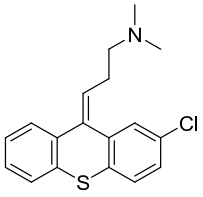		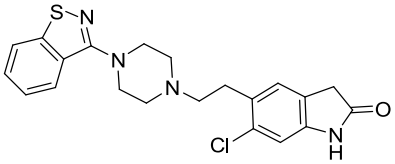	
Thiothixene	Chlorprothixene		Ziprasidone	
NT / **RS**			**NT** / **RS**	
Dopamine / D_2			**Serotonin** / $5\text{-}HT_{2A}$, $5\text{-}HT_{2C}$	
Histamine / H_1			**Dopamine** / D_2	
Adrenaline / α_1			**Adrenaline** / α_1	

2.1.1 Historical background

Psychiatric application of neuroleptic drugs in management of psychotic disorders spans over many decades. Neuroleptic drugs, phenothiazines in particular, structurally evolved from methylene blue. Chlorpromazine was first prepared by a French chemist, Paul Charpentier, in 1951 and became available as a prescription drug around 1952 in France.[1,5] The psychotherapeutic use of chlorpromazine was deemed a significant breakthrough in neuropsycopharmacology. Shortly thereafter, other structurally related antipsychotics were introduced between 1953 and 1960. Thioridazine with milder side effects was introduced in 1959.[6]

In 1971, clozapine, the first atypical antipsychotic was marketed in Europe. The discovery of structurally similar atypical drugs such as olanzapine followed a few years later.[1,7] By the early 2000s, drugs such as ziprasidone and risperidone were introduced as psychotropics. The low risk of extrapyramidal effects development associated with these tetracyclic atypical antipsychotics is reportedly due to their unique chemical structures.[5,8,9,10] A simplified timeline of clinically approved antipsychotic therapeutics is shown in Figure 2.1.

As discussed in chapter 1, phenothiazines have attracted notable research interest not only in neuropsychology but also for other indications.[1,2,11,12] Therefore, the privileged phenothiazine scaffold and scaffolds of related neuroleptics are of interest to this research study partly for their potential as a novel class of therapeutics in various non-neuroleptic indications.

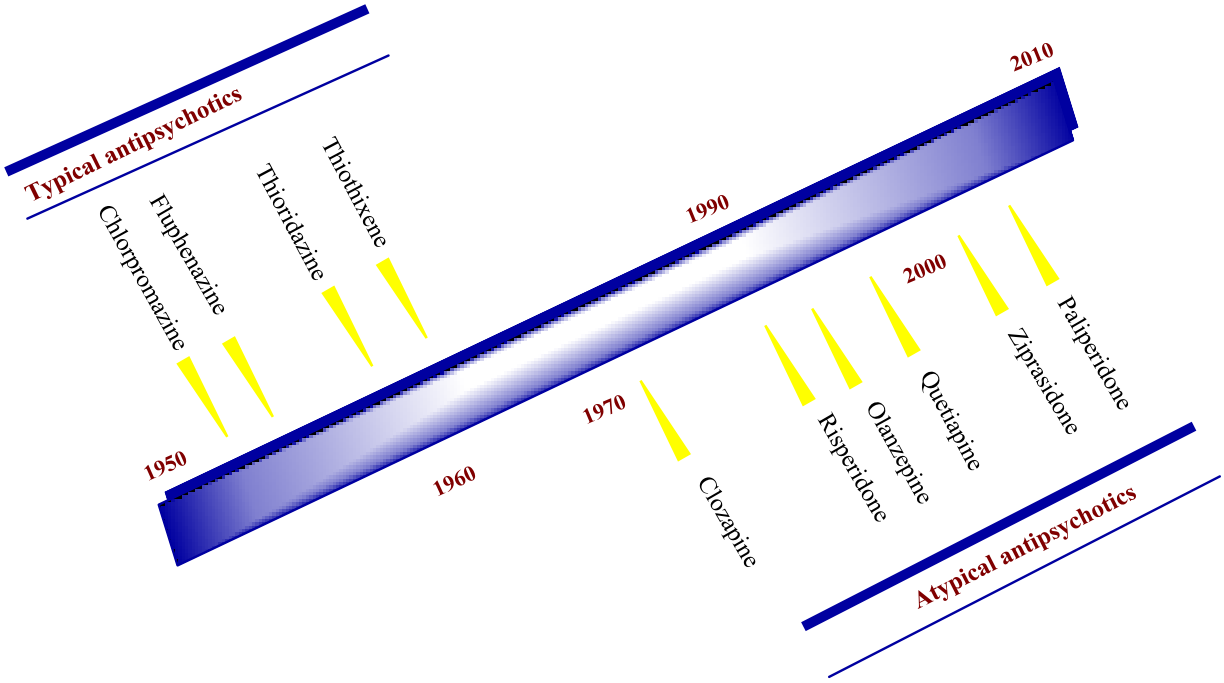

Figure 2.1: A timeline of antipsychotic therapeutics since the early 1950s**.**

2.1.2 General structures of phenothiazines and related drugs

Various classes of antipsychotic drugs obey a lipophilic chromophore/basic side chain paradigm including phenothiazines as exemplified in Figure 2.2. The first preparation of a phenothiazine chromophore was achieved by August Bernthsen in 1883 *via* fusion of diphenylamine with sulfur to afford 10*H*-dibenzo-1,4-thiazine.[11,13]

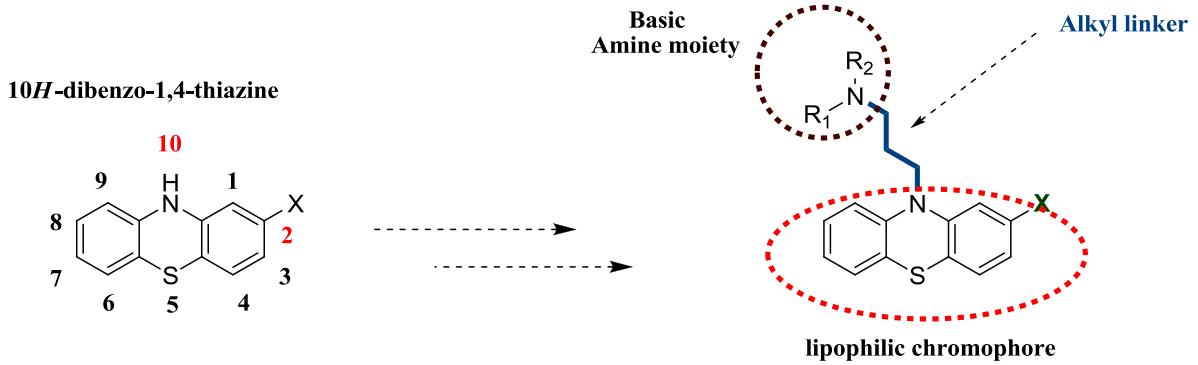

Figure 2.2: The phenothiazine chromophore showing the adopted nomenclature (left) and the general structure of phenothiazine drugs illustrating the lipophilic chromophore/basic side chain paradigm (right).

The tricyclic phenothiazine chromophore is related to the thiazine class of heterocycles. Derivatization of the phenothiazine scaffold mostly occurs by substitution at the thiazine nitrogen and /or 2nd position of the tricyclic ring system. Derivatives formed by substitution at the thiazine nitrogen are referred to as 10-*H* derivatives.[2,11] Phenothiazine drugs currently in clinical use for treatment of psychosis are classified according to the type of terminal nitrogen moiety. The subgroups of these drugs include (i) aliphatics (bearing acyclic moieties); (ii) piperidines (bearing piperidine-derived moieties) and (iii) piperazines (bearing piperazine-derived moieties) as shown in Figure 2.3.[1,2,11]

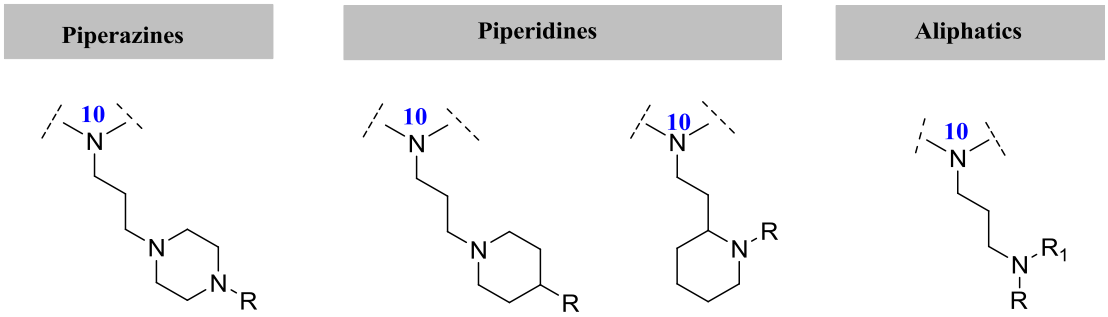

Figure 2.3: Alkylaminoalkyl structure moieties for determining classes of phenothiazine drugs.

Literature reports rank the intensity of their neuroleptic action based on the nature of the terminal amine moiety. The ranking (in decreasing order) is as follows: piperazine > piperidine > aliphatic. Other structural features essential for their neuroleptic action is nature of substitution at C-2 and length of alkyl chain linking thiazine and distal nitrogens. Electron-withdrawing substituents at C-2 are known to intensify neuroleptic action as follows: -SO_2NR_2 > -CF_3 > -$COCH_3$ > -Cl.[2,14] A full account of structural traits associated with their neuroleptic activity is provided below.

2.2 Structural traits and physicochemical properties for neuroleptic action

2.2.1 Conformational resemblance to dopamine

The three-dimensional configuration of phenothiazines and other structurally related drugs closely resembles that of dopamine, hence their strong affinity for CNS dopaminergic receptors (Figure 2.4).[2,15]

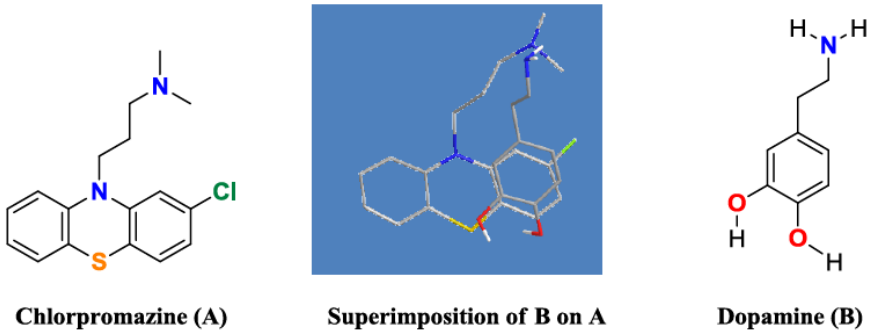

Chlorpromazine (A) **Superimposition of B on A** **Dopamine (B)**

Figure 2.4: An illustration of the resemblance between chlorpromazine (A) and dopamine (B); Superimposition of B on part of A, 3-D structure obtained using ChemBio3D Ultra version 11.0**.**

In 1975, Feinberg *et al.* conducted computational modelling studies to investigate the role of phenothiazine chemical structures in their interaction with dopaminergic receptors. In their findings, the nature of substituents at position-2 of the chromophore and the type of alkylamino side chain were determinants of binding affinity for dopaminergic receptors. This was attributed to the favourable Van der Waals interactions between the side chain (Ring A) and position-2 substituents as illustrated in Figure 2.5.[15]

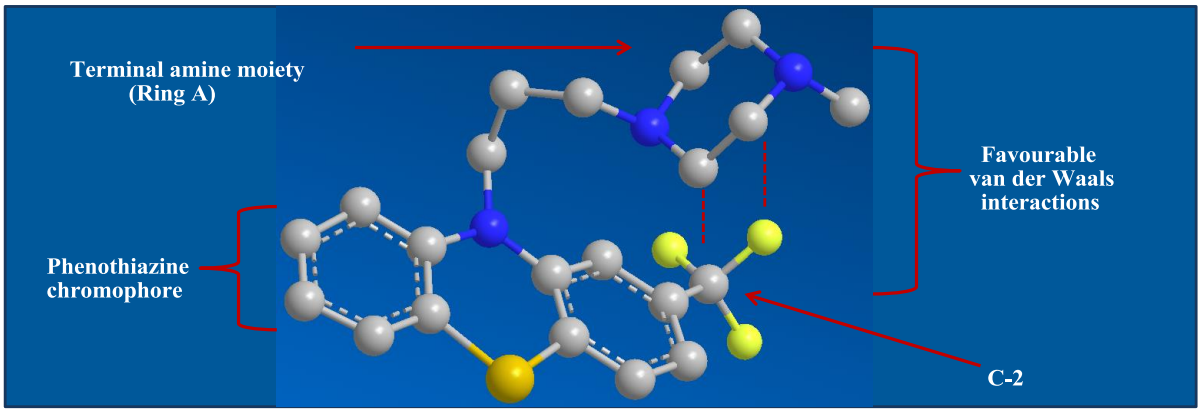

Figure 2.5: An energy-minimized conformation of trifluoperazine to illustrate the adopted dopamine-like configuration owing to Van der Waals forces (ChemBio3D Ultra version 11.0.). Alkylamino side chain tilts towards C-2 substituent promoting a dopamine-like configuration.

2.2.2 Higher degree of lipophilicity: Facilitates BBB penetration

Permeation of the blood-brain barrier (BBB) is a prerequisite for CNS-active agents. A restrictive layer of endothelial cells with tight junctions constitutes the BBB. The protective barrier prevents passive diffusion of molecules from the blood stream into the CNS, particularly those greater than 20 Å in diameter.[16,17,18] CNS drugs possess characteristic physicochemical parameters owing to the selectivity of the BBB membrane. Lipid solubility is amongst others a crucial property of CNS drugs and is known to facilitate diffusion across the BBB. In contrast, highly polar molecules with a topological surface area (TPSA) greater than 90 $Å^2$ are likely to be prohibited from crossing the BBB.[19,20,21]

2.2.3 Ionizability: Protonation of the distal amine moiety

Phenothiazines are known to be amphiphilic in nature.[2] In conjunction with a lipophilic chromophore, the majority of these drugs possess a basic alkylamino side chain.[1,2,11] Apart from their lipophilic nature, the presence of a proton accepting amine species is known to

favor penetration of the BBB. It is also known that at physiological pH, the distal amine moiety of these drugs acquires a positive charge.[2,11,22] The strength of acidity and basicity is a crucial pK_a determinant of diffusion across the BBB. Strongly acidic species (pK_a < 4) and strongly basic species (pK_a > 10) are prohibited from penetrating the barrier.[19,23]

2.3 Overview of remodelling strategies reported in literature

Seemingly trivial structural transformations such as substitution at position-2 of the ring have shown strong correlations to potency of these drugs. Numerous libraries of phenothiazine derivatives and related structures are documented in literature for biological activity or non-biological applications.[2,11,19] The tricyclic chromophore has several sites of possible modifications, hence the large number of structural diversifications reported.[2,11,22,24]

Structural modifications reported in literature include substitution around the tricyclic ring system, introduction of cyclic and non-cyclic alkyl side chains, increase in steric volume *via* dimerization or linkage to other heterocycles, introduction of heteroatoms into the ring system, oxidation of the thiazine sulfur, ring expansions and many more.[11] In most cases structural modifications of these drugs are carried out to find potential drug candidates for other indications.[25,26,27,28,29]

Apart from understanding the minimum structural requirements for neuroleptic action of phenothiazines and related drugs, it is also important to understand drug metabolism and pharmacokinetics (DMPK) properties including ADMET properties that are associated with drug development, a discussion is provided below.

2.4 Significance of early ADMET evaluation

Prior to the early 2000s, poor DMPK profiles were primary contributors to attrition in late-stage drug development. Apart from poor pharmacokinetics, other factors such as toxicity, adverse effects and lack of efficacy largely contributed to failures of many drug candidates.[30,31] It has therefore become routine for the aforementioned properties to be determined early in the drug development process.[30,32,33]

2.4.1 Overview of DMPK including ADMET

In simple terms, pharmacokinetics is usually referred to as 'what the body does to the drug' as opposed to pharmacodynamics which is 'what the drug does to the body'. Pharmacokinetics is the investigation of the time course of a drug within the body post-administration and thus incorporates ADME processes. Pharmacodynamics involves the relationship between concentration of a drug and the effects elicited at the site of action including mechanisms of its action.[30,34] ADME encapsulates the processes involved in the fate of a drug within the body thus affects various parameters including the percentage of drug concentration that reaches the systemic circulation i.e. bioavailability.[30]

An orally-administered drug (non-intravenous administration) could either get excreted from the body without any biotransformation or could get absorbed through the gut wall followed by transportation to the liver. Many drug molecules transverse biological membranes by passive diffusion or as substrates of transporter proteins.[35] Transporters could either promote or hinder permeability of molecules across membranes. Proteins such as P-glycoprotein and cytochrome P450 3A4 are known to serve as a barrier to absorption of drugs from the

gastrointestinal tract.[30] The drug that is absorbed through the gut wall is transported to the liver *via* the hepatic portal vein. From the liver, the drug reaches the systemic circulation followed by distribution to various organs, tissues including its biomolecular target.[36]

Elimination of foreign molecules (xenobiotics) including drug molecules primarily occurs *via* metabolism. Biotransformation of drugs to respective metabolites could occur before the drug reaches the systemic circulation. This happens primarily in the liver and/or sometimes in the gut wall and is referred to as first-pass metabolism.[30] Metabolism is traditionally categorized into two phases i.e. phase I metabolism and phase II metabolism. The former involves functionalization of a drug molecule *via* redox reactions or hydrolysis whereby enzyme classes such as cytochrome P450s (CYP450s) play a crucial role.[37] The latter involves further transformation of the functionalized molecule, although not necessarily sequential, *via* processes such as conjugation with glutathione or glucuronidation.[30,38]

2.4.2 Evaluation of properties associated with ADMET

As alluded to earlier, determination of ADMET *via in silico* predictions and subsequently *in vitro* or *in vivo* approaches is crucial at very early stages of drug development. *In silico* approaches are advantageous in that a virtual library of compounds is required hence less time-consuming and more cost-effective. Reliable ADMET predictive models may provide useful information prior to synthesis and subsequent *in vitro* and *in vivo* evaluation.

2.4.3 *In vitro* and *in vivo* ADMET

Various *in vitro* and *in vivo* models are utilized as standardised procedures for early hit-to-lead optimization.[30,32] Liver microsomal stability and whole hepatocyte models are the most

common studies carried out for *in vitro* metabolism.[39] The models involve major metabolic enzymes including CYP450 (Phase I metabolism) as well as UDP-glucuronosyltransferase (phase II metabolism).[32,38] For evaluation of cell permeability, key *in vitro* assays include Caco-2 or MDCK cell-based models.[30,38,40] Studying the aforementioned factors including others such solubility helps in decision-making and selection of compounds with desirable pharmacokinetic properties for further *in vivo* studies.

In vivo pharmacokinetics studies (either using mice or other non-human primates) provide information on factors such as drug clearance, volume of distribution, bioavailability and half-life.[30,40] Most DMPK/ADMET-related assays are conducted using automated technology platforms in combination with high-throughput liquid chromatography-mass spectrometry (LC/MS/MS).[38]

Another aspect of early evaluation of DMPK/ADMET properties includes drug metabolite identification and profiling.[32,41] This provides a better understanding as to whether the toxicity of a drug candidate is a result of exposure to the parent drug or toxic metabolites.[38] Additionally, other safety-related studies include human Ether-á-go-go-Related Gene (hERG) inhibition for prediction of cardiotoxicity.[32,42]

2.4.4 *In silico* prediction of ADMET and associated physicochemical properties

In silico prediction tools use molecular descriptors derived from 3D molecular interaction fields as inputs to build mathematical/ statistical models.[17] The predictive capacity and reliability of such models vary based on various factors such as molecular descriptor inputs

used in building the models, the chemical space/ diversity covered by set of compounds used to train models as well as data quality of the training set of compounds.[20,21]

In general, *in silico* predictions are associated with a number of limitations. *In silico* ADMET prediction is limited by complexities arising from participating organs and multiple biological processes that occur *in vivo.* Therefore, *in silico* predicted results are merely guidelines and are not over-interpreted. Furthermore, where possible the results are usually corroborated by *in vitro* and *in vivo* ADMET evaluations.

2.4.5 Physicochemical parameters associated with ADMET

Various physicochemical properties affect ADMET processes and their determination either experimentally or *in silico* is of utmost importance (Table 2.2). Drug-likeness can be predicted *in silico* on the basis of rules such as Lipinski's rule of five (RO5) and this aids in filtering out compounds with poor physical properties (Table 2.2).[21] Over the years, RO5 has been amended to include other properties such as polar surface area and rotatable bonds. Similar to RO5, the rule of three has also been introduced to describe compounds with lead-like properties.[43] RO5 remains popular even though it has limitations. Its simplicity allows easy prediction of drug-like properties associated with orally-administered drugs.[21]

Table 2.2: Physicochemical parameters that affect ADME processes [21,30]

	Description	Association with ADME and related processes	Lipinski's rule of five (RO5)
Lipophilicity	Affinity of drug for a lipophilic environment; Expressed as logP or clogP or logD. P is the partition coefficient between lipophilic and aqueous environments, for example octanol/water system. D is the distribution coefficient at pH 7.4 and 6.5 (more relevant for ionizable drugs).	**Affects dissolution rate and permeability, hence absorption and bioavailability.**	logP or clogP ≤ **5** and ≥ **0**
Molecular weight (MW)	Mass per one mole of a substance.	**Linked to ability of a drug to cross membranes e.g. blood-brain barrier.**	MW ≤ **500 g/mol**
Hydrogen bonding (HB)	Takes into account the number of hydrogen bond donors (HBD) and acceptors (HBA). Involves the interaction of a drug molecule with its aqueous environment.	**Strong HB linked to low permeability and absorption.**	HBD ≤ **5** HBA ≤ **10**
Solubility	A drug has to dissolve in an aqueous environment e.g. gastrointestinal tract contents or blood plasma prior to absorption. In case of ionizable molecules, solubility is affected by the pH of the aqueous environment.	**Poor solubility is detrimental to absorption.**	
Permeability	Ability to cross lipid bilayers of biological membranes.	**Affects absorption and bioavailability.**	

2.5. Research Aims and Objectives

Apart from clinical application of phenothiazines in psychiatry, their diverse range of antimicrobial and other non-neuroleptic properties has been extensively investigated (Chapter 1). However at clinically effective doses, they elicit adverse side effects including extrapyramidal symptoms, in addition to their neuroleptic effects. Therefore, their extensive application in other indications is limited. In full knowledge of the minimum structural requirements for their neuroleptic action, it was postulated that the selectivity of phenothiazines and related neuroleptics for other indications could be improved through rationalized structural remodelling.

2.5.1 Overall objective

The overall objective of this study is to structurally remodel neuroleptic phenothiazines and related drugs such that their inherent neuroleptic effects are abrogated whilst their antitubercular or anticancer properties are retained.

2.5.2 Specific aims and objectives

(i) To remodel phenothiazines and related neuroleptics to generate a focused library of new chemical entities (NCEs) with reduced likelihood to exhibit neuroleptic effects.

In consideration of the minimum structural requirements of phenothiazines for neuroleptic action, remodelling strategies were rationally considered in order to generate NCEs that are less likely to exhibit neuroleptic effects. *In silico* tools will be employed to assess drug-likeness of the NCEs as well as their likelihood of exhibiting neuroleptic effects. The *in silico* predictions can be obtained using QikProp, a Schrödinger program that computes

pharmaceutically relevant properties of potential drug candidates. NCEs with promising drug-like properties would be prioritized for chemical synthesis.

(ii) To evaluate the remodelled phenothiazines as potential antitubercular agents.

Chemically synthesized remodelled phenothiazines will be evaluated against virulent *Mycobacterium tuberculosis* (M.*tb*H37Rv) by screening the library of NCEs for *in vitro* extracellular growth inhibition against M.*tb*H37Rv. Further assessment will include screening selected NCEs for their ability to inhibit intracellular M.*tb*H37Rv in bone marrow-derived macrophages, which will also be indicative of cytotoxicity.

(iii) To investigate the neuroleptic potential of the remodelled phenothiazines using experimental approaches.

To corroborate the *in silico* CNS activity predictions, selected NCEs will be screened in dopamine and serotonin receptor radioligand binding assays offered as a commercial service by Perkin Elmer (formerly Caliper Life Sciences) Maryland USA.

(iv) To elucidate the pharmacokinetic profiles of NCEs with promising antimycobacterial properties and more importantly, reduced likelihood of neuroleptic effects.

In vitro microsomal metabolic stability, kinetic solubility and *in vivo* toxicity of selected NCEs will be evaluated to corroborate *in silico* predictions.

(iv) To evaluate the remodelled phenothiazines as potential anticancer agents.

To investigate the anticancer properties of selected NCEs, they will be subjected to an MTT cell viability screen.

2.6 Strategies employed in the remodelling of phenothiazines and related drugs

Phenothiazines are among the most widely prescribed neuroleptic drugs worldwide.[44] As mentioned earlier, they exert their neuroleptic effects by blockade of various CNS receptors including dopaminergic and serotonergic receptors.[1,2] The structural traits and properties of neuroleptic drugs delineated in section 2.2 were thoroughly examined pre-remodelling. These include conformational resemblance to dopamine, high degree of lipophilicity for blood-brain barrier penetration and presence of a proton accepting distal amine moiety.

The overall rational approach taken herein was to design NCEs with novel functionalities that deviate from the minimum structural requirements for neuroleptic activity. In consideration of the significance of early ADMET evaluation discussed in section 2.4, *in silico* tools were incorporated into the remodelling process to generate NCEs with desirable drug-like properties that are less likely to exhibit neuroleptic effects.

2.6.1 Strategy 1: Replacement of the distal amine with a sulfonate functionality

2.6.1.1 Rationale behind the selected remodelling strategy

A high degree of hydrophobicity is known to facilitate diffusion across the BBB.[2] To decrease the propensity of BBB penetration, the distal amine moiety was replaced with a polar sulfonate functionality (Figure 2.6). Furthermore, the presence of a proton accepting alkylamine species is also known to favor BBB penetration as discussed earlier. Therefore, replacement with a sulfonate moiety not only results in an increase in aqueous solubility but also a change in charge from a protonated positively charged alkylamine species to a negatively charged alkylsulfonate moiety at physiological pH (Figure 2.6).

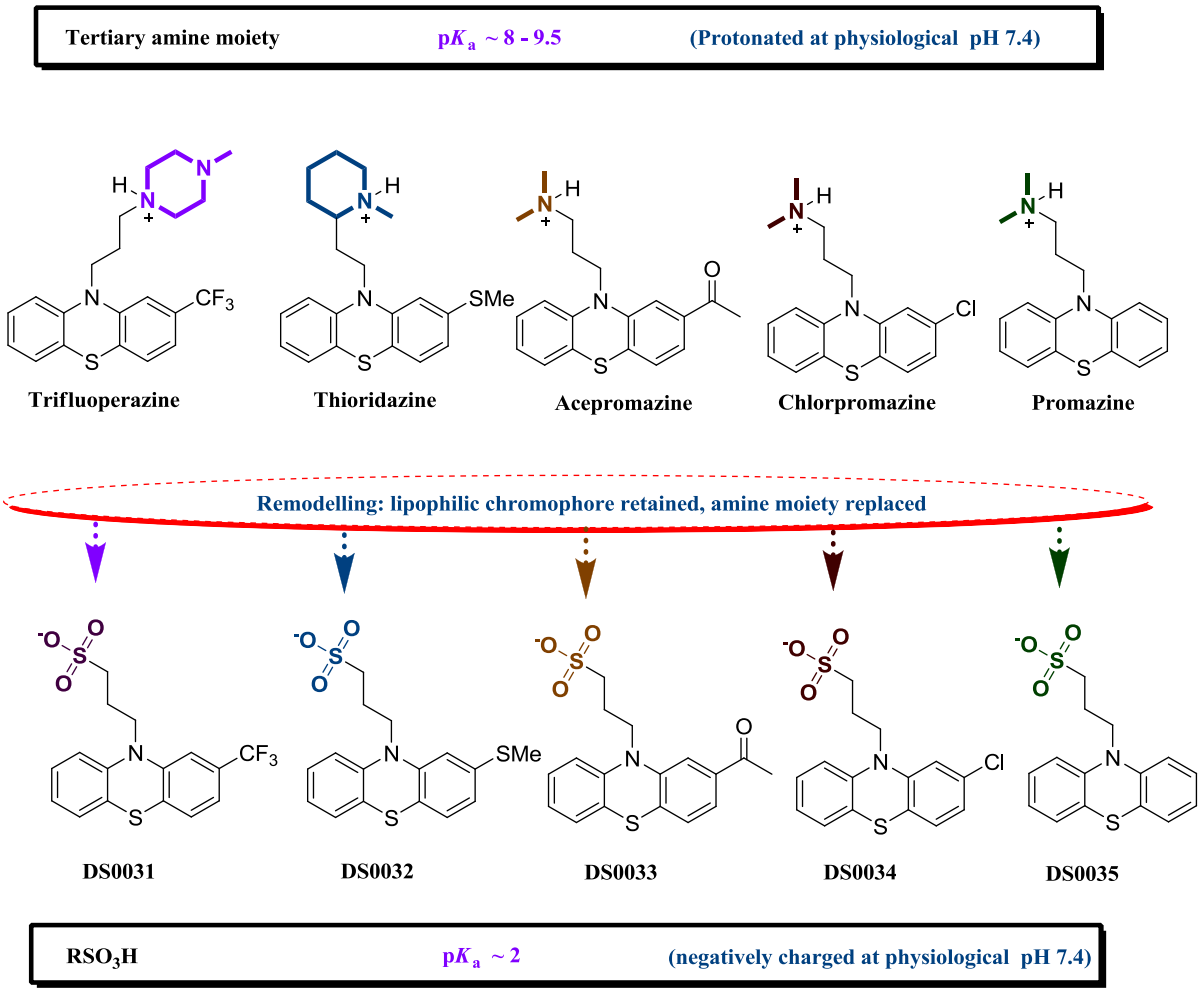

Figure 2.6: Remodelling of typical antipsychotics to form NCEs with increased aqueous solubility. It is accepted that sulfonates are negatively charged at physiological pH. Therefore, the lack of a proton accepting alkylamine species further reduces the potential of the remodelled phenothiazines (**DS0031-35)** to cross the BBB.

2.6.1.2 *N*-butylsulfonates of phenothiazines: Rationale behind alkyl linker extension

Reportedly, variation of alkyl linker length of phenothiazines affects their affinity for CNS receptors.[2,14] From a structure-activity relationship (SAR) perspective, extension of the alkyl linker of NCEs described in section 2.6.1.1 would shed some light on the effect of chain length variation on the bio-activities of interest. The phenothiazines were remodelled accordingly as shown in Figure 2.7.

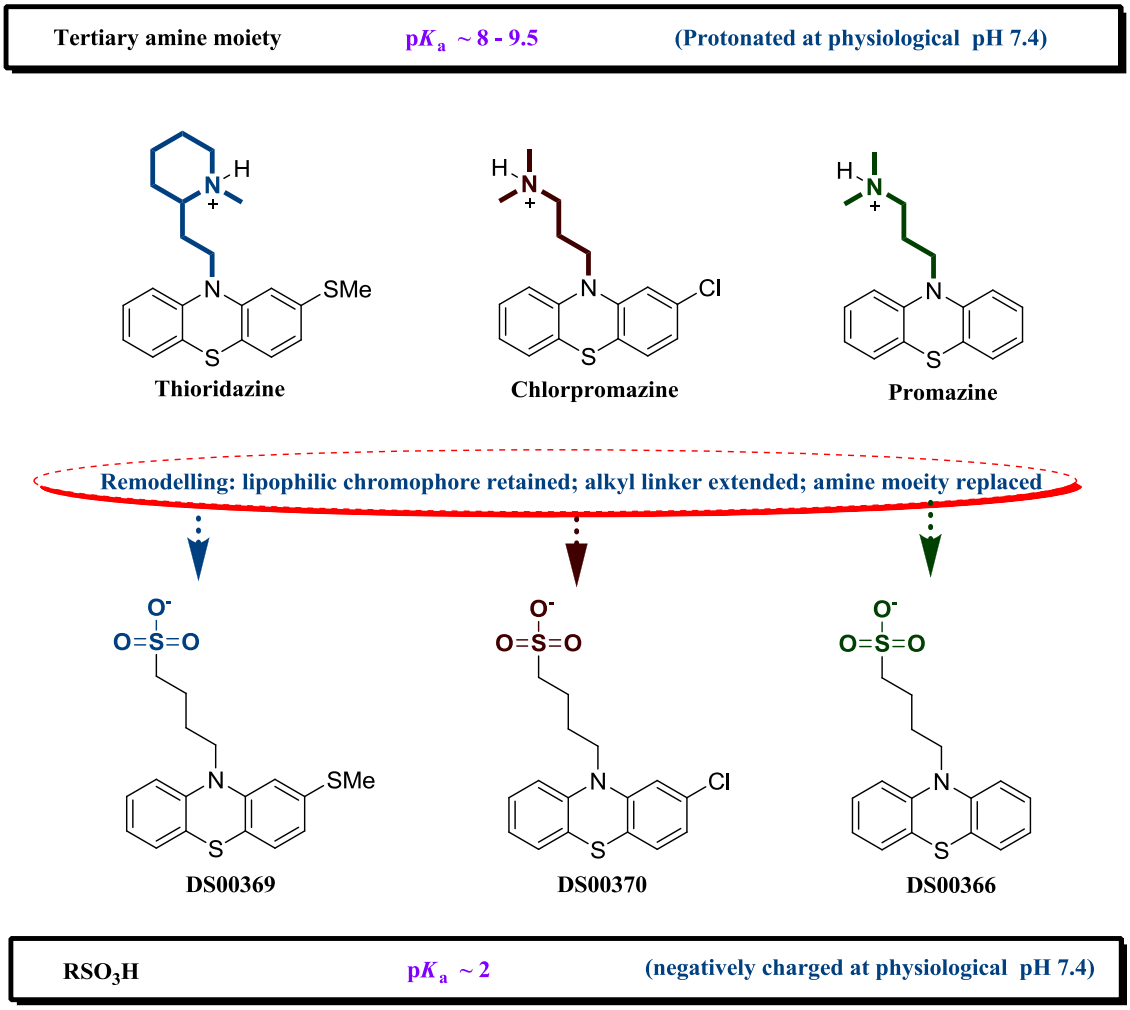

Figure 2.7: Alkyl chain extension and application of the strategy 1 delineated in section 2.6.1 to form *N*-butylsulfonates NCEs **(DS00366, DS00369** and **DS00370)**.

2.6.1.3 *N*-propylsulfonates of ring-expanded phenothiazine-like scaffolds

2.6.1.3.1 Rationale behind ring expansion

Atypical antipsychotics such as clozapine and imipramine have seven-membered rings as part of their tricyclic heteroaromatic ring system. The non-neuroleptic biological properties of the majority of these drugs have not been extensively investigated. As alluded to earlier, these atypical drugs bear structural resemblance to the phenothiazine class of antipsychotics.[1] To

broaden the scope of investigation into remodelled CNS drugs, it was decided to design NCEs that closely resemble the structures of atypical antipsychotics as depicted in Figure 2.8.

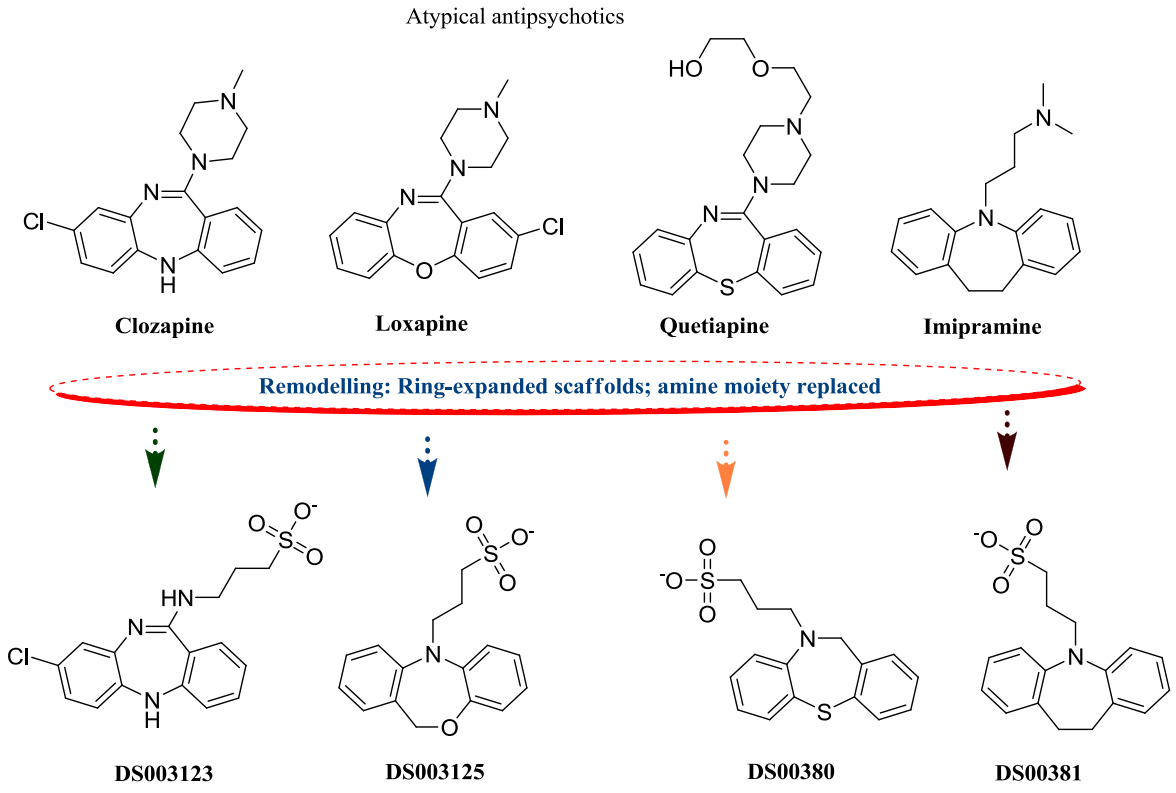

Figure 2.8: Water-soluble ring-expanded phenothiazine-like NCEs mimicking atypical antipsychotic structures. Sulfonates are expected to exist as negatively charged species at physiological pH.

2.6.1.4 Propylsulfonates of non-thiazine tricyclic scaffolds

2.6.1.4.1 Rationale behind replacement of phenothiazine central thiazine ring

In efforts to widen the scope of investigation into remodelling of phenothiazines and to determine the importance of the central thiazine ring of phenothiazines in bio-activities of interest, the central ring was replaced as depicted in Figure 2.9.

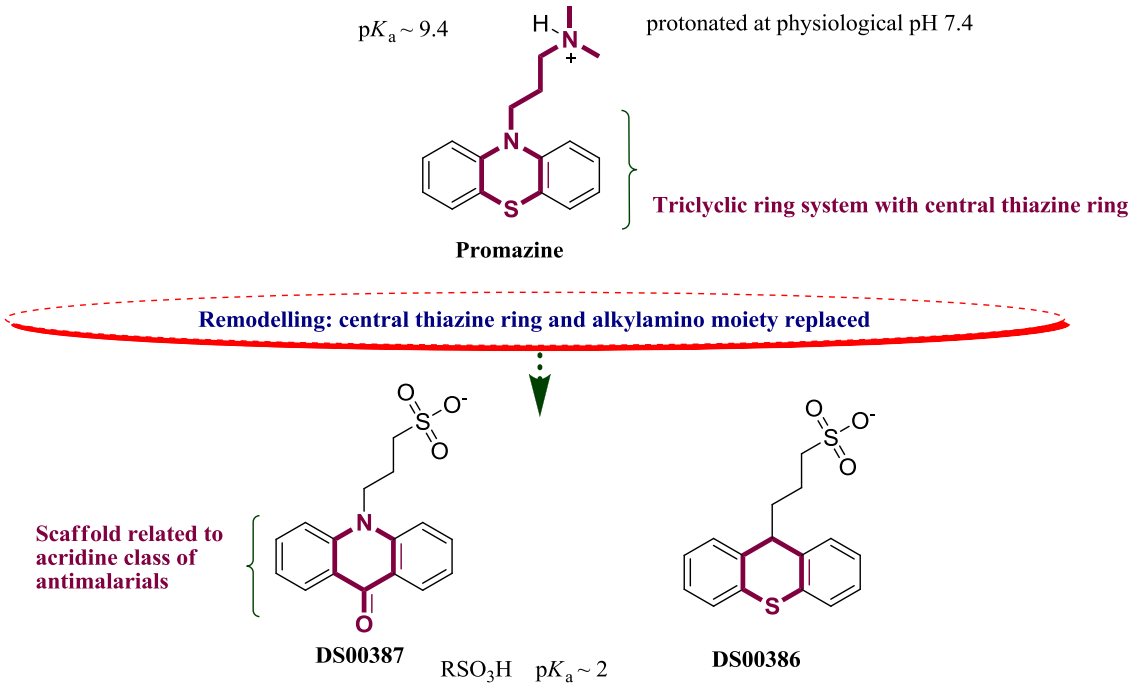

Figure 2.9: Non-thiazine scaffolds and application of remodelling strategy 1 delineated in section 2.6.1.

2.6.1.5 Prediction of physicochemical properties associated with Lipinski's rule of five

Physicochemical properties associated with Lipinski's rule of five (RO5) were predicted *in silico* to assess drug-likeness of the generated NCEs. These properties including molecular weight, lipophilicity (log P), hydrogen bond donors and acceptors affect lipid solubility and hence BBB penetration. The *in silico* predictions revealed distinctions among properties of derived NCEs and those of parent drugs. As discussed earlier, the replacement of the distal alkylamine moiety with a sulfonate functionality is expected to result in a decrease in hydrophobicity. In general, the decrease in lipophilicity was evident in the clogP values of the NCEs in comparison to parent drugs (Table 2.3). Furthermore, all the NCEs were compliant to the RO5.

Table 2.3: Prediction of molecular descriptors associated with solubility and permeation on the basis of Lipinski's rule of five (Propylsulfonates of phenothiazines and phenothiazine-like scaffolds)

NCE or **parent CNS drug**	**MW**	**clogP**	**HBD**	**HBA**
N-propylsulfonates of phenothiazines				
DS0031	389.4	4.213	1	4
Trifluoperazine	**407.5**	**4.759**	**0**	**3**
DS0032	367.5	3.772	1	4
Thioridazine	**370.6**	**5.90**	**0**	**2**
DS0033	363.5	2.592	1	5
Acepromazine	**326.4**	**4.479**	**0**	**3**
DS0034	355.9	3.556	1	4
Chlorpromazine	**318.9**	**5.291**	**0**	**2**
DS0035	321.4	2.906	1	4
Promazine	**284.4**	**4.550**	**0**	**2**
N-butylsulfonates of phenothiazines				
DS00369	381.1	4.438	1	4
DS00370	369.9	4.274	1	4
DS00366	335.4	3.754	1	4
N-propylsulfonates of ring-expanded scaffolds				
DS00381	317.4	2.573	1	4
Imipramine	**280.4**	**4.4.21**	**0**	**2**
DS003123	331.4	3.122	2	6
Clozapine	**326.8**	**3.379**	**1**	**4**
DS003125	319.4	2.193	1	5
Loxapine	**293.4**	**3.307**	**0**	**4**
DS00380	335.4	2.660	1	4
Quetiapine	**383.5**	**3.524**	**1**	**5**
Propylsulfonates of non-thiazine scaffolds				
DS00386	320.4	3.749	1	4
DS00387	317.4	2.163	1	6

Predictions obtained using StarDrop 5.5; **MW**: Molecular weight; **clogP**: log of octanol-water partition coefficient; **HBD**: Hydrogen-bond donor count (NH, NH_2 & OH groups) **HBA**: Hydrogen Bond Acceptors count (O & N atoms).

2.6.2 *In silico* prediction of blood-brain barrier penetration and ADMET properties

In addition to assessment of drug-likeness on the basis of RO5, *in silico* tools were also employed to predict properties associated with ADMET. Neuroleptic drugs have the propensity to cross the blood-brain barrier (BBB).[2] Therefore, it was important to predict BBB penetration and CNS activity so as to evaluate the likelihood of the NCEs to exhibit neuroleptic effects. Other predicted parameters include solubility, permeability (Caco-2 and MDCK cell permeability), number of metabolic reactions and hERG inhibition.

The abovementioned ADMET properties were evaluated using QikProp. QikProp is a Schödinger program that computes pharmaceutically relevant properties of potential drug candidates.[31] Contrary to properties that can be calculated directly from molecular structure (e.g. molecular weight and rotatable bonds), the prediction of more complex properties (e.g. solubility, BBB penetration, intestinal permeability and hERG inhibition) largely relies on data used in training the models. This poses a great challenge in accurately modelling such properties. Therefore, the results obtained from these models are only viewed as rough estimations to guide the remodelling. Radar plots were used for comparison of predicted properties of the generated NCEs with that of native neuroleptic drugs. Shortened NCE codes were used on all the plots for aesthetic purposes e.g. **DS0035** is the same as **DS35**.

2.6.2.1 *In silico* prediction of BBB penetration and CNS activity

CNS activity of the remodelled phenothiazines and parent neuroleptic drugs was predicted on a scale ranging from -2 (considered inactive) to +2 (considered active) using Qikprop.[31] All the remodelled phenothiazines were predicted to be inactive (values $\leq$ -1) in comparison to

parent drugs (values = +2). The radar plot of predicted blood/brain partition coefficients (QPlogBB) exhibited the same pattern as that of predicted CNS activity (Figure 2.10).

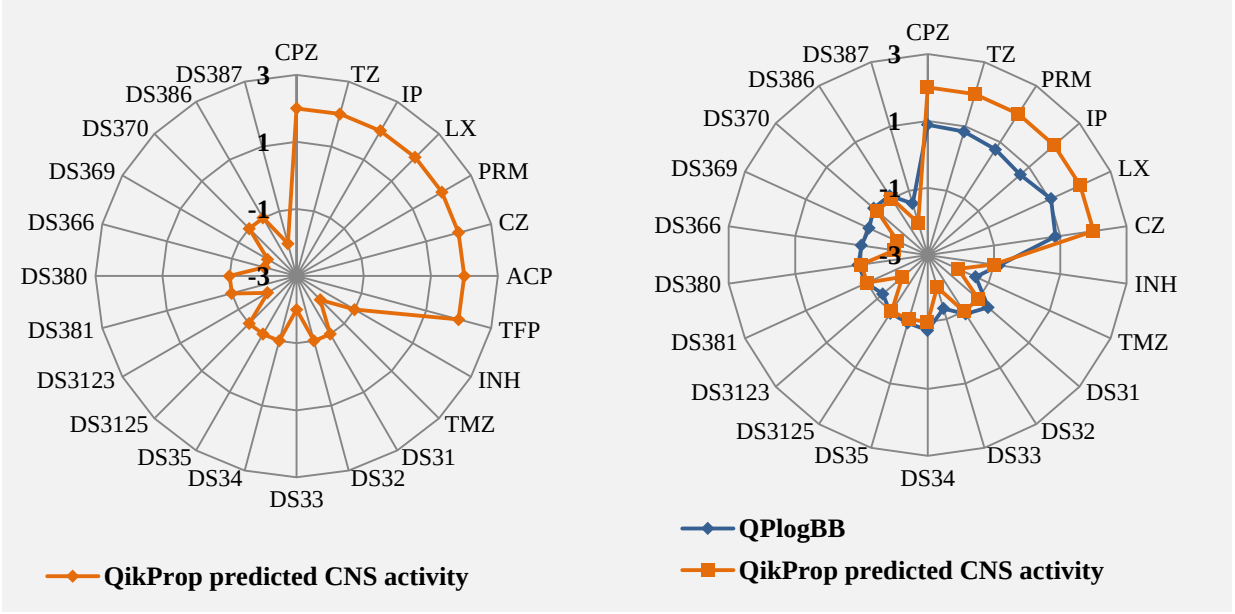

Figure 2.10: QikProp predicted CNS activity and Blood/Brain partition coefficient (QPlogBB). QP- QikProp; CNS activity scale -2 (inactive) to +2 (active); CNS drugs: Chlorpromazine (**CPZ**), Thioridazine (**TZ**), Imipramine (**IP**), Loxapine (**LX**), Promazine (**PRM**), Clozapine (**CZ**), Acepromazine (**ACP**), Trifluoperazine (**TFP**); antitubercular Isoniazid (**INH**); anticancer Temozolomide (**TMZ**); **QikProp scale for CNS activity: -2 (inactive) to +2 (active)**; All neuroleptic drugs were predicted to be CNS active (+2). All alkylsulfonates described in section **2.5.1.1 -2.5.1.4** were predicted to be CNS inactive (-1); Note: Shortened NCE codes were used on all the radar plots e.g. DS0035 is the same as DS35.

2.6.2.2 *In silico* prediction of properties associated with ADMET

In addition to prediction of CNS activity of the remodelled phenothiazines, other properties associated with ADMET were also predicted using QikProp (Figure 2.11).

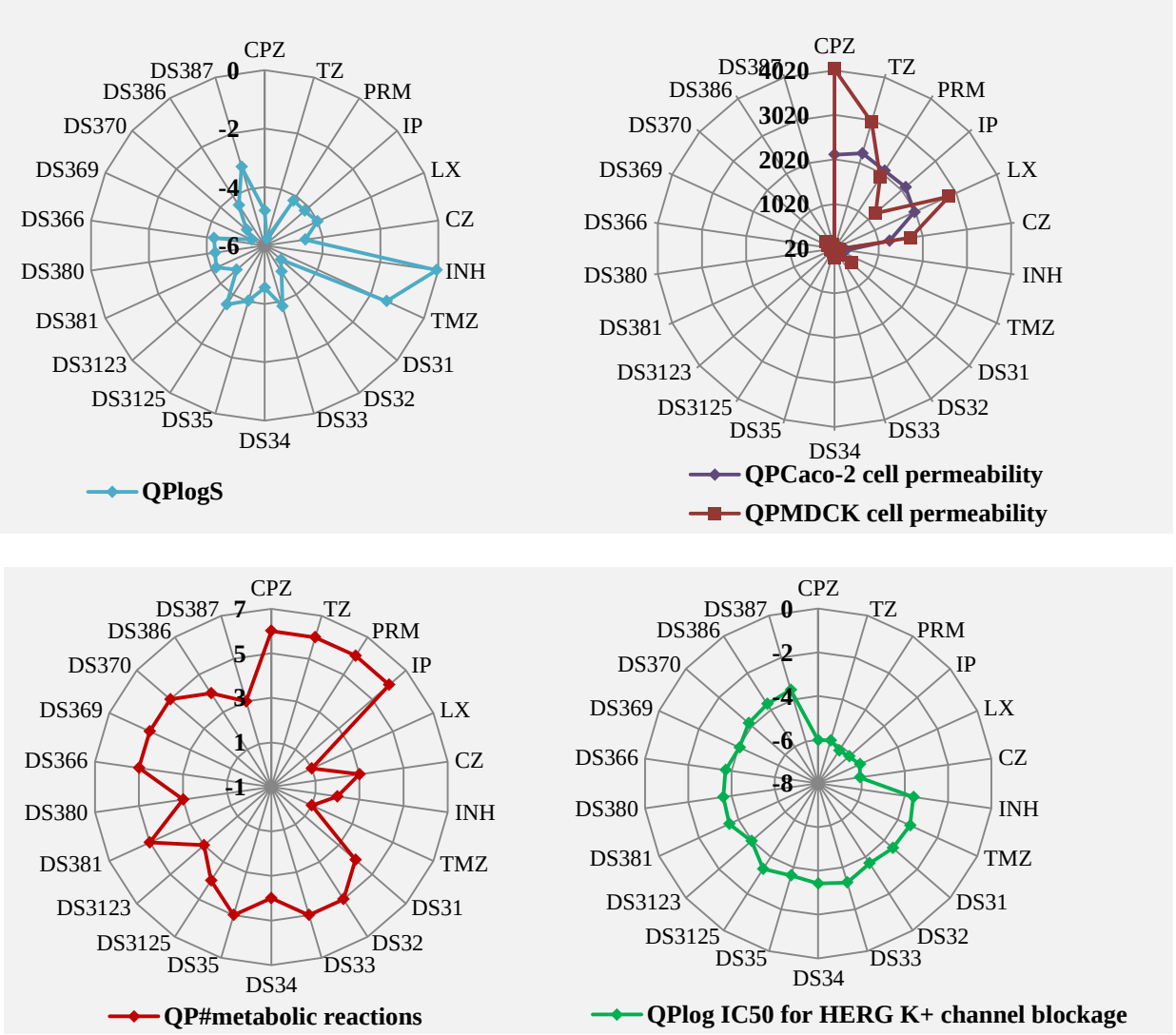

Figure 2.11: QikProp predicted aqueous solubility (QPlogS), predicted Caco-2 cell permeability, predicted MDCK cell permeability, predicted number of metabolic reactions and predicted hERG inhibition; QP-QikProp; CNS drugs: Chlorpromazine (**CPZ**), Thioridazine (**TZ**), Imipramine (**IP**), Loxapine (**LX**), Promazine (**PRM**), Clozapine (**CZ**); antitubercular Isoniazid (**INH**); anticancer Temozolomide (**TMZ**). **QikProp ranges for 95% of known drugs**: QPlogS (-6 to 0.5), Caco-2 (< 25 poor, > 100 high) MDCK (<25 poor, >500 great), # metabolic reactions (1-8); loghERG < -5 raises concern.

As discussed earlier, aqueous solubility and permeability are one of the key determinants of drug absorption. All the predicted aqueous solubility values fell within the QikProp solubility range for 95% of known drugs i.e. -6 to 0.5 (Figure 2.11).[31] The aqueous solubility of these

remodelled phenothiazines is expected to be greater than that of parent drugs due to the presence of a polar alkylsulfonate moiety. The plot reveals slight differences in the predicted solubility values (Figure 2.11).

For prediction of metabolic stability, the predicted number of likely metabolic reactions (≤ 5) fell within the Qikprop number of likely metabolic reactions range (1-8) for 95% of known drugs (Figure 2.11).[31]

The QikProp predicted permeability values in nm/sec are interpreted as (< 25 poor, > 100 high) for Caco-2 and (< 25 poor, > 500 great) for MDCK.[31] The NCEs showed good predicted Caco-2 and MDCK cell permeability. All parent CNS drugs showed greater permeability which could be attributable to their relatively high lipophilicity (Figure 2.11).

As mentioned earlier, evaluation of hERG inhibition is important for determination of possible cardiac toxicity.[38] QikProp predicted hERG inhibition values ($logIC_{50}$ for hERG K^+-channel inhibition) less than -5 suggest possible toxicity.[31] For all the remodelled phenothiazines, values were greater than -5.Chlorpromazine and other neuroleptic drugs were predicted to be cardio-toxic with loghERG values over -6 (Figure 2.11).

2.6.3 Strategy 2: Replacement of the tricyclic phenothiazine core with bicyclic quinoline

2.6.3.1 Rationale behind *N*-propylsulfonates of quinolines

Phenothiazines share ancestral roots with quinoline and acridine based antimalarial drug classes, hence the striking structural resemblance.[28] Various well-known antimalarial drugs structurally evolved from the phenothiazinium dye, methylene blue. Substitution of the

phenothiazine ring system with that of acridine or quinoline furnished highly potent antimalarial drugs such as quinacrine and chloroquine, respectively.[28,45] These antimalarial drug classes display the same lipophilic chromophore/ basic side chain paradigm observed in tricyclic phenothiazines.[46,47] For this reason, the bicyclic quinoline scaffolds became appealing to this research study and were remodelled as illustrated in Figure 2.12.

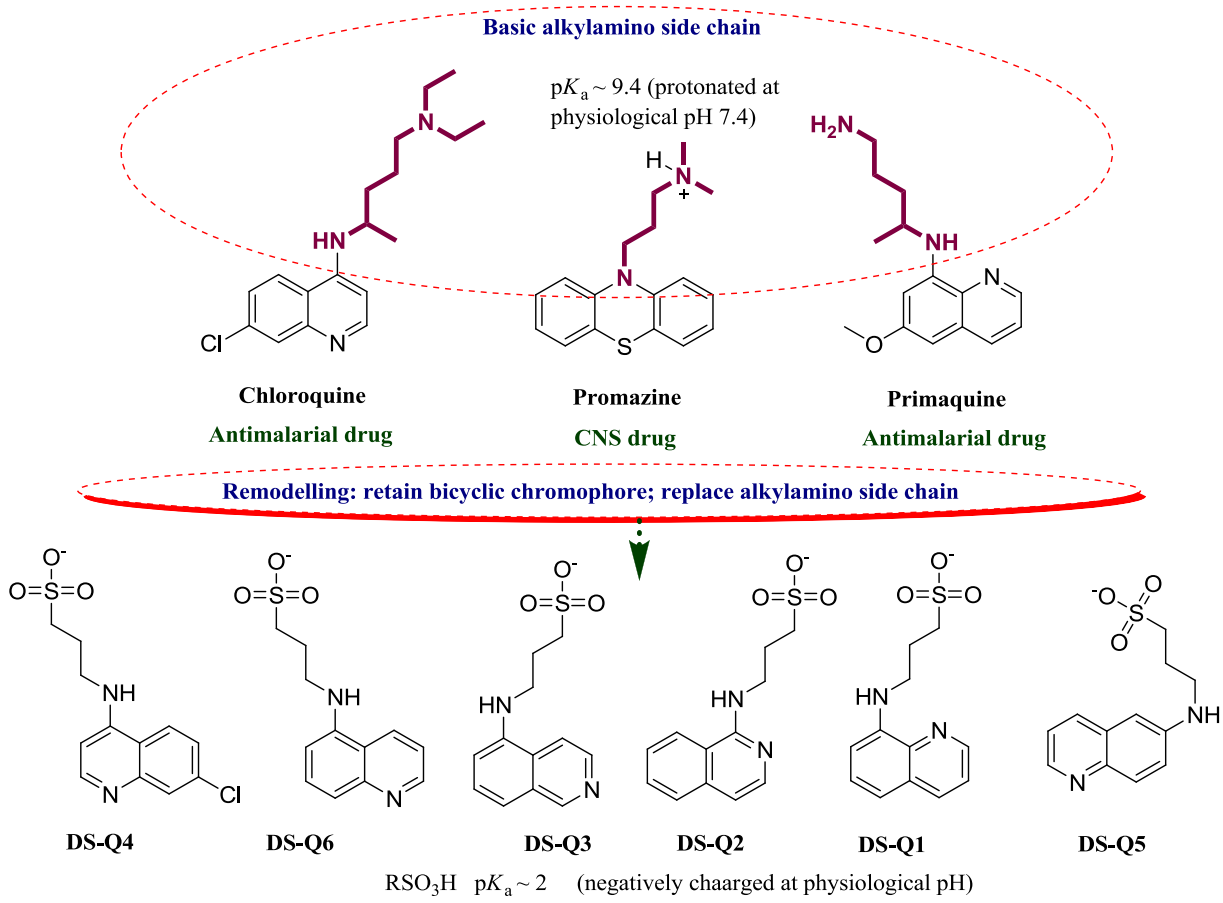

Figure 2.12: Application of remodelling strategy delineated in section 2.6.1 and replacement of the lipophilic tricyclic ring system of phenothiazines. Sulfonates are expected to exist as negatively charged species at physiological pH.

Similar to propylsulfonates NCEs described in section 2.6.1, the bicyclic quinoline NCEs also complied with the RO5 (Table 2.4). Furthermore, in comparison to the propylsulfonates of phenothiazines, these quinoline NCEs are the least lipophilic.

Table 2.4: Prediction of molecular descriptors associated with solubility and permeation on the basis of Lipinski's rule of five (*N*-propylsulfonates of quinolines)

NCE or **parent CNS drug**	**MW**	**clogP**	**HBD**	**HBA**
DSQ1	266.3	1.669	2	5
DSQ2	266.3	1.799	2	5
DSQ3	266.3	1.407	2	5
DSQ4	300.8	2.037	2	5
DSQ5	266.3	1.609	2	5
DSQ6	266.3	1.567	2	5
Chloroquine	**319.9**	**4.327**	**1**	**4**
Primaquine	**315.4**	**3.992**	**1**	**5**

Predictions obtained using StarDrop 5.5; **MW**: Molecular weight; **clogP**: log of octanol-water partition coefficient; **HBD**: Hydrogen-bond donor count (NH, NH_2 & OH groups) **HBA**: Hydrogen Bond Acceptors count (O & N atoms).

2.6.3.2 *In silico* prediction of BBB penetration and CNS activity

The predicted blood/brain partition coefficients and CNS activity were in accordance with the decrease in hydrophobicity observed earlier for the quinoline NCEs. The NCEs were all predicted to be CNS inactive (values = -2) as illustrated in Figure 2.13. Interestingly, antimalarial chloroquine and primaquine were predicted to be moderately CNS active (values = +1) which could be attributable to their structural similarity to phenothiazine drugs.

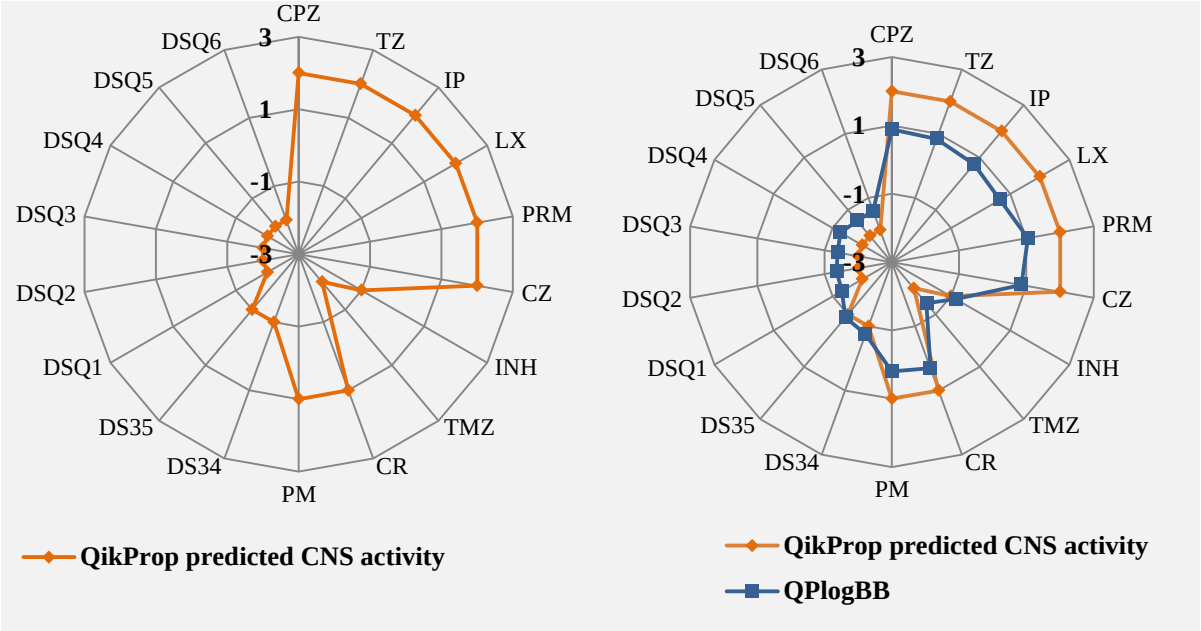

Figure 2.13: QikProp predicted CNS activity and Blood/Brain partition coefficient (QPlogBB)**.** QP- QikProp; CNS drugs: Chlorpromazine (**CPZ**), Thioridazine (**TZ**), Imipramine (**IP**), Loxapine (**LX**), Promazine (**PRM**), Clozapine (**CZ**); antitubercular Isoniazid (**INH**); anticancer Temozolomide (**TMZ**); antimalarial Chloroquine (**CR**), antimalarial Primaqine (**PR**); **QP CNS activity scale: -2 (inactive) to +2 (active)**; All neuroleptic drugs were predicted to be CNS active (+2). All *N*-propylsulfonates of quinolines **(DSQ1-Q6)** were predicted to be CNS inactive (-2).

2.6.3.3 *In silico* prediction of properties associated with ADMET

The predicted ADMET properties of the quinoline NCEs displayed the same radar plot patterns as with *N*-propylsulfonates of phenothiazines described earlier in section 2.6.1 (Figure 2.14). In contrast, chloroquine was predicted to be a hERG inhibitor (loghERG <-5) whereas the quinoline-based NCEs were not (Figure 2.14).

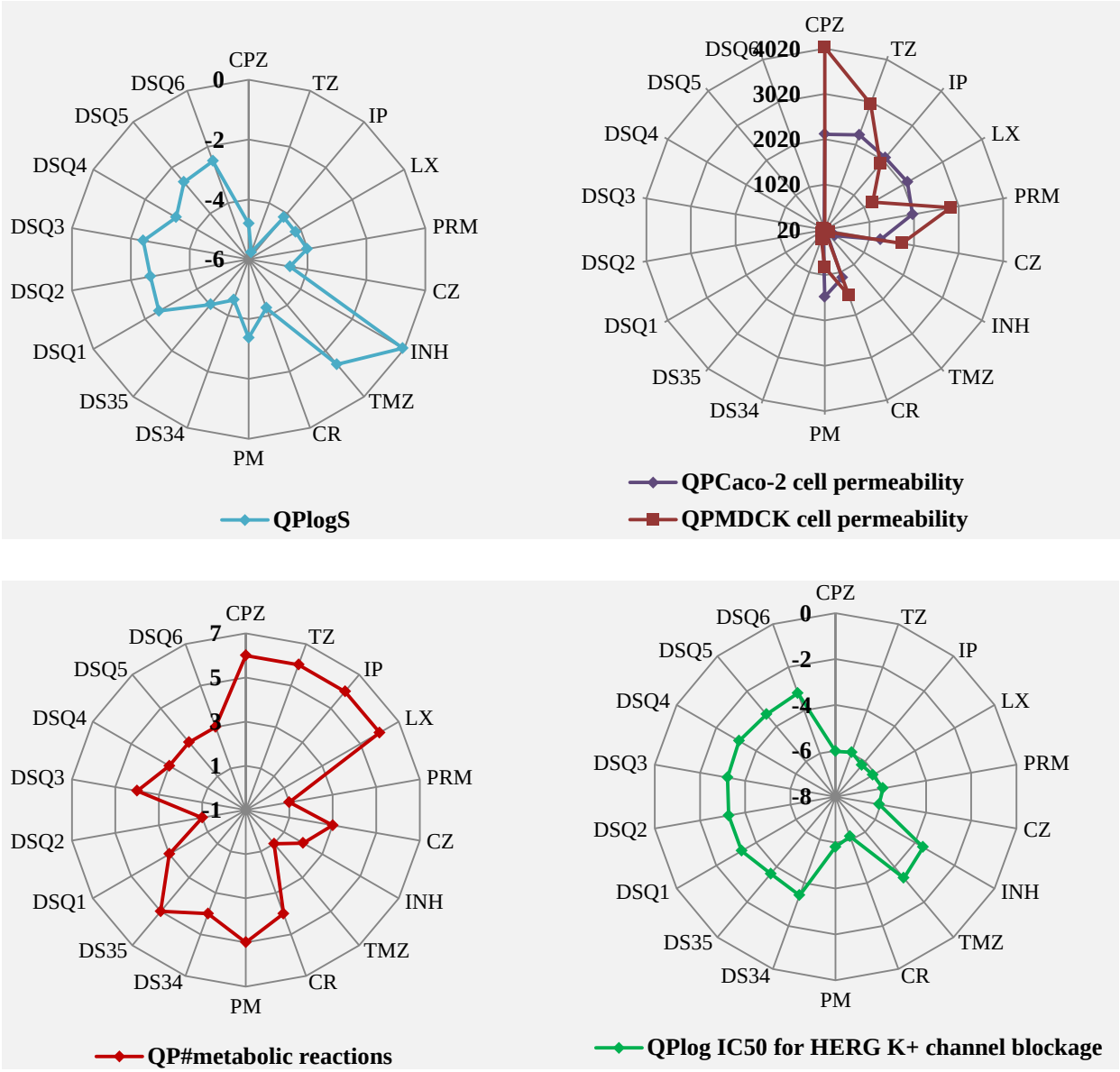

Figure 2.14: QikProp predicted aqueous solubility (QPlogS), predicted Caco-2 cell permeability, predicted MDCK cell permeability, predicted number of likely metabolic reactions and predicted hERG inhibition; QP-QikProp; CNS drugs: Chlorpromazine (**CPZ**), Thioridazine (**TZ**), Imipramine (**IP**), Loxapine (**LX**), Promazine (**PRM**), Clozapine (**CZ**); antitubercular Isoniazid (**INH**); anticancer Temozolomide (**TM)**; Chloroquine (**CR**); Primaquine (**PM**).**QikProp ranges for 95% of known drugs**: QPlogS (-6 to 0.5), Caco-2 (< 25 poor, > 100 high) MDCK (<25 poor, >500 great), # metabolic reactions (1-8); loghERG < -5 raises concern.

2.6.4 Strategy 3: Molecular hybridization

2.6.4.1 Rationale behind molecular hybrids of phenothiazines

Molecular hybridization is a rational design strategy that involves combination of two or more pharmacophoric subunits to form hybrids. This strategy aims to produce bioactive agents with better efficacy than parent drugs.[48,49,50] Furthermore, hybrids generated may show different selectivity profiles, fewer side effects, different and/or dual mechanisms of action compared to parent drugs.[48] This concept also paves the way for targeting multifactorial diseases such as neurodegenerative disorders and cancer.[50,51] Hybrids of repurposed psychoactive drugs such as phenothiazines have been reported for biological and non-biological properties.[51,52]

Using this pharmacophoric hybridization strategy, a series of isoniazid hybrids were generated by combination with phenothiazine core structures. Additionally, another series of phenothiazine hybrids was generated from hybridization with *ortho-/para*-nitrobenzenesulfonyl chlorides to form sulfonamides found in a class of antibiotics called sulfanilamides (Figure 2.15).

Non-*N*-alkylated phenothiazine derivatives linked to various heterocyclic rings have been reported to exhibit a range of biological properties including antibacterial, antifungal and anticancer activities. This includes monocyclics such as pyrazoles, tetrazoles and thiazoles.[11] Substitution at C-2 of phenothiazines is known to greatly influence the intensity of their neuroleptic action due to favourable van der Waals interactions.[2,15] Herein, phenothiazine was linked to pyrazole and isoxazole heterocyclic moieties at C-2 (Figure 2.15).

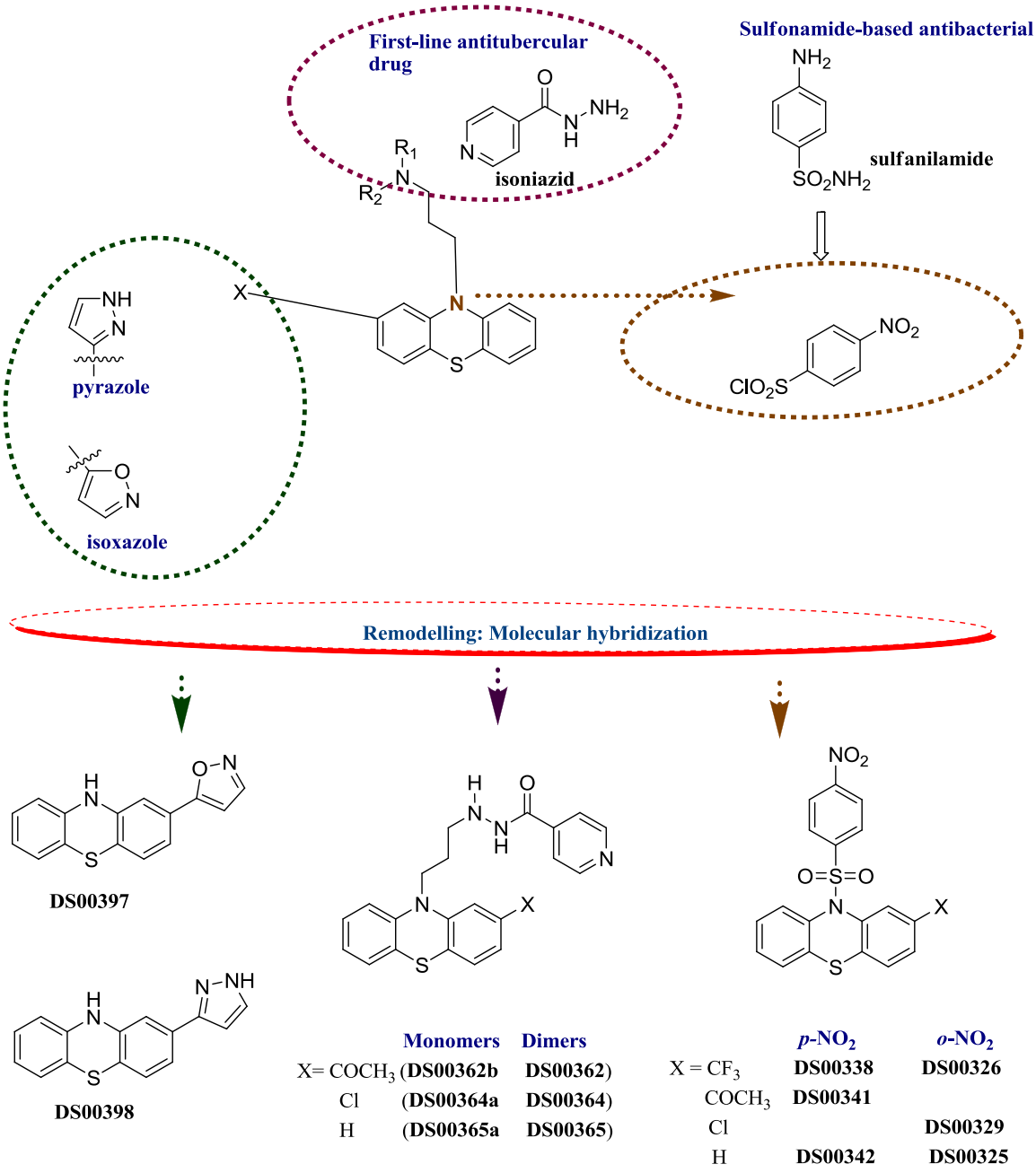

Figure 2.15: Molecular hybridization of phenothiazines with antibacterial pharmacophores including isoniazid and sulfanilamide precursors. Phenothiazines were also linked to monocyclic heterocycles (pyrazole and isoxazole) which are common in biologically active molecules.

All the NCEs were compliant to the RO5 except dimers of isoniazid hybrids which have molecular weights greater than 500 and clogPs greater than 5 (Table 2.5). As discussed earlier, a higher degree of lipophilicity is known to facilitate BBB penetration. As with propylsulfonates of phenothiazines, a decrease in hydrophobicity was also evident herein.

Table 2.5: Prediction of molecular descriptors associated with solubility and permeation on the basis of Lipinski's rule of five (Hybrids of phenothiazines). Values violating RO5 are shown in red

NCE or **parent CNS drug**	**MW**	**clogP**	**HBD**	**HBA**
Isoniazid hybrids				
DS00362b	418.5	3.821	2	8
Acepromazine	**326.4**	**4.479**	**0**	**3**
DS00362 (dimer)	699.9	7.567	1	6
DS00364a	410.9	4.755	2	6
Chlorpromazine	**318.9**	**5.291**	**0**	**2**
DS00364 (dimer)	684.7	9.514	1	5
DS00365a	376.5	4.267	2	6
Promazine	**284.4**	**4.550**	**0**	**2**
DS00365 (dimer)	615.8	9.030	1	5
Nitrobenzenesulfonamides				
DS00325	384.4	3.084	0	6
DS00342	384.4	2.939	0	6
DS00326	452.4	4.123	0	6
Trifluoperazine	**407.5**	**4.759**	**0**	**3**
DS00338	452.4	3.806	0	6
DS00329	418.9	3.516	0	6
DS00341	426.4	2.089	0	7
Pyrazole and isoxazole linked phenothiazines				
DS00397	266.3	3.729	1	2
DS00398	265.3	3.482	2	2

Predictions obtained using StarDrop 5.5; **MW**: Molecular weight; **clogP**: log of octanol-water partition coefficient; **HBD**: Hydrogen-bond donor count (NH, NH_2 & OH groups) **HBA**: Hydrogen Bond Acceptors count (O & N atoms).

2.6.4.2 *In silico* prediction of BBB penetration and CNS activity.

The predicted blood/brain partition coefficients as well as predicted CNS activity exhibited the same radar plot patterns as observed before. The predicted CNS activity values for the

hybrids ranged from -2 (inactive) to +1 (moderately active). Notably, the presence of an acetyl group at the 2-position of the phenothiazine chromophore appeared to influence predicted CNS activity. All NCEs with an acetyl group at C-2 (**DS00341**, **DS00362** and **DS00362b**) were predicted to be CNS inactive (values = -2). Phenothiazines linked to pyrazole (**DS00398**) and isoxazole (**DS00397**) were predicted to be moderately CNS active (values = +1) (Figure 2.16).

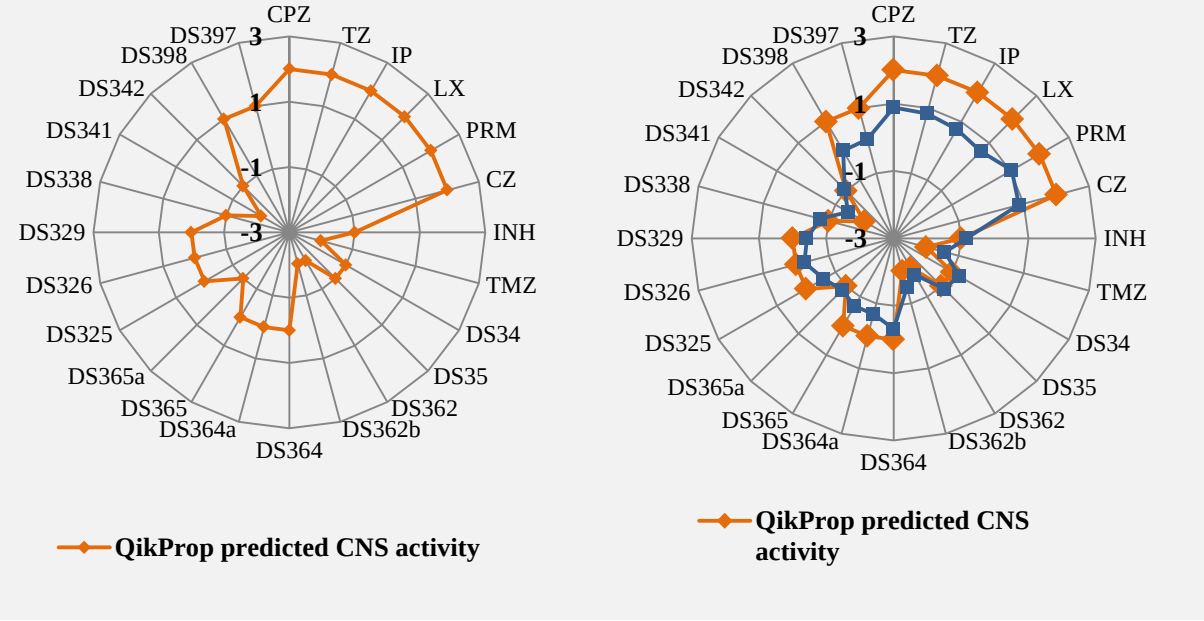

Figure 2.16: QikProp predicted CNS activity and Blood/Brain partition coefficient (QPlogBB). QP- QikProp; Activity scale -2 (inactive) to +2 (active); CNS drugs: Chlorpromazine (**CPZ**), Thioridazine (**TZ**), Imipramine (**IP**), Loxapine (**LX**), Promazine (**PRM**), Clozapine (**CZ**); antitubercular Isoniazid (**INH**); anticancer Temozolomide (**TMZ**); **QP CNS activity scale: -2 (inactive) to +2 (active)**; All neuroleptic drugs were predicted to be CNS active (values = +2). Predicted CNS activity values ranged from -2 to 1 with NCEs **DS00397** and **DS00398** showing moderate CNS activity. DS00341, DS00362 and DS00362b were predicted to be the most CNS inactive (-2) of this series; Note: Shortened NCE codes were used on all the radar plots e.g. DS0035 is the same as DS35.

2.6.4.3 *In silico* prediction of properties associated with ADMET

As before, four properties were predicted using QikProp including aqueous solubility, number of likely metabolic reactions, permeability and hERG inhibition (Figure 2.17).

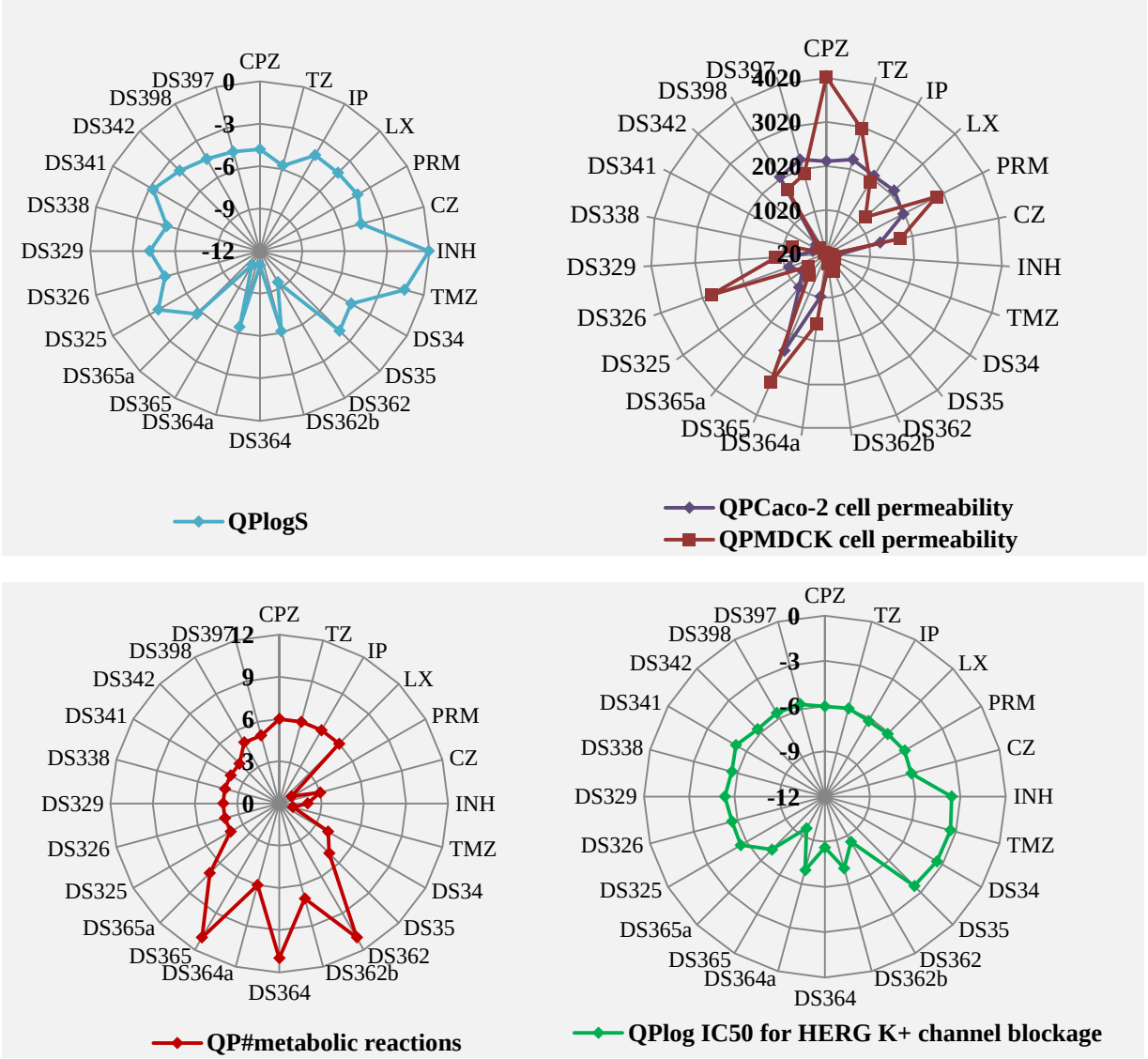

Figure 2.17: QikProp predicted aqueous solubility (QPlogS), predicted Caco-2 cell permeability, predicted MDCK cell permeability, predicted number of metabolic reactions and predicted hERG inhibition; QP-QikProp; CNS drugs: Chlorpromazine (**CPZ**), Thioridazine (**TZ**), Imipramine (**IP**), Loxapine (**LX**), Promazine (**PRM**), Clozapine (**CZ**); antitubercular Isoniazid (**INH**); anticancer Temozolomide (**TMZ**). **QikProp ranges for 95% of known drugs**: QPlogS (-6 to 0.5), Caco-2 (< 25 poor, > 100 high) MDCK (<25 poor, >500 great), # metabolic reactions (1-8); loghERG < -5 raises concern. Predicted values for isoniazid dimers (**DS00362**, **DS00364** and **DS00365**) suggested they possess poor pharmacokinetic properties.

The predicted logS values fell within the QikProp solubility range for 95% of known drugs (i.e. -6 to 0.5) except for isoniazid hybrids dimers (values greater than -9.).[31] The isoniazid dimers also had the highest number of likely metabolic reactions and were predicted to be

hERG channel blockers (Figure 2.17). This suggested that these hybrid dimers did not possess desirable ADMET properties and were thus of least priority for chemical synthesis.

2.6.5 Strategy 4: Replacement of amine moiety with other non-basic functionalities

2.6.5.1 Rationale behind the design

Apart from conversion of the amine moiety to a sulfonate group, neutral species such as nitriles and esters were also considered to further probe replacement of the basic distal amine of phenothiazines (Figure 2.18). Since the presence of proton accepting nitrogen moieties promotes BBB penetration, substitution with non-basic moieties could impede the penetration.[2,19]

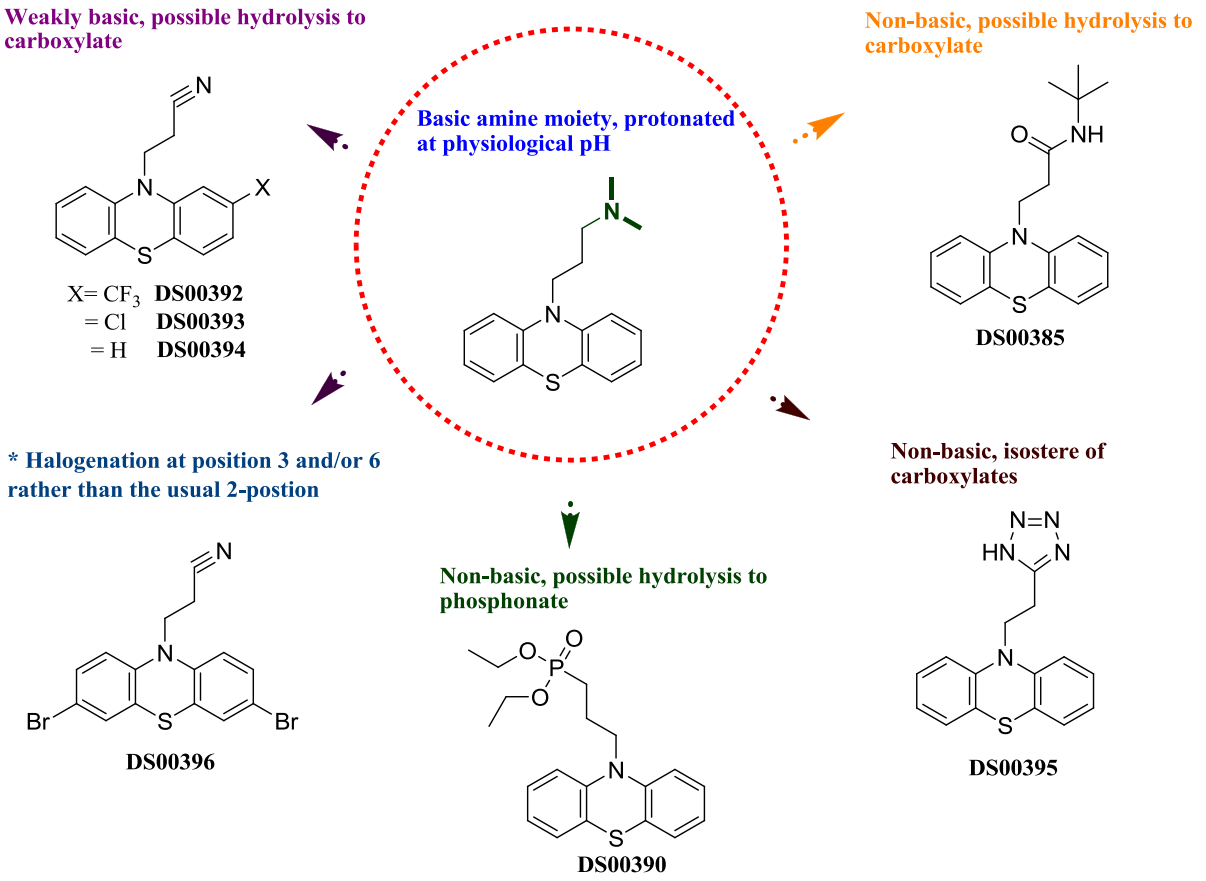

Figure 2.18: Replacement of tertiary amine moiety of phenothiazine with non-basic functionalities. * Mono-bromination would allow evaluation of the effect of a halogen substituent at an unusual position 3 or 6 on bio - activity. Interestingly, a dibrominated NCE **DS00396** would bear some structural similarity to DNA intercalators such as ethidium bromide.[53]

This series of NCEs also showed compliance to the RO5. Furthermore, replacement of the distal amine moiety with a nitrile functionality resulted in lower clogP values (Table 2.6). Ester **DS00390**, amide **DS00385** as well as dibromo-substitued NCE **DS00396** showed slightly higher clogP values in comparison to promazine. This raised concern as an increase in hydrophobicity could favour BBB penetration.

Table 2.6: Prediction of molecular descriptors associated with solubility and permeation on the basis of Lipinski's rule of five (Phenothiazines with other non-basic side chains)

NCE or **CNS drug**	**MW**	**clogP**	**HBD**	**HBA**
DS00385	326.4	4.572	1	3
Promazine	**284.4**	**4.550**	**0**	**2**
DS00392	320.3	4.835	0	2
Trifluoperazine	**407.5**	**4.759**	**0**	**3**
DS00393	286.8	4.395	0	2
Chlorpromazine	**318.9**	**5.291**	**0**	**2**
DS00394	252.3	3.955	0	2
DS00395	295.4	3.103	1	4
DS00396	410.1	4.834	0	2
DS00390	377.4	4.569	0	6

Predictions obtained using StarDrop 5.5; **MW**: Molecular weight; c**logP**: log of octanol-water partition coefficient; **HBD**: Hydrogen-bond donor count (NH, NH_2 & OH groups) **HBA**: Hydrogen Bond Acceptors count (O & N atoms).

2.6.5.2 *In silico* prediction of BBB penetration and CNS activity

The radar plot of predicted blood/brain barrier partition coefficients displayed the same pattern as that of predicted CNS activity. This series of NCEs were predicted to be moderately CNS active (values range from 0 to +1) except for tetrazole **DS00395** (value = -1)

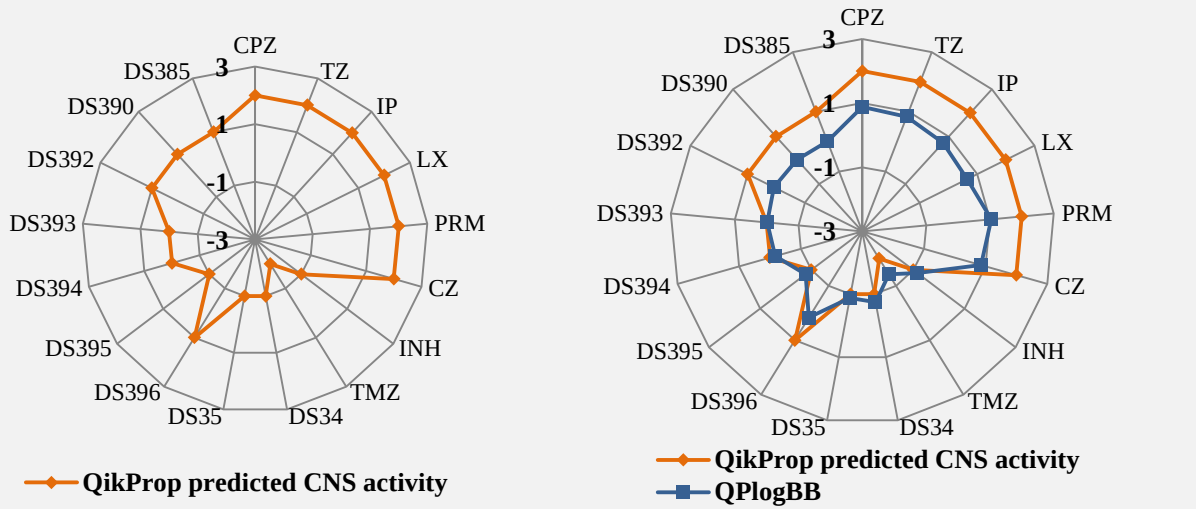

Figure 2.19: QikProp predicted CNS activity and Blood/Brain partition coefficient (QPlogBB). QP- QikProp; **QP CNS activity scale -2 (inactive) to +2 (active)**; CNS drugs: Chlorpromazine (**CPZ**), Thioridazine (**TZ**), Imipramine (**IP**), Loxapine (**LX**), Promazine (**PRM**), Clozapine (**CZ**); antitubercular Isoniazid (**INH**); anticancer Temozolomide (**TMZ**); all neuroleptic drugs were predicted to be CNS active (+2). Predicted CNS acivity values ranged from -1 to 1; Note: Shortened NCE codes were used on all the radar plots e.g. DS0035 is the same as DS35.

2.6.5.3 *In silico* prediction of properties associated with ADMET

Predicted properties fell within the QikProp ranges for 95% of known drugs.[31] The NCEs were predicted to have good Caco-2 and MDCK cell permeability. NCE **DS00396** displayed the highest MDCK cell permeability (greater than 7300, not shown on the plot). Furthermore, the NCEs were not predicted to be inhibitors of hERG (Figure 2.20).

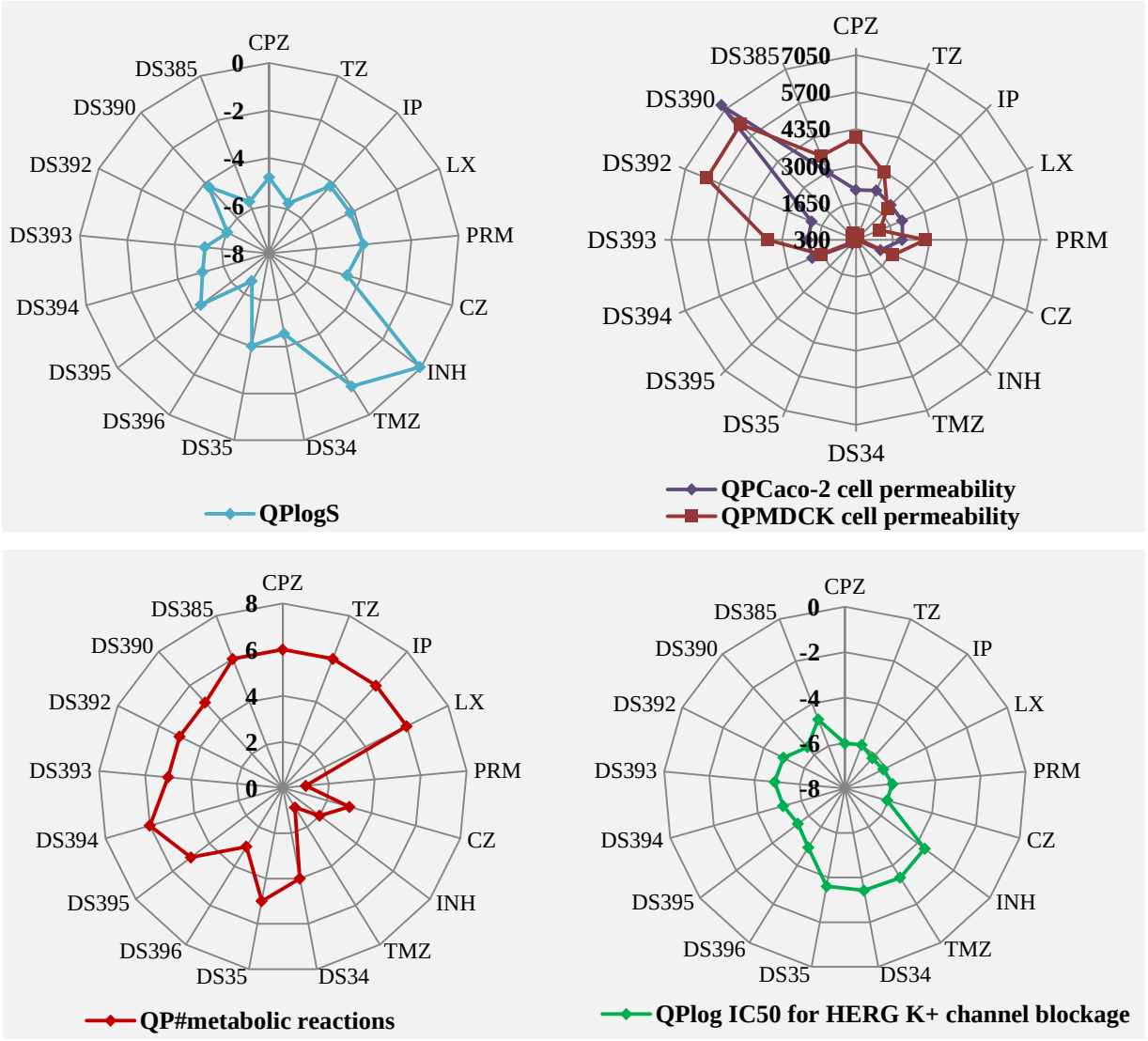

Figure 2.20: QikProp predicted aqueous solubility (QPlogS), predicted Caco-2 cell permeability, predicted MDCK cell permeability, predicted number of metabolic reactions and predicted hERG inhibition; QP-QikProp; CNS drugs: Chlorpromazine (**CPZ**), Thioridazine (**TZ**), Imipramine (**IP**), Loxapine (**LX**), Promazine (**PRM**), Clozapine (**CZ**); antitubercular Isoniazid (**INH**); anticancer Temozolomide (**TMZ**). **QikProp ranges for 95% of known drugs**: QPlogS (-6 to 0.5), Caco-2 (< 25 poor, > 100 high) MDCK (<25 poor, >500 great), # metabolic reactions (1-8); loghERG < -5 raises concern.

2.7 Concluding Remarks

An in depth evaluation of minimum structural requirements for neuroleptic activity guided the remodelling of existing CNS drugs to create a diverse focused library of non-neuroleptic NCEs for bio-activities of interest i.e. antitubercular and anticancer activities. The library comprises novel functionalities such as alkylsulfonates which resulted in increased aqueous solubility, a property that deviates from a considerably high degree of hydrophobicity exhibited by CNS drugs. The other remodelling strategies included molecular hybridization with antibacterial pharmacophores and introduction of other non-basic moieties such as nitriles and esters. The overall remodelling approach applied herein was to deviate from the lipophilic chromophore/basic side chain paradigm obeyed by phenothiazines and structurally related drugs.

In silico predictions tools were integrated into the structural remodelling to assess drug-likeness of the resulting NCEs on the basis of Lipinski's rule of five. Most NCEs were compliant to the rule. ADMET properties including aqueous solubility, Caco-2 & MDCK cell permeability, number of likely metabolic reactions and hERG inhibition were also predicted *in silico*. *In silico* evaluation of these ADMET properties suggested that most of the remodelled phenothiazines had favourable drug-like properties. Furthermore *in silico* prediction of CNS activity suggested the NCEs had reduced likelihood of exhibiting neuroleptic effects.

In the next chapter, an extensive discussion of synthetic methods employed for chemical synthesis of these remodelled phenothiazines (for *in vitro* evaluation as antitubercular or anticancer agents) is provided.

References

(1) Jafari, S.; Fernandez-Enright, F.; Huang, X. F. Structural Contributions of Antipsychotic Drugs to Their Therapeutic Profiles and Metabolic Side Effects. *J. Neurochem.* **2012**, *120* (3), 371–384.

(2) Jaszczyszyn, A.; Gąsiorowski, K.; Świątek, P.; Malinka, W.; Cieślik-Boczula, K.; Petrus, J.; Czarnik-Matusewicz, B. Chemical Structure of Phenothiazines and Their Biological Activity. *Pharmacol. Reports* **2012**, *64* (1), 16–23.

(3) Mauri, M. C.; Paletta, S.; Maffini, M.; Colasanti, A.; Dragogna, F.; Pace, C. Di; Altamura, A. C. Review Article : Clinical Pharmacology of Atypical Antipsychotics: An Update. *EXCLI J.* **2014**, *13*, 1163–1191.

(4) Meltzer, H. Y. Update on Typical and Atypical Antipsychotic Drugs. *Annu. Rev. Med.* **2013**, *64*, 394–406.

(5) Carpenter, D. T. Another View of the History of Antipsychotic Drug Discovery and Development. *Mol. Psychiatry* **2012**, *17* (12), 1168–1173.

(6) Van Soolingen, D.; Hernandez-Pando, R.; Orozco, H.; Aguilar, D.; Magis-Escurra, C.; Amaral, L.; Van Ingen, J.; Boeree, M. J. The Antipsychotic Thioridazine Shows Promising Therapeutic Activity in a Mouse Model of Multidrug-Resistant Tuberculosis. *PLoS One* **2010**, *5* (9), 1–6.

(7) Seeman, P. Clozapine , a Fast-Off -D2 Antipsychotic. *ACS Chem. Neurosci.* **2014**, *5*, 24–29.

(8) Colpaert, F. C. Discovery of Risperidone: The LSD Model of Psychopathology. *Nat. Rev. Drug Discov.* **2003**, *2* (4), 315–320.

(9) Shen, W. W. A History of Antipsychotic Drug Development. *Compr Psychiatry* **1999**, *40* (6), 407–414.

(10) Ban, A. T. Fifty Years Chlorpromazine: A Historical Perspective. *Neuropsychiatry Dis Treat* **2007**, *3* (4), 495–508.

(11) Pluta, K.; Morak-Młodawska, B.; Jeleń, M. Recent Progress in Biological Activities of Synthesized Phenothiazines. *Eur. J. Med. Chem.* **2011**, *46* (8), 3179–3189.

(12) Sudeshna, G.; Parimal, K. Multiple Non-Psychiatric Effects of Phenothiazines: A Review. *Eur. J. Pharmacol.* **2010**, *648* (1-3), 6–14.

(13) Massie, S. P. The Chemistry of Phenothiazine. *Chem. Rev.* **1954**, *54* (5), 797–833.

(14) De Ruiter, J. Dopamine Antagonists: Phenothiazine/thioxanthene SAR. In *Principles of Drug Action: The Basis of Pharmacology.* Ed. Pratt WB and Taylor P, Churchill Livingstone, New York; **1990**; pp 1–14.

(15) Feinberg, A. P.; Snyder, S. H. Phenothiazine Drugs : Structure-Activity Relationships Explained by a Conformation That Mimics Dopamine. *Proc. Nat. Acad. Sci.* **1975**, *72* (5), 1899–1903.

(16) Seelig, A.; Gottschlich, R.; Devant, R. M. A Method to Determine the Ability of Drugs to Diffuse through the Blood-Brain Barrier. *Proc. Natl. Acad. Sci. U. S. A.* **1994**, *91* (1), 68–72.

(17) Ooms, F.; Weber, P.; Carrupt, P. A.; Testa, B. A Simple Model to Predict Blood-Brain Barrier Permeation from 3D Molecular Fields. *Biochim. Biophys. Acta* **2002**, *1587* (2-3), 118–125.

(18) Martins, I. F.; Teixeira, A. L.; Pinheiro, L.; Falcao, A. O. A Bayesian Approach to in Silico Blood-Brain Barrier Penetration Modeling. *J. Chem. Inf. Model.* **2012**, *52* (6), 1686–1697.

(19) Kharkar, P. S. Drugs Acting on Central Nervous System (CNS) Targets as Leads for Non-CNS Targets. *F1000Research* **2014**, *3* (40), 1–7.

(20) Lipinski, C. A.; Lombardo, F.; Dominy, B. W.; Feeney, P. J. Experimental and Computational Approaches to Estimate Solubility and Permeability in Drug Discovery and Development. *Adv. Drug Deliv. Rev.* **2001**, *46*, 3–26.

(21) Lipinski, C. A. Drug-like Properties and the Causes of Poor Solubility and Poor Permeability. *J. Pharmacol. Toxicol. Methods* **2000**, *44* (1), 235–249.

(22) Warman, A. J.; Rito, T. S.; Fisher, N. E.; Moss, D. M.; Berry, N. G.; O'Neill, P. M.; Ward, S. a.; Biagini, G. a. Antitubercular Pharmacodynamics of Phenothiazines. *J. Antimicrob. Chemother.* **2013**, *68* (4), 869–880.

(23) Pajouhesh, H.; Lenz, G. R. Medicinal Chemical Properties of Successful Central Nervous System Drugs. *NeuroRx* **2005**, *2* (4), 541–553.

(24) Morak-Młodawska, B.; Suwińska, K.; Pluta, K.; Jeleń, M. 10-(3′-Nitro-4′-Pyridyl)-1,8-Diazaphenothiazine as the Double Smiles Rearrangement Product. *J. Mol. Struct.* **2012**, *1015*, 94–98.

(25) Mekky, A. E. M.; Saleh, T. S.; Al-Bogami, A. S. Synthesis of Novel Pyrazoles Incorporating a Phenothiazine Moiety: Unambiguous Structural Characterization of the Regioselectivity in the 1,3-Dipolar Cycloaddition Reaction Using 2D HMBC NMR Spectroscopy. *Tetrahedron* **2013**, *69* (33), 6787–6798.

(26) Belei, D.; Dumea, C.; Samson, A.; Farce, A.; Dubois, J.; Bîcu, E.; Ghinet, A. New Farnesyltransferase Inhibitors in the Phenothiazine Series. *Bioorganic Med. Chem. Lett.* **2012**, *22* (14), 4517–4522.

(27) Lu, M.; Zhu, Y.; Ma, K.; Cao, L.; Wang, K. Facile Synthesis and Photo-Physical Properties of Cyano-Substituted Styryl Derivatives Based on Carbazole/phenothiazine. *Spectrochim. Acta - Part A Mol. Biomol. Spectrosc.* **2012**, *95*, 128–134.

(28) Wainwright, M.; Amaral, L. The Phenothiazinium Chromophore and the Evolution of Antimalarial Drugs. *Trop. Med. Int. Heal.* **2005**, *10* (6), 501–511.

(29) Dunn, E. A.; Roxburgh, M.; Larsen, L.; Smith, R. A. J.; McLellan, A. D.; Heikal, A.; Murphy, M. P.; Cook, G. M. Incorporation of Triphenylphosphonium Functionality Improves the Inhibitory Properties of Phenothiazine Derivatives in Mycobacterium Tuberculosis. *Bioorg. Med. Chem.* **2014**, *22* (19), 5320–5328.

(30) Van de Waterbeemd, H.; Gifford, E. ADMET in Silico Modelling: Towards Prediction Paradise? *Nat. Rev. Drug Discov.* **2003**, *2* (3), 192–204.

(31) Ntie-Kang, F. An in Silico Evaluation of the ADMET Profile of the StreptomeDB Database. *Springerplus* **2013**, *2* (353), 1–11.

(32) Moroy, G.; Martiny, V. Y.; Vayer, P.; Villoutreix, B. O.; Miteva, M. a. Toward in Silico Structure-Based ADMET Prediction in Drug Discovery. *Drug Discov. Today* **2012**, *17* (1-2), 44–55.

(33) Waring, M. J.; Arrowsmith, J.; Leach, A. R.; Leeson, P. D.; Mandrell, S.; Owen, R. M.; Pairaudeau, G.; Pennie, W. D.; Pickett, S. D.; Wang, J.; Wallace, O.; Weir, A. An Analysis of the Attrition of Drug Candidates from Four Major Pharmaceutical Companies. *Nat. Rev. Drug Discov.* **2015**, *14*, 475–486.

(34) Van Bambeke, F.; Barcia-Macay, M.; Lemaire, S.; Tulkens, P. M. Cellular Pharmacodynamics and Pharmacokinetics of Antibiotics: Current Views and Perspectives. *Curr. Opin. Drug Discov. Devel.* **2006**, *9* (2), 218–230.

(35) Alavijeh, M. S.; Chishty, M.; Qaiser, M. Z.; Palmer, A. M. Drug Metabolism and Pharmacokinetics , the Blood-Brain Barrier , and Central Nervous System Drug Discovery. *J. Am. Soc. Exp. Neurother.* **2005**, *2*, 554–571.

(36) Crowley, P. J.; Martini, L. G. Formulation Design: New Drugs from Old. *Drug Discov. Today Ther. Strateg.* **2004**, *1* (4), 537–542.

(37) Kortagere, S.; Ekins, S. Troubleshooting Computational Methods in Drug Discovery. *J. Pharmacol. Toxicol. Methods* **2014**, *61* (2), 67–75.

(38) Wan, H. What ADME Tests Should Be Conducted for Preclinical Studies? *Admet Dmpk* **2013**, *1* (3), 19–28.

(39) Masimirembwa, C. M.; Bredberg, U.; Andersson, T. B. Metabolic Stability for Drug Discovery and Development: Pharmacokinetic and Biochemical Challenges. *Clin. Pharmacokinet.* **2003**, *42* (6), 515–528.

(40) Hughes, J. P.; Rees, S. S.; Kalindjian, S. B.; Philpott, K. L. Principles of Early Drug Discovery. *Br. J. Pharmacol.* **2011**, *162* (6), 1239–1249.

(41) Cook, D.; Brown, D.; Alexander, R.; March, R.; Morgan, P. Lessons Learned from the Fate of AstraZeneca's Drug Pipeline: A Five-Dimensional Framework. *Nat. Rev. Drug Discov.* **2014**, *13* (6), 419–431.

(42) Raunio, H. In Silico Toxicology Non-Testing Methods. *Front. Pharmacol.* **2011**, *JUN* (June), 1–8.

(43) Over, B.; Wetzel, S.; Gru, C.; Nakai, Y.; Renner, S.; Rauh, D. Natural-Product-Derived Fragments for Fragment-Based Ligand Discovery. *Nat. Chem.* **2013**, *5*, 21–28.

(44) Fourrier, A., Gasquet, I., Allicar, M.P., Bouhassira, M., Lepine, J.P., Begaud, B. Patterns of Neuroleptic Drug Prescription: A National Cross-Sectional Survey of a Random Sample of French Psychiatrists. *Br. J. Clin. Pharmacol* **2000**, *49*, 80–86.

(45) Wainwright, M. The Evolution of Antimycobacterial Agents from Non- Antibiotics. *Open J. Pharmacol.* **2012**, 2–1.

(46) Kristiansen, J. E.; Amaral, L. The Potential Management of Resistant Infections with Non-Antibiotics. *J. Antimicrob. Chemother.* **1997**, *40* (3), 319–327.

(47) Go, M. L. Novel Antiplasmodial Agents. *Med. Res. Rev.* **2003**, *23* (4), 456–487.

(48) Viegas-junior, C.; Danuello, A.; Bolzani, S.; Barreiro, E. J.; Alberto, C.; Fraga, M. Molecular Hybridization : A Useful Tool in the Design of New Drug Prototypes. *Curr. Med. Chem.* **2007**, *14*, 1829–1852.

(49) Manohar S; Tripathi M; Rawat D S. 4-Aminoquinoline Based Molecular Hybrids as Antimalarials: An Overview. *Curr Top Med Chem* **2014**, *14* (14), 1706–1733.

(50) Decker M. Hybrid Molecules Incorporating Natural Products: Applications in Cancer Therapy, Neurodegenerative Disorders and beyond. *Curr Med Chem* **2011**, *18* (10), 1464–1475.

(51) Hui A; Chen A; Zhu S; Gan S; Pan J; Zhou A. Design and Synthesis of Tacrine-Phenothiazine Hybrids as Multitarget Drugs for Alzheimer's Disease. *Med. Chem. Res.* **2014**, *23* (7), 3546–3557.

(52) Addla, D.; Jallapally, A.; Gurram, D.; Yogeeswari, P.; Sriram, D.; Kantevari, S. Rational Design, Synthesis and Antitubercular Evaluation of Novel 2-(trifluoromethyl)phenothiazine[1,2,3]triazole Hybrids. *Bioorg. Med. Chem. Lett.* **2014**, *24* (1), 233–236.

(53) Laursen, J. B.; Nielsen, J. Phenazine Natural Products: Biosynthesis, Synthetic Analogues, and Biological Activity. *Chem. Rev.* **2004**, *104* (3), 1663–1685.

Chapter 3

Chemical synthesis of remodelled phenothiazines as potential antitubercular or anticancer agents

Preface

In the previous chapter, strategies selected for remodelling phenothiazines and related drugs for non-neuroleptic bioactivities were discussed. Furthermore, *in silico* prediction tools were incorporated to assess drug-likeness on the basis of Lipinski's rule of five (RO5). Properties associated with ADMET (A: Absorption; D: Distribution; M: Metabolism; E: Excretion; T: Toxicity) such as aqueous solubility, Caco-2 and MDCK cell permeability, a number of likely metabolic reactions as well as hERG inhibition were also predicted *in silico*. *In silico* prediction of CNS activity also guided the selection of NCEs that are less likely to exhibit neuroleptic effects. The resulting new chemical entities (NCEs) with promising drug-like properties were prioritized for chemical synthesis.

In this chapter, an extensive discussion of employed synthetic methods and spectroscopic characterization of the NCEs is provided. The synthesis afforded a focused library comprising pairs of remodelled phenothiazine NCEs and parent neuroleptic drugs for biological evaluation as potential antitubercular or anticancer agents.

3.1 Remodelled phenothiazines and related neuroleptic drugs

The remodelling strategies described in chapter 2 include replacement of the basic terminal amine moiety of phenothiazines with a polar sulfonate functionality and other non-basic funtionalities, introduction of bicyclic quinoline scaffolds and molecular hybridization with

antibacterial pharmacophores. Using these strategies, a diverse library of remodelled phenothiazines including *N*-alkylsulfonates, isoniazid molecular hybrids, nitrobenzene sulfonamides and *N*-alkylnitriles was generated. The chemical synthesis of these remodelled phenothiazines is discussed herein.

3.2 *N*-propylsulfonates of phenothiazines

N-propylsulfonates of phenothiazines (**3.1a-e**) were obtained by replacement of the amine moiety of phenothiazine drugs with a sulfonate functionality as described in chapter 2 (Figure 3.1).

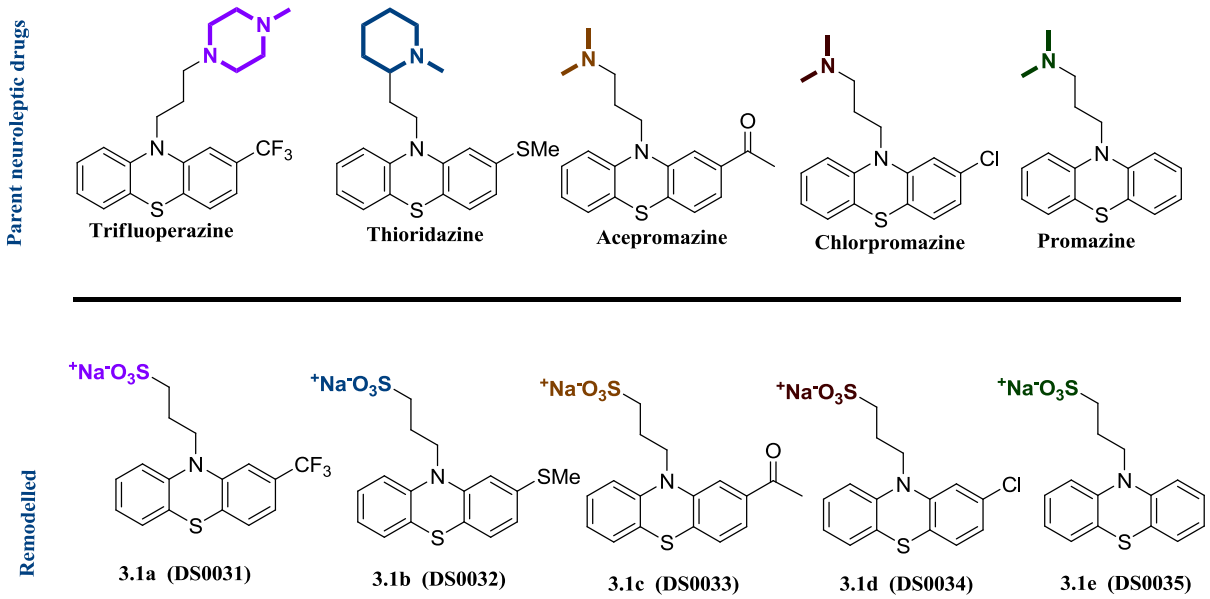

Figure 3.1: Remodelled phenothiazine drugs illustrating deviation from the lipophilic chromophore/basic side chain paradigm.

3.2.1 Retrosynthetic analysis, synthesis and analytical characterization

The classic preparation of alkylsulfonates (RSO_3^-) was first introduced by a German chemist, Aldoph Strecker, in 1868. The Strecker sulfite alkylation reaction involves nucleophilic

substitution of alkyl halides by sulfite salts in the presence of an iodide as a catalyst.[1] Other synthetic procedures for preparation of alkylsulfonic acid (RSO_3H) or their conjugate bases (RSO_3^-) include oxidation of free thiols (RSH) via formation of sulfenic acids (RSOH) and sulfinic acids (RSO_2H) using oxidants such as hydrogen peroxide, and alkaline hydrolysis of sulfonate esters.[2,3] Herein, the oxidation route (**A**) was ruled out to protect the structural integrity of the phenothiazine chromophore. A nucleophilic, *N*-alkylating, ring-opening methodology **B** was adopted (Scheme 3.1).

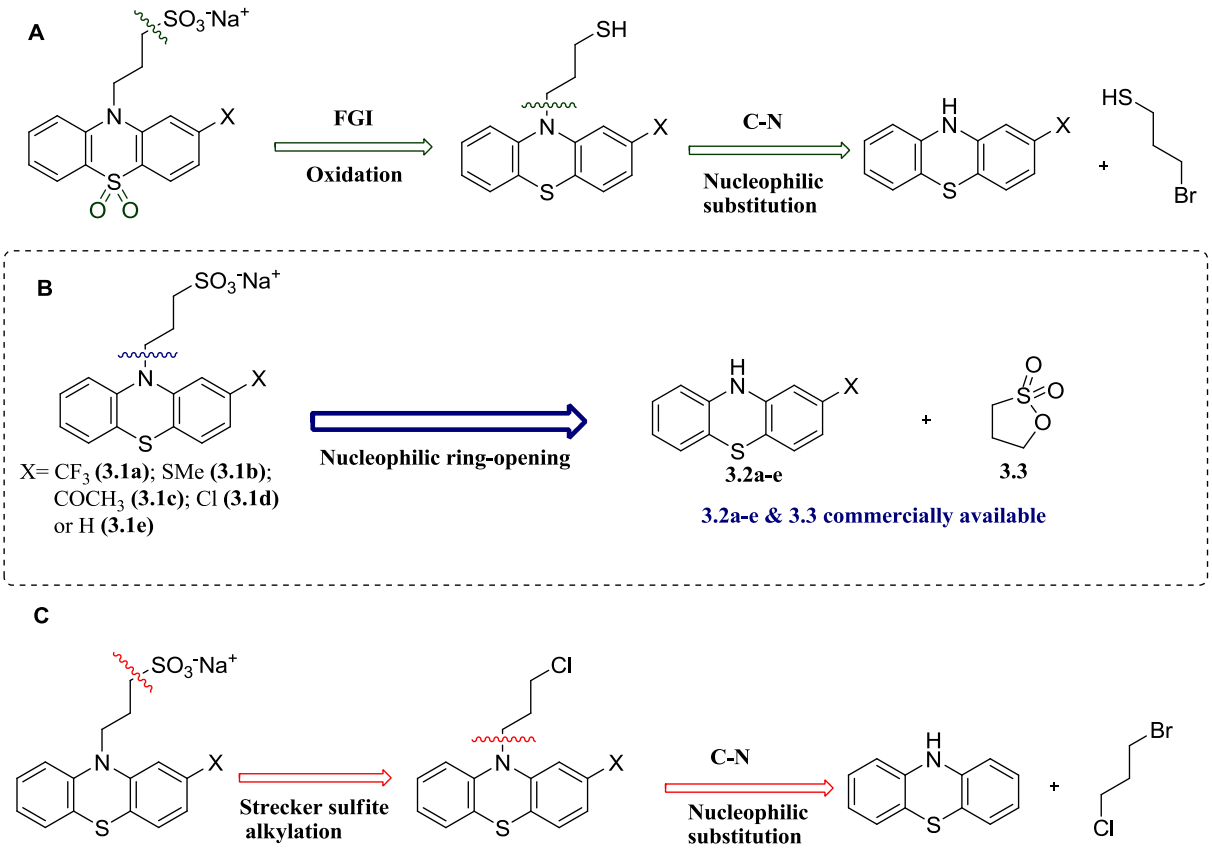

Scheme 3.1: Possible routes to synthesis of *N*-propylsulfonates **3.1a-e**; One-step route **B** was a better choice over **A** and **C** as it involved the use of readily accessible starting materials.

The synthesis of phenothiazine-based *N*-propylsulfonates **3.1a-e** was envisaged as achievable *via* a non-concerted *N*-alkylation reaction involving deprotonation of phenothiazine under

strong basic conditions subsequently followed by nucleophilic ring-opening of cyclic sulfonate ester **3.3** (Figure 3.2). Resonance and electron-withdrawing inductive effects of the sulfonate group in **3.3** render the neighbouring carbon (R**C**-OSO_2R_1) electron-deficient hence susceptible to nucleophiles.

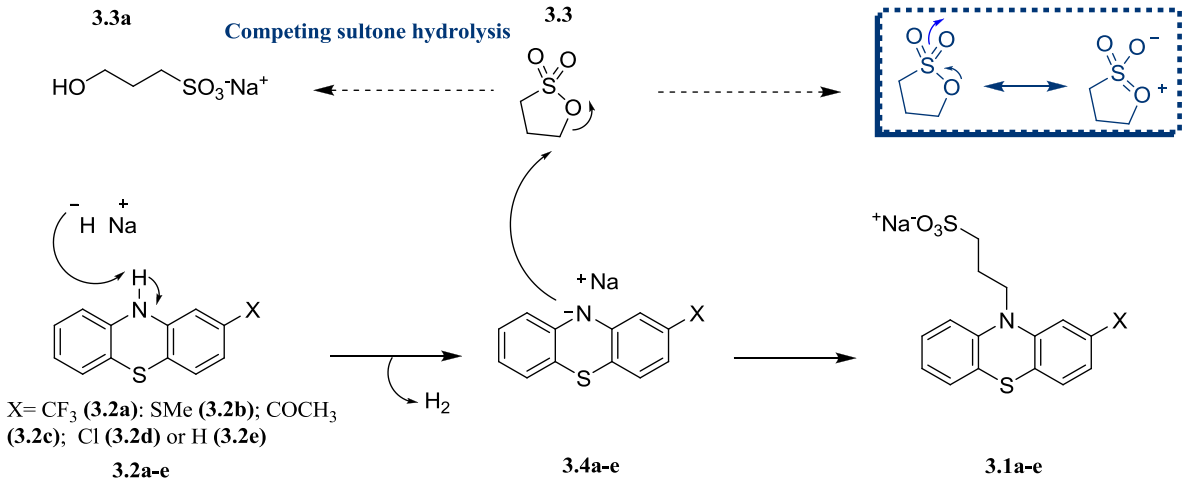

Figure 3.2: Proposed reaction mechanism for nucleophilic ring-opening of sultone **3.3** to afford NCEs **3.1a-e**.

The detailed reaction conditions for the *N*-alkylation are outlined in Scheme 3.2. It was mandatory to work under anhydrous and inert atmospheric conditions owing to the pyrophoric nature of sodium hydride and possible sultone hydrolysis under the slightest wet basic conditions. Furthermore, working under an inert atmosphere of nitrogen was necessary to avoid possible air oxidation of the phenothiazine core. Moreover, solutions of phenothiazines are prone to free radical reactions under exposure to light thus the reactions were kept in the dark as a matter of precaution.[4]

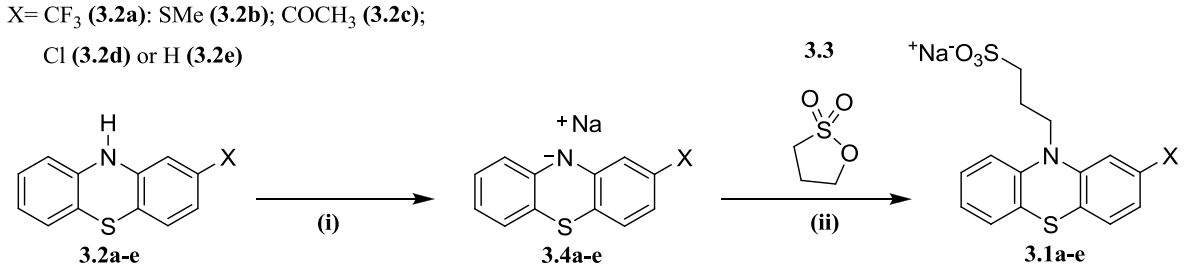

Scheme 3.2: *Reagents and conditions*: **(i)** NaH (60% dispersion in mineral oil, 1.1 eq), dry DMF, rt → 50 °C, N_2, 1.5 h; **(ii) 3.3** (1.1 eq) in dry DMF, rt, N_2, 16 h. **3.1a** (27%), **3.1b** (17%), **3.1c** (23%), **3.1d** (40%), **3.1e** (38%).

Isolation and purification of these *N*-propylsulfonates **3.1a-e** was carried out using reversed-phase chromatography due to the presence of a polar sulfonate side chain imparting aqueous solubility. In general, the reversed-phase mobile phase for elution is primarily aqueous and may include organic modifiers such as methanol and acetonitrile. Gradient elution was preferred over isocratic elution for better separation. Water was used as the eluent and methanol was gradually (0-10%) introduced. Unreacted hydrophobic starting materials were retained on the column using the above-mentioned solvent system. Notably, the amphiphilic salts **3.1a-e** displayed considerable retention on the column compared to the sultone hydrolysis product **3.3a**. This purification process avoids the use of large quantities of organic solvents, which is advantageous from a commercial and "green" perspective.

The desired compounds **(3.1a-e)** were obtained as coloured solids in relatively low yields of less than 40%. The plausible explanation for the low yields is the occurrence of a competing reaction i.e. hydrolysis of sultone **3.3** as alluded to earlier. Although significant efforts were put into place maintaining dry reaction conditions when using DMF as a solvent, the presence

of any trace of moisture would promote the formation of 'naked' hydroxide ions from hydride ions. These hydroxide ions in DMF are much more nucleophilic hence the significant sultone hydrolysis. Initially, no significant attempts were made in yield optimization as the amounts isolated were sufficient for *in vitro* bio-activity screening. Large-scale synthesis of NCEs **3.1a-e** was carried out at a later stage for preclinical *in vivo* toxicity and *in vivo* efficacy evaluation. In consideration of the high-boiling point and environmental unfriendly nature of DMF, THF was the solvent of choice for the large-scale reactions. Furthermore, anhydrous THF is commercially available on large scale and its use contributed to greater than 90% product yield. Moreover, purification was carried out by trituration with ethyl acetate to extract the minimal amount of sultone by-product and recover unreacted starting material.

In general, the following analytical techniques were employed for structure elucidation, confirmation and purity assessment of the synthesized NCEs: Melting point; 1D NMR spectroscopy (^{1}H and ^{13}C); LCMS and/or HRMS; IR. Full characterization details are outlined in chapter 7.

Inductive effects and anisotropic effects produced by the π-system of aromatic rings along with the presence of electron-donating/withdrawing groups were evident in resonance patterns observed in ^{1}H and ^{13}C NMR spectra of NCEs **3.1a-e**. Their ^{1}H NMR spectra revealed sets of peaks in the aromatic region downfield and three sets of methylene peaks upfield. Figure 3.3 shows the general pattern of resonance signals that was observed. The three methylene signals resonating at chemical shifts (δ) ranging between δ_H 2-4 ppm displayed the expected multiplicities i.e. two triplets and a quintet with vicinal coupling

constants, ^{3}J, around 7 Hz. For derivatives **3.1b** (X= SMe) and **3.1c** (X= $COCH_3$), the methyl resonance peaks were observed as singlets at δ_H 2.28 ppm and 2.43 ppm, respectively. Some of the signals were not well-resolved presumably due to salt/D_2O/H_2O solvent effects. Resonance signals in the aromatic region integrated for the correct number of protons i.e. seven for substituted derivatives **3.1a-d** and eight protons for the symmetrical derivative **3.1e**.

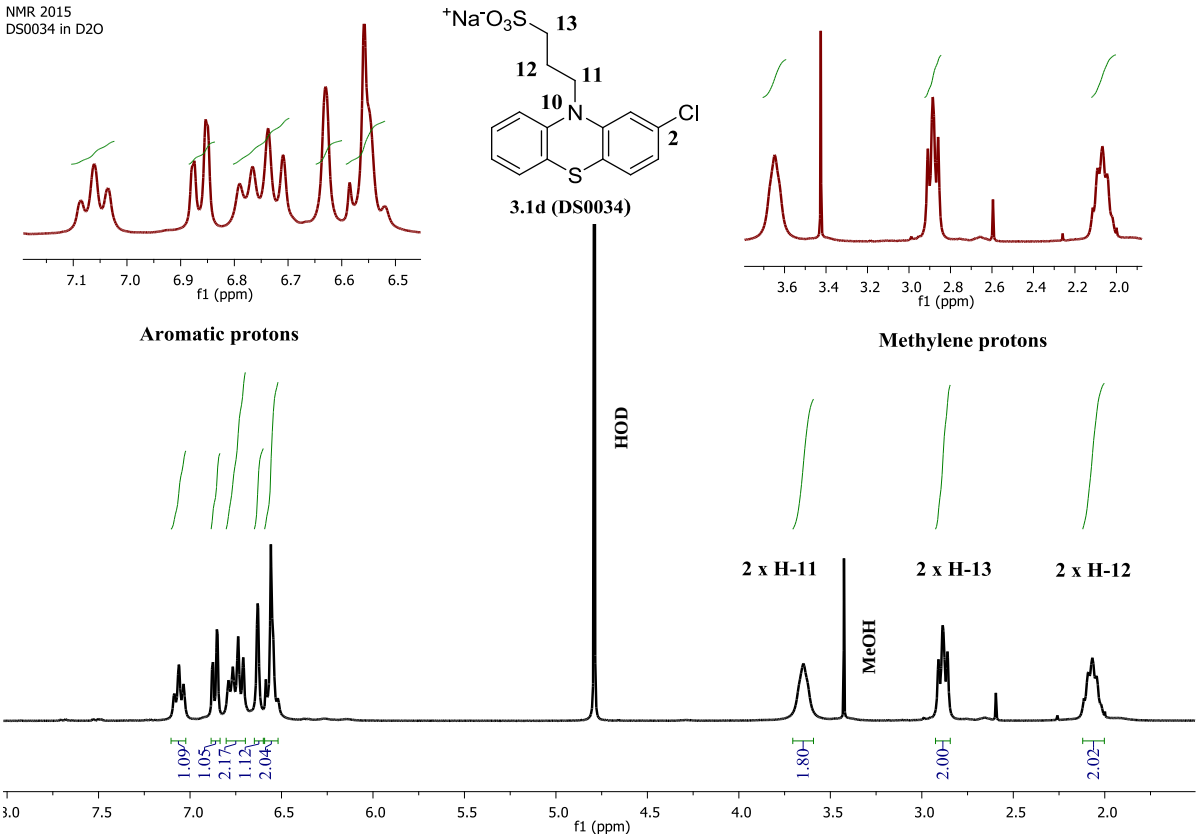

Figure 3.3: ^{1}H NMR spectrum of **3.1d** (**DS0034**) to illustrate the general pattern of resonances for NCE **3.1a-e**.

The number resonances in ^{13}C NMR spectra of all five derivatives (**3.1a-e)** were in accordance with ^{1}H NMR spectra observations. For **3.1e (DS0035)** only 6 resonance signals were observed downfield owing to an existing plane of symmetry. Derivatives **3.1b (DS0032)** and **3.1c (DS0033)** showed additional signals in the upfield region confirming the

presence of thiomethyl and acetyl groups, respectively. Also distinct in the spectrum of **3.1c (DS0033),** was a deshielded carbonyl signal resonating at δ_C 201.88 ppm. The NMR observations were further corroborated by LCMS thereby confirming the structures of the compounds and their purity. An accurate mass spectrum of **3.1d (DS0034)** with a molecular ion peak $[M]^+$ of 377.9991 calculated for $C_{15}H_{13}ClNNaO_3S_2$ (*m/z*) 377.9957 $[M]^+$ is given in Figure 3.4 as an example. The base peak ion 356.0180 corresponded to $[(M + 2H) – Na]^+$. The doubling of peaks (intensity ratio 3:1) in the mass spectrum of **3.1d** is indicative of the presence of two isotopes of chlorine i.e. ^{35}Cl and ^{37}Cl, respectively.

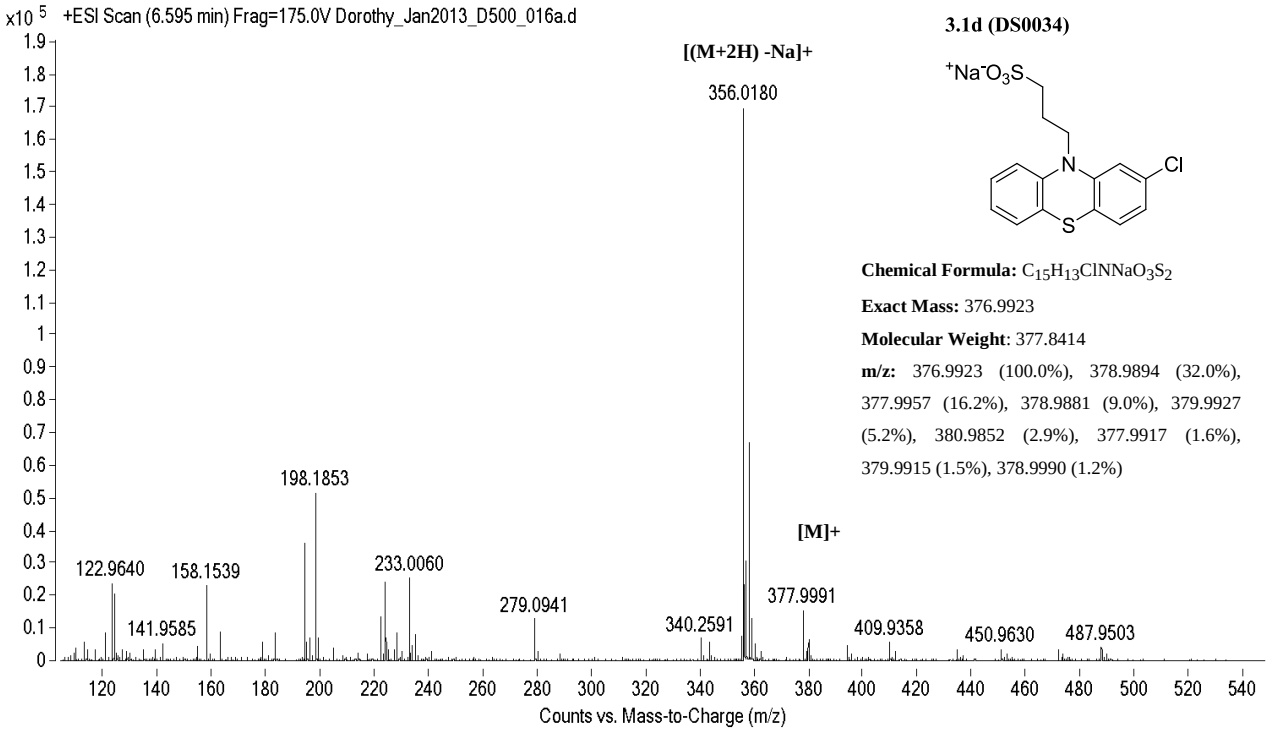

Figure 3.4: An accurate mass spectrum of **3.1d** (**DS0034**) from LCMS analysis showing isotope peaks due to the presence of chlorine. Molecular ion peak of $[M]^+$ of 377.9991 calculated for $C_{15}H_{13}ClNNaO_3S_2$ (m/z) 377.9957 $[M]^+$ was observed.

3.3 *N*-butylsulfonates of phenothiazines

Application of same strategy used to obtain *N*-propylsulfonates **3.1a-e** afforded remodelled phenothiazines **3.5a-e** with an extended alkyl linker (Figure 3.5).

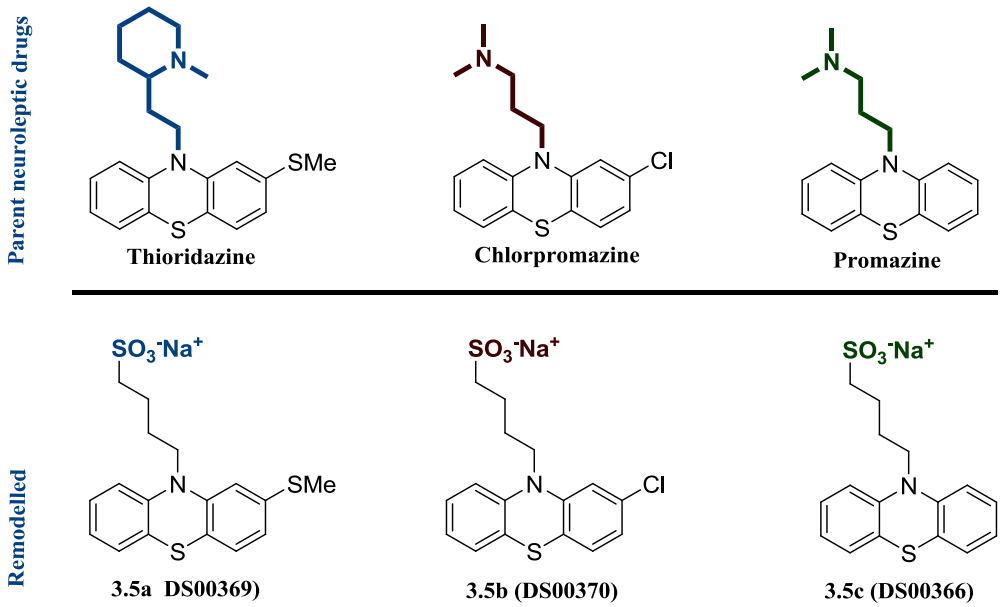

Figure 3.5: Remodelled phenothiazines with an extended alkyl linker.

3.3.1 Synthesis and analytical characterization

The synthesis of *N*-butylsulfonates NCEs **3.5a-c** was envisaged as achievable using the same approach described in section 3.2.1, similar reaction conditions and purification method were employed. However, the electrophilic alkylating agent used to afford a butyl linker was 1,4-butane sultone **(3.8)** (Scheme 3.3). Due to butane sultone being a more stable ring system than propane sultone, the rate nucleophilic attack was much slower than the competing sultone hydrolysis, hence lower yields were obtained. Sufficient materials were obtained for bio-activity testing and yield optimization using THF as a solvent was not attempted.

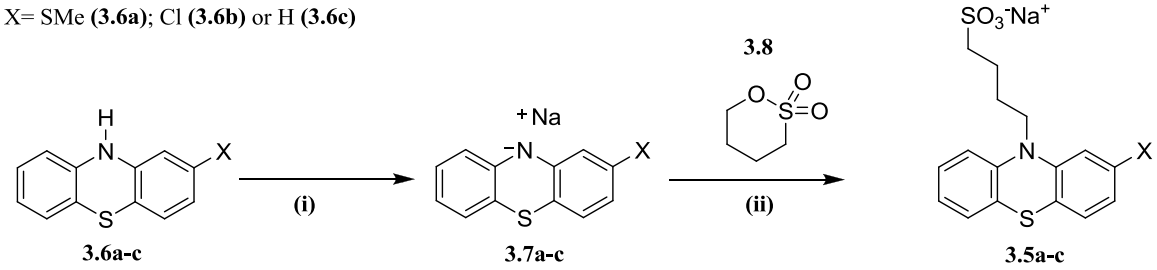

Scheme 2.3: *Reagents and conditions*: **(i)** NaH (60% dispersion in mineral oil, 1.1 eq), dry DMF, rt to 50 °C, N_2, 1.5 h; **(ii) 3.8** (1.1 eq) in dry DMF, rt, N_2, 20 h. **3.5a** (19%), **3.5b** (20%), **3.5c** (14%).

A thorough analysis of ^{1}H NMR spectra of **3.5a (DS00369)**, **3.5b (DS00370)** and **3.5c (DS00366)** revealed the same pattern of resonance signals as observed earlier for *N*-propylsulfonates **3.1a-e**. The only noticeable distinction was the presence of an extra methylene resonance in the upfield region belonging to the butyl moiety (Figure 3.6). Additional support from ^{13}C NMR spectra and LCMS analysis confirmed the structures.

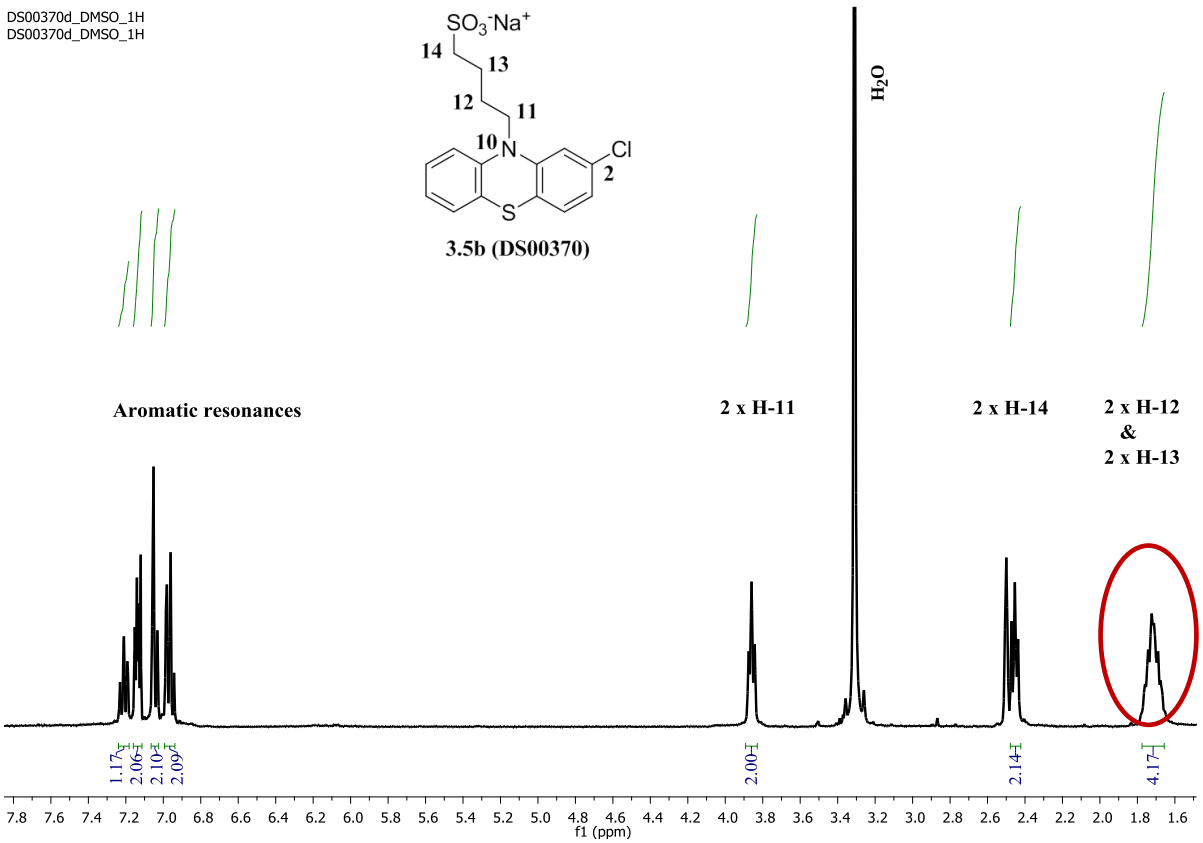

Figure 3.6: ^{1}H NMR spectrum of **3.5b** (**DS00370**) as example to illustrate the pattern observed.

3.4. *N*-propylsulfonates of ring expanded phenothiazine-like scaffolds

A ring-expansion strategy was applied to create phenothiazine-like scaffolds that mimic atypical neuroleptic drugs shown in Figure 3.7.

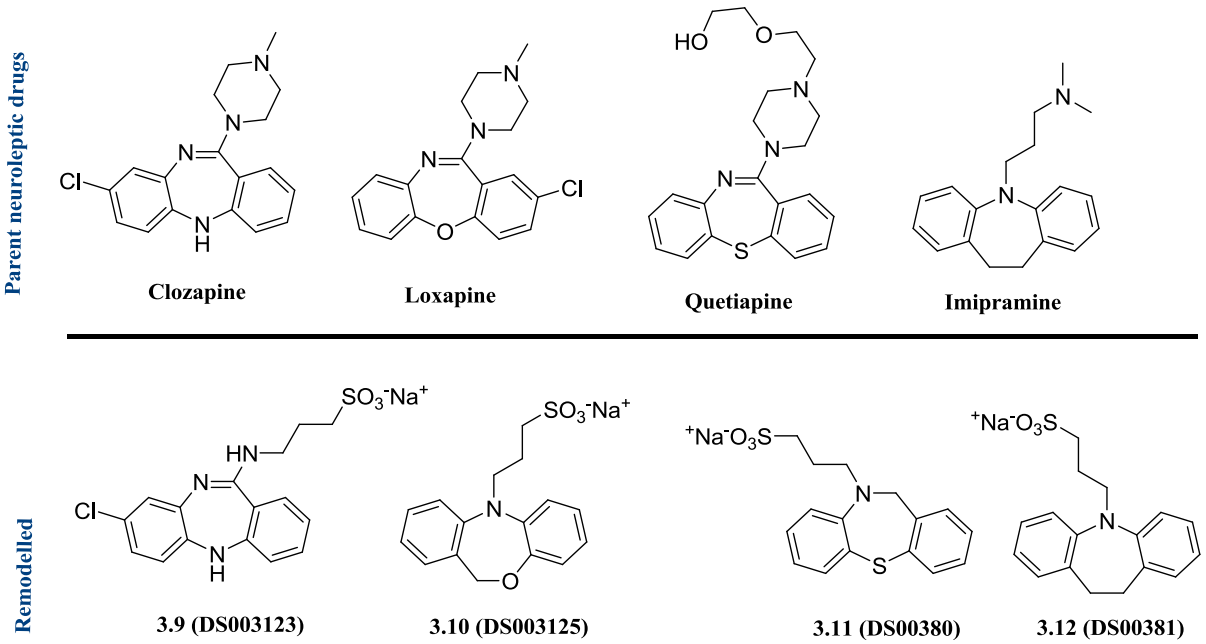

Figure 3.7: Remodelled phenothiazines mimicking structures of atypical neuroleptic drugs.

3.4.1 Synthesis of ring-expanded scaffolds

Tricyclic/ tetracyclic ring systems with central seven-membered rings are common scaffolds in numerous therapeutic agents. CNS drugs such as clozapine, imipramine, quetiapine and loxapine possess such scaffolds.[5,6,7] Accessibility of these scaffolds is in most cases hindered by multistep synthetic routes and/ or low-yielding nature of the reactions. Significant efforts were put into designing routes that could afford scaffolds which closely resemble those found in the above-mentioned atypical antipsychotics.

3.4.1.1 Synthesis of a clozapine scaffold

The synthesis of azaheterocycles was first reported in the mid-1960s.[8,9] The routes designed for the preparation of clozapine scaffolds were inspired by traditional clozapine synthesis methods reported in literature.[10] Retrosynthetic approaches to synthesis of these are depicted in Scheme 2.4. Route A shows the traditional route to synthesis of azaheterocycles involving copper-catalyzed *N*-arylation and intramolecular cyclization. Route B was of interest as it involved fewer steps to the synthesis of scaffold **3.19** and **3.20** that closely resemble clozapine (Scheme 3.4).

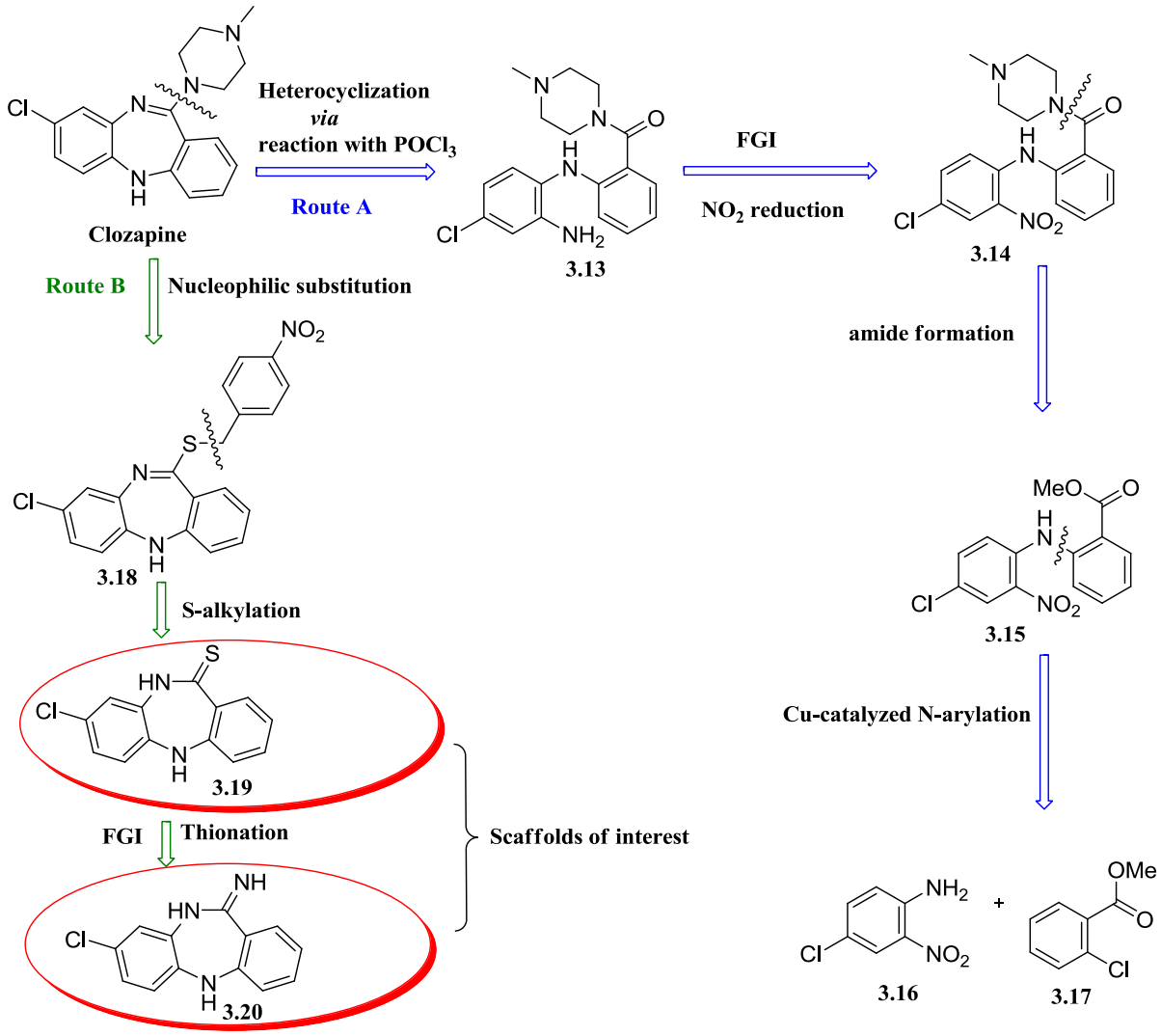

Scheme 3.4: Possible routes to preparation of clozapine scaffolds *via* Cu-catalyzed *N*-arylation or thionation.

(i) Initial approach: Copper-catalyzed *N*-arylation

Documented routes to the synthesis of dibenzodiazepines generally rely on multi-step reactions including copper-catalyzed intramolecular *N*-arylation or cross couplings under Buchwald-Hartwig conditions, iron-catalyzed nitro-group reduction as well as amide coupling.[11,8,12] Initially, the preparation of clozapine scaffold **3.25** was conceived as achievable from an adaptation of a dibenzodiazapinones synthesis procedure reported by Zhang *et al*.[12] The reaction proceeded *via* copper-catalyzed cross coupling of diamine **3.23** and benzoic ester **3.22** (Scheme 3.5). Apart from the route being shorter, the readily available starting materials made the reaction worthwhile.

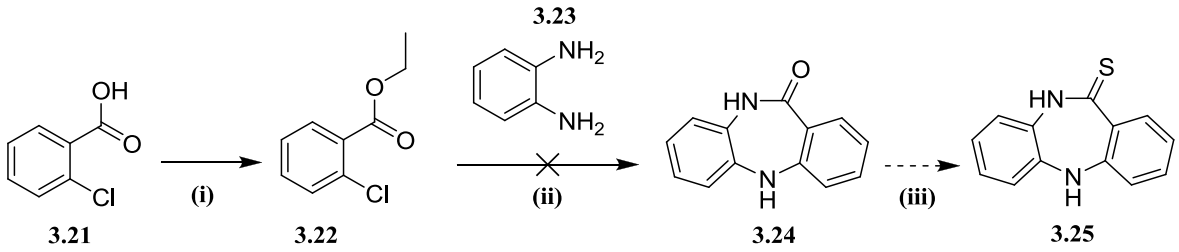

Scheme 3.5: *Reagents and conditions*: **(i) 3.21**, EtOH, HCl (aq), reflux; **(ii) 3.22** (1.0 eq), **3.23** (2.0 eq)**,** Na_2CO_3 (2.,0 eq), CuI (10 mol%); ethylene glycol, 100 °C, 4 h; **(iii)** Lawsesson's reagent (1.0 eq), THF, reflux.

The esterification reaction was conducted successfully to give benzoate **3.22**. However, the subsequent step did not afford the desired product **3.24** and hydrolysed starting material **3.21** was recovered. Failure of the *N*-arylation might be that the benzoate moiety of **3.22** is not sufficiently electron-withdrawing to favour S_NAr substitution at the *ortho* position. Additionally, Zhang *et al*. observed this reaction with iodo-/bromo-substituted benzoates and not with poorer leaving groups like chlorides (Scheme 3.5).

ii) Second approach: Acid-catalyzed *N*-arylation

The second approach was also inspired by Route B depicted in Scheme 3.4. The first step of preparation of thioamide **3.29** involved a process reported by Meshram *et al*, (US Patent 2010/0228023 Al).[13] This process appeared desirable in that formation of the clozapine scaffold **3.28** would occur in one step using inexpensive starting materials *via* an *in situ* condensation subsequently followed by cyclization. The preparation involved a reaction between isatoic anhydride **3.26** with diamine **3.27** in aqueous acetic acid heated at 75 °C for 3h (Scheme 3.6).

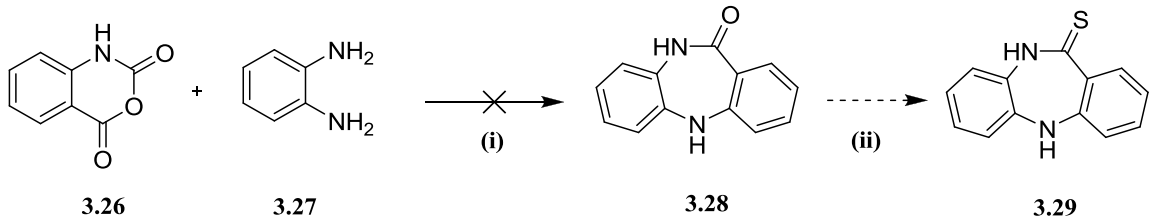

3.26 **3.27** **3.28** **3.29**

Scheme 3.6: *Reagents and conditions*: **(i) 3.26** (1.0 mmol), **3.27** (1.1 mmol), Glacial acetic acid, 75 °C, 3 h; **(ii)** Lawesson's reagent (1.0 eq), THF, reflux.

^{1}H NMR analysis of the solid precipitate revealed multiple products based on the number of resonance signals observed. None of these signals corresponded to either one of the starting materials (**3.26** and **3.27**). Therefore it was presumed that the isolated precipitate was a mixture of uncyclized intermediates and product **3.28**. No purification was attempted as the precipitate appeared as a single spot on TLC using different solvent systems and no further characterization was carried out to identify components of the mixture. Consequently, this method was not pursued any further.

(iii) Third approach: intramolecular amidine synthesis

Given the failure of the first two approaches, the focus was shifted to clozapine scaffold **3.35** (Scheme 3.7). The synthesis was envisaged as achievable from an adaptation of an intramolecular amidine synthesis procedure reported by Aicher and co-workers as illustrated in Scheme 3.7 below.[14]

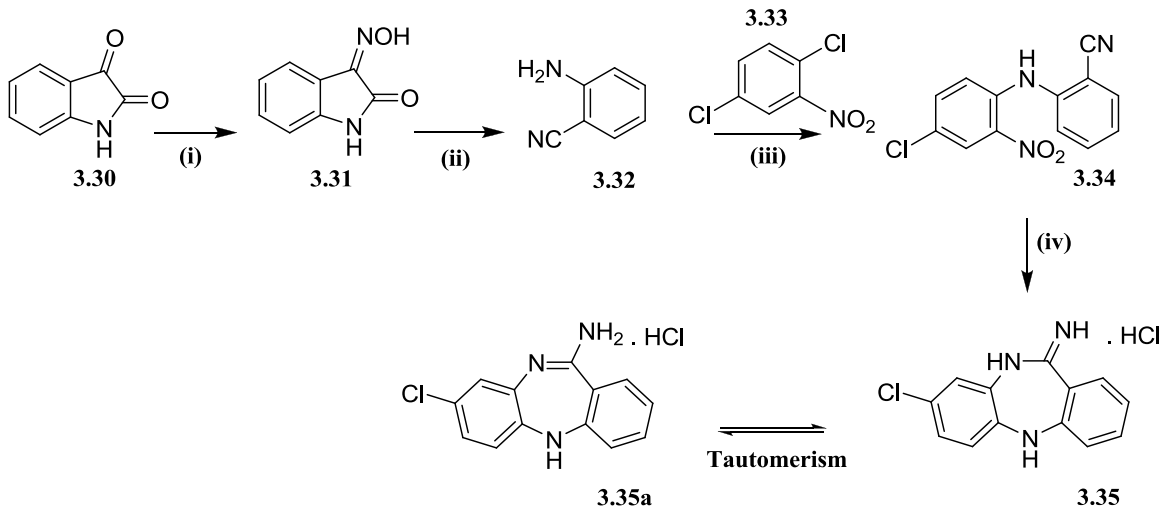

Scheme 3.7: *Reagents and conditions*: **(i)** $NH_2OH.HCl$, H_2O , reflux, 1h, 96%; **(ii)** Na_2CO_3 (0.10 eq), DMF, 135 °C, 2.5 h, 82%; **(iii) 3.32** (1.0 eq), **3.33** (1.1 eq), K_2CO_3 (1.1 eq), DMF, 120 °C, 16 h, 20% ; **(iv)** $SnCl_2.2H_2O$ (3.0 eq) in 1N HCl, absolute EtOH, reflux, 8 h, 93%.

The reaction proceeded *via* nucleophilic aromatic substitution between aminobenzonitrile **3.32** with 1,4-dichloronitrobenzene **3.33**. The *N*-arylation in this case was successful due to the presence of a strong electron-withdrawing nitro group *ortho* to a chloro leaving group. Moreover, the reaction was conducted at a relatively high temperature of 120 ° C. The subsequent step involved nitro-reduction followed by intramolecular amidine formation. The possible mechanism of this latter step is similar to the Pinner reaction whereby a protonated

nitrile group is subjected to an intramolecular nucleophilic attack.[15,16] Apart from aromatic resonances observed in the ^{1}H NMR spectrum, three distinct broad signals were observed downfield thus confirming presence of three NH protons of the tautomeric form **3.35**. The structure was further confirmed by ^{13}C NMR and LCMS analysis.

3.4.1.2 Synthesis of a 'loxapine-like' scaffold

The traditional method for synthesis of dibenzoxazepine is *via* a multi-step synthetic route that involves a key intramolecular *N*-arylation using either copper-based or palladium-based catalyst/ligand systems.[17] Herein two approaches were explored for the synthesis of dibenzoxazepine **3.39** (Scheme 3.8).

(i) Initial approach: Copper/L-proline-catalyzed intramolecular aryl amination

Initially, the synthesis of dibenzoxazepine scaffold **3.39** was conceived as achievable from a procedure reported by Guo and his co-workers.[18] The key step of this two-step procedure was intramolecular aryl amination catalyzed by a copper/L-proline system (Scheme 3.8).

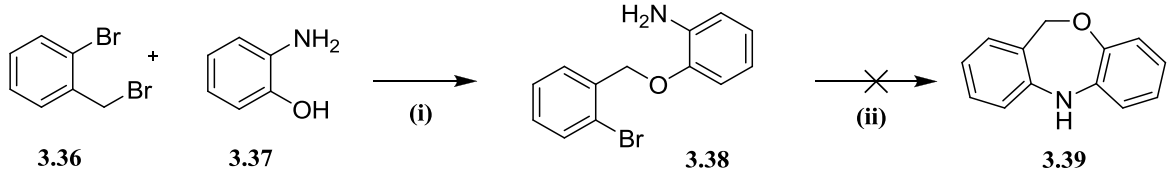

3.36 **3.37** **3.38** **3.39**

Scheme 3.8: *Reagents and conditions*: **(i)** (a) **2.37** (2.0 eq), Na_2CO_3 (4.0 eq), DMF (b) **2.36** (1.0 eq) 0°C to rt, 4 h, 45% **(ii)** Na_2CO_3 (2 eq), CuI (10 mol%), L-proline (20 mol%), DMF, 90 °C N_2, 62 h.

The etherification reaction was successful but the subsequent aryl amination step could not afford the desired product **3.39** even after the reaction was allowed to continue for prolonged hours. Guo *et al.* only isolated the desired dibenzoxazepine **3.39** in poor yields under reaction conditions represented in Scheme 3.8.[18] As difficulties were encountered with copper-catalysed *N*-arylations before, it was decided to consider palladium/ligand systems.

(ii) Second Approach: Palladium-catalyzed intramolecular *N*-arylation

The second approach involved a catalytic $Pd_2(dba)_3/P(t\text{-}Bu)_3$ system as reported by Margolis and co-workers.[9] The first step was etherification, subsequently followed by nitro-reduction and then Pd-catalyzed *N*-aryl amination as depicted in Scheme 3.9.

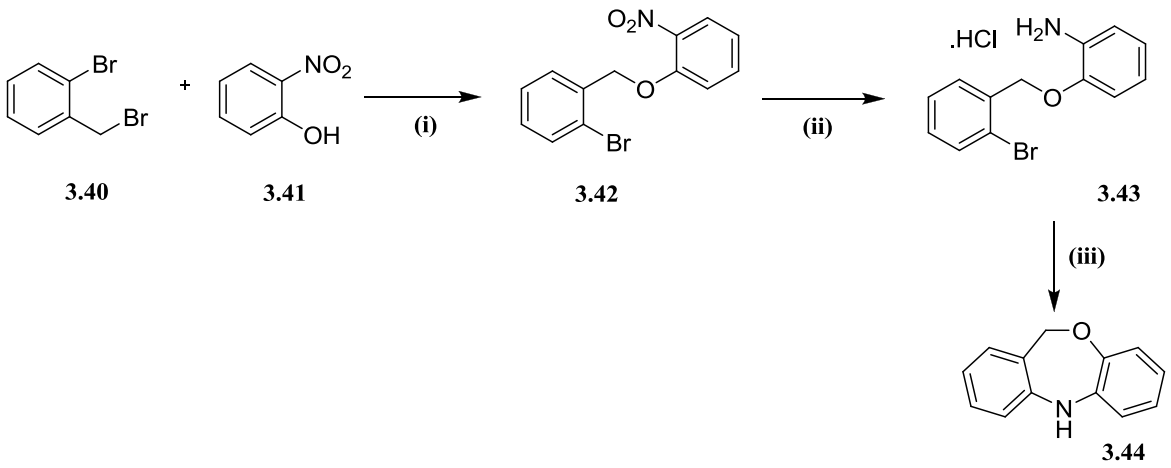

3.40 **3.41** **3.42** **3.43** **3.44**

Scheme 3.9: *Reagents and conditions*: **(i)** (a) **3.41** (2.0 eq), K_2CO_3 (2.5 eq), **3.40** (1.1 eq), 70°C, 3 h, 64%; **(ii)** Fe filings (15.0 eq), 10 N HCl, Isopropanol, 60 °C , 17 h, 88%; **(iii) 3.43** (1.0 eq) NaO-*t*-Bu (2.0 eq), K_2CO_3 (2.0 eq), $Pd_2(dba)_3$ (10 mol%), $P(t\text{-}Bu)_3$ (0.5 mol%), 95 °C, N_2, 10 h, 22%.

The first two steps of the reaction afforded product **3.42** and **3.43** in relatively good yields (Scheme 3.9). The subsequent *N*-aryl amination yielded the desired cyclized dibenzooxazepine **3.44** in a yield of 22% and unreacted starting material **3.43** was recovered.

Structure confirmation was achieved by NMR and LCMS analysis. The expected number of resonance signals was observed downfield along with a benzyl methylene resonating at δ_H 5.03 ppm. A broad resonance signal at δ_H 5.93 ppm integrated for only one NH proton as confirmation of a successful cyclization.

3.4.1.3 Synthesis of a dibenzothiazepine scaffold

Synthetic approaches to thiazepine-based ring systems vary from cross couplings to rearrangements of existing rings.[9,19,20] Approaches that were attempted for preparation of dibenzothiazepine to mimic a quetiapine scaffold are discussed below.

(i) Schmidt rearrangement Approach

The Schmidt reaction is a useful method of insertion of nitrogen next to a carbonyl group. It involves reaction of azides with electrophilic carbonyls in the presence of an acid catalyst to form an amide. This goes *via* an azidohydrin intermediate which rearranges with expulsion of nitrogen.[21,22,23] The preparation of thiazepine **3.47** was conceived as achievable using this reaction followed by reductive deoxygenation using BH_3.THF complex (Scheme 3.10).[24] Due to the symmetrical nature of **3.45**, regioselectivity issues would be avoided.

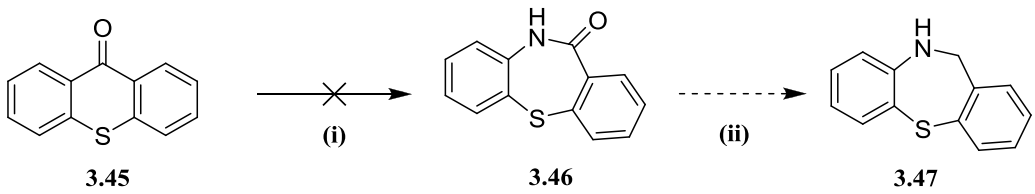

Scheme 3.10: *Reagents and conditions*: **(i)** NaN_3 (3 eq), conc. H_2SO_4**,** CH_3CN, 0 °C to rt (12 h); **(ii)** BH_3.THF complex, dry THF, -10 °C, reflux, N_2.

The ^{1}H NMR spectrum of the isolated compound was consistent with that of pure starting material **3.45** hence, no reaction took place. Other attempts using different reaction conditions, i.e. changing the source of azide (trimethylsilyl azide) and varying the solvent (e.g. THF and DCM), were also not successful.

(ii) Beckmann rearrangement approach

The second approach chosen involved the use of oximes to form amides *via* the Beckmann rearrangement. The rearrangement is envisioned to proceed *via* alkyl migration induced by an electropositive oxime nitrogen under acid conditions.[21,25] An attempt to synthesize the desired thiazepine **3.51** under the conditions outlined in Scheme 3.11 was futile and starting material **3.48** was recovered.

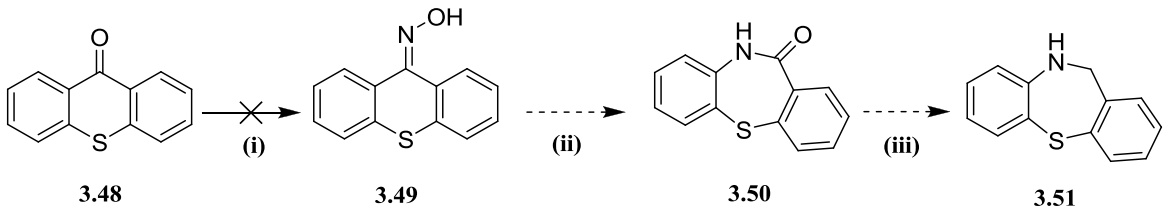

3.48 **3.49** **3.50** **3.51**

Scheme 3.11: *Reagents and conditions*: **(i)** $NH_2OH.HCl$ (5.0eq) NH_4OAc (5.0 eq), EtOH, reflux, 10h; **(ii)** conc. H_2SO_4, Δ. **(iii)** BH_3.THF complex, dry THF, -10 °C, reflux, N_2.

The first two approaches to dibenzothiazepine i.e. *via* Beckmann rearrangement or Schmidt rearrangement were unsuccessful presumably due to the limited accessibility of the thioxanthone keto-group to nucleophilic addition.

(iii) S-arylation approach

After futile attempts to synthesize the desired thiazepine scaffold *via* rearrangement approaches, another route was designed as shown in Scheme 3.12. The first step of the route involved one-pot imine formation and S-arylation. The subsequent step was a facile reduction of imine **3.54** using sodium borohydride in methanol.

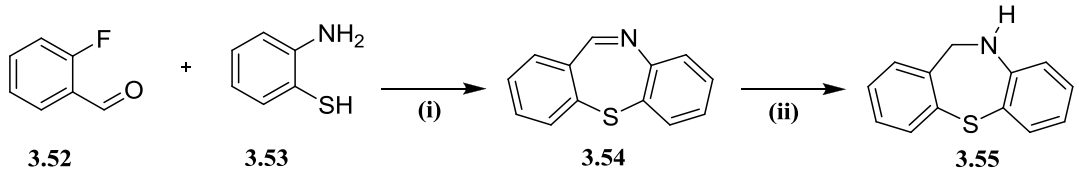

3.52 **3.53** **3.54** **3.55**

Scheme 3.12: *Reagents and conditions*: **(i) 3.52** (1.0 eq), **3.53** (1.0 eq), K_2CO_3 (0.80 eq), DMF, 100 °C, 20 h, 53%; **(ii)** $NaBH_4$ (1.0 eq), MeOH, 0 °C → rt, 91%.

The S-arylation route successfully afforded thiazepine **3.55**. The structures were confirmed by NMR and LCMS analysis. ^{1}H NMR of **3.54** revealed a characteristic imine signal downfield resonating at δ_H 8.92 ppm. After reduction, the imine resonance signal disappeared and a methylene resonance of **3.55** was observed at δ_H 4.85 ppm.

3.4.2 Synthesis of *N*-alkylsulfonates of ring-expanded phenothiazine-like scaffolds

NCEs **3.9-3.12** were prepared from the ring-expanded scaffolds (**3.35**, **3.44**, **3.55** & commercially available 10,11-dihydro-5H-dibenzoazepine (**3.56)** *via* the general sultone ring-opening procedure described in section 3.2.1 (Scheme 3.13). For NCE **3.9**, the alkylation was envisaged as achievable *via* thionation as illustrated in Scheme 3.4 (Route B). However a direct sultone ring-opening attempt under mild basic conditions was successful using sodium

carbonate as a base. The reactions were all extremely low yielding due to a competing sultone hydrolysis side reaction. However, the amounts isolated were sufficient for bio-activity screening. Optimization of yields was not prioritized and unreacted starting materials were recovered.

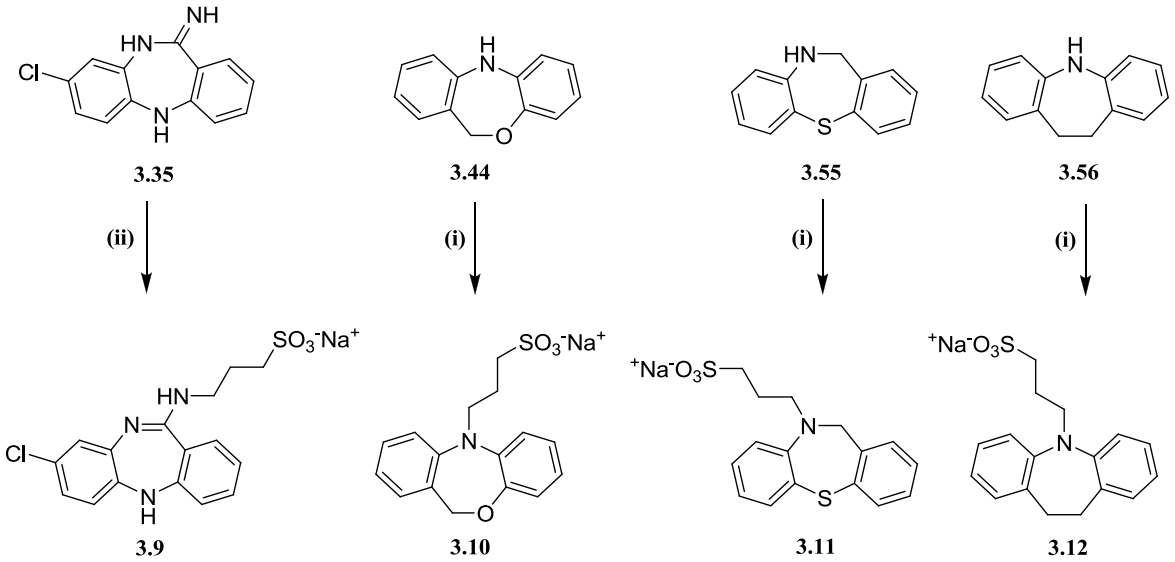

Scheme 3.13: *Reagents and conditions*: **(i)** NaH (60% dispersion in mineral oil, 1.1 eq), dry DMF, rt → 50 °C, N_2, 1.5 h; 1,3-propane sultone **3.3** (1.1 eq) in dry DMF, rt, N_2, 16 h → 18 h. **3.10** (22%), **3.11** (18%), **3.12** (18%); **(ii)** Na_2CO_3 (1.1 eq), dry DMF, rt → 50 °C, N_2, 1.5 h; 1,3-propane sultone **3.3** (1.1 eq) in dry DMF, rt, N_2, 12 h **3.9** (11%).

The structures and purity were confirmed by NMR and LCMS analysis. Figure 3.8 exemplifies the general pattern of resonances observed in the ^{1}H NMR spectrum of oxazepine **3.10**. The distinctive feature in the spectrum is the methylene resonance at δ_H 5.40 ppm indicative of a central seven-membered ring. The rest of the NCEs **3.9**, **3.11** and **3.12** also displayed similar patterns of resonances in the upfield and downfield regions.

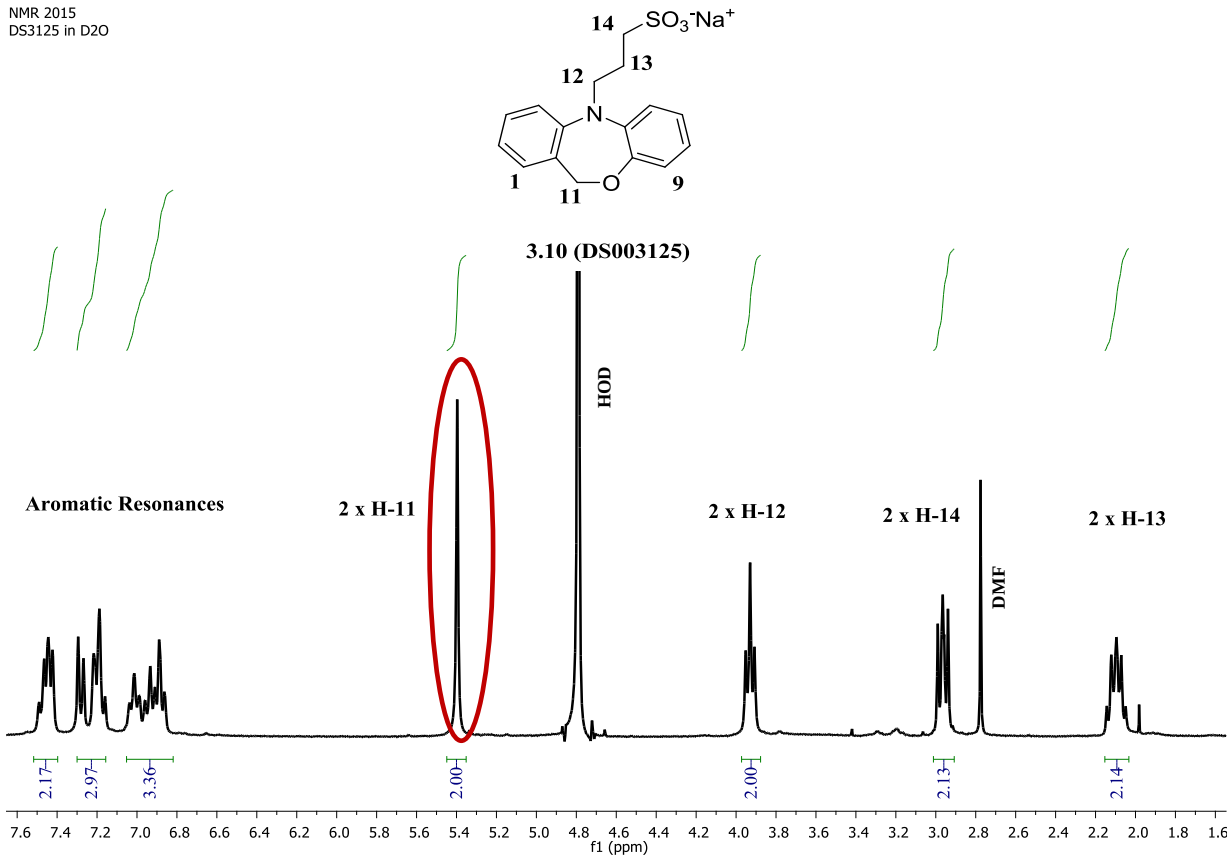

Figure 3.8: ^{1}H NMR spectrum of **DS003125** (**3.10**) to illustrate the pattern of resonance signals observed.

3.5 *N*-propylsulfonates of quinolines

As discussed in chapter 2, quinolines are of interest to this research study owing to their structural resemblance to neuroleptic phenothiazines. The strategy that was applied in remodelling phenothiazines in section 3.2.1 was also used generate *N*-propylsulfonates of quinolines (Figure 3.9).

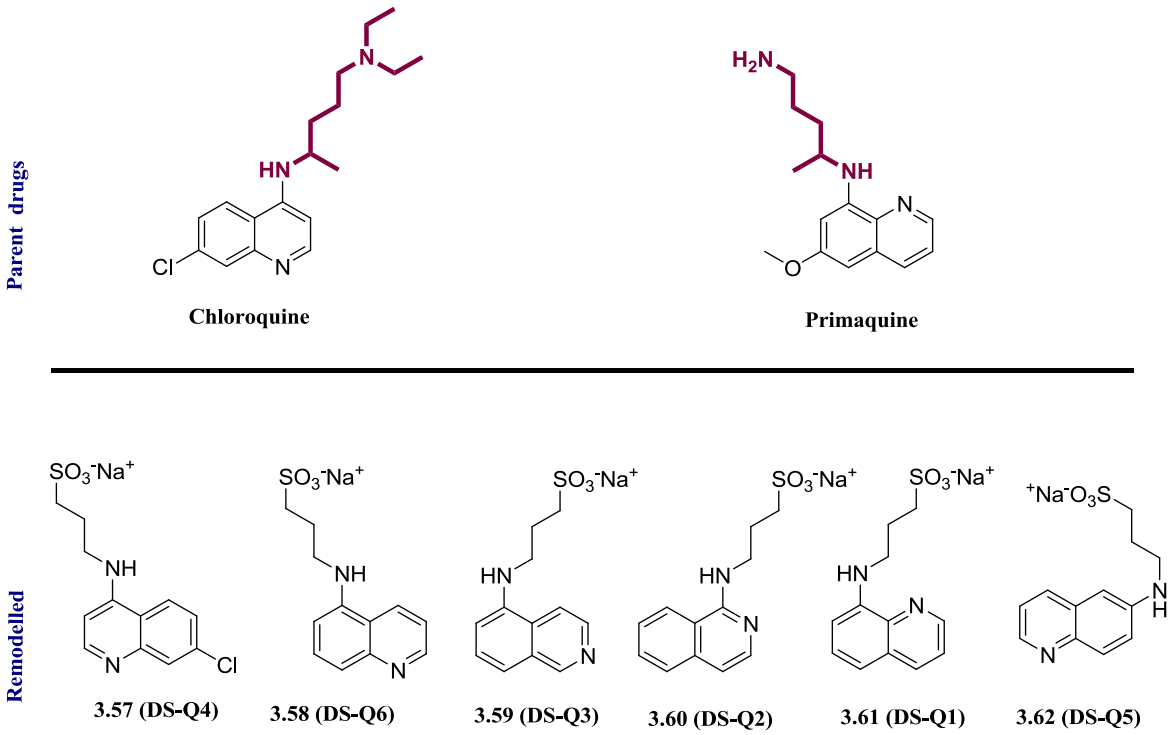

Figure 3.9: *N*-propylsulfonates of bicyclic quinolines.

3.5.1 Synthesis of *N*-propylsulfonates of quinolines

The approach described in section 3.2.1 was employed in preparation of quinoline and isoquinoline-based *N*-propylsulfonates (Scheme 3.14). Contrary to the appreciable retention displayed by phenothiazine-based *N*-alkylsulfonates **(3.1a-e)**, the quinoline-based derivatives **(3.57-3.62)** showed poor retention on reversed-phase columns. Consequently, co-elution with sultone hydrolysis product **3.3a** occurred. Repeated chromatography was necessary to afford NCEs **3.57-3.62** in pure form. The compounds were obtained in low yields due to a competing sultone hydrolysis side reaction as discussed previously.

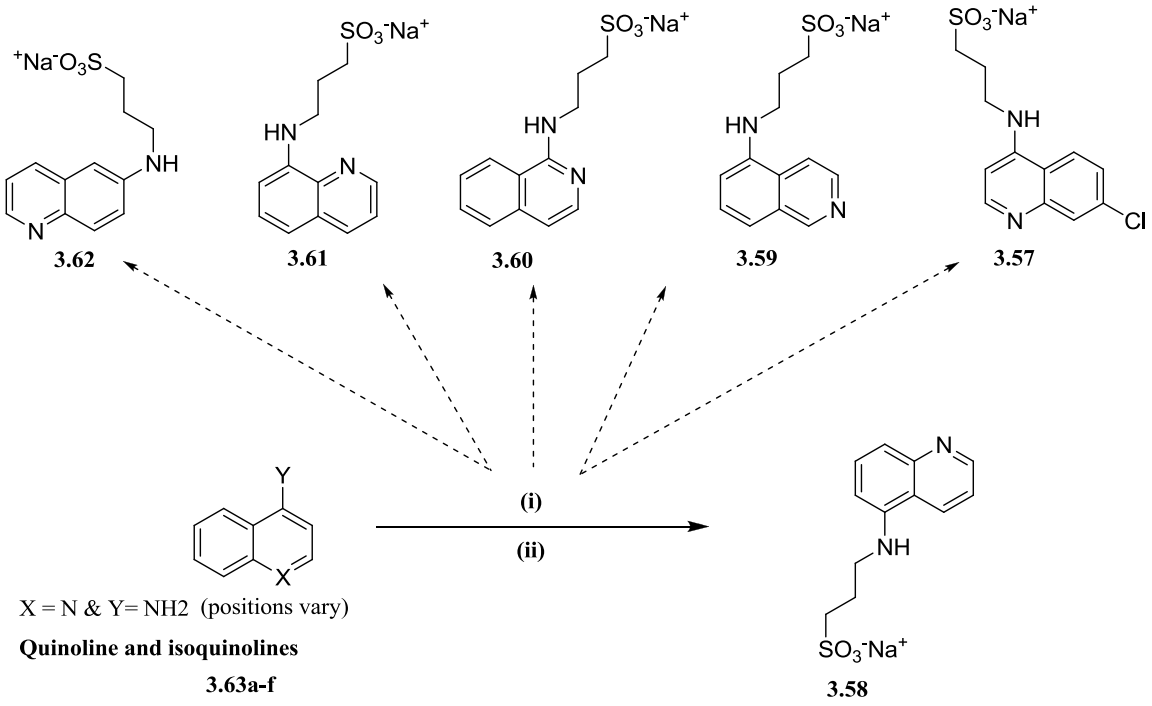

Scheme 3.14: *Reagents and conditions*: **(i)** NaH (60% dispersion in mineral oil, 1.1 eq), dry dioxane, rt to 40 °C, N_2, 1 h; **(ii)** propane sultone **3.3** (1.0 eq) in dry dioxane, rt, N_2, 14 h. **3.58** (10%), **3.59** (11%), **3.60** (16%), **3.61** (22%), **3.62** (11%), **3.57** (13%).

^{1}H and ^{13}C NMR spectra corroborated by LCMS analysis confirmed the structures of the desired NCEs **3.57-3.62**. A thorough analysis of ^{1}H NMR spectra further confirmed that all the derivatives were mono-alkylated as the resonance signals integrated for the expected number of protons. The resonance patterns differed based on the position of the quinoline nitrogen and the side chain (Figure 3.10). Given the nature of the structures, intramolecular/ intermolecular hydrogen bonding is expected to affect chemical shifts of the amine protons in particular. However due to D_2O exchange, the amine protons were not observed.

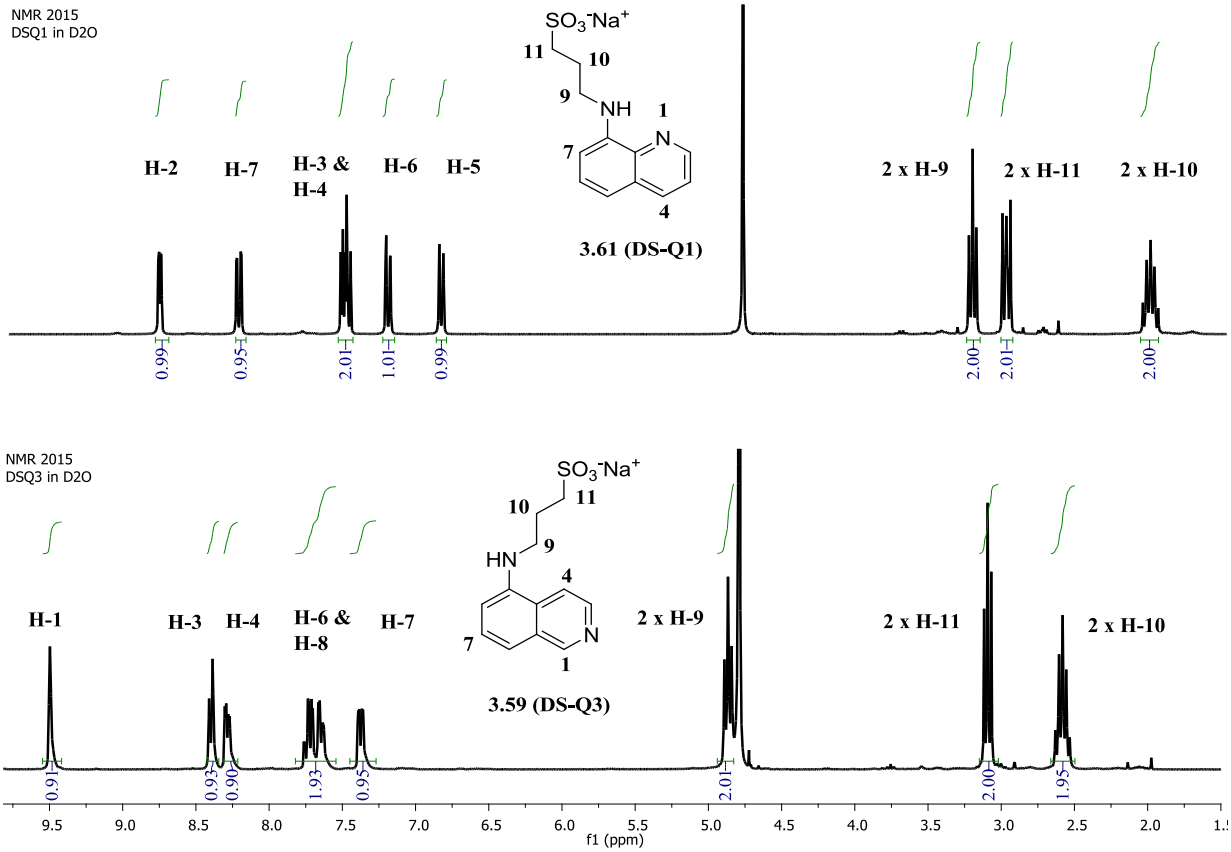

Figure 3.10: ^{1}H NMR spectra of **3.61** and **3.57** to illustrate the differing patterns of resonance signals.

3.6 Propylsulfonates of scaffolds without a thiazine central ring

Replacement of the central thiazine ring of phenothiazines with a thiane and acridine ring afforded NCEs shown in Figure 3.11.

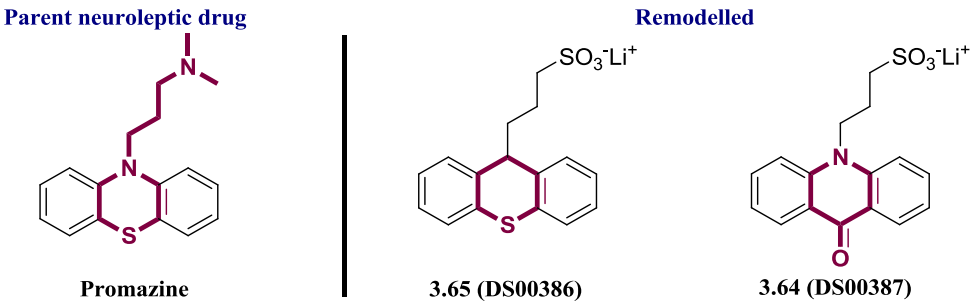

Figure 3.11: Propylsulfonates of non-thiazine phenothiazine-like scaffolds.

3.6.1 Thiane ring from reductive deoxygenation of thioxanthone

Conversion of ketones to the corresponding hydrocarbons is traditionally achieved *via* the use of methods such as Clemmensen reduction and Wolff-Kishner reduction. Clemmensen reduction of ketones occurs at the surface of a zinc metal catalyst under very strong acidic conditions with heating.[21] The alternative Wolff-Kishner reduction occurs under strong basic conditions *via* the formation of a hydrazone using hydrazine.[21] Reductive deoxygenation of ketones/aldehydes has been reported under milder conditions using reducing agents such as borane complexes or copper-based catalyst systems.[24] Herein, a BH_3.THF complex method was employed for preparation of thioxanthene **3.67** from thioxanthone **3.66** (Scheme 3.15).

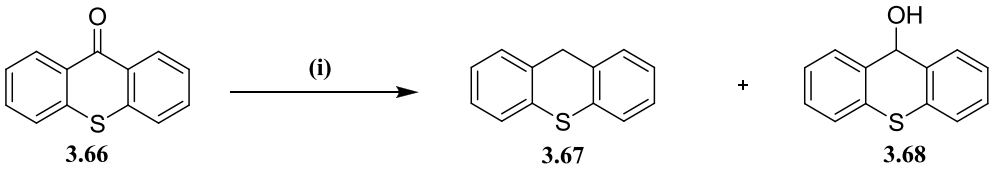

3.66 **3.67** **3.68**

Scheme 3.15: *Reagents and conditions*: **(i)** 1M BH_3.THF complex (2.0 eq), dry THF, -10 °C, rt → reflux, 14h, **3.67** 51%, alcohol **3.68** (15%) **+** unreacted starting material **3.66**.

The reductive deoxygenation reaction afforded desired product **3.67** including alcohol **3.68**. The structure of product **3.67** was confirmed by ^{1}H NMR and ^{13}C NMR analysis which revealed a methylene signal resonating at δ_H 3.89 ppm and disappearance of a ketone resonance, respectively.

3.6.1 Propylsulfonates of thioxanthene and acridone

The preparation of NCEs **3.64** and **3.65** was conceived as achievable *via* the general sultone ring-opening procedure described in section 3.2.1. However, a much stronger base, *n*-butyl lithium (pK_a ~ 50), was chosen to facilitate C-alkylation of thioxanthene **3.66** (Scheme 3.16).

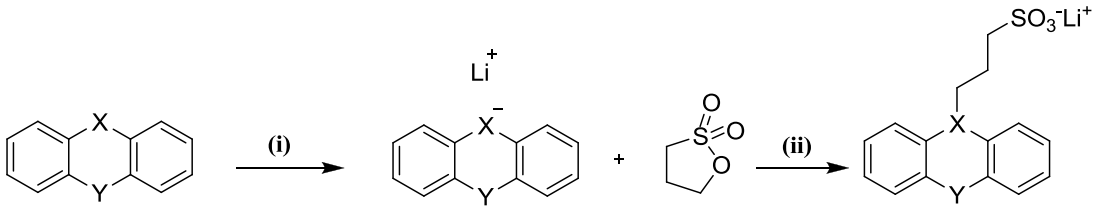

3.66 X= CH_2; Y=S
3.69 X= N; Y C(O)

3.66a & **3.69a**

3.3

3.65 X= CH, Y= S
3.64 X= N, Y= C(O)

Scheme 3.16: *Reagents and conditions*: **(i)** n-BuLi (1.0 eq), dry THF, -20 °C → rt, N_2, 0.5 h; **(ii) 3.3** (1.3 eq) in dry THF, rt, N_2, 16 h. **3.64** (24%), **3.65** (12%).

The purification was carried out using reversed-phase chromatography which was advantageous in that the sulfonate product (**3.64** or **3.65**) was eluted before unreacted starting material. NMR and LCMS analysis confirmed structures of desired products **3.64** and **3.65**. In the ^{1}H NMR spectrum of **3.65**, a triplet resonating at δ_H 3.85 ppm with a ^3J of 6.9 Hz confirmed C-alkylation.

3.7 Molecular hybrids of phenothiazines

3.7.1 Phenothiazine-isoniazid hybrids

The synthesis of phenothiazine-isoniazid hybrids was envisaged as achievable from a two-step synthesis route. This included an *N*-alkylation with 1-bromo-3-chloropropane followed by nucleophilic substitution on the side chain. The reaction conditions employed to achieve

this are outlined in Scheme 3.17. In chapter 2, the isoniazid dimers were predicted to have poor drug-like properties and were thus of least priority. However, step (ii) of the synthesis yielded both monomers **3.72a-c** and dimers **3.73a-c**. Therefore, the dimers were also isolated for biological evaluation.

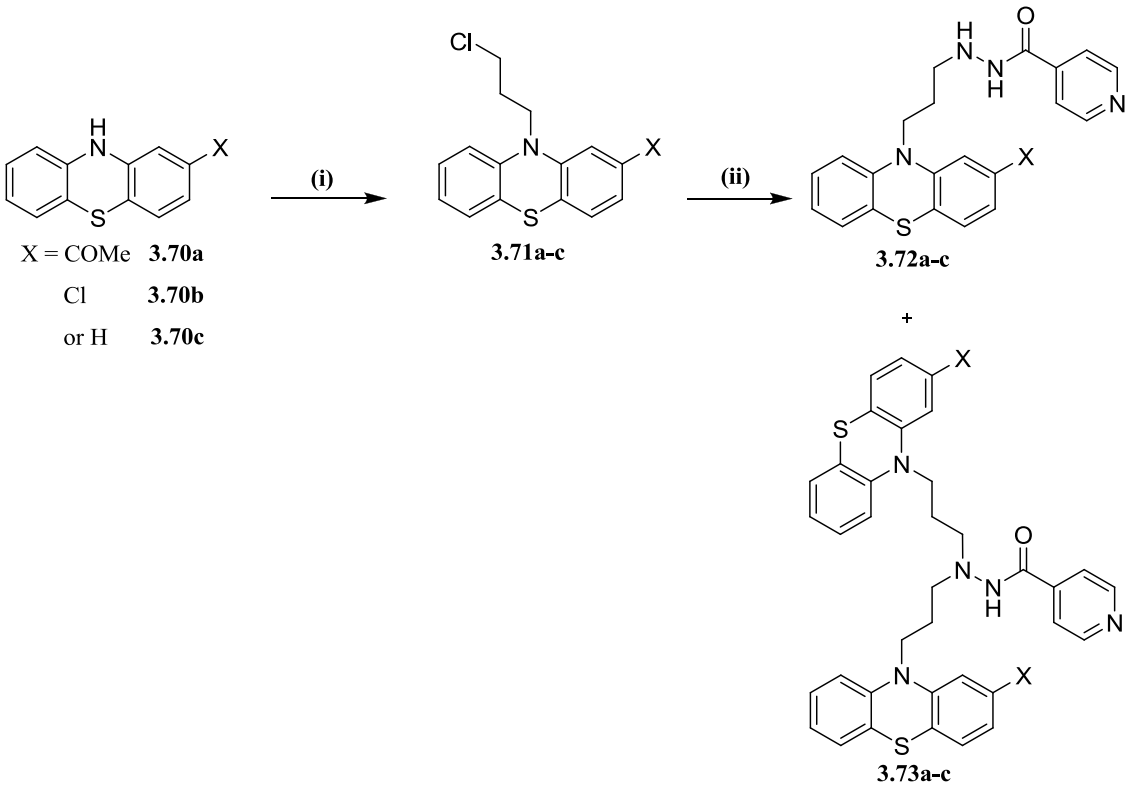

Scheme 3.17: *Reagents and conditions*: **(i)** NaH (1.1 eq), dry DMF, N_2, 0 °C → rt, 1.5 h, 1-bromo-3-chloropropane (1.0 eq), rt, 21 h. **3.70a** (38%), **3.70b** (79%), **3.70c** (26%) ; **(ii)** Isoniazid (1.0 eq), NaH (1.0 eq), dry DMF, N_2, 0 °C → rt, 0.5 h, **3.71a-c** (1.0 eq), rt, 36 h. **3.72a** (20%), **3.72b** (22%), **3.72c** (26%)., **3.73a** (13%), **3.73b** (15%), **3.73c** (18%).

^{1}H NMR spectra of the hybrids displayed two distinct sets of deshielded signals resonating in the δ_H range 7.70-8.73 ppm which were assigned to the pyridine ring. Integrals for all methylene and phenothiazine resonances doubled for the dimers. The structures were further confirmed by ^{13}C NMR and LCMS analysis.

3.7.2 *Ortho- and para-* nitrobenzenesulfonamides of phenothiazines

The synthesis of nitrobenzenesulfonamides of phenothiazines **3.74a-c** and **3.76a-c** was envisaged as achievable from a direct condensation of *ortho*- or *para*-nitrobenzenesulfonyl chlorides with the respective phenothiazines as illustrated in Scheme 3.18.

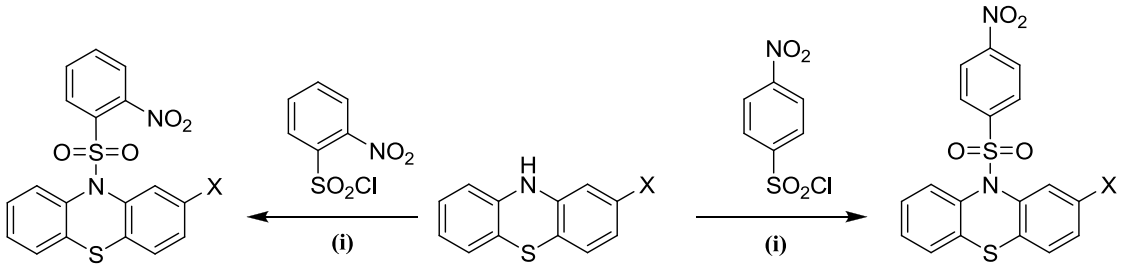

Scheme 3.18: *Reagents and conditions*: **(i) 3.75a-c** (1.0 eq), *ortho*- or *para*-nitrobenenzesulfonyl chloride (1.0 eq), dry pyridine, 50 °C, N_2, 32 h. **3.74a** (49%), **3.74b** (12%), **3.74c** (22%), **3.76a** (21%), **3.76b** (38%), **3.76c** (46%).

^{1}H NMR and ^{13}C NMR spectra revealed aromatic resonances with differing patterns depending on the type of substitution. For *ortho*-nitro derivatives **3.74a-c**, the aromatic resonances were observed in the range δ_H 6.75-9.22 ppm and for the *para*-nitro derivatives **3.76a-c** the range was δ_H 7.37-8.92 ppm. The formation of the sulfonamide bond was confirmed with IR spectra showing sulfonamide absorption bands in the frequency range 1344-1351 cm^{-1}. These results were further corroborated by LCMS analysis.

3.7.3 Pyrazole- and isoxazole-linked phenothiazine derivatives

The synthesis of pyrazole-linked and isoxazole-linked phenothiazines (**3.79** & **3.80**, respectively) was achieved from adaptation of a procedure reported by Mekky *et al*.[26] The reaction conditions are outlined in Scheme 3.19.

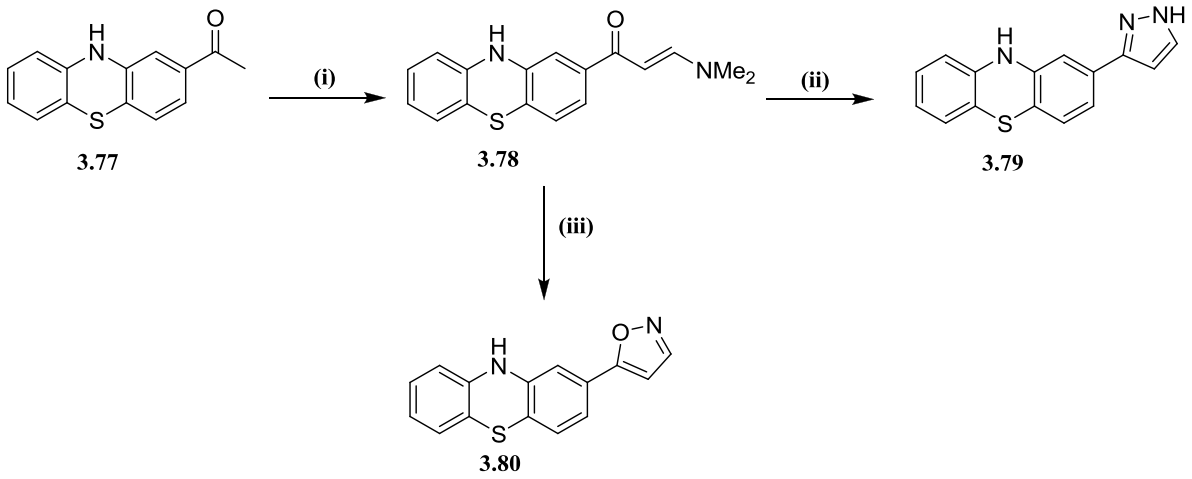

Scheme 3.19: *Reagents and conditions*: **(i) 3.77** (1.0 eq), Dimethylformamide-dimethylacetal (DMF-DMA) (2.0 eq), dry toluene, reflux, N_2, 47%; **(ii) 3.78** (1.0 eq), $NH_2NH_2.H_2O$ (excess), EtOH, rt, 14h, 83%; **(iii) 3.78** (1.0 eq), $NH_2OH.HCl$ (3.0 eq), EtOH, rt, 14 h, 85%.

The ^{1}H NMR spectrum of enaminone **3.78** revealed two ethylenic protons resonating at δ_H 7.69 and 5.69 ppm with a ^3J of 12.3 Hz which is indicative of an *E*-configuration. In addition two singlets were observed at δ_H 3.14 ppm and 2.90 ppm, which were assigned to the *N,N*-dimethyl protons. The ^{1}H NMR spectra of pyrazole **3.79** and isoxazole **3.80** revealed aromatic resonances in the ranges δ_H 7.71-6.56 ppm and 8.62-6.70 ppm respectively. ^{13}C NMR and LCMS analysis corroborated these observations.

3.8 Phenothiazines with non-basic side chains

Apart from *N*-propylsulfonates of phenothiazines, other derivatives with non-basic side chains were designed as described in chapter 2 (Scheme 3.20).

3.8.1 Retrosynthetic analysis and synthesis details

Scheme 3.20 illustrates the retrosynthetic plan undertaken which involved four key one-step routes to afford desired NCEs **3.82a-d** and **3.83-3.84**. Three of the routes (B-C) were designed from aza-Michael addition product **3.82a** as depicted in Scheme 3.20.

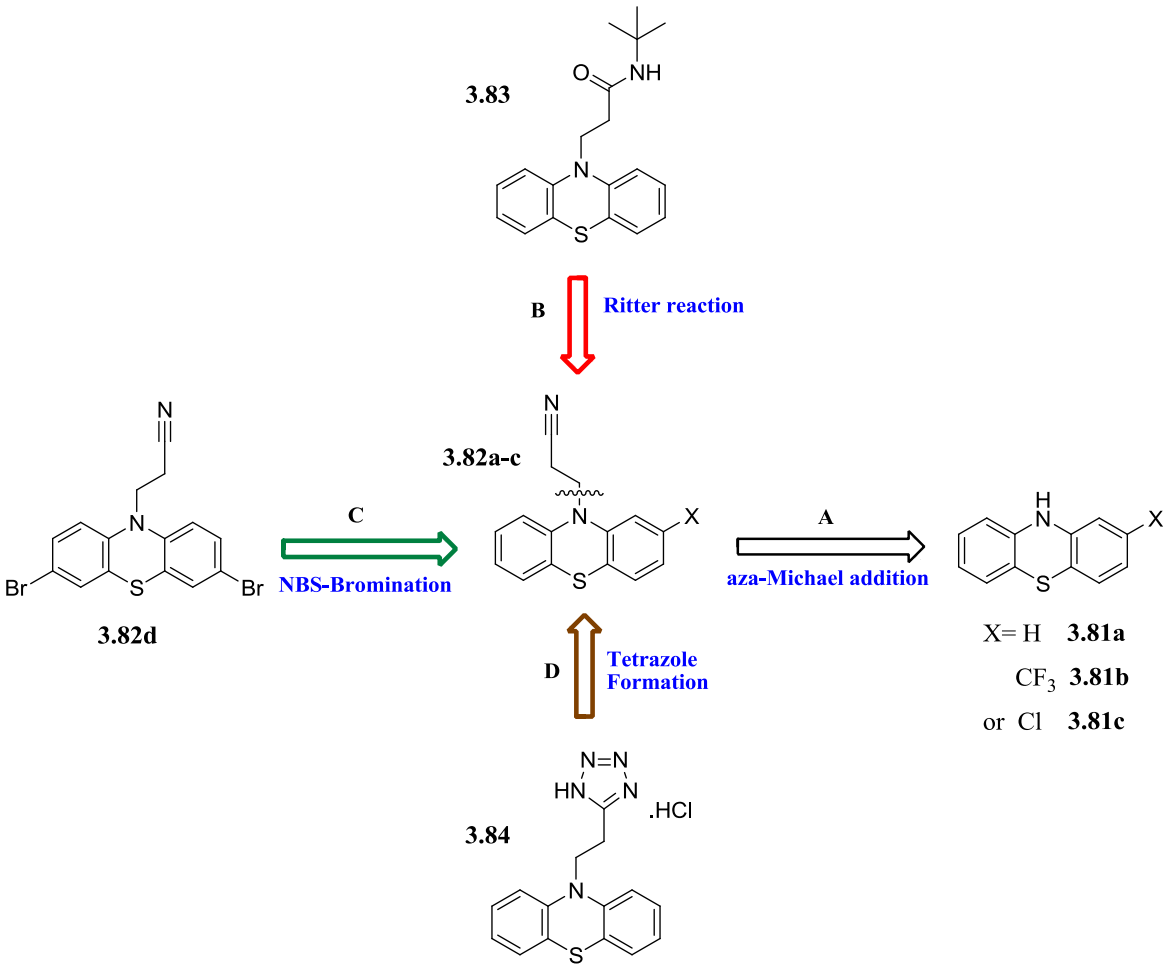

Scheme 3.20: The retrosynthetic plan for preparation of desired NCEs **3.82a-d** and **3.83-3.84**

3.8.1.1 Synthesis of nitrile 3.82a-c via aza-Michael addition

The aza-Michael addition was achieved by a reaction of the phenothiazines **3.81a-c** with acrylonitrile as a Michael-acceptor using the conditions outlined in Scheme 3.21.[27] ^{1}H NMR confirmed the addition by showing aromatic resonances along with two triplets resonating in the range δ_H 2.92 – 4.23 ppm. These were assigned to the two methylene groups derived from the Michael acceptor. ^{1}H NMR results were corroborated by ^{13}C NMR and LCMS analysis.

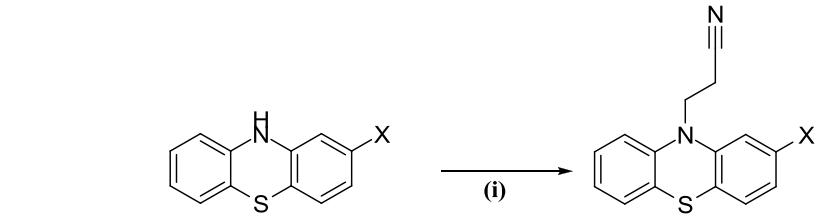

3.81a (X= H), **3.81b** (X= CF_3), **3.81c** (X= Cl) **3.82a-c**

Scheme 3.21: *Reagents and conditions:* **(i)** Acrylonitrile (excess), Triton B (10 mol%), 0 °C, 0.5 h; Dioxane, reflux, 1h, **3.82a** (67%), **3.82b** (54%), **3.82c** (60%).

3.8.1.2 Synthesis of tetrazole 3.84

The preparation of tetrazole derivative **3.84** was achieved using sodium azide in the presence of ammonium chloride (Scheme 3.22). In comparison to the ^{1}H NMR of the unsubstituted nitrile derivative **3.82a**, a clear shift of methylene resonances from δ_H 4.23 & 2.93 ppm to δ_H 4.35 & 3.32 ppm, respectively, was observed. This was ascribed to strong electron-withdrawing inductive effects exhibited by the tetrazole ring.

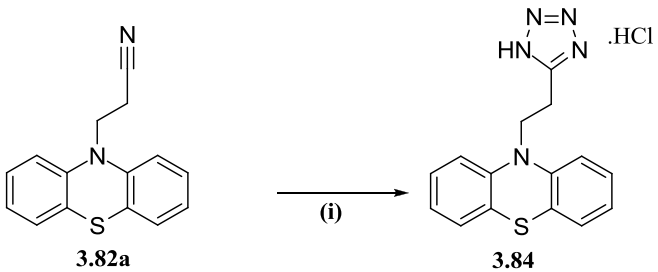

3.82a **3.84**

Scheme 3.22: *Reagents and conditions:* **(i)** NaN_3 (3.0 eq), NH_4Cl (3.0 eq), DMF, 125 °C, 16 h, **3.84** (45%).

3.8.1.3 Synthesis of dibromo-10*H*-phenothiazine propanenitrile 3.82d

A monobrominated product was initially of interest to this study to evaluate the effect of halogen substitution, at a position other than the usual 2-position, on bio-activity. However, attempts to synthesize the mono-brominated product yielded dibromo **3.82d** as the major product. Interestingly, dibromo product **3.82d** bears structural resemblance to DNA intercalators such as ethidium bromide, thus was also of interest to this study.[28] Consequently, the reaction conditions were optimized and the dibromo derivative **3.82d** was obtained after recrystallization from a mixture of ethyl acetate and hexane (Scheme 3.23).

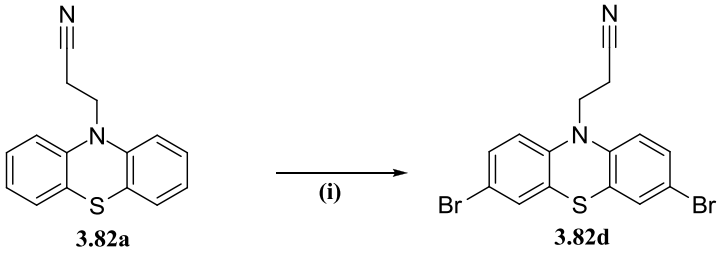

Scheme 3.23: *Reagents and conditions:* **(i)** *N*-bromosuccinimide (2.3 eq; optimized for dibromination), dry THF, 0 °C, 1 h → rt 12 h, **3.82d** (65%).

Dibromo **3.82d** was the major product presumably due to *ortho, para*-directing effects of the thiazine ring. Selectivity amongst the available positions is known to be determined by steric hindrance.[29,30] Two sets of aromatics resonances at δ_H 7.41 ppm & 7.04 ppm integrated for four and two protons, respectively. This was a confirmation that the electrophilic disubstitution was successful.

3.8.1.4 Synthesis of amide 3.83 *via* the Ritter reaction

The amide derivative **3.83** was prepared *via* an acid-catalyzed nucleophilic addition of nitrile **3.82a** to a carbenium ion generated from *t*-butyl acetate (Scheme 3.24). This reaction is known as the Ritter reaction.[31] Nitriles are known to be poor nucleophiles and weak bases

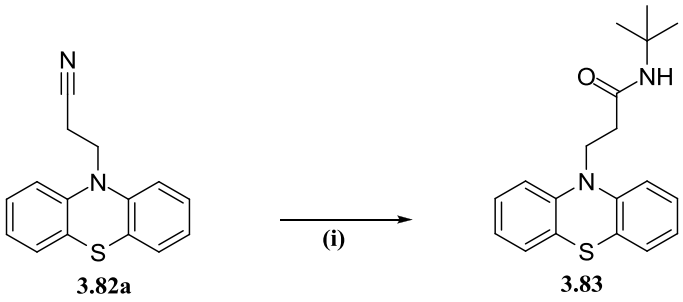

Scheme 3.24: *Reagents and conditions*: **(i)** *tert*-butyl acetate, conc. H_2SO_4, rt → 42 °C., 12 h, **3.83** (20%).

due to the lone pair on the nitrogen atom being in a low-energy sp orbital.[30] The carbocation generated in this reaction is reactive enough to combine with the weakly nucleophilic nitrile. The proposed mechanism of this reaction is illustrated in Figure 3.12.

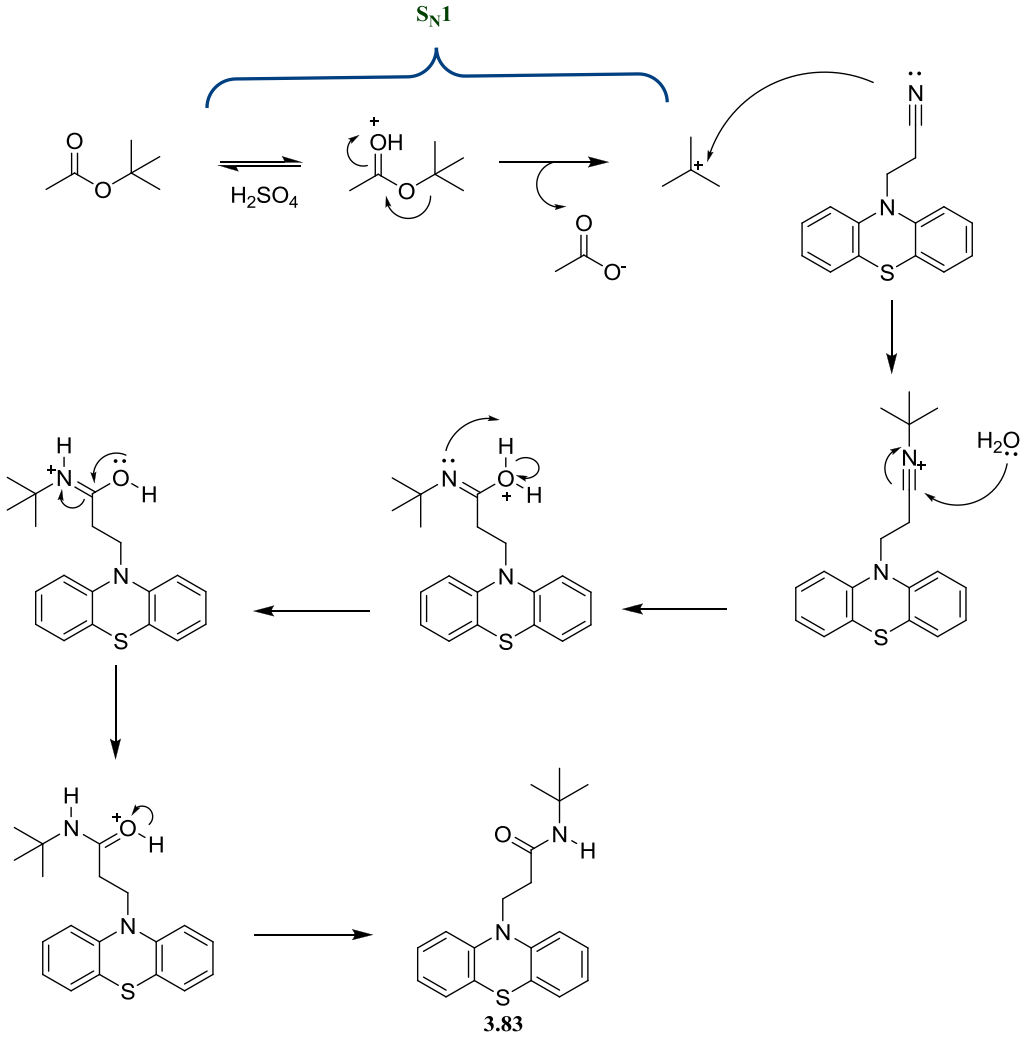

Figure 3.12: Proposed mechanism of the Ritter reaction illustrating the series of intermediates involved.

The Ritter product **3.83** was characterized by NMR and LCMS. The ^{1}H NMR spectrum showed a characteristic *tert*-butyl resonating upfield at δ_H 1.23 ppm. An amide proton was observed downfield at δ_H 7.46 ppm. ^{13}C NMR revealed a carbonyl signal resonating at δ_C 169.66 ppm. One of the methylene resonances appeared to overlap with the DMSO-d_6 peak at δ_H 2.48 ppm, thus the signal integration was ambiguous. This ambiguity was resolved using an ^{13}C-APT (Attached Proton Test) NMR experiment for distinguishing between carbons based on the number of protons attached. The ^{13}C-APT spectrum of **3.83** showed two positive resonance peaks at δ_C 34.17 ppm and 43.32 ppm, thus confirming the presence of two methylene carbons (Figure 2.13).

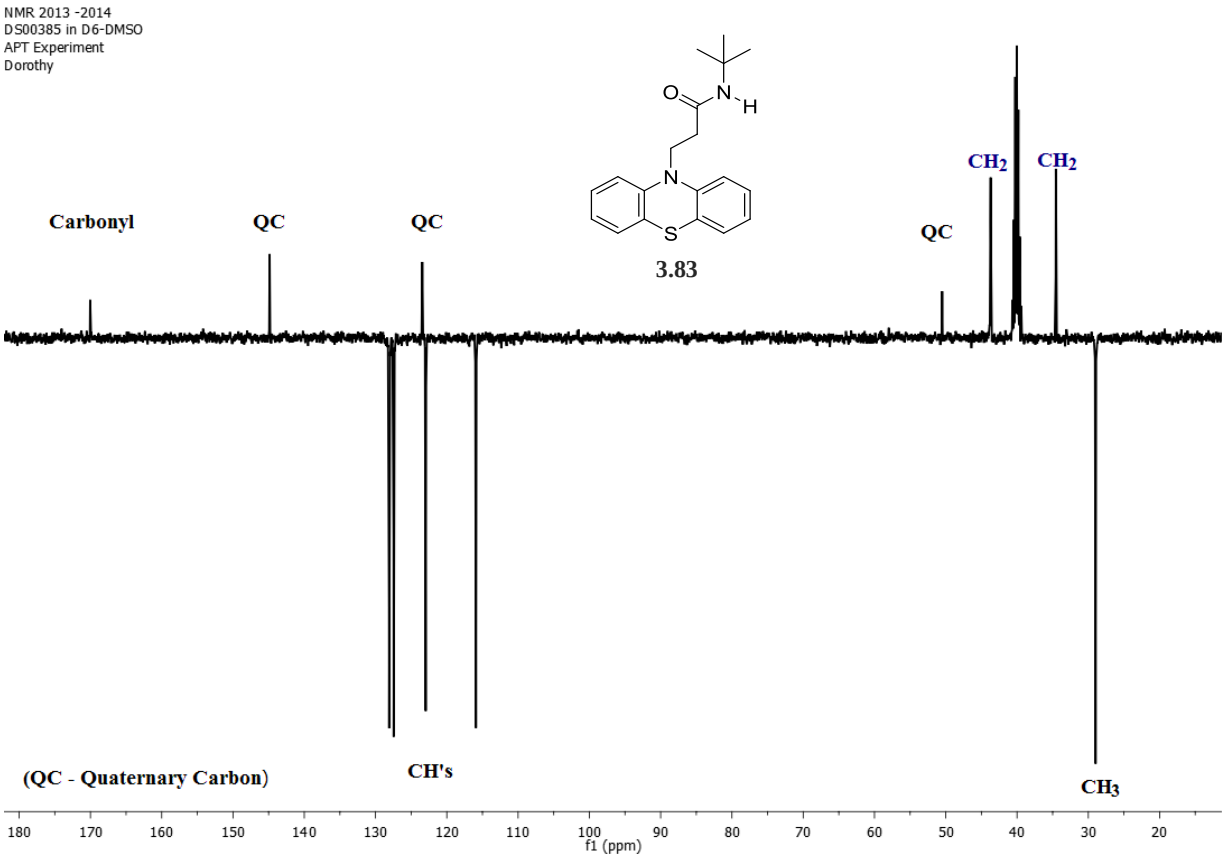

Figure 3.13: ^{13}C-APT NMR for confirmation of two methylenes in the chemical structure of **3.83** (**DS00385**). Quaternary and methylene carbons point upwards whereas CH's and CH_3's point downwards.

3.8.1.5 *N*-propylphosphonate ester 3.87 from the Michaelis-Arbuzov reaction

The Michaelis-Arbuzov reaction is a useful method for preparing phosphonates from alkyl halides. One of the drawbacks from this classical synthetic method is the need for elevated temperatures for the reaction to occur. Adaptations of the original method have been reported including the use of Lewis acid-catalysts.[32] The synthesis of the *N*-propylphosphonate ester **3.87** was conceived as achievable using the Michaelis-Arbuzov reaction method under the conditions outlined in Scheme 3.25.

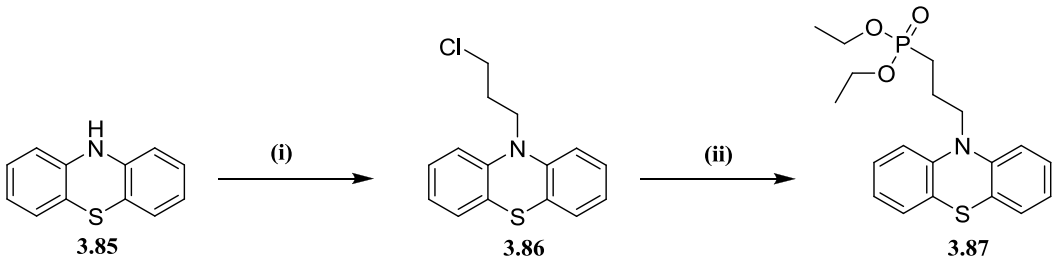

Scheme 3.25: *Reagents and conditions*: **(i)** NaH (1.1 eq), dry DMF, N_2, 0 °C → rt, 1.5 h, 1-bromo-3-chloropropane (1.0 eq), rt, 26 h. 53 %; **(ii) 3.86** (1.0 eq), triethyl phosphite (5.0 eq), $ZnCl_2$ (1M in DCM) (1.2 eq), dry toluene, 75 °C, N_2, 18 h. 10%.

The Michaelis-Arbuzov reaction proceeded *via* an S_N2 reaction between nucleophilic triethylphosphite and an alkyl halide followed by an S_N2 dealkylation to form phosphonate ester **3.87**. The proposed mechanism is depicted in Figure 3.14.

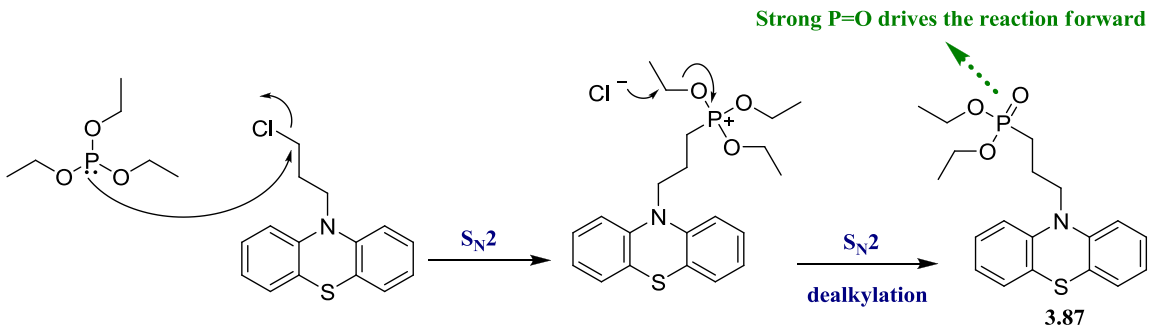

Figure 3.14: Proposed mechanism of Michaelis-Arbuzov reaction illustrating the formation of phosphonate ester **3.87** from an alkyl halide.

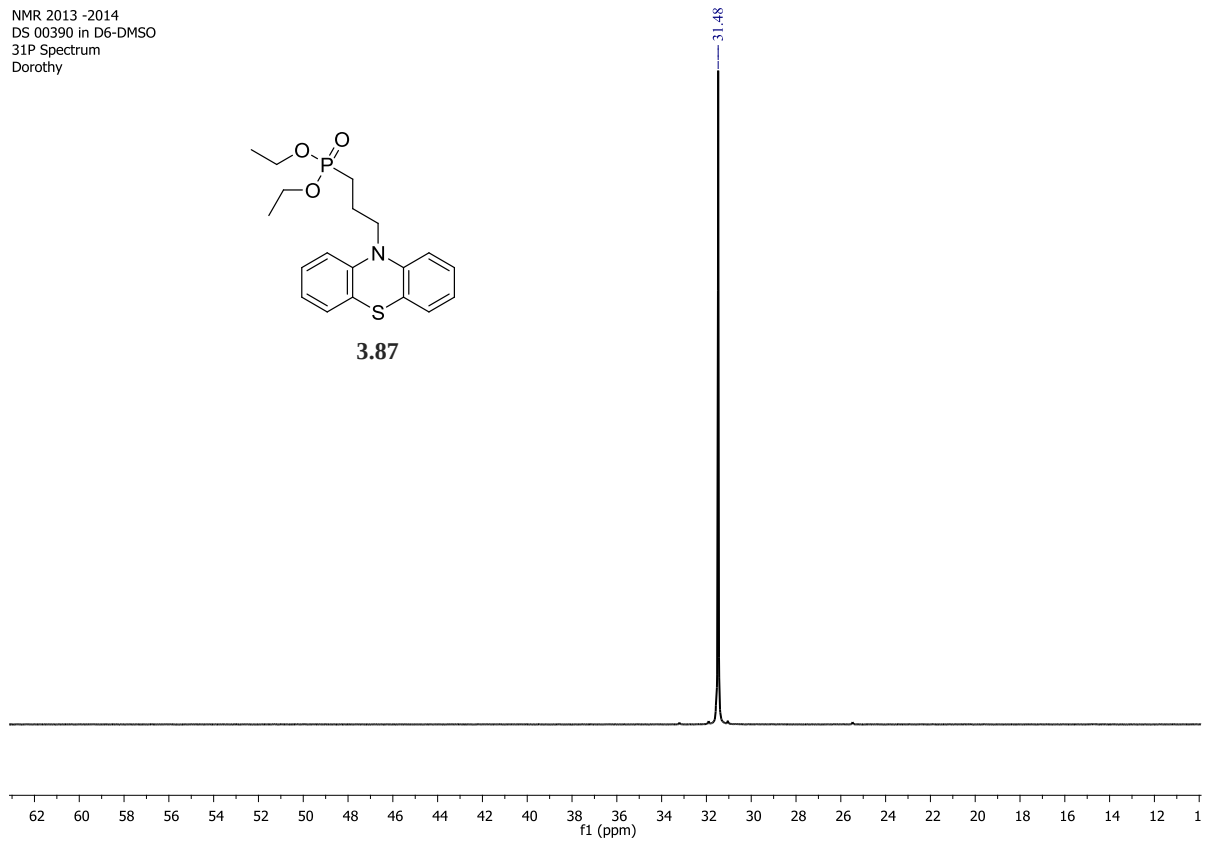

Figure 3.15: ^{31}P NMR (proton-decoupled) of **3.87** as confirmation of the presence of a phosphonate group.

The ^{1}H NMR spectrum of phosphonate ester **3.87** revealed the right number of aromatic resonating in the range δ_H 7.20-6.96 ppm along with sets of methylene and methyl resonances in the upfield region. Furthermore, a resonance peak was observed at δ_P 31.48 ppm in the ^{31}P NMR spectrum, thus confirming the presence of a phosphonate moiety (Figure 3.15).

3.9 Concluding remarks

Adaptation of well-known organic reactions and literature reported synthetic methods led to the design of shorter and concise routes to the library of desired NCEs. The attachment of side chains was afforded *via* reactions such as nucleophilic ring-opening *N*-alkylation and aza-Michael addition. Other mechanistically interesting reactions such as the Arbuzov-Michaelis reaction and Ritter reaction also afforded desired NCEs. In cases where the tricyclic-ring system had to be assembled from functionalized benzenes, the Buchwald-Hartwig reaction conditions were employed. In general, most of the chemical reactions were low yielding particularly due to incomplete consumption of starting materials and/or competing side reactions (e.g. sultone hydrolysis). However, the amount of products isolated was sufficient for bio-activity screening thus optimization of yields was not prioritized.

Isolation and purification techniques common in organic synthesis were employed with reversed-phase chromatography being an exception for purification of alkylsulfonate NCEs. This method involved the use of aqueous-based mobile phase and introduction of organic modifiers where necessary. Spectroscopic techniques such as NMR, LCMS and IR were employed for structure elucidation, confirmation and purity analysis.

The next two chapters (Chapter 4 & 5) report on the biological evaluation of the library of NCEs for antitubercular and anticancer activities.

References

(1) Strecker A. About a New Mode of Formation and the Constitution of Sulfonic Acids. *Ann. der Chemie und Pharm.* **1868**, *148* (1), 90–96.

(2) Van Bergen, L. A.; Roos, G.; De Proft, F. From Thiol to Sulfonic Acid: Modeling the Oxidation Pathway of Protein Thiols by Hydrogen Peroxide. *J. Phys. Chem. A* **2014**, *118* (31), 6078–6084.

(3) Duarte F, Geng T, Marloie G, Al hussain AO, Williams NH, K. S. The Alkaline Hydrolysis of Sulfonate Esters: Challenges in Interpreting Experimental and Theoretical Data. *J. Org. Chem.* **2014**, *79* (7), 2816–2828.

(4) Bell J; Geng T; Blount JF; Briscoe OV; Freeman HC. The Crystal Structure of Phenothiazine. *Chem. Commun.* **1968**, *0* (24), 1656–1657.

(5) Jafari, S.; Fernandez-Enright, F.; Huang, X. F. Structural Contributions of Antipsychotic Drugs to Their Therapeutic Profiles and Metabolic Side Effects. *J. Neurochem.* **2012**, *120* (3), 371–384.

(6) Seeman, P. Clozapine , a Fast-O Ff -D2 Antipsychotic. *ACS Chem Neurosci* **2014**, *5*, 24–29.

(7) Froimowitz, M.; Cody, V. Biologically Active Conformers of Phenothiazines and Thioxanthenes. Further Evidence for a Ligand Model of Dopamine D2 Receptor Antagonists. *J. Med. Chem.* **1993**, *36* (15), 2219–2227.

(8) Tsvelikhovsky, D.; Buchwald, S. L. Concise Palladium-Catalyzed Synthesis of Dibenzodiazepines and Structural Analogues. *J. Am. Chem. Soc.* **2011**, *133* (36), 14228–14231.

(9) Margolis, B. J.; Swidorski, J. J.; Rogers, B. N. An Efficient Assembly of Heterobenzazepine Ring Systems Utilizing an Intramolecular Palladium-Catalyzed Cycloamination. *J. Org. Chem* **2003**, 68, 644–647.

(10) Hunziker F; Fischer E; Shmutz J. 11-Amino-5H-Dibenzo[b,e]-1,4-Diazepine. *Helv. Chim. Acta* **1967**, *50* (6), 1588–1599.

(11) Joshua, A. V.; Sharma, S. K.; Strelkov, A.; Scott, J. R.; Martin-Iverson, M. T.; Abrams, D. N.; Silverstone, P. H.; McEwan, A. J. B. Synthesis and Biodistribution of 8-Iodo-11-(4-Methylpiperazino)-5H-dibenzo[b,e][1,4]-Diazepine: Iozapine. *Bioorganic Med. Chem. Lett.* **2007**, *17* (14), 4066–4069.

(12) Zhang, Q. Y.; Wang, X. J.; Tian, Y. L.; Qi, J. G.; Li, C.; Yin, D. L. One Pot Synthesis of Dibenzodiazepinones via CuI Catalysis in Ethylene Glycol. *Chinese Chem. Lett.* **2013**, *24* (9), 825–828.

(13) Meshram, H. M.; Ramesh, P.; Reddy, C.; Singhyadav, J. One Step Process for the Synthesis of Subtituted 5,10-dihydrodibenzo[b,e][1,4]diazepines-11-Ones. US 2010/0228023 Al, 2010.

(14) Aicher T; Chen Z; Faul M; Krushinski J; Le Huerou Y; Pineiro-nunez M; Rocco V; Ruley K; Schaus J; Thompson D; TuperD. Piperazine Substituted Aryl Benzodiazepine and Their Use as Dopamine Receptor Antagonists for the Treatment of Psychotic Disorders. WO 03/082877 Al, **2003**.

(15) Wigbers, C.; Prigge, J.; Mu, Z.; Fröhlich, R.; Chi, L.; Würthwein, E. U. Synthesis, Structures, and Aggregation Properties of N-Acylamidines. *European J. Org. Chem.* **2011**, No. 5, 861–877.

(16) Pinner A. About Amidines and Pyrimidines. *Ber. Dtsch. Chem. Ges.* **1889**, *22*, 1600–1612.

(17) Sang, P.; Yu, M.; Tu, H.; Zou, J.; Zhang, Y. Highly Regioselective Synthesis of Fused Seven-Membered Rings through Copper-Catalyzed Cross-Coupling. *Chem. Commun. (Camb).* **2013**, *49* (7), 701–703.

(18) Guo, L.; Li, B.; Huang, W.; Pei, G.; Ma, D. Elaboration of the Oxazepine Ring System via cuI/L-Proline-Catalyzed Intramolecular Aryl Amination. *Synlett* **2008**, *12*, 1833–1836.

(19) Khoobi, M.; Foroumadi, A.; Emami, S.; Safavi, M.; Dehghan, G.; Alizadeh, B. H.; Ramazani, A.; Ardestani, S. K.; Shafiee, A. Coumarin-Based Bioactive Compounds: Facile Synthesis and Biological Evaluation of Coumarin-Fused 1,4-Thiazepines. *Chem. Biol. Drug Des.* **2011**, *78* (4), 580–586.

(20) Shirude, P. S.; Paul, B.; Roy Choudhury, N.; Kedari, C.; Bandodkar, B.; Ugarkar, B. G. Quinolinyl Pyrimidines: Potent Inhibitors of NDH-2 as a Novel Class of Anti-TB Agents. *ACS Med. Chem. Lett.* **2012**, *3* (9), 736–740.

(21) Sykes P. *A Guidebook to Mechanism in Organic Chemistry*, 6th ed.; Pearson: Harlow, 1986.

(22) Cho, H.; Iwama, Y.; Sugimoto, K.; Mori, S.; Tokuyama, H. Regioselective Synthesis of Heterocycles Containing Nitrogen Neighboring an Aromatic Ring by Reductive Ring Expansion Using Diisobutylaluminum Hydride and Studies on the Reaction Mechanism. *J. Org. Chem.* **2010**, *75* (3), 627–636.

(23) Kantorowski, E. J.; Kurth, M. J. Expansion to Seven-Membered Rings. **2000**, *56* (530), 4317–4353.

(24) Zaccheria, F.; Ravasio, N.; Ercoli, M.; Allegrini, P. Heterogeneous Cu-Catalysts for the Reductive Deoxygenation of Aromatic Ketones without Additives. *Tetrahedron Lett.* **2005**, *46* (45), 7743–7745.

(25) De Luca, L.; Giacomelli, G.; Porcheddu, A. Beckmann Rearrangement of Oximes under Very Mild Conditions. *J. Org. Chem.* **2002**, *67* (17), 6272–6274.

(26) Mekky, A. E. M.; Saleh, T. S.; Al-Bogami, A. S. Synthesis of Novel Pyrazoles Incorporating a Phenothiazine Moiety: Unambiguous Structural Characterization of the Regioselectivity in the 1,3-Dipolar Cycloaddition Reaction Using 2D HMBC NMR Spectroscopy. *Tetrahedron* **2013**, *69* (33), 6787–6798.

(27) Rajasekaran, A.; Thampi, P. P. Synthesis and Analgesic Evaluation of Some 5-[β-(10-Phenothiazinyl) Ethyl]-1-(acyl)-1,2,3,4-Tetrazoles. *Eur. J. Med. Chem.* **2004**, *39* (3), 273–279.

(28) Laursen, J. B.; Nielsen, J. Phenazine Natural Products: Biosynthesis, Synthetic Analogues, and Biological Activity. *Chem. Rev.* **2004**, *104* (3), 1663–1685.

(29) Smith M; March J. *March's Advanced Organic Chemistry Reactions, Mechanisms and Structures*, 6th ed.; John Wiley and Sons: New Jersey, 2007.

(30) Clayden J; Greeves N; Warren S; Wothers P. *Organic Chemistry*, 1st ed.; Oxford University Press: New York, 2001.

(31) Reddy, K. L. An Efficient Method for the Conversion of Aromatic and Aliphatic Nitriles to the Corresponding N-Tert-Butyl Amides: A Modified Ritter Reaction. *Tetrahedron Lett.* **2003**, *44*, 1453–1455.

(32) Rajeshwaran, G. G.; Nandakumar, M.; Sureshbabu, R.; Mohanakrishnan, A. K. Lewis Acid-Mediated Michaelis - Arbuzov Reaction at Room Temperature : A Facile Preparation of Arylmethyl/ Heteroarylmethyl Phosphonates. *Org. Lett.* **2010**, *6*, 1270–1273.

Chapter 4

Structurally remodelled phenothiazines as potential antitubercular agents without neuroleptic effects

Preface

Various strategies were applied in remodelling phenothiazines and related neuroleptic drugs. The strategies were rationally selected to ensure deviation from minimum structural requirements for neuroleptic action of phenothiazines. In so doing, a focused library comprising remodelled phenothiazines that are less likely to exhibit neuroleptic effects was generated. In the previous chapter, remodelled phenothiazines and related drugs were chemically synthesized for biological evaluation.

Tuberculosis remains one of the leading causes of death from an infectious disease, worldwide. In this chapter, the library of remodelled phenothiazines including parent drugs was evaluated against drug-susceptible *Mycobacterium tuberculosis*. Moreover, a selected series was screened for binding to serotonin and dopamine receptors to corroborate *in silico* predictions. Furthermore, *in vitro* and *in vivo* preclinical evaluation studies are also reported herein. This chapter thus addresses one of the key objectives of this research study i.e. to identify potential antitubercular agents from remodelled phenothiazines with less likelihood of neuroleptic effects.

4.1 The Tuberculosis scourge

4.1.1 Tuberculosis and HIV co-epidemics: global statistics

The prevalence of Tuberculosis (TB) is a grave global concern. An estimated 9.0 million new TB cases were reported in 2013 of which 16% resulted in death and 13% tested positive for Human Immunodeficiency Virus (HIV) (Figure 4.1). Significant progress has been made over the years since TB was declared a global public health emergency by the World Health Organization (WHO) in 1993. The TB mortality rate has gone down by 45% since 1990 and there is a notable decrease in TB incidence rates in some parts of the world.[1]

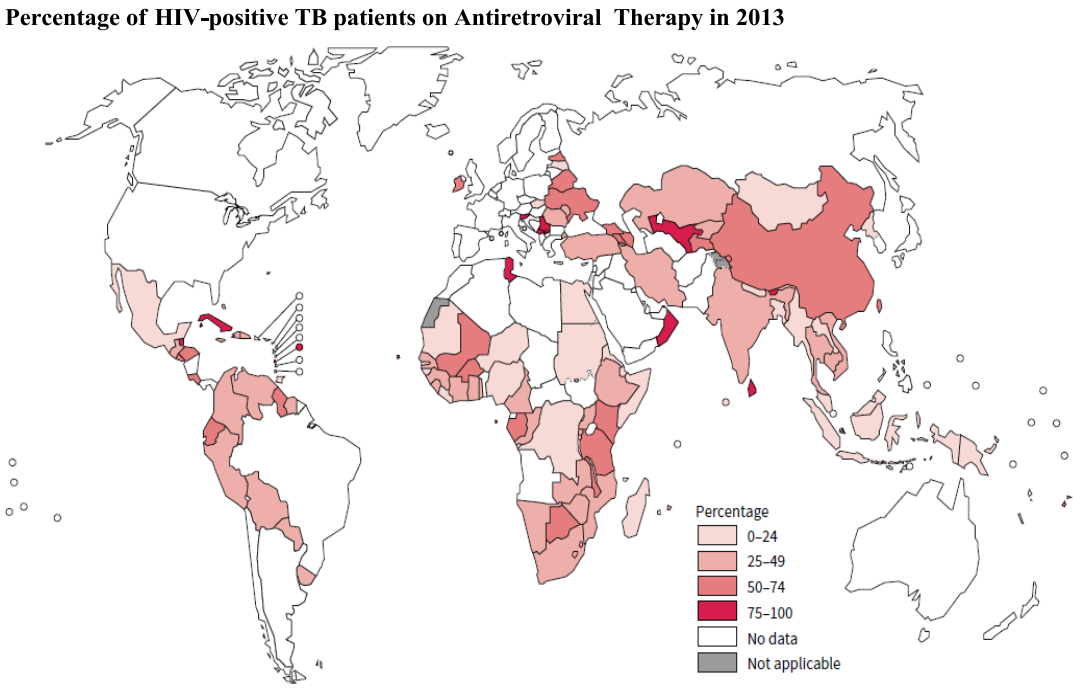

Figure 4.1: 2013 Global statistics of HIV co-infection with TB**.** Data and map courtesy of WHO Global Tuberculosis Report, 2014. **Key Facts**: HIV-positive people are 29 times more likely get infected with TB; 13% of 9 million TB patients tested positive for HIV in 2013; There is a decrease in the number of people dying from TB and HIV co- infection:540 000 cases in 2004 to 360 000 cases in 2013.[1]

Emergence of drug resistance continues to be a threat to the management of TB. More than 480 000 cases of multidrug-resistant TB (MDR-TB) occur annually across the globe. Of these, 9% is associated with extensively drug-resistant TB (XDR-TB).[2] In 2014, the WHO reported 54 countries that confirmed treating XDR-TB patients in 2013. Amongst these are Ukraine (1006 XDR-TB cases), South Africa (612 XDR-TB cases), India (364 XDR-TB cases) and Kazakhstan (305 XDR-TB cases).[1]

4.1.2 *Mycobacterium tuberculosis*: the causative agent of TB

Mycobacterium tuberculosis (M.*tb*) typically affects the lungs to cause pulmonary TB or other sites of the body (extrapulmonary).[3] TB infection is acquired from inhalation of micro-droplets of sputum from a TB patient. These micro-droplets are about 2.5 μm in diameter with 1-3 bacilli. Once the bacteria reach the alveolar sacs of the pulmonary system, they get phagocytosed by macrophages. The host responds to this infection by apoptosis of infected macrophages.

Virulent strains may escape apoptosis by subversion of the immune system resulting in prolonged survival in host cells. The bacteria may remain dormant in the macrophages and this is referred to as latent TB. The latent stage of TB infection is asymptomatic and non-infectious.[3] Poor hygienic conditions, poverty, immune system suppression and co-infection with other diseases, e.g. HIV, may lead to active TB. A simplified depiction of TB infection is given in Figure 2.2.

Diagnosis of TB is commonly carried out *via* sputum smear microscopy, a method that was developed over a century ago. Diagnosis may also be done using culture methods especially in regions where there is a more developed laboratory infrastructure.[1,4]

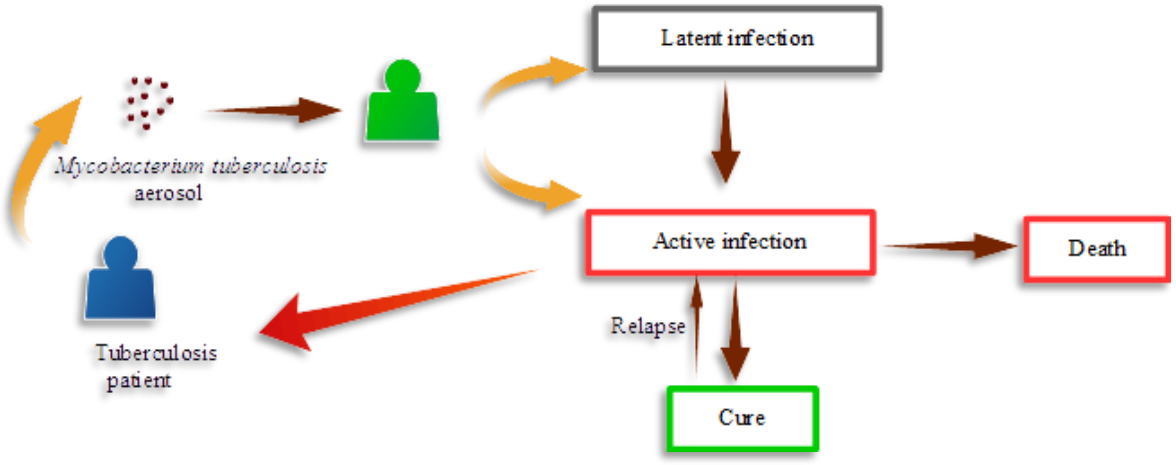

Figure 4.2: A simplified depiction of TB infection cycle caused by *Mycobacterium tuberculosis*.

4.1.3 Treatment of TB infections and drug resistance as a setback

Prior to the discovery of M.*tb* in 1882 by Robert Koch, a German physician and scientist, different types of collapse therapy and surgical interventions e.g. thoracoplasty were used for TB treatment. By the early 1950s, surgical interventions for TB treatment began to recede as antitubercular drugs were introduced.[3] The principal issue with the management of TB is the necessity to have lengthy drug treatment regimens of six to nine months. The lengthy treatment regimens have several drawbacks including non-compliance with therapy, relapse and drug resistance.[5,6]

Amongst these drawbacks, drug resistance remains the major setback in TB treatment. The Direct Observed Treatment (DOT) of drug-susceptible TB involves a four-drug regimen of first-line anti-TB drugs. The first phase (intensive phase – rate of bacteria growth very high) includes isoniazid, pyrazinamide, rifampicin and ethambutol for a period of two months. Subsequently, a continuation phase (bacilli in slow growth persister form) including only isoniazid and rifampicin follows for at least 4 months.[3]

The existence of drug-resistant M.*tb* strains was first reported in 1944 right after streptomycin was introduced. Subsequently, resistance to other TB drugs was demonstrated.[7] M.*tb* strains resistant to first-line anti-TB drugs are termed multidrug-resistant (MDR), while those resistant to second-line anti-TB drugs e.g. fluoroquinolones and aminoglycoside injectables like amikacin are termed extremely drug-resistant (XDR) (Figure 4.3).[8,9] Treatment of drug-susceptible TB has up to 95% cure rates in comparison to MDR-TB which has less than 70% cure rates.[3]

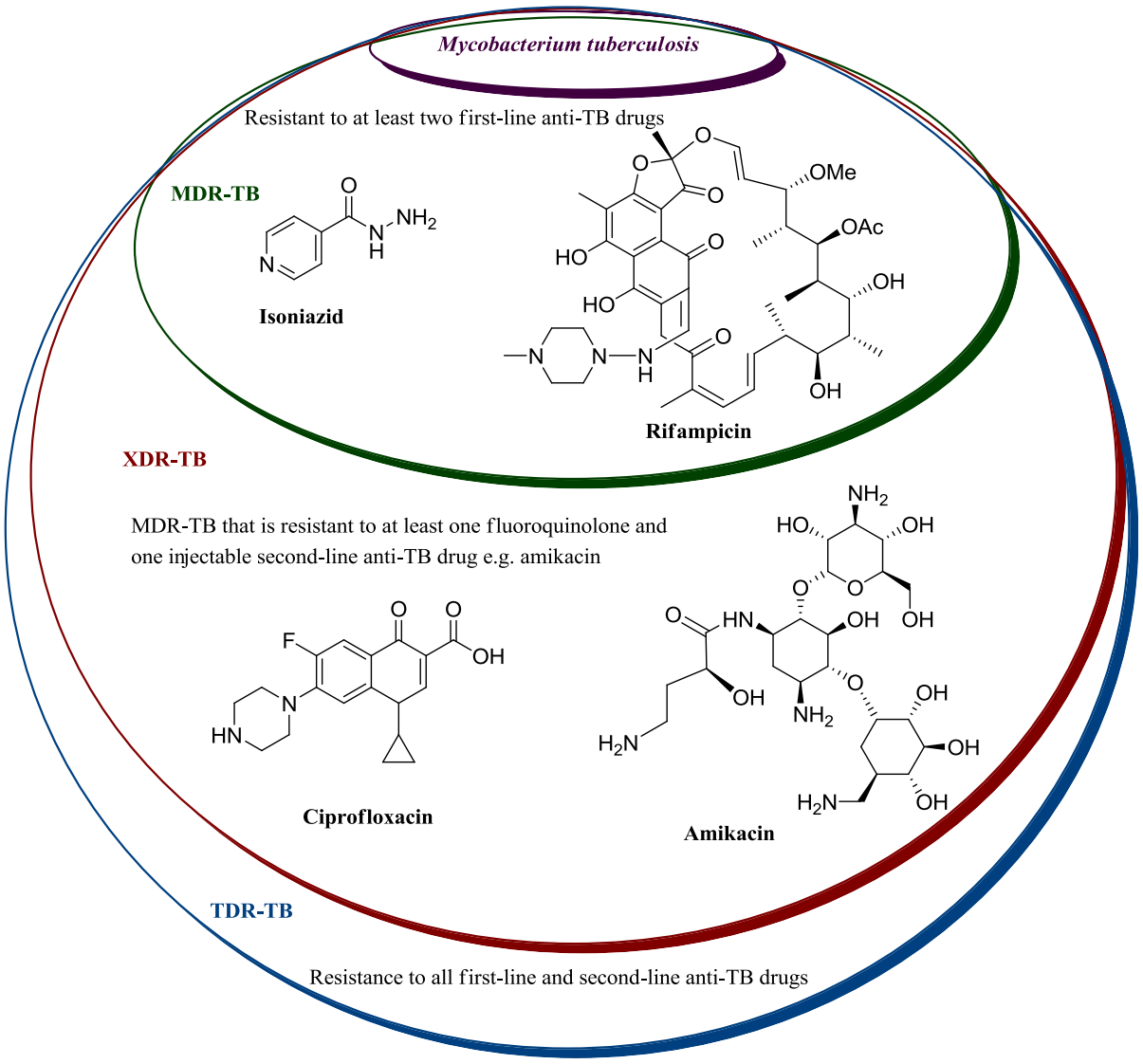

Figure 4.3: Resistance of *Mycobacterium tuberculosis* - a threat to management of TB.

More recently, totally-drug resistant (TDR) M.*tb* strains have been reported as a serious threat to TB therapy. TDR-TB is virtually untreatable and shows resistance to all first-line and second line anti-TB drugs. The earliest observation of TDR-TB was in Italy over a decade ago followed by Iran in the late 2000s.[10,11] In 2011, Udwadia *et al*. reported patients with TDR-TB in India.[12] Additionally, in 2013, the Center for Disease Control and Prevention reported first incidents of TDR-TB in South Africa.[11]

Anti-TB chemotherapeutics are categorized into five groups on the basis of factors such as efficacy, mode of administration (oral or injectable) and structural identity (Table 4.1).[2]

Table 4.1: Classification of anti-TB drugs

Group 1	**Group 2**	**Group 3**	**Group 4**	**Group 5**
Oral	*Injectable*	*Oral & Injectable* **(Fluroquinolones)**	*Oral Bacteriostatic*	*Miscellaneous roles*
Isoniazid	*Streptomycin	Levofloxacin	Cycloserine	Linezolid
Ethambutol	*Amikacin	Moxifloxaxin	Terizidone	Clofazimine
Pyrazinamide	*Kanamycin	Ciprofloxacin	Thionamide,	Amoxicillin/clavulanate
Rifampicin	$Capreomycin	Ofloxacin	Protionamide	thioacetazone,
Rifabutin	$Viomycin	Gatifloxacin	*para*-amino- glyco-	Imipenem/cilastatin
Rifapentin			salicylic acid	High dose isoniazid
				Clarithromycin

***Aminoglycosides** **$Polypeptides**

As discussed in chapter 1, novel therapeutic drug classes are urgently required to curb the rising tide of antibiotic resistance. Several drug candidates with novel modes of action are in late-stage clinical development or have been approved for TB chemotherapy (Figure 4.4).[13] Examples include bedaquiline (a diarylquinoline), delamanid (a nitroimidazo-oxazole), sutezolid (an oxazolidinone) and SQ109 (a 1,2-diamine).[10,13,14]

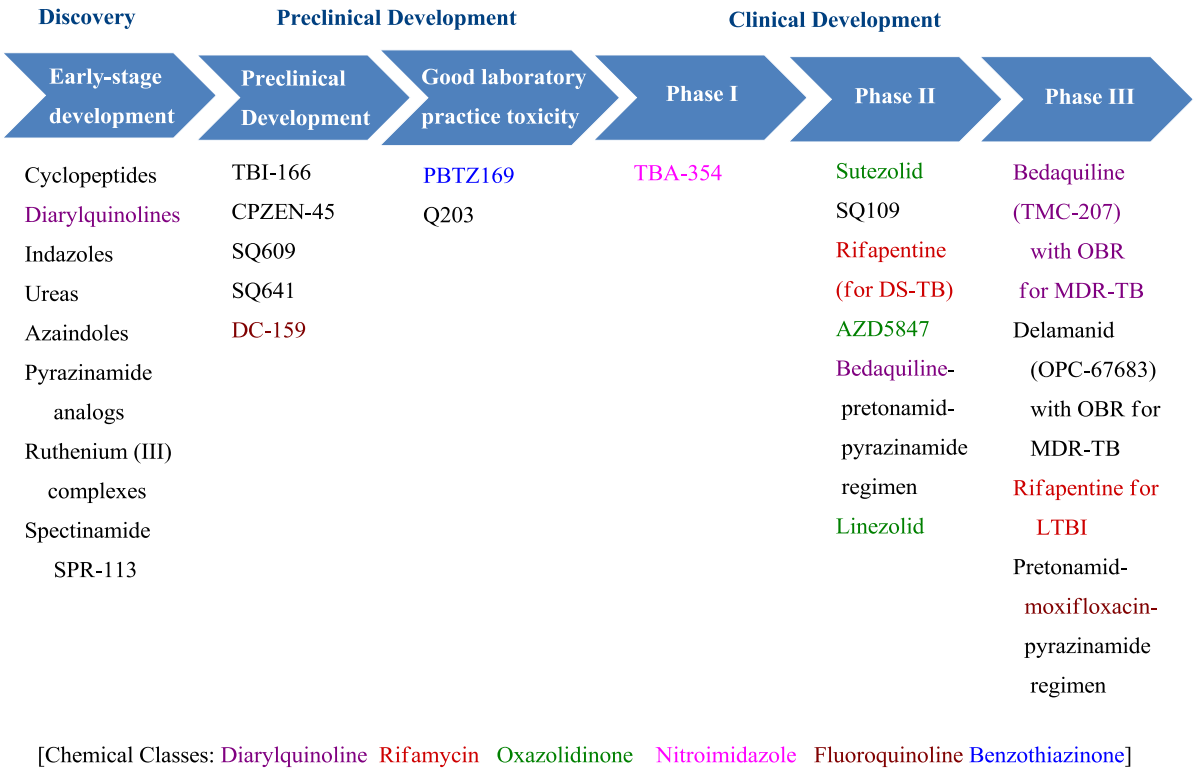

Figure 4.4: The tuberculosis drug pipeline. OBR - optimised background regimen; DS-TB: drug-susceptible tuberculosis; MDR-TB: multidrug-resistant tuberculosis; LTBI: latent tuberculosis infection.[13]

Drug repurposing (chapter 1) has garnered significant research interest as an alternative strategy for the management of antimicrobial drug resistance. A number of drugs, including neuroleptic thioridazine and linezolid, have been repurposed and are under investigational use as adjuvants in treatment of MDR-TB and XDR-TB.[2,12,15]

4.1.4 Drug targets in TB drug discovery

The cell wall is crucial for survival of M.*tb* particularly under unfavourable conditions post-phagocytosis by the host. Its biosynthesis is appealing for discovery of new drugs for several reasons. It is absent in the mammalian system and many enzymes involved in this pathway

are attractive biomolecular targets. An illustration of processes targeted by the majority of anti-TB agents is given in Figure 4.5. The bacterial cell wall synthesis is targeted by first-line anti-TB drugs, ethambutol and isoniazid.[5] The newly developed nitroimidazo-oxazole, delamanid, also targets cell wall synthesis by blocking the synthesis of mycolic acids.[14] Inhibition of calcium-dependent enzymes interferes with processes such as ATP hydrolysis which is essential for cellular energy.[7,8] Bedaquiline targets the proton pump of ATP synthesis which is essential for bacterial metabolism.[16]

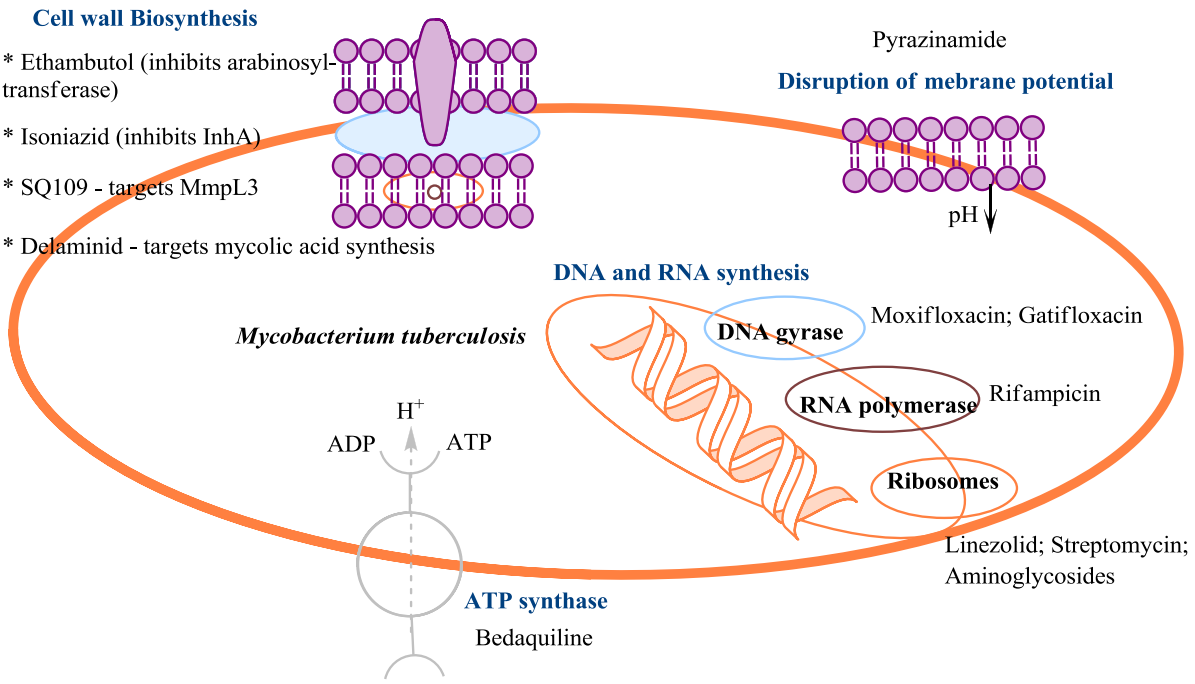

Figure 4.5: Examples of biological processes targeted by the majority of anti-TB drugs**.** InhA (2-trans-enoyl-acyl carrier protein reductase); MmpL3 (membrane transporter of trehalose monomycoclate).[2,17]

A number of biosynthetic pathways have been well documented as potential anti-TB drug targets. Mycothiol and ergothioneine are primary low molecular weight thiols that play a crucial role in maintaining cellular redox homeostasis thereby ensuring the survival and

persistence of M.*tb*. Therefore, enzymes involved in the biosynthesis of small molecule thiols and the associated detoxification pathways are appealing targets.[18] Another pathway that is appealing is amino acid biosynthesis which involves synthesis of aromatic and non-aromatic amino acids.[5] Other attractive targets include enzymes involved in the respiratory chain of M.*tb*.[19] Oxidoreductases such as type II NADH:menaquinone odixoreductase (NDH-2) are viable anti-TB drug targets.[8] Mutations of genes associated with processes such as cell wall synthesis and DNA metabolism play a major role in drug resistance. They may cause upregulation of bacterial efflux pumps thus decreasing its susceptibility to several drug classes. These pumps are thus attractive targets for discovery of novel anti-TB drugs and management of resistance.[7,20]

Phenothiazines have been reported to interfere with some of the above-mentioned biological processes.[8] In particular, thioridazine and other phenothiazines, have been reported as inhibitors of M.*tb* NDH-2 and bacterial efflux pumps.[9,21,22] Moreover, they have also been reported to inhibit NDH-2 in other pathogens e.g. *Staphylococcus aureus*.[23]

4.1.5 Reports of antimycobacterial properties of phenothiazines

There is a growing interest in the antimycobacterial properties of native phenothiazine drugs and their derivatives (Chapter 1).[24,25,26] The most recent libraries reported include phenothiazine-based 1,3,4-thiadiazole hybrids,[27] phenothiazine-based dihydropyrazolo[3,4-d]pyrimidines,[28] 2-trifluoromethylphenothiazine-triazole hybrids,[29] and phenothiazines bearing a triphenylphosphonium moiety.[16] These reports reveal the great potential of phenothiazines as antitubercular agents through minimal structural remodelling.

4.2 Biological evaluation of a focused library of remodelled phenothiazines

4.2.1 Brief overview

Phenothiazines produce adverse side effects in addition to their inherent neuroleptic effects at clinically effective concentrations. Therefore, their extended clinical use as antimycobacterial agents is limited. In this study, it was postulated that these drugs could be remodelled such that their inherent neuroleptic effects are abrogated whilst antimycobacterial activity is retained. The overall rationale applied in the remodelling involved deviating from structural traits and properties associated with their neuroleptic action (Chapter 2). The library of the new chemical entities generated was taken through several stages to identify potential antitubercular agents with reduced likelihood of neuroleptic effects (Figure 4.6).

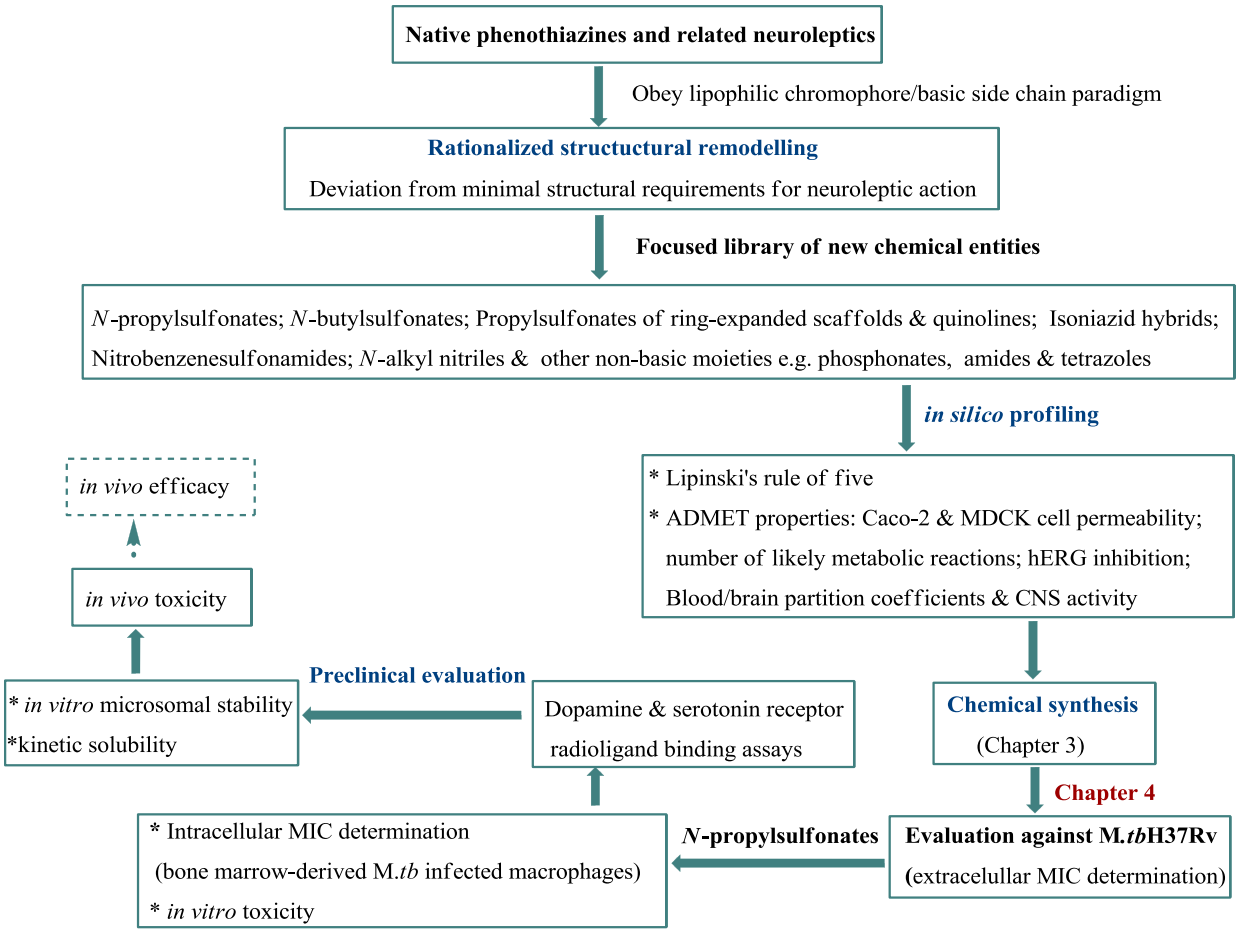

Figure 4.6: Biological evaluation of new chemical entities from remodelling phenothiazines and related drugs.

4.2.2 Antimycobacterial evaluation against M.*tb*H37Rv

The biological screening against M.*tb* was conducted in collaboration with University of Cape Town (UCT) Institute of Infectious diseases and Molecular Medicine (IIDMM). Detailed assay methods are provided in Chapter 7. Neuroleptic drugs with unknown antitubercular activity were purchased from Sigma-Aldrich and AK Scientific (Figure 4.7).

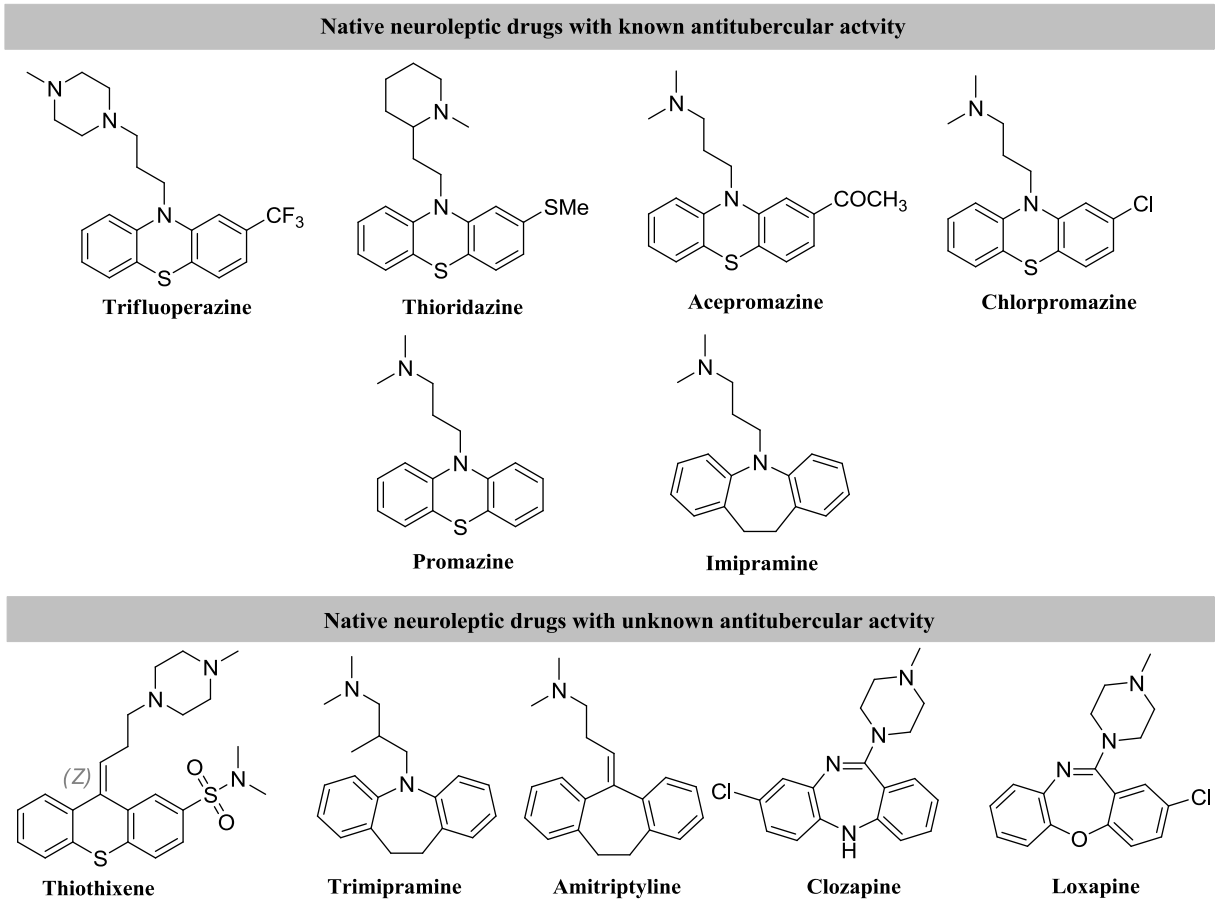

Figure 4.7: Parent neuroleptic drugs that were structurally remodelled for antimycobacterial evaluation.

The library of NCEs (Figure 4.8) and commercially available parent drugs (Figure 4.7) were evaluated *in vitro* against virulent *M.tb*H37Rv using the Green Fluorescent Protein Microplate Assay (GFPMA) in a GAST/Fe medium.[30] The minimum inhibitory concentrations (MICs) were determined at 14 days (Table 4.2).

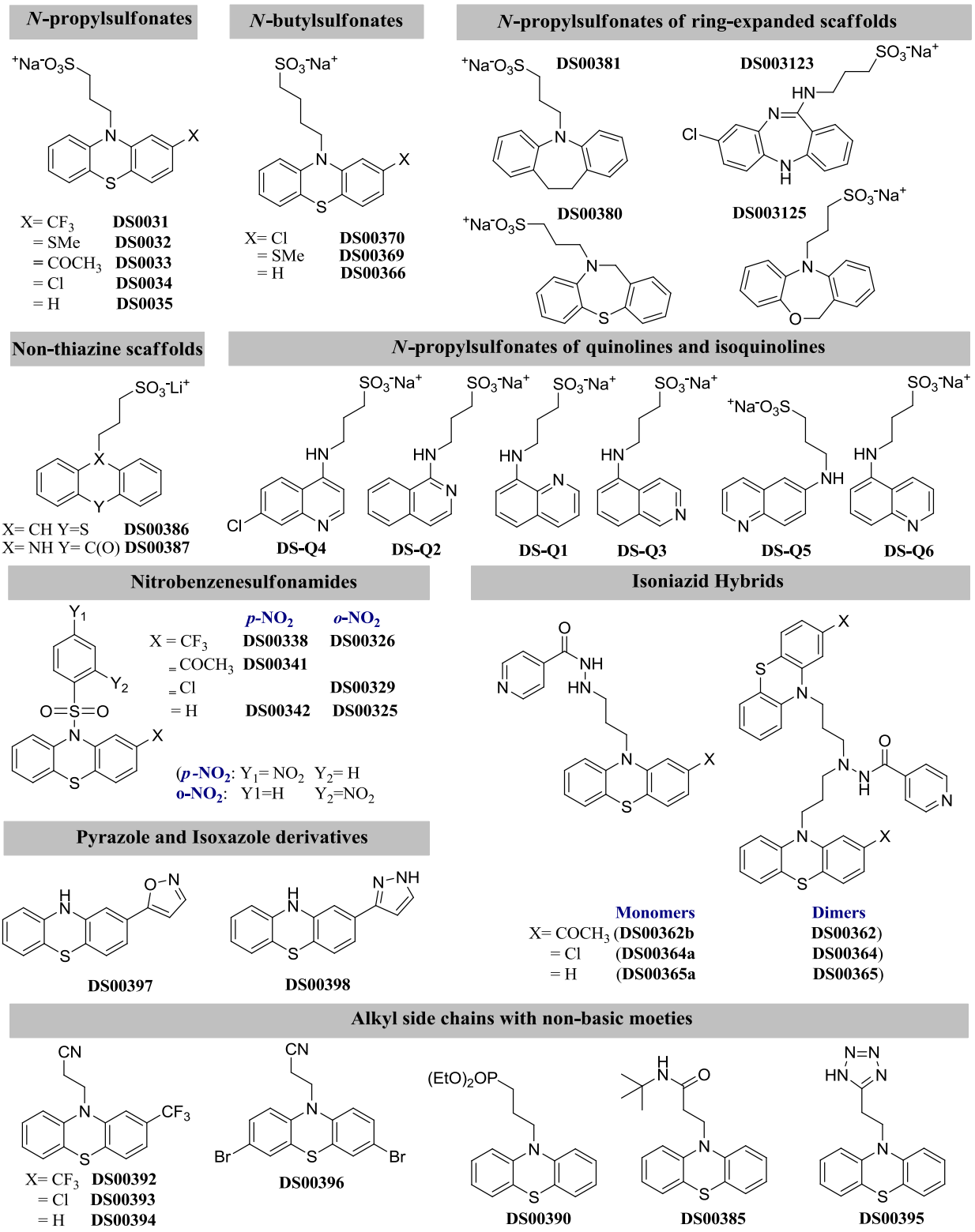

Figure 4.8: Library of new chemical entities derived from phenothiazines and related neuroleptics for evaluation as antitubercular agents.

Table 4.2: *in vitro* activity of remodelled phenothiazines against M.*tb*H37Rv in comparison to parent neuroleptic drugs and their *in silico* predicted CNS activity

NCE	*in silico* predicted CNS activity	M.*tb*H37Rv MIC_{90} (µM)	M.*tb*H37Rv MIC_{99} (µM)	Parent neuroleptic drug	MIC_{90} & MIC_{99} (µM) [a]lit MIC (µg/mL)
***N*-propylsulfonates**					
DS0031	-1 (inactive)	> 125	> 125	Trifluoperazine	[a] 8-32 (cfu)[31]
DS0032	-1 (inactive)	> 125	> 125	Thioridazine	9.9 & 12.9
DS0033	-2 (inactive)	> 125	> 125	Acepromazine	[a] > 20[32]
DS0034	-1 (inactive)	> 125	> 125	Chlorpromazine	[a] 4-32 (Bactec)[33]
DS0035	-1 (inactive)	> 125	> 125	Promazine	[a] > 25 (Bactec)[34]
***N*-butylsulfonates**					
DS00369	-2 (inactive)	> 125	> 125	Thioridazine	9.9 & 12.9
DS00370	-1 (inactive)	> 125	> 125	Chlorpromazine	
DS00366	-2 (inactive)	23.5	29.6	Promazine	[a] > 25 (Bactec)[34]
Ring-expanded scaffolds					
DS00381	-1 (inactive)	> 125	> 125	Imipramine	[a] 250 µM[35]
				Amitriptyline	75.1 & 99.6
DS003123	-2 (inactive)	> 125	> 125	Clozapine	> 125
DS003125	-1 (inactive)	> 125	> 125	Loxapine	> 125
DS00380	-1 (inactive)	> 125	> 125	Trimipramine	> 125
Non-thiazine scaffolds					
DS00386	-1 (inactive)	> 125	> 125	Thiothixene	30.8 & 40.6
DS00387	-2 (inactive)	> 125	> 125		
Quinoline scaffolds				**(Antimalarial drugs)**	
DSQ1	-2 (inactive)	> 125	> 125	Primaquine	
DSQ2	-2 (inactive)	> 125	> 125	Chloroquine	
DSQ3	-2 (inactive)	> 125	> 125	Primaquine	
DSQ4	-2 (inactive)	> 125	> 125	Chloroquine	
DSQ5	-2 (inactive)	> 125	>125	Chloroquine	
DSQ6	-2 (inactive)	> 125	> 125	Primaquine	

Table 4.2 continued…

NCE	*in silico* predicted CNS activity	M.*tb*H37Rv MIC_{90} (µM)	M.*tb*H37Rv MIC_{99} (µM)	Parent neuroleptic drug	MIC_{90} & MIC_{99} (µM) [a]lit MIC (µg/mL)
Isoniazid hybrids					
DS00362b	-2 (inactive)	92.8	120	Acepromazine	[a] > 20[32]
DS00362 (dimer)	-2 (inactive)	10.6	11.3	Acepromazine	[a] > 20[32]
DS00364a	0 (moderate)	> 125	> 125	Chlorpromazine	[a] 4-32 (Bactec)[33]
DS00364 (dimer)	0 (moderate)	>125	>125	Chlorpromazine	[a] 4-32 (Bactec)[33]
DS00365a	-1 (inactive)	101	> 125	Promazine	[a] > 25 (Bactec)[34]
DS00365 (dimer)	0 (moderate)	> 125	> 125	Promazine	[a] > 25 (Bactec) [34]
Nitrobenzenesulfonamides					
DS00325	0 (moderate)	> 125	> 125	Promazine	[a] > 25 (Bactec)[34]
DS00342	-1 (inactive)	> 125	> 125	Promazine	[a] > 25 (Bactec)[34]
DS00326	0 (moderate)	> 125	> 125	Trifluoperazine	[a] 8-32 (cfu)[31]
DS00338	-1 (inactive)	>125	> 125	Trifluoperazine	[a] 8-32 (cfu)[31]
DS00329	0 (moderate)	66.2	73.8	Chlorpromazine	[a] 4-32 (Bactec)[33]
DS00341	-2 (inactive)	>125	>125	Acepromazine	[a] > 20[32]
Pyrazole & Isoxazole derivatives					
DS00397	1 (moderate)	> 125	> 125	Promazine	[a] > 25 (Bactec)[34]
DS00398	1 (moderate)	90.9	117	Promazine	[a] > 25 (Bactec)[34]
Other non-basic side chains					
DS00385	1 (moderate)	> 125	> 125	Promazine	[a] > 25 (Bactec)[34]
DS00392	1 (moderate)	> 125	> 125	Trifluoperazine	[a] 8-32 (cfu)[31]
DS00393	0 (moderate)	> 125	> 125	Chlorpromazine	[a] 4-32 (Bactec)[33]
DS00394	0 (moderate)	> 125	> 125	Promazine	[a] > 25 (Bactec)[34]
DS00395	-1 (inactive)	38.1	44.4	Promazine	[a] > 25 (Bactec)[34]
DS00396	1 (moderate)	11.4	15.4	Promazine	[a] > 25 (Bactec)[34]
DS00390	1 (moderate)	> 125	> 125	Promazine	[a] > 25 (Bactec)[34]

MIC-minimum inhibitory concentration; MIC_{90} –concentration that inhibits 90% of bacterial isolates; MIC_{99}- concentration that inhibits 99% of bacterial isolates; Positive control-Rifampicin MIC_{90} (0.003129) & MIC_{99} (0.00503) µM; Concentration range tested 0.244-125 µM, MIC less than 125 are highlighted; [a] MICs from literature and system used for determination of direct antitubercular activity; cfu- colony-forming units; QikProp predicted CNS activity scale: -2 (inactive) to +2 (active).

The evaluation of the library of remodelled phenothiazines including native neuroleptic drugs against virulent M.*tb*H37Rv led to identification of several interesting hits from each subclass (Table 4.2). The library displayed MICs ranging from as low as 9.9 µM to 125 µM, the highest concentration tested. The remodelled phenothiazines as well as neuroleptic drugs that displayed MIC_{90} values less than 125 µM are shown in Figure 4.9.

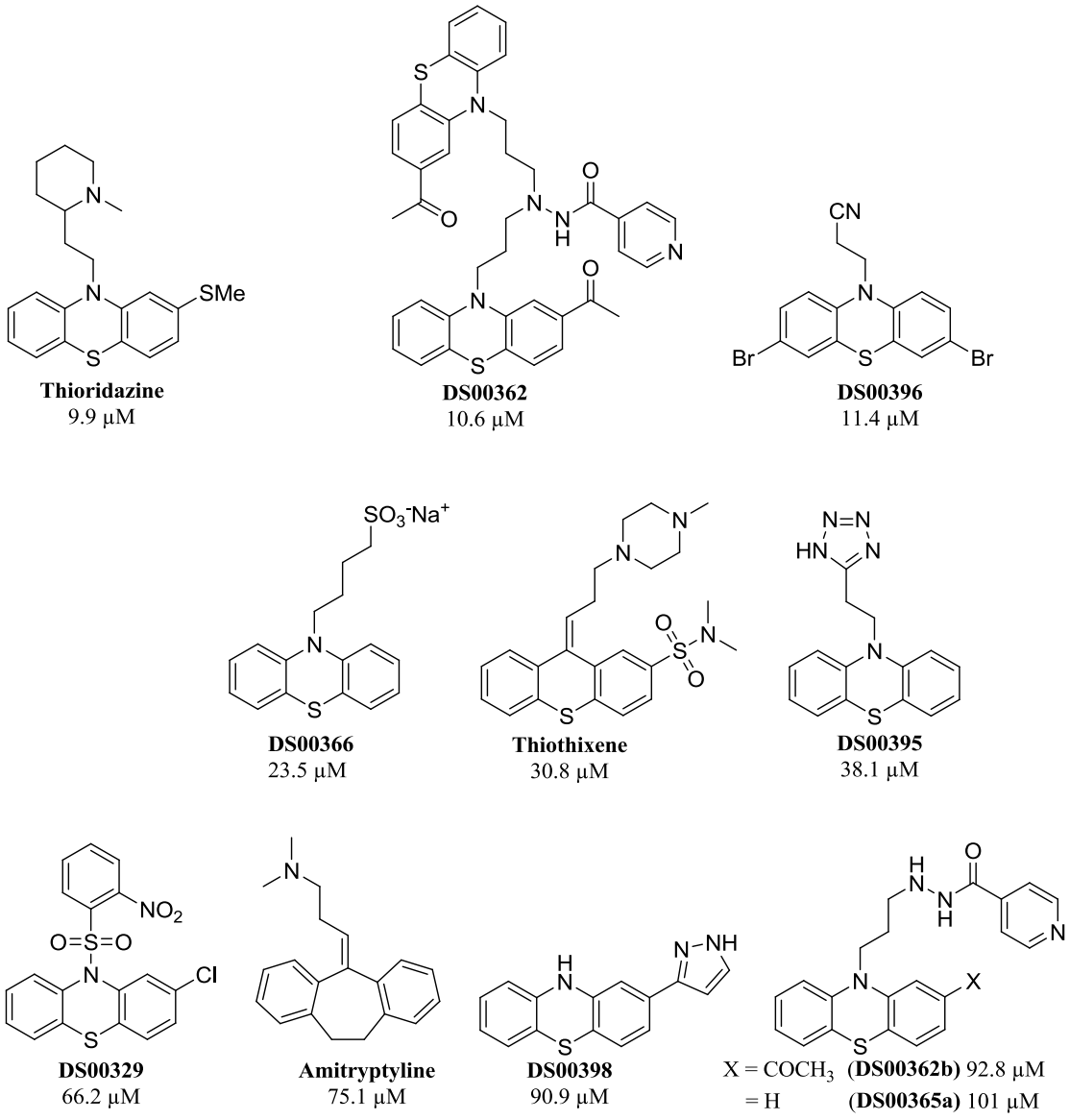

Figure 4.9: Remodelled phenothiazines and neuroleptic drugs with MIC_{90} below 125 µM. The MICs were determined using the GFPMA in a GASTE/Fe medium.

Alkyl chain extension, from propyl to butyl, yielded a hit compound, **DS00366** (Figure 4.9). The butylsulfonate NCE **DS00366** displayed a lower MIC_{90} of 23.5 µM relative to its analogue **DS0035** (> 125 µM). The parent thioridazine drug had the lowest MIC_{90}, 9.9 µM. Amitriptyline and thiothixene displayed MIC_{90} of 75.1 and 30.8 µM, respectively. It is important to note that the aforementioned antidepressants, amitriptyline and thiothixene, have not been previously evaluated as antitubercular agents. Therefore, their potential use as adjuvants or drug resistance-reversal agents in TB chemotherapy remains to be investigated.

Introduction of ring-expanded scaffolds did not lower MIC_{90} values in comparison to parent drugs and six-membered phenothiazine tricyclic systems. Moreover, replacement of the phenothiazine ring system with bicyclic quinolines and non-thiazine scaffolds had no effect on MICs. Substitution patterns in bicyclic quinolines and isoquinolines also had no effect on MICs as all NCEs displayed MICs greater than 125 µM.

Of the isoniazid hybrids, only **DS00365a, DS00362** and **DS00362b** displayed MIC_{90} less than 125 µM (Figure 4.9). Interestingly, **DS00362** whose molecular weight (699.88 Da) lies out of the conventional oral drug space (300-500 Da), displayed the lowest MIC_{90} of 10.6 µM (Table 4.2). The presence of an acetyl group at C-2 of the phenothiazine appeared to have an effect on MICs as observed for isoniazid hybrid dimer **DS00362** (10.6 µM) and monomer **DS00362b** (92.8 µM). Nitrobenzenesulfonamide **DS00329** and pyrazole **DS00398** also exhibited lower MICs of 66.2 µM and 90.9 µM, respectively.

Dibromo-substituted NCE **DS00396** emerged as the most active of the *N*-alkyl nitrile series with the lowest MIC_{90} of 11.4 µM (Figure 4.9). Furthermore, the MIC is 2-fold lower than that of NCE **DS00366** (23.5 µM) from the *N*-alkylsulfonates series. Another NCE, tetrazole **DS00395**, also displayed a relatively low MIC_{90} of 38.1 µM (Figure 4.9).

It is noteworthy that the hit compounds identified from the antimycobacterial screening were predicted to be CNS-inactive and also less likely to cross the blood/brain barrier. Therefore, these hit compounds hold great potential for further development as antitubercular agents that are devoid of neuroleptic effects.

Although *N*-propylsulfonates (**DS0031**, **DS0032**, **DS0034** & **DS0035)** displayed MIC_{90} and MIC_{99} values greater than 125 µM, they were of particular interest to this study for various reasons. They are analogous to clinically approved neuroleptics trifluoperazine, thioridazine, chlorpromazine and promazine, which have known physical and pharmacological properties. Additionally, the replacement of the alkylamine moiety with an alkylsulfonate as the only structural modification, created the greatest contrast between the parent neuroleptic drugs and the NCEs. Contrary to the lipophilic chromophore/basic side chain paradigm, an alkyl sulfonate functionality is expected to impart aqueous solubility and to exist as negatively charged species at physiological pH. It was therefore decided to carry out further investigations to establish their structure-antimycobacterial activity relationships and structure-neuroleptic activity relationships.

4.2.3 Investigation of *N*-propylsulfonates as non-neuroleptic antitubercular agents

4.2.3.1 Inhibition of M.*tb* growth and determination of cell viability

The *N*-propylsulfonates (**DS0031**, **DS0032**, **DS0034** & **DS0035**) were selected for further evaluation against M.*tb*H37Rv (UCT IIDMM). The GFPMA was used to evaluate bactericidal/ bacteriostatic activity against extracellular M.*tb* in a Middlebrook 7H9 medium.[36] Isoniazid and the neuroleptic thioridazine were selected as positive controls. Additionally, their ability to inhibit intracellular M.*tb* replication was assessed. For intracellular inhibition of M.*tb* growth, bone marrow-derived macrophages infected with M.*tb* were treated for five days with the respective remodelled phenothiazines. Furthermore, cell viability was determined using CellTiter-Blue® Reagent as an indicator of cytotoxicity in infected macrophages.

The remodelled phenothiazines displayed a concentration-dependent inhibitory effect on replication of *M.tb*H37Rv.gfp (Figure 4.10). Interestingly, the order of antimycobacterial activity of the NCEs (i.e. **DS0035** & **DS0034 > DS0032 *&* DS0031**) did not follow the order of potency of the neuroleptic drugs they are analogous to i.e. trifluoperazine > thioridazine > chlorpromazine > promazine.[8] The structures of NCEs only varied from each other by substituents at C-2 of the tricyclic ring system. Unsubstituted NCE (**DS0035**) and a chloro-substituted NCE (**DS0034**) displayed MICs of 12.5 µg/mL. The MICs of the other two NCEs (trifluoromethyl-substituted **DS0031** and thiomethyl-substituted **DS0032**) were 2-fold higher (Table 4.3). These observations demonstrate that although MICs of the NCEs were higher than that of parent neuroleptic drugs, antimycobacterial activity could still be retained after structural manipulation.

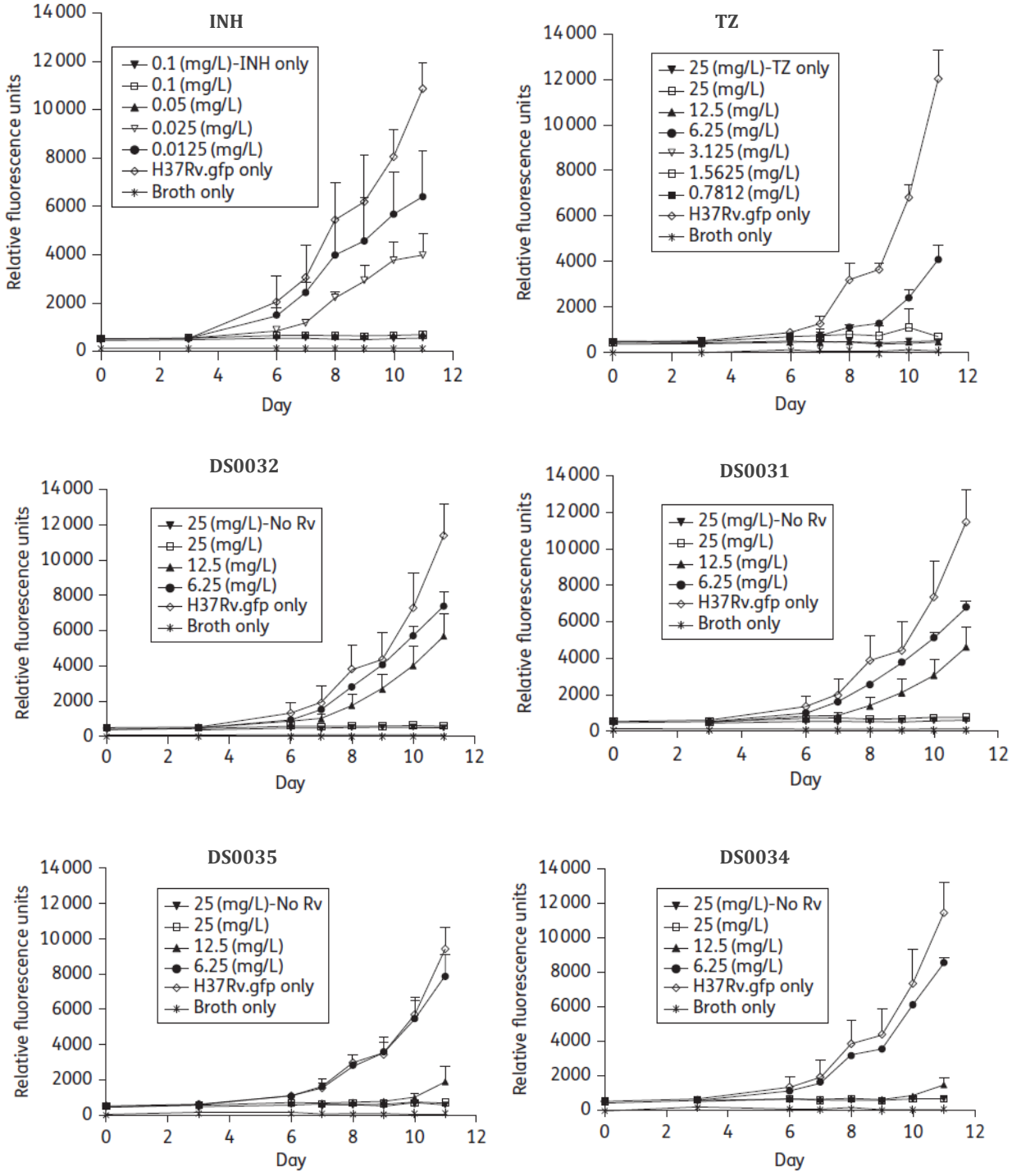

Figure 4.10: Direct antibacterial activity of the four remodelled phenothiazines (**DS0031**, **DS0032**, **DS0034** & **DS0035**) against M.*tb*H37Rv using the GFPMA in a Middlebrook 7H9 medium. Isoniazid (INH) and neuroleptic thioridazine (TZ) were used as positive controls and were evaluated at concentration ranges of 0.0125-0.1 and 0.7812-25 µg/mL, respectively. The fluorescence of M.*tb*H37Rv.gfp was measured for 12 days to determine the effects of the respective compounds on M.*tb* replication.

Table 4.3: *In vitro* antimycobacterial activity of remodelled phenothiazines in comparison to literature-reported MICs of parent neuroleptic drugs

Remodelled Phenothiazine	MIC against *M.tb*H37Rv.gfp (µg/mL)	Parent Neuroleptic drug	*MIC of parent drug ((µg/mL)
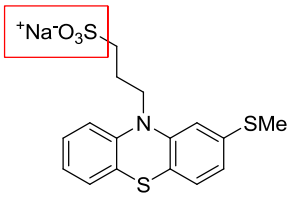 **DS0032**	25	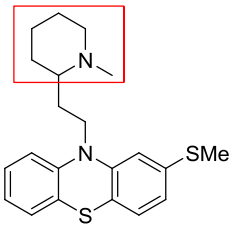 **Thioridazine**	8-32 (Bactec)[37] 6-12 (Bactec) [34]
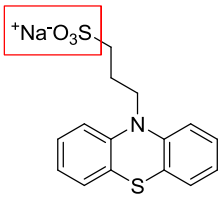 **DS0035**	12.5	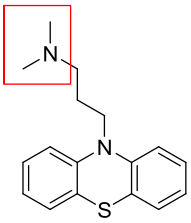 **Promazine**	> 25 (Bactec)[34]
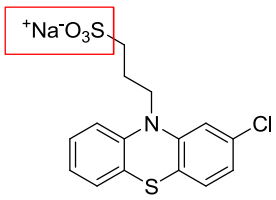 **DS0034**	12.5	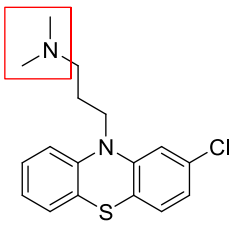 **Chlorpromazine**	12.5 (cfu)[38] 4-32 (Bactec)[33] 6-12 (Bactec)[34]
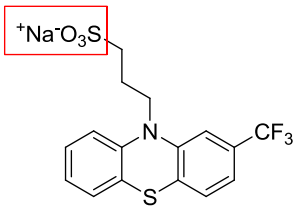 **DS0031**	25	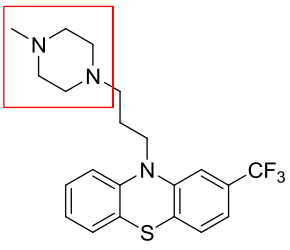 **Trifluoperazine**	5-8 (cfu)[39] 4-16 (cfu)[40] 8-32 (cfu)[31]

MIC- minimum inhibitory concentration; Isoniazid and neuroleptic thioridazine were used as positive controls and were evaluated at concentration ranges of 0.0125-0.1 and 0.7812-25 µg/mL, respectively; * MIC obtained from literature, system used for determination of direct antitubercular activity is given in brackets; cfu- colony-forming units.

The NCEs with the lowest MICs showed between 40% and 60% inhibition against intracellular M.*tb* at 25µg/mL thus demonstrating their ability to transverse cell membrane systems (Figure 4.11). Furthermore, it is possible that the NCEs also retained the capacity to concentrate within macrophages, as described for the parent neuroleptic drugs.[37]

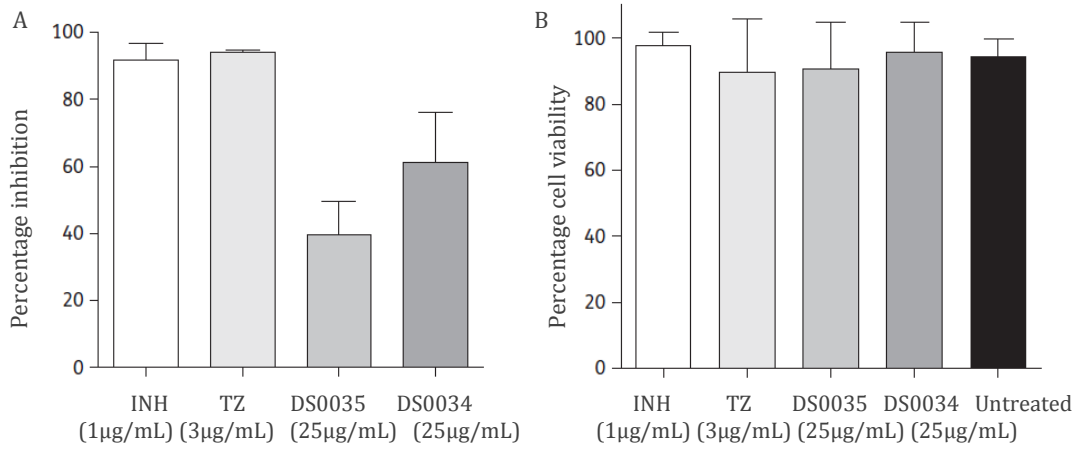

Figure 4.11: The activity of phenothiazine derivatives (**DS0034** & **DS0035**) against intracellular M.*tb*H37Rv to evaluate efficacy and cell viability. **A**- Bone marrow-derived macrophages infected with M.*tb*H37Rv were treated for five days with the respective NCEs. They were then lysed and plated for cfu determination. Isoniazid (INH) and thioridazine (TZ) were used as positive controls. **B**- Post treatment, cell viability was determined using CellTiter-Blue® Reagent as measure of cytotoxicity in infected macrophages.

Moreover, infected macrophages were almost completely viable (> 95%) post-treatment with the respective remodelled phenothiazines, thus pointing to their lack of cytotoxicity. The percentages of cell viability for all four NCEs are tabulated in Table 4.4. It is important to note that at the highest concentration tested, 25 µg/mL, thioridazine was cytotoxic whereas its analogue **DS0032** was not. Furthermore, at the same concentration, the rest of the NCEs displayed negligible cytotoxicity.

Table 4.4: Cell viability as a measure of cytotoxicity, bone marrow-derived macrophages were treated for five days, after which cell viability was determined using CellTiter-Blue® Reagent. TZ- thioridazine

Concentration	Cell Viability (%)				
	TZ	**DS0035**	**DS0034**	**DS0031**	**DS0032**
25.00 µg/mL	**0.00**	98.36	98.05	98.41	**100.00**
12.50 µg/mL	**0.00**	100.00	97.87	100.00	**100.00**
6.25 µg/mL	**0.00**	100.00	97.92	100.00	**99.54**
3.13 µg/mL	87.45	99.95	97.96	100.00	98.85
1.56 µg/mL	98.75	100.00	100.00	96.620	100.00
0.78 µg/mL	99.93	100.00	99.13	98.36	100.00
0.39 µg/mL	99.15	98.80	98.72	98.93	100.00
0.20 µg/mL	99.89	100.00	99.78	96.86	100.00

4.2.3.2 Investigation of the neuroleptic potential of *N*-propylsulfonates

Having established the ability of the four NCEs (**DS0031**, **DS0032**, **DS0034** & **DS0035**) to inhibit both extracellular and intracellular M.*tb* replication, their neuroleptic potential was investigated next. The NCEs were screened in dopamine and serotonin receptor radioligand binding assays to corroborate *in silico* predicted CNS activity results (Perkin Elmer, formerly Caliper Life Sciences, Maryland USA). They were evaluated for binding to dopaminergic receptor subtypes D_1, D_2 and D_3 as well as serotonergic receptor subtypes 5-HT_{1A}, 5-HT_{2A} and 5-HT_{2C} (Figure 4.12).

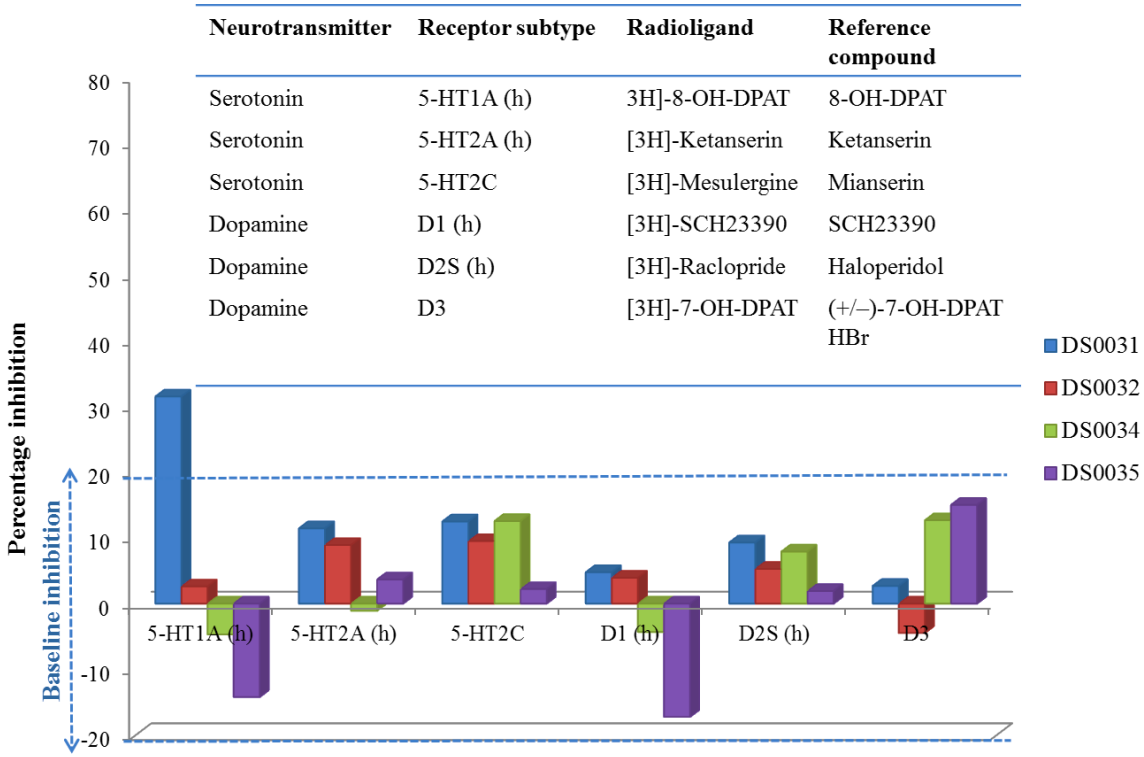

Figure 4.12: Results from dopamine and serotonin receptor radioligand binding assay showing percentage inhibition of binding for remodelled phenothiazines (**DS0031**, **DS0032**, **DS0034** & **DS0035)**; Table embedded lists ligands used in the assay; NovaScreen radio-ligand binding assay standard baseline range -20% to + 20% ; Inhibition of binding -20% to + 20% (inactive); 20% to 49% (marginal activity) ; > 50% (active); h- human recombinant; All the remodelled phenothiazines displayed no binding to the respective receptors except **DS0031**which exhibited marginal serotonin receptor (5-HT_{1A}) binding .

The results demonstrated that there was no dopamine and serotonin receptor binding by any of the remodelled phenothiazines except for **DS0031** which displayed marginal serotonin receptor (5-HT_{1A}) binding. It is known that substitution at C-2 of phenothiazines influences CNS receptor binding affinity. In particular, the presence of a trifluoromethyl substituent at C-2 in conjunction with an alkylamine moiety is known to increase CNS receptor binding affinity.[41,42] It is therefore possible that **DS0031** retained marginal serotonin receptor binding due to the presence of a trifluoromethyl group at C-2 position.

Overall, these observations demonstrated that it is possible to abolish binding of phenothiazines to CNS receptors whilst retaining antimycobacterial activity through rationalized structural remodelling. Successfully switching off CNS receptor binding without losing antimycobacterial activity is a challenge in itself. Others have reported remodelled phenothiazines which displayed antitubercular activity but still retained 40-50% dopamine receptor binding affinity.[43]

Herein, the key to successful abolishment of dopamine and serotonin receptor binding involved increasing polarity by introducing a sulfonate functionality at a critical receptor recognition site. Furthermore, the polar sulfonate moiety imparts aqueous solubility thus deviating from the lipophilic chromophore/basic side chain obeyed by native phenothiazine drugs. This strategy also relied on the change of charge i.e. at physiological pH the distal amine moiety (pKa 8-9.5) of phenothiazine drugs acquires a positive charge whereas sulfonates ((pKa ~ 2) would be negatively charged (Chapter 2). These findings were fundamental to this study and encouraged further investigation of the NCEs (Salie, S.; Hsu, N.; Semenya, D.; Jardine, A.; Jacobs, M. Novel Non-Neuroleptic Phenothiazines Inhibit Mycobacterium Tuberculosis Replication. *J. Antimicrob. Chemother.* **2014**, *69* (6), 1551–1558).[36]

4.2.3.3 Preclinical evaluation of *N*-propylsulfonates of phenothiazines

4.2.3.3.1 *In vitro* microsomal metabolic stability and kinetic solubility

Preclinical evaluation of the NCEs was inspired by the positive outcomes from antimycobacterial screening as well as dopamine and serotonin receptor binding studies. To corroborate *in silico* predicted ADMET properties, *in vitro* microsomal metabolic stability and kinetic solubility studies were conducted (UCT Division of Clinical Pharmacology) (Table 4.5).

Table 4.5: *In vitro* microsomal stability and kinetic solubility of remodelled phenothiazines

Remodelled phenothiazines	µM solubility pH 2	µM solubility pH 6.5	µM solubility FaSSIF* pH 6.5	Liver microsomal species	Percentage NCE remaining	Projected Half- life (min)**
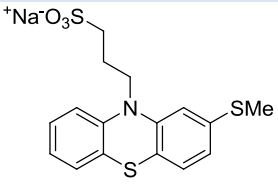 **DS0032**	181.0	179.2	182.4	Mouse	72.4	64.9
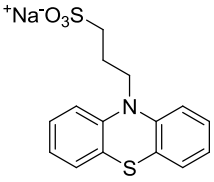 **DS0035**	184.3	167.3	172.3	Mouse	88.1	> 100
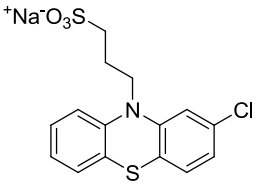 **DS0034**	177.0	184.1	194.7	Mouse	90.0	> 100
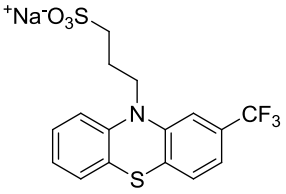 **DS0031**	167.0	158.9	187.0	Mouse	87.3	> 100

* FaSSIF- bio-relevant buffer that simulates the small intestine juices in fasted state; **A single time point assay (30 min) was used to establish ranking of the NCEs for prediction of half-life; Quality control standards for validation of metabolic stability include (i) Propanolol (8.1; 8.3) (ii) Midazolom (6.9, 7.8) (iii) MMV390048 (96.1, > 100) [% remaining (first value) and projected half-life (second value)].

As discussed in Chapter 2, solubility is a key determinant of absorption and oral bioavailability.[44] The kinetic solubility of the NCEs was measured at pH 2 and pH 6.5 in

fasted state simulated intestinal fluid (FaSSIF) medium.[45] All compounds had solubility values greater than 100 which were interpreted as highly soluble (Table 4.5). These observations were anticipated as the presence of a highly polar sulfonate moiety is expected to impart aqueous solubility.

Early assessment of microsomal stability provides crucial information on metabolic liabilities of potential drug candidates. Low metabolic stability is associated with high hepatic clearance as well as a short half-life.[46] The metabolic stability of the NCEs was assessed in mouse liver microsomes using a single time point assay that involved 30 min incubation and measurement of the percentage of compound remaining.[46] The metabolic stability of the NCEs was comparable to the positive control MMV390048 (Table 4.5). The percentage residual NCE ranged between 72.4 and 90.0. These NCEs do not have any apparent highly reactive groups excluding **DS0032** which might be more susceptible to sulfoxidation. This could potentially explain why NCE **DS0032** displayed the lowest percentage NCE remaining (72.4) and a shorter half-life (64.9).

4.2.3.3.2 *In vivo* toxicity in mice

The toxicity potential of two *N*-propylsulfonates NCEs (**DS0034** & **DS0035**) was evaluated in a small animal model at a dose of 100mg/kg as the maximum starting dose and outcomes were measured against thioridazine or against no treatment. For this purpose, 6-8 week old adult female C57Bl/6 mice were used. Preliminary observations revealed that while a daily dose administration of either 100mg/kg or 40mg/kg thioridazine caused 100% mortality within 48h, all the animals challenged with 100mg/kg of **DS0034** or **DS0035** survived. Moreover, mice that were treated with **DS0034** or **DS0035** lost approximately 10% of their body weight. Of the body organs assessed, brains, livers, lungs, kidneys and hearts showed normal weight distribution whereas spleens were significantly reduced. Overall, the

comparative toxicity profiles of **DS0034** and **DS0035** were significantly better than that of thioridazine even when the latter was tested at a dose 10-fold lower. The full details of the *in vivo* toxicity evaluation will be reported elsewhere at a later stage as the investigation is still in progress.

4.4 Concluding remarks

Phenothiazines possess desirable antitubercular properties including multi-drug resistance reversal properties. At clinically relevant doses, their extended use may lead to adverse side effects, hence the resistance to their application in TB chemotherapy. Thioridazine, a milder phenothiazine, has recently been successfully repurposed for XDR-TB therapy.

Herein, rationalized remodelling strategies were employed to generate a focused library of NCEs that would less likely exhibit neuroleptic effects, but still retain antimycobacterial properties. The general remodelling approach was to eliminate minimum structural requirements for neuroleptic action. The library comprised *N*-propylsulfonates of phenothiazines; *N*-butylsulfonates phenothiazines; *N*-propylsulfonates of quinolines; *N*-propylsulfonates of ring-expanded scaffolds & non-thiazine scaffolds; molecular hybrids and *N*-alkyl phenothiazines with other non-basic terminal moieties.

Chapter 4 addressed one of the key objectives of this study by identifying interesting hits through screening the library against virulent M.*tb*H37Rv and probing their neuroleptic potential. The hit compounds with MIC_{90} (GAST/Fe) less than 25 µM included *N*-butylsulfonate **DS00366** (23.5 µM), nitrile **DS00396** (11.4 µM) and isoniazid hybrid dimer **DS00362 (**10.6 µM). Furthermore, a lower MIC_{90} of butylsulfonate **DS00366** (23.5 µM) in comparison to its analogue propylsulfonate **DS0035** (MIC_{90} > 125 µM), indicated that efficacy could be improved through alkyl chain extension. Moreover, for the first time, the antitubercular activity of the neuroleptics amitriptyline and thiothixene was demonstrated.

Further evaluation of *N*-propylsulfonates (**DS0031**, **DS0032**, **DS0034** & **DS0035**) also gave interesting results. The conclusions drawn from the observations include: (i) The remodelled phenothiazines retained antitubercular properties against M.*tb*H37Rv.gfp (7H9 MIC 12.5- 25 µg/mL); (ii) They displayed between 40% and 60% inhibition of intracellular M.*tb*H37Rv thus demonstrating their ability to transverse cell membrane systems and access intracellular bacilli; (iii) Cell viability measurements indicated that in contrast to the parent neuroleptic thioridazine which was toxic to bone-marrow derived macrophages at higher concentrations (6.25-25 µg/mL, Table 4.4), the remodelled phenothiazines were not toxic.

The neuroleptic potential of this series of *N*-propylsulfonates was investigated through dopamine and serotonin receptor radioligand binding assays. The results demonstrated that, through careful structural manipulation undesirable CNS receptor binding could be abolished. Additionally, preclinical evaluation of the *N*-propylsulfonates revealed favourable *in vitro* metabolic stability, kinetic solubility and *in vivo* toxicity profiles. These observations led to a conclusion that these NCEs possess promising drug-like properties, thus evaluation of their *in vivo* efficacy against M.*tb* in mice is currently underway.

Overall, this chapter reports on subclasses of remodelled phenothiazines that hold potential for further development as non-neuroleptic antitubercular agents. Lowering MICs and hit-to-lead optimization would require standard medicinal chemistry approaches that involve iterative structural modification processes.

The anticancer properties of phenothiazines have been demonstrated in various literature reports.[47,48,49,50] Therefore, it was decided to evaluate the same library of compounds as potential anticancer agents, to evaluate whether their anticancer effects were retained post-remodelling. A report on the anticancer screening is given in the next chapter.

References

(1) WHO. http://www.who.int/tb/publications/global_report/en/ *(accessed 30/05/2015)*, Global Tuberculosis Report; 2014.

(2) Ambrosio, L. D.; Centis, R.; Sotgiu, G.; Pontali, E.; Spanevello, A.; Migliori, G. B. New Anti-Tuberculosis Drugs and Regimens : 2015 Update. *ERJ Open Res.* **2015**, *1*, 1–15.

(3) Koul, A.; Arnoult, E.; Lounis, N.; Guillemont, J.; Andries, K. The Challenge of New Drug Discovery for Tuberculosis. *Nature* **2011**, *469* (7331), 483–490.

(4) Ernst, J. D. The Immunological Life Cycle of Tuberculosis. *Nat. Rev. Immunol.* **2012**, *12*, 581–591.

(5) Sarkar, S.; Suresh, M. R. An Overview of Tuberculosis Chemotherapy - A Literature Review. *J. Pharm. Pharm. Sci.* **2011**, *14* (2), 148–161.

(6) Dutta, N. K.; Mehra, S.; Kaushal, D. A Mycobacterium Tuberculosis Sigma Factor Network Responds to Cell-Envelope Damage by the Promising Anti-Mycobacterial Thioridazine. *PLoS One* **2010**, *5* (4), 1–10.

(7) Field, S. K.; Fisher, D.; Jarand, J. M.; Cowie, R. L.; Field, S. K.; Fisher, D.; Jarand, J. M.; Cowie, R. L. New Treatment Options for Multidrug-Resistant Tuberculosis. *Ther. Adv. Respir. Dis.* **2012**, *6* (5), 255–268.

(8) Warman, A. J.; Rito, T. S.; Fisher, N. E.; Moss, D. M.; Berry, N. G.; O'Neill, P. M.; Ward, S. a.; Biagini, G. a. Antitubercular Pharmacodynamics of Phenothiazines. *J. Antimicrob. Chemother.* **2013**, *68* (4), 869–880.

(9) Amaral, L.; Martins, M.; Viveiros, M. Enhanced Killing of Intracellular Multidrug-Resistant Mycobacterium Tuberculosis by Compounds That Affect the Activity of Efflux Pumps. *J. Antimicrob. Chemother.* **2007**, *59* (6), 1237–1246.

(10) Parida, S. K.; Rao, M. V; Singh, N.; Master, I.; Lutckii, A.; Keshavjee, S.; Andersson, J.; Zumla, A.; Maeurer, M. Totally Drug-Resistant Tuberculosis and Adjunct Therapies. *J. Int. Med.* **2015**, *277* (4), 388–405.

(11) Velayati, A. A.; Farnia, P.; Masjedi, M. R. Letter to Editor The Totally Drug Resistant Tuberculosis (TDR-TB). *Int J Clin Exp Med* **2013**, *6* (4), 307–309.

(12) Udwadia, Z. F.; Sen, T.; Pinto, L. M. Safety and Efficacy of Thioridazine as Salvage Therapy in Indian Patients with XDR-TB. *Recent Pat Antiinfect Drug Discov* **2011**, *6*, 88–91.

(13) Pontali, E.; Sotgiu, G.; Ambrosio, L. D.; Centis, R.; Migliori, G. B. Tuberculosis : A Systematic and Critical Analysis of the Evidence. *Eur. J. Respir.* **2016**, *47*, 394–402.

(14) Lienhardt, C.; Raviglione, M.; Spigelman, M.; Hafner, R.; Jaramillo, E.; Hoelscher, M.; Zumla, A.; Gheuens, J. New Drugs for the Treatment of Tuberculosis: Needs, Challenges, Promise, and Prospects for the Future. *J. Infect. Dis.* **2012**, *205* (SUPPL. 2), 1–9.

(15) Amaral, L.; Boeree, M.; Gillespie, S.; Udwadia, Z.; van Soolingen, D. Thioridazine Cures Extensively Drug-Resistant Tuberculosis (XDR-TB) and the Need for Global Trials Is Now! *Int. J. Antimicrob. Agents* **2010**, *35* (6), 524–526.

(16) Dunn, E. A.; Roxburgh, M.; Larsen, L.; Smith, R. A. J.; McLellan, A. D.; Heikal, A.; Murphy, M. P.; Cook, G. M. Incorporation of Triphenylphosphonium Functionality Improves the Inhibitory Properties

of Phenothiazine Derivatives in Mycobacterium Tuberculosis. *Bioorg. Med. Chem.* **2014**, *22* (19), 5320–5328.

(17) Zhang, Y. The Magic Bullets and Tuberculosis Drug Targets. *Annu. Rev. Pharmacol. Toxicol.* **2005**, *45* (2), 529–564.

(18) Kumar, A.; Farhana, A.; Guidry, L.; Saini, V.; Houndalus, M.; Steyn, A. J. C. Redox Homeostasis in Mycobacteria: The Key to Tuberculosis Control. *Expert Rev Mol Med* **2011**, *13*, e39.

(19) Shirude, P. S.; Paul, B.; Roy Choudhury, N.; Kedari, C.; Bandodkar, B.; Ugarkar, B. G. Quinolinyl Pyrimidines: Potent Inhibitors of NDH-2 as a Novel Class of Anti-TB Agents. *ACS Med. Chem. Lett.* **2012**, *3* (9), 736–740.

(20) Kristiansen, J. E.; Amaral, L. The Potential Management of Resistant Infections with Non-Antibiotics. *J. Antimicrob. Chemother.* **1997**, *40* (3), 319–327.

(21) Yano, T.; Lin-Sheng, L.; Weinstein, E.; Teh, J. S.; Rubin, H. Steady-State Kinetics and Inhibitory Action of Antitubercular Phenothiazines on Mycobacterium Tuberculosis Type-II NADH-Menaquinone Oxidoreductase (NDH-2). *J. Biol. Chem.* **2006**, *281* (17), 11456–11463.

(22) Teh, J. S.; Yano, T.; Rubin, H. Type II NADH: Menaquinone Oxidoreductase of Mycobacterium Tuberculosis. *Infect. Disord. Drug Targets* **2007**, *7* (2), 169–181.

(23) Schurig-briccio, L. A.; Yano, T.; Rubin, H.; Gennis, R. B. Characterization of the Type 2 NADH : Menaquinone Oxidoreductases from Staphylococcus Aureus and the Bactericidal Action of Phenothiazines. *Biochim. Biophys. Acta* **2014**, *1837*, 954–963.

(24) Pluta, K.; Morak-Młodawska, B.; Jeleń, M. Recent Progress in Biological Activities of Synthesized Phenothiazines. *Eur. J. Med. Chem.* **2011**, *46* (8), 3179–3189.

(25) Kristiansen, J. E.; Dastidar, S. G.; Palchoudhuri, S.; Roy, D. S.; Das, S.; Hendricks, O.; Christensen, J. B. Phenothiazines as a Solution for Multidrug Resistant Tuberculosis : From the Origin to Present. *Int. Microbiol.* **2015**, *18*, 1–12.

(26) He, C.-X.; Meng, H.; Zhang, X.; Cui, H.-Q.; Yin, D.-L. Synthesis and Bioevaluation of Phenothiazine Derivatives as New Antituberculosis Agents. *Chinese Chem. Lett.* **2015**, *26* (08), 951–954.

(27) Ramprasad, J.; Nayak, N.; Dalimba, U. Design of New Phenothiazine-Thiadiazole Hybrids via Molecular Hybridization Approach for the Development of Potent Antitubercular Agents. *Eur. J. Med. Chem.* **2015**, *106*, 75–84.

(28) Siddiqui, A. B.; Trivedi, A. R.; Kataria, V. B.; Shah, V. H. Phenothiazines as Antitubercular Agents. *Bioorg. Med. Chem. Lett.* **2014**, *24*, 1493–1495.

(29) Addla, D.; Jallapally, A.; Gurram, D.; Yogeeswari, P.; Sriram, D.; Kantevari, S. Rational Design, Synthesis and Antitubercular Evaluation of Novel 2-(trifluoromethyl)phenothiazine[1,2,3]triazole Hybrids. *Bioorg. Med. Chem. Lett.* **2014**, *24* (1), 233–236.

(30) Westhuyzen, R. Van Der; Winks, S.; Wilson, C. R.; Boyle, G. A.; Gessner, R. K.; Melo, C. S. De; Taylor, D.; Kock, C. De; Njoroge, M.; Brunschwig, C.; Lawrence, N.; Rao, S. P. S.; Sirgel, F.; Helden, P. Van; Seldon, R.; Moosa, A.; Warner, D. F.; Arista, L.; Manjunatha, U. H.; Smith, P. W.; Street, L. J.; Chibale, K. Pyrrolo[3,4-C]pyridine-1,3(2H)-Diones: A Novel Antimycobacterial Class Targeting Mycobacterial Respiration. *J. Med. Chem.* **2015**, *58* (23), 9371–9381.

(31) Gadre, D. V.; Talwar, V. In Vitro Susceptibility Testing of Mycobacterium Tuberculosis Strains to Trifluoperazine. *J. Chemother.* **1999**, *11*, 203–206.

(32) Ratnakar, P.; Rao, S. P.; Sriramarao, P.; Murthy, P. S. Structure-Antitubercular Activity Relationship of Phenothiazine-Type Calmodulin Antagonists. *Int. Clin. Psychopharmacol.* **1995**, *10* (1), 39–44.

(33) Amaral, L.; Kristiansen, J. E.; Abebe, L. S.; Millett, W. Inhibition of the Respiration of Multi- Drug Resistant Clinical Isolates of Mycobacterium Tuberculosis by Thioridazine: Potential Use for Initial Therapy of Freshly Diagnosed Tuberculosis. *J. Antimicrob. Chemother.* **1996**, *38*, 1049–1053.

(34) Viveiros M B; Bosne-David S; Amaral L. Comparative in Vitro Activity of Phenothiazines against Multi-Drug Resistant Mycobacterium Tuberculosis. *Int. J. Antimicrob. Agents* **2000**, *16*, 69–71.

(35) Godbole, A. A.; Ahmed, W.; Bhat, R. S.; Bradley, E. K.; Ekins, S.; Nagaraja, V. Targeting Mycobacterium Tuberculosis Topoisomerase I by Small-Molecule Inhibitors. *Antimicrob. Agents Chemother.* **2015**, *59* (3), 1549–1547.

(36) Salie, S.; Hsu, N.; Semenya, D.; Jardine, A.; Jacobs, M. Novel Non-Neuroleptic Phenothiazines Inhibit Mycobacterium Tuberculosis Replication. *J. Antimicrob. Chemother.* **2014**, *69* (6), 1551–1558.

(37) Amaral, L.; Kristiansen, J. E.; Viveiros, M.; Atouguia, J. Activity of Phenothiazines against Antibiotic-Resistant Mycobacterium Tuberculosis: A Review Supporting Further Studies That May Elucidate the Potential Use of Thioridazine as Anti-Tuberculosis Therapy. *J. Antimicrob. Chemother.* **2001**, *47* (5), 505–511.

(38) Kristiansen J E; B, V. The Antibacterial Effect of Selected Phenothiazines and Thioxanthenes on Slow-Growing Mycobacteria. *Acta Pathol. Microbiol. Immunol. Scand.* **1986**, *94*, 393–398.

(39) Ratnakar P.; Murthy P. S. Antitubercular Activity of Trifluoperazine, a Calmodulin Antagonist. *FEMS Microbiol. Lett.* **1992**, *76*, 73–76.

(40) Gadre, D. V.; Talwar, V.; Gupta, H. C.; Murthy, P. S. Effect of Trifluoperazine, a Potential Drug for Tuberculosis with Psychotic Disorders, on the Growth of Clinical Isolates of Drug Resist- Ant Mycobacterium Tuberculosis. *Int. Clin. Psycho- Pharmacol.* **1998**, *13*, 129–131.

(41) Jaszczyszyn, A.; Gąsiorowski, K.; Świątek, P.; Malinka, W.; Cieślik-Boczula, K.; Petrus, J.; Czarnik-Matusewicz, B. Chemical Structure of Phenothiazines and Their Biological Activity. *Pharmacol. Reports* **2012**, *64* (1), 16–23.

(42) Feinberg, A. P.; Snyder, S. H. Phenothiazine Drugs : Structure-Activity Relationships Explained by a Conformation That Mimics Dopamine. *Proc. Nat. Acad. Sci.* **1975**, *72* (5), 1899–1903.

(43) Madrid, P. B.; Polgar, W. E.; Tanga, M. J. Synthesis and Antitubercular Activity of Phenothiazines with Reduced Binding to Dopamine and Serotonin Receptors. *Bioorg. Med. Chem. Lett.* **2007**, *17*, 3014–3017.

(44) Abay, E. T.; Westuizen, J. H. Van Der; Swart, K. J.; Gibhard, L.; Lawrence, N.; Dambuza, N.; Wilhelm, A.; Pravin, K.; Wiesner, L. Efficacy and Pharmacokinetic Evaluation of a Novel Anti-Malarial Compound (NP046) in a Mouse Model. *Malar. J.* **2015**, *14* (8), 1–7.

(45) Frank, K. J.; Westedt, U.; Rosenblatt, K. M.; Hölig, P.; Rosenberg, J.; Mägerlein, M.; Brandl, M.; Fricker, G. European Journal of Pharmaceutical Sciences Impact of FaSSIF on the Solubility and Dissolution- / Permeation Rate of a Poorly Water-Soluble Compound. *Eur. J. Pharm. Sci.* **2012**, *47* (1), 16–20.

(46) Di, L. I.; Kerns, E. H.; Gao, N.; Li, S. Q.; Huang, Y.; Bourassa, J. I. M. L.; Huryn, D. M.; Al, D. I. E. T. Experimental Design on Single-Time-Point High-Throughput Microsomal Stability Assay. *J. Pharm. Sci.* **2004**, *93* (6), 1537–1544.

(47) Cheng, H.; Liang, Y.; Kuo, Y.; Chuu, C.; Lin, C.; Lee, M.; Wu, A. T. H.; Yeh, C.; Chen, E.; Su, C. Identification of Thioridazine , an Antipsychotic Drug , as an Antiglioblastoma and Anticancer Stem Cell Agent Using Public Gene Expression Data. *Cell Death Dis.* **2015**, *3*, 1–13.

(48) Abuhaie, C.-M.; Bîcu, E.; Rigo, B.; Gautret, P.; Belei, D.; Farce, A.; Dubois, J.; Ghinet, A. Synthesis and Anticancer Activity of Analogues of Phenstatin , with a Phenothiazine A-Ring , as a New Class of Microtubule-Targeting Agents. *Bioorg. Med. Chem. Lett.* **2013**, *23* (1), 147–152.

(49) Belei, D.; Dumea, C.; Samson, A.; Farce, A.; Dubois, J.; Bîcu, E.; Ghinet, A. New Farnesyltransferase Inhibitors in the Phenothiazine Series. *Bioorganic Med. Chem. Lett.* **2012**, *22* (14), 4517–4522.

(50) Sudeshna, G.; Parimal, K. Multiple Non-Psychiatric Effects of Phenothiazines: A Review. *Eur. J. Pharmacol.* **2010**, *648* (1-3), 6–14.

Chapter 5

Structurally remodelled phenothiazines as potential anticancer chemotherapeutics

Preface

In the previous chapter, the antimycobacterial activity of remodelled phenothiazines and related drugs was reported. The screening led to the identification of several antimycobacterial hits with reduced likelihood of neuroleptic effects. Additionally, preclinical evaluation revealed favourable *in vitro* microsomal stability, kinetic solubility and *in vivo* toxicity profiles of selected new chemical entities (NCEs).

Phenothiazines are known to exhibit broad-spectrum biological activities and their anticancer potential has been demonstrated in multiple tumor cell lines. The key findings in chapter 4 demonstrated that careful structural manipulation of native phenothiazine drugs could lead to abrogation of unwanted neuroleptic effects whilst antimycobacterial activity was retained. Herein, a preliminary investigation of the library of remodelled phenothiazines reported in chapter 4 was carried out, to test whether application of the same principles could potentiate their anticancer effects.

5.1 Overview of Cancer

5.1.1 Brief overview and global statistics

Cancer is undoubtedly among the most devastating non-communicable diseases known to humankind and has been claiming millions of lives for years. There is mounting evidence that links the development of cancer to a rare population of cells termed cancer stem cells (CSCs).[1,2] CSCs are found within tumors and they possess characteristics similar to that of

normal stem cells such as self-renewal and the ability to differentiate into various cell types.[3] Moreover, they have the unique ability to initiate and sustain the disease.[1,4] As an example, a comparison of stem cell self-renewal during haematopoiesis (the formation of blood cellular components) and leukaemic transformation is given in Figure 5.1.[1]

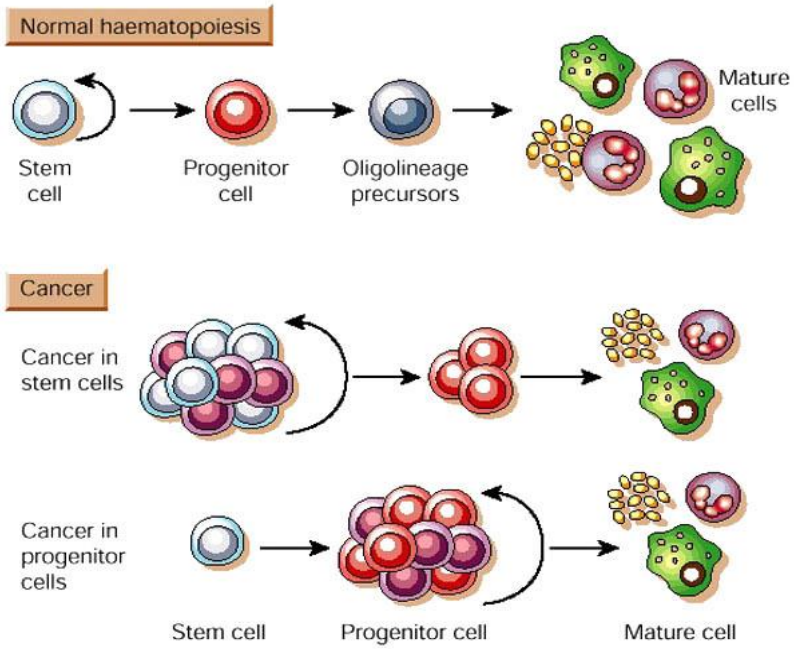

Figure 5.1: The transformation of stem cells in normal and leukaemic haematopoiesis. The signalling pathways that are associated with self-renewal of stem cells are tightly regulated, their dysregulation promotes uncontrollable self-renewal.[1]

Over half of cancer deaths that occur annually are attributable to the most common types including lung, breast, colorectal, liver and stomach cancers. In 2012, an estimated 14.1 million new cancer cases and 8.2 million deaths occurred. Of the various malignancies, lung cancer remains the most prevalent with an estimated 1.8 million cases in 2012. In the same year, brain and central nervous system cancers accounted for 1.8% of the new cases and 2.3%

of the deaths.[5] The percentage contribution to deaths caused by the most commonly diagnosed cancers is represented in Figure 5.2. Types of cancer treatment include radiation, chemotherapy, targeted therapy, immune therapy, hormone therapy and surgical interventions.[6,7]

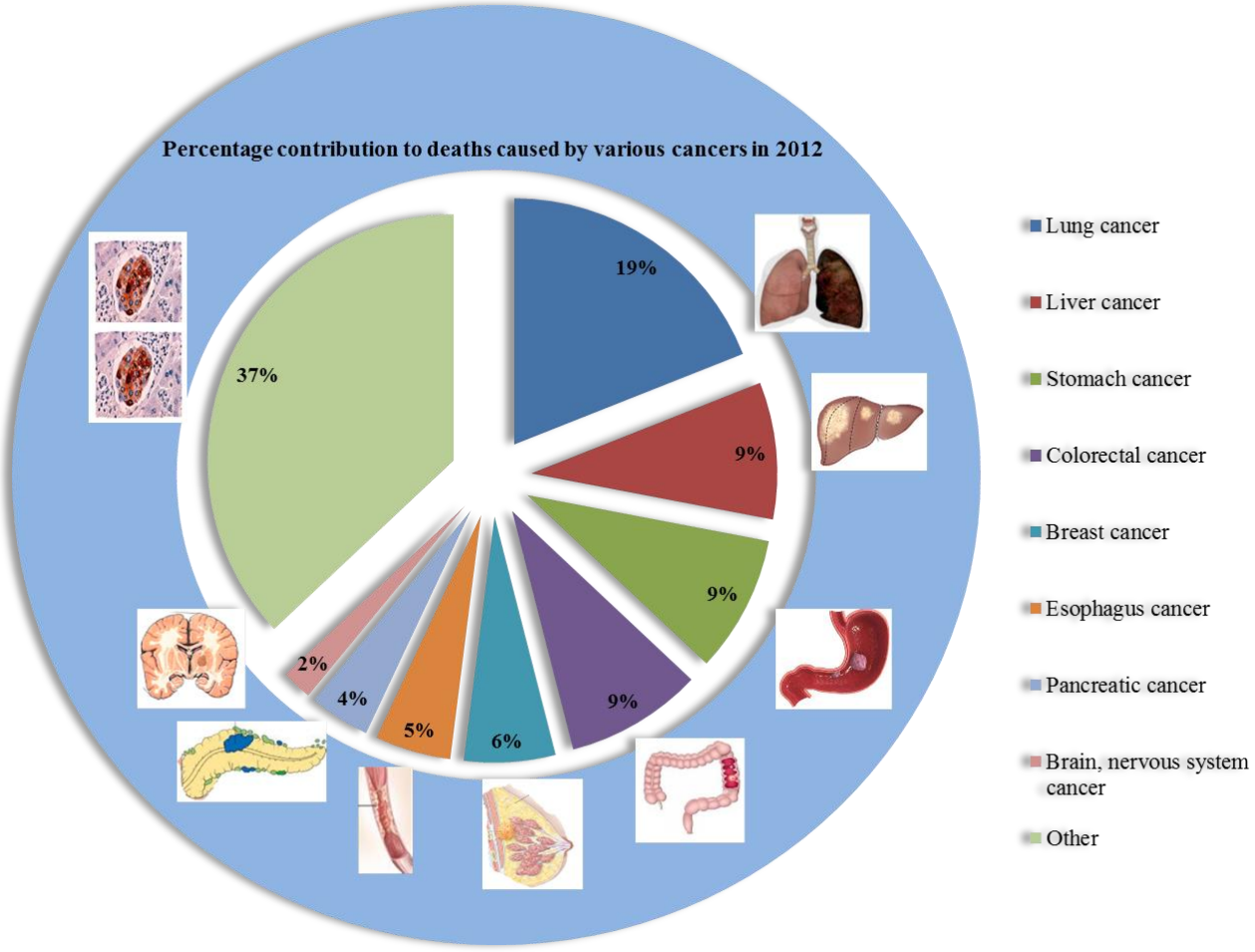

Figure 5.2: Estimated percentage contribution to deaths caused by various types of cancers in 2012.[5]

5.1.2 Cancer chemotherapy

The normal functioning of the cell cycle is regulated by multiple mechanisms and their dysregulation is implicated in the development of tumors.[8] The phases of the cell cycle include resting stage (G0 phase), growth phase 1 (G1), DNA synthesis (S phase), growth phase 2 (G2) and mitosis (M). It also involves critical checkpoints that are regulated by

complex mechanisms such as cyclin-dependent kinases (CDKs). The cell cycle represents an opportunity for development of new chemotherapeutics, thus the majority of antineoplastics target the proliferation cycle of cells.[9] Due to the inability of anticancer drugs to differentiate between healthy cells and tumor cells, cancer chemotherapy is associated a plethora of side effects including gastrointestinal tract lesions, bone marrow suppression and hair loss.[10]

Various classes of drugs are in clinical use for cancer chemotherapy including alkylating agents, antimetabolites, antitumor antibiotics, topoisomerase inhibitors, mitotic inhibitors and corticosteroids (Figure 5.3).

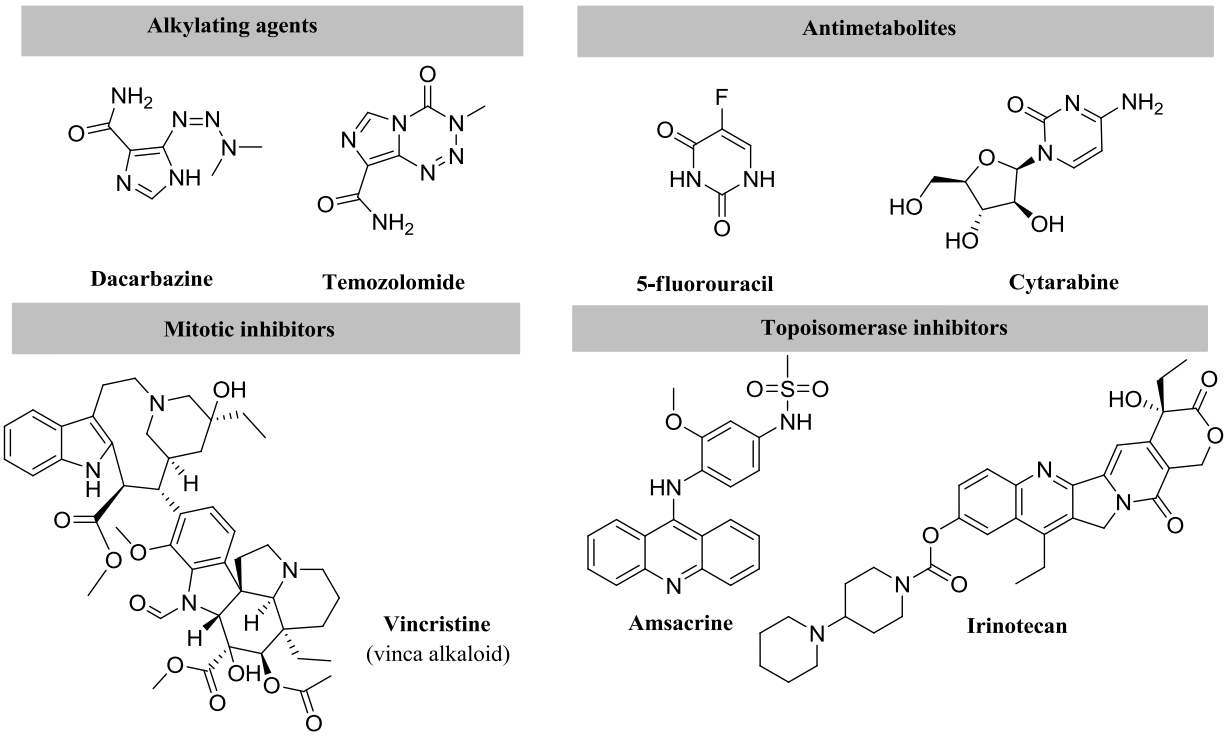

Figure 5.3: Examples of different classes of antineoplastics.[10]

Chemotherapeutics such as cytarabine, 5-fluorouracil, fludarabine and pentostatin inhibit DNA synthesis.[11] Other anticancer agents including paclitaxel or docetaxel and vinca alkaloids such as vinblastine, vincristine, vindesine, and vinorelbine interfere with the normal

functioning of mitosis.[12,13] Reportedly, antimitosis drugs bind at three major sites of tubulin (a component of microtubules) namely the vinca, taxane and colchicine sites.[14] Other examples of potent antimitotic agents include combretastatin A-4 (a natural product extracted from a South African tree, *Combretum caffrum*) and epothilones.[12] An illustration of the cell cycle events that are targeted by most anticancer drugs is given in Figure 5.4.

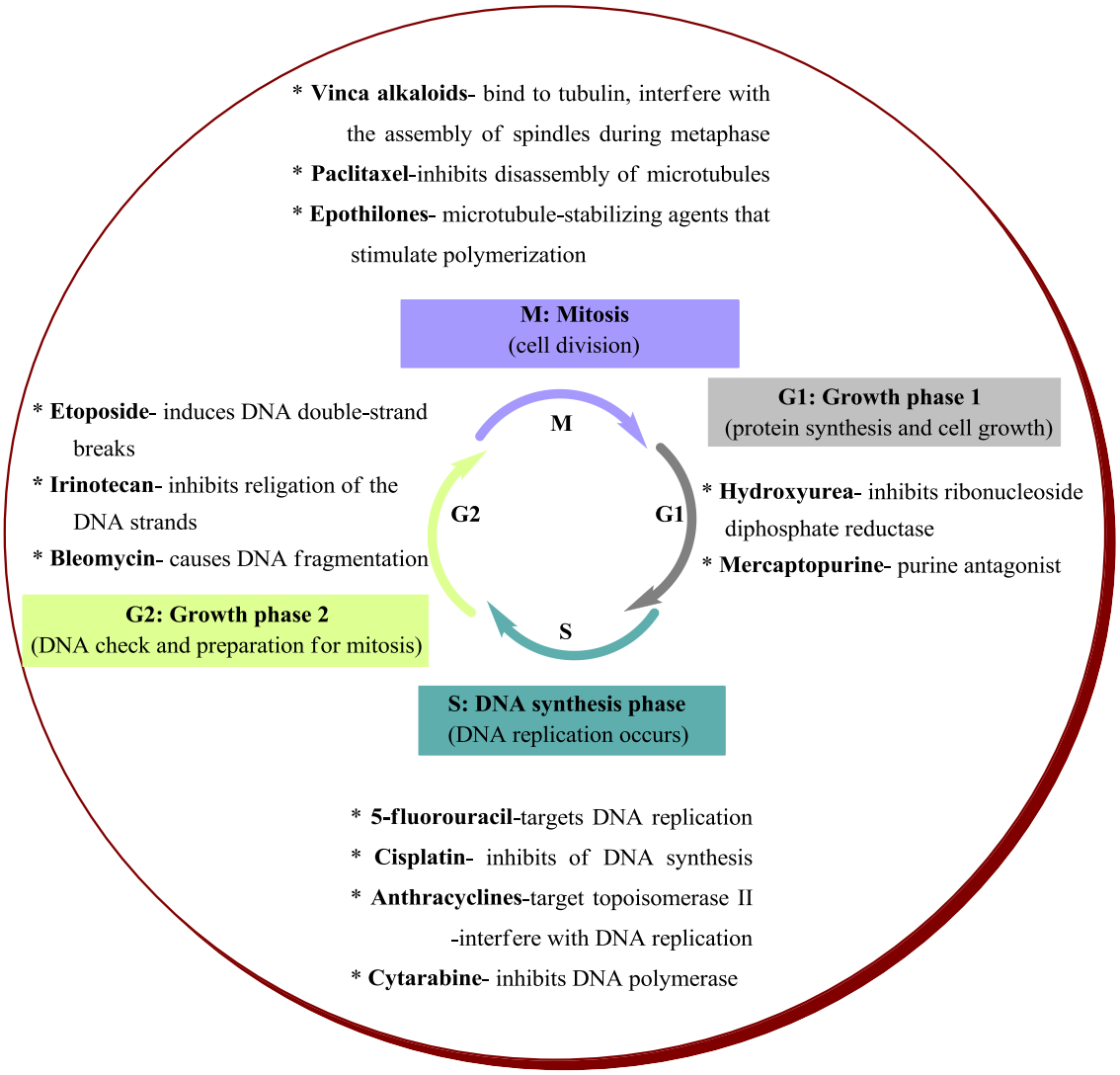

Figure 5.4: Four major phases of the cell cycle and the events targeted by the majority of antineoplastics.[9,15,16]

5.2 Phenothiazines as promising anticancer chemotherapeutic agents

As alluded to in chapter 1, the anticancer chemotherapeutic properties of phenothiazines have been extensively studied for decades. Native phenothiazines and their derivatives have been reported to display cytotoxic activities against various tumor cell lines including colon, leukemia, lung, central nervous system (CNS), melanoma, breast, ovarian, prostate and renal tumors.[17,18,19,20]

Trifluoperazine has been reported to augment the cytotoxicity of bleomycin against human non-small cell lung carcinoma U1810. Additionally, it was reported to sensitize H23 cells to DNA-damaging antineoplastics, bleomycin and cisplatin. Triflupromazine and fluphenazine were also reported as sensitizers and enhanced cytotoxicity of cisplatin to U1810.[21] The cytotoxicity of five native phenothiazines (thioridazine, chlorpromazine, trifluoperazine, perphenazine and fluphenazine) was demonstrated against human neuroblastoma SH-SY5Y and rat glioma C6 cells with IC_{50} ranges of 11-15 and 13-22 μM, respectively.[22] Others reported thioridazine as a potent antiglioblastoma and antiglioblastoma stem cells agent.[23] Chlorpromazine has also been reported to induce cell death in human U-87MG glioma cells.[24]

Motohashi and co-workers were among the first to report the anticancer effects of functionalized phenothiazines including benzophenothiazines, phenothiazines bearing naphthalenes and "half-mustard type" phenothiazines.[25] Other reports include phenothiazine-based thiazole derivatives which displayed cytotoxicity against cancer cell lines MCF-7 and HT29.[26] Phenothiazines and dibenzazepines with neutral polar side chains were also reported to display activity against H1650 lung adenocarcinoma cells.[27] Prinz *et al.* reported a series of *N*-benzolyated phenoxazine and phenothiazine derivatives with cytotoxicity against human

chronic myelogenous leukemia K562 cells.[28] Another series of phenothiazine analogues bearing a 1,2,3-triazole motif was reported to exhibit cytotoxicity against different human tumor cell lines.[19] Abuhaie *et al.* demonstrated the anticancer activities of phenstatin analogues bearing a phenothiazine ring against various cancer cell types including leukemia, non-small cell lung cancer, breast, melanoma, central nervous system and colon.[14]

The phenothiazine cancer chemopreventive effect is accounted for by their anti-calmodulin activity, inhibition of protein kinase C, inhibition of P-glycoprotein and anti-proliferative effects.[29,30,31] Resistance to anticancer chemotherapeutics poses severe limitations on their efficacy. Therefore, the chemosensitizing properties possessed by phenothiazines hold significant promise for cancer chemotherapy regimens.[21] Amongst the various anticancer properties possessed by phenothiazines, they also show great potential as chemotherapeutics for the treatment of brain cancer. [22,32,33]

5.2.1 Potentiating non-neuroleptic CNS-related effects of phenothiazines

Phenothiazines are notably unselective and they elicit adverse side effects in addition to neuroleptic effects through binding to multiple CNS receptor subtypes including dopaminergic and serotonergic receptor subtypes.[34,35] In this study, the general remodelling approach involved elimination of structural traits associated with neuroleptic activity (Chapter 2-4). The cytotoxicity of phenothiazines has been demonstrated against different cell lines.[14,19] Herein, brain cancer was first to be investigated given that phenothiazines are native CNS agents. Furthermore, in consideration of the structural remodelling strategies employed in this study, brain cancer was considered an interesting avenue for exploration (Figure 5.5). To potentiate cytotoxicity of phenothiazines against brain cancer, the challenge

would be carrying out the remodelling such that their ability to cross the blood-brain barrier is not compromised whereas neuroleptic-related structural traits are eliminated. Therefore, as a starting point, the library of NCEs reported in chapter 4 was evaluated against the U-251 glioblastoma cell line. The preliminary investigation would reveal whether the anticancer properties of the remodelled phenothiazines were retained after structural remodelling.

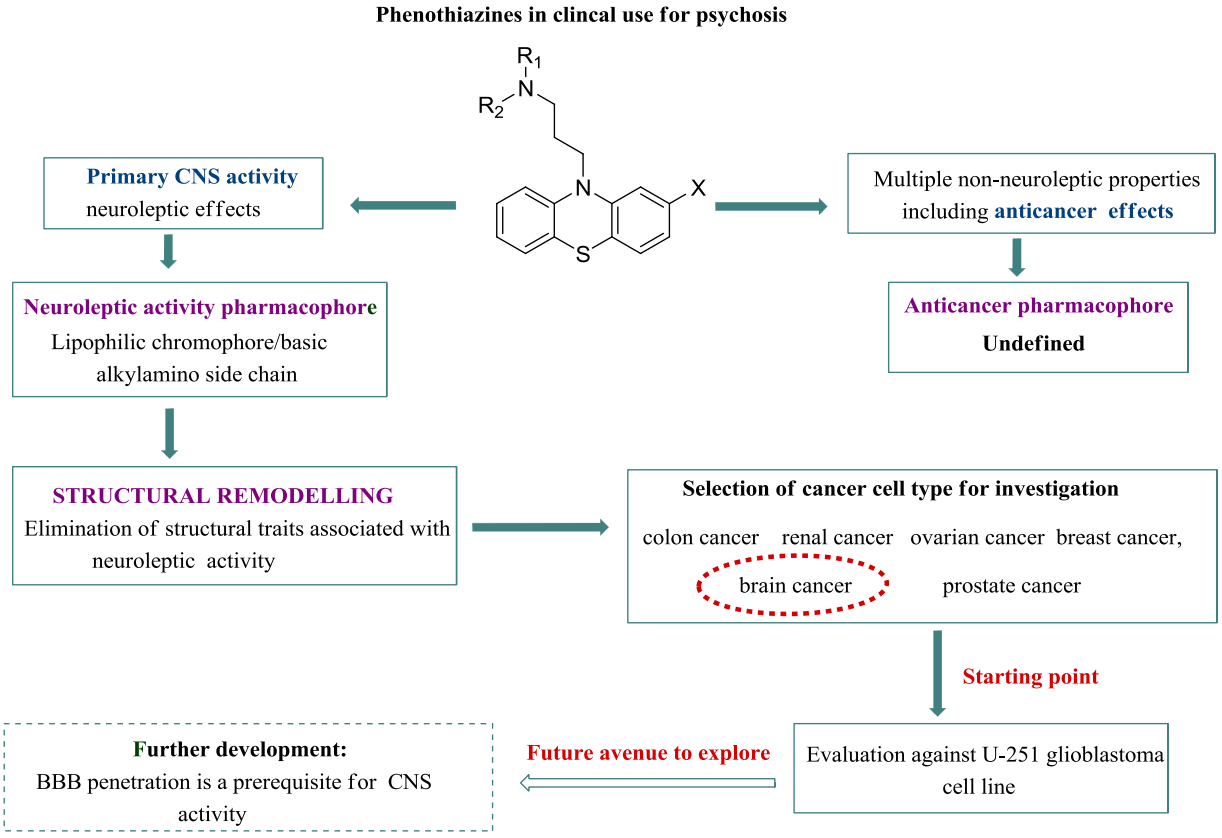

Figure 5.5: The pharmacophore of phenothiazines in clinical use for psychosis and their remodelling for evaluation as anticancer agents. BBB - Blood brain barrier.

5.2.2 Epidemiology of glioblastoma

Classification of brain tumors may be based on their anatomical location or histophathologic characteristics. Gliomas are the most common type of brain tumors including astrocytomas,ependymomas and oligodendrogliomas.[36,37] The types of gliomas that are not of

glial tissue origin include schwannomas, craniopharyngiomas, meningiomas and germ cell tumors.[37] Glioblastoma is one of the most aggressive and lethal type of malignant astrocytoma.[36] The highly invasive nature of the tumor cells renders surgical interventions virtually impossible. Glioblastoma and related malignant gliomas only infiltrate the surrounding brain parenchyma and metastasis does not occur. Moreover, resistance to radiation and cytotoxic chemotherapy reduces survival chances of glioblastoma patients.[38, 39]

Gliomas are more prevalent among white rather than black populations and also in males than females. A family history of glioma only increases the risk of developing glioma by 2-fold.[39,40] Post-surgery, adjuvant radiotherapy in combination with chemotherapy is usually considered for glioblastoma patients.[39] Frequently used glioblastoma chemotherapy regimens include a DNA alkylating agent, temozolomide, concomitant with radiotherapy.[41] Virtually all glioblastoma patients experience tumor progression after first-line chemotherapy. Apart from surgical resection for treatment of recurrent glioblastoma, salvage chemotherapy options include the use of temozolomide, bevacizumab and various alkylating agents such as nitrosoureas and carboplatin. No treatment options are available in case of unsuccessful salvage chemotherapy and the median survival is 3 to 4 months.[39,42] This points to an urgent need for novel chemotherapeutic treatment approaches for glioblastoma.

5.3 Evaluation of remodelled phenothiazines against glioblastoma cell line

The anticancer potential of remodelled phenothiazines in this study and parent neuroleptic drugs was assessed by an MTT assay,[43] to determine their effects on U-251 glioblastoma cells after 48 h exposure. Of the various subclasses evaluated, nitrobenzenesulfonamides (**DS00325**, **DS00326**, **DS00329**, & **DS00341**) and two native phenothiazines (thioridazine and thiothixene) displayed potent inhibition effects against the glioblastoma cell line (Table

5.1). At the highest concentration tested, 15 µM, the rest of the remodelled phenothiazines and parent neuroleptic drugs were not cytotoxic to the U-251 glioblastoma cells.

Table 5.1: The anticancer effects of phenothiazines on U-251 glioblastoma cell line after 48 h exposure. (NC- Not cytotoxic at the highest concentration tested, 15 µM)

NCE/ parent neuroleptic drug	U-251 glioblastoma IC_{50} (µM)	NCE/ parent neuroleptic drug	U-251 Glioblastoma IC_{50} (µM)
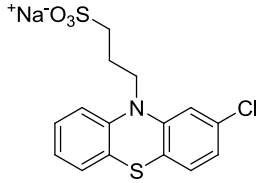 **DS0034**	NC	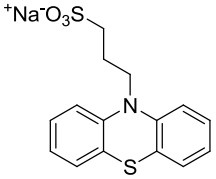 **DS0035**	NC
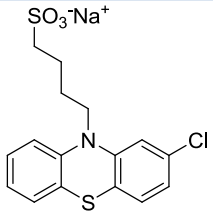 **DS00370**	NC	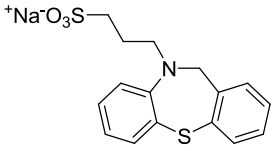 **DS00380**	NC
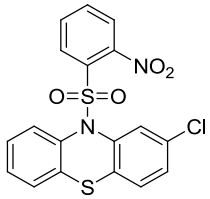 **DS00329**	6.63	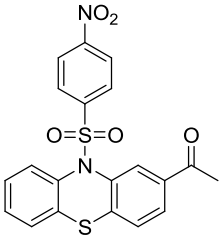 **DS00341**	*IC_{50}
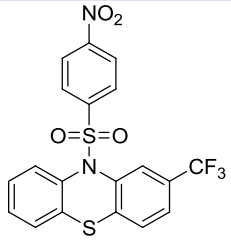 **D00338**	NC	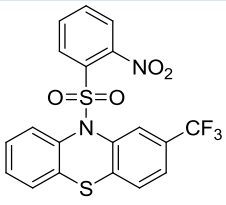 **DS00326**	4.51
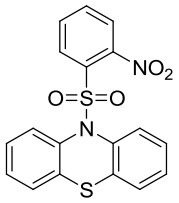 **DS00325**	8.06	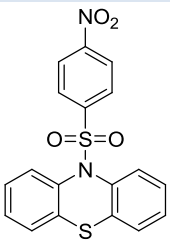 **DS00342**	NC

Table 5.1 continued…

NCE/ parent neuroleptic drug	U-251 glioblastoma IC_{50} (µM)	NCE/ parent neuroleptic drug	U-251 Glioblastoma IC_{50} (µM)
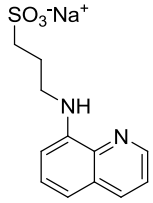 **DS-Q1**	NC	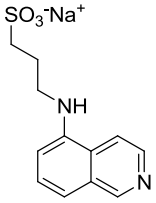 **DS-Q3**	NC
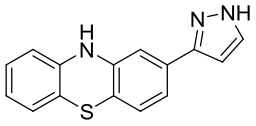 **DS00398**	NC	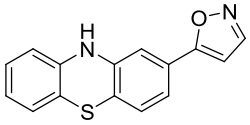 **DS00397**	NC
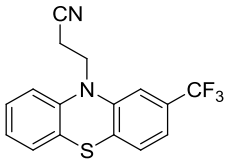 **DS00392**	NC	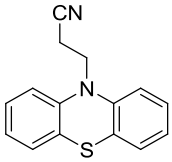 **DS00394**	NC
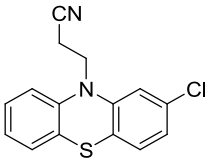 **DS00393**	NC	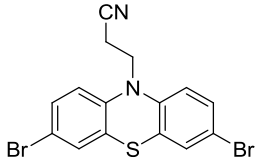 **DS00396**	NC
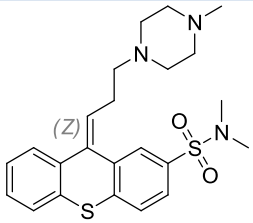 **Thiothixene**	12.43	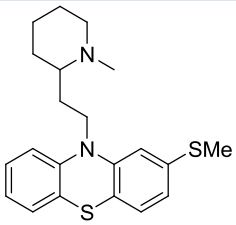 **Thioridazine**	8.83
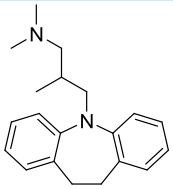 **Trimipramine**	NC	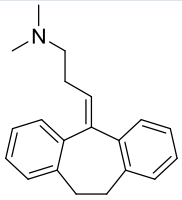 **Amitriptyline**	NC

IC_{50}- Half maximal inhibitory concentration; NC- Not cytotoxic at the highest concentration tested, 15 µM; *A dose-dependent decrease in cell viability was observed but 50% cell death was not observed at 15 µM.

In chapter 4, *N*-propylsulfonates **DS0034** & **DS0035** displayed negligible cytotoxicity against bone marrow-derived macrophages (Table 5.1). Interestingly, herein they also displayed no cytotoxicity against the U-251 glioblastoma cells. The compounds with potent inhibition effects induced a dose-dependent decrease in cell-viability as shown in Figure 5.6.

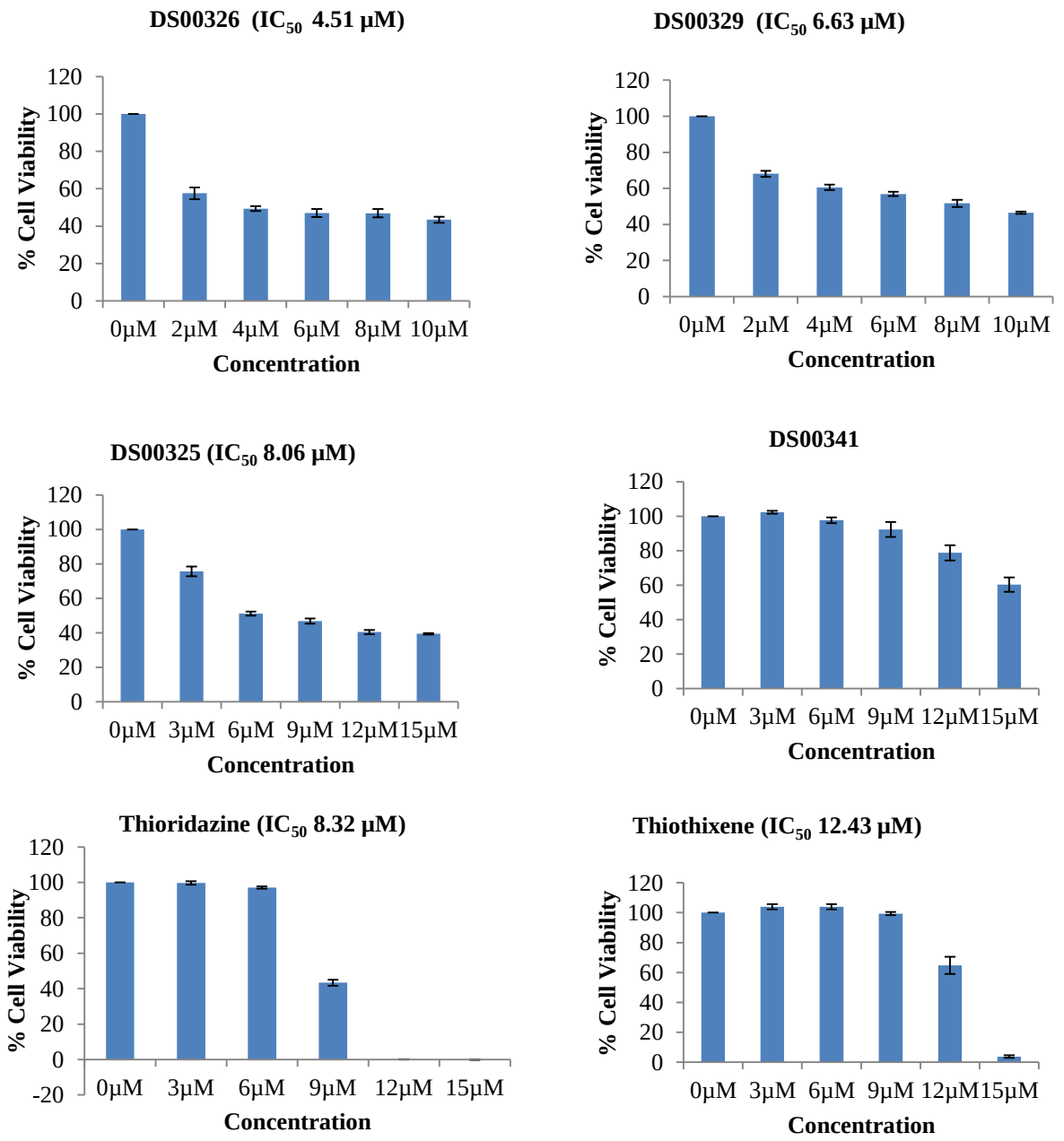

Figure 5.6: The anticancer effects of remodelled phenothiazines and native neuroleptic drugs on U-251 glioblastoma cell line after 48 h exposure**.** MTT assay was used to determine cell viability.

The IC_{50} values ranged from 4.51-12.43 μM. Furthermore, the remodelled phenothiazines (**DS00325**, **DS00326**, **DS00329**) were more potent than the native neuroleptics, thioridazine and thiothixene. Thiothixene and thioridazine also displayed interesting effects on the cells. At lower concentrations, there was no significant effect on the cells followed by a drastic decrease in cell viability at higher concentrations, 9-15 μM. The cytotoxic effect of native phenothiazines including thioridazine on neuroblastoma and glioma cell lines was reportedly mediated by apoptosis.[22] Herein, the mode of action of the remodelled phenothiazines remains to be ascertained. Although conclusive structure-activity relationships could not be established, these preliminary observations demonstrate that the anticancer effects of native phenothiazines could be retained after structural remodelling.

5.4 Concluding Remarks

In this chapter, the preliminary results demonstrated that it is possible to potentiate the anticancer effects of phenothiazines through structural remodelling. In particular, the remodelled phenothiazines [**DS00325** (IC_{50} 8.06 μM), **DS00326** (IC_{50} 4.51 μM), **DS00329** (IC_{50} 6.63 μM)] displayed more potent cytotoxic effects than the native neuroleptics [thioridazine (IC_{50} 8.32 μM), thiothixene (IC_{50} 12.43 μM)]. Furthermore, the remodelled phenothiazines are devoid of structural traits associated with neuroleptic action i.e. a lipophilic chromophore in conjunction with a basic alkylamino moiety. *In silico* predictions (Chapter 2) also revealed that they are less likely to exhibit CNS activity. The ability to cross the blood-brain barrier is a crucial characteristic of therapeutics that target CNS-related indications. Therefore, further development of the remodelled phenothiazines as antiglioblastoma agents would require introduction of some degree of lipophilicity to facilitate blood-brain barrier penetration.

References

(1) Reya, T.; Morrison, S. J.; Clarke, M. F.; Weissman, I. L. Stem Cells, Cancer, and Cancer Stem Cells. *Nature* **2001**, *414* (6859), 105–111.

(2) Clevers, H. The Cancer Stem Cell: Premises, Promises and Challenges. *Nat Med* **2011**, *17* (3), 313–319.

(3) Lobo, N. A.; Shimono, Y.; Qian, D.; Clarke, M. F. The Biology of Cancer Stem Cells. *Annu Rev Cell Dev Biol* **2007**, *23*, 675–699.

(4) Yeh, C.; Wu, A. T. H.; Chang, P. M.; Chen, K.; Yang, C. Trifluoperazine , an Antipsychotic Agent , Inhibits Cancer Stem Cell Growth and Overcomes Drug Resistance of Lung Cancer. *Am J Respir Crit Care Med* **2012**, *186* (11), 1180–1188.

(5) Ferlay, J.; Soerjomataram, I.; Dikshit, R.; Eser, S.; Mathers, C.; Rebelo, M.; Parkin, D. M.; Forman, D.; Bray, F. Cancer Incidence and Mortality Worldwide : Sources , Methods and Major Patterns in GLOBOCAN 2012. *Int. J. Cancer* **2014**, *136*, E359–E386.

(6) American Cancer Society. Cancer Facts and Figures 2015. *Atlanta Am. Cancer Soc.* **2015**, 1–56.

(7) Wrensch, M.; Minn, Y.; Chew, T.; Bondy, M.; Berger, M. S. Epidemiology of Primary Brain Tumors : Current Concepts and Review of the Literature. *Neuro. Oncol.* **2002**, *4*, 278–299.

(8) Stewart, Z. A.; Westfall, M. D.; Pietenpol, J. A. Cell-Cycle Dysregulation and Anticancer Therapy. *Trends Pharmacol Sci* **2003**, *24* (3), 139–145.

(9) Senese, S.; Lo, Y. C.; Huang, D.; Zangle, T. A.; Gholkar, A. A.; Robert, L.; Homet, B.; Ribas, A.; Summers, M. K.; Teitell, M. A.; Damoiseaux, R.; Torres, J. Z. Chemical Dissection of the Cell Cycle: Probes for Cell Biology and Anti-Cancer Drug Development. *Cell Death Dis.* **2014**, *5* (10), e1462.

(10) Nussbaumer, S.; Bonnabry, P.; Veuthey, J.; Fleury-souverain, S. Analysis of Anticancer Drugs : A Review. *Talanta* **2011**, *85* (5), 2265–2289.

(11) Rangel-Vega, A.; Bernstein, L. R.; Mandujano-tinoco, E. A.; Debabov, D.; Visca, P. Drug Repurposing as an Alternative for the Treatment of Recalcitrant Bacterial Infections. *Front. Microbiol.* **2015**, *6* (282), 1–8.

(12) Prinz, H.; Chamasmani, B.; Vogel, K.; Böhm, K. J.; Aicher, B.; Gerlach, M.; Günther, E. G.; Amon, P.; Ivanov, I.; Müller, K. N-Benzoylated Phenoxazines and Phenothiazines: Synthesis, Antiproliferative Activity, and Inhibition of Tubulin Polymerization. *J. Med. Chem.* **2011**, *54* (12), 4247–4263.

(13) Pantziarka, P.; Bouche, G.; Meheus, L.; Sukhatme, V.; Sukhatme, V. P. Repurposing Drugs in Oncology (ReDO)-Mebendazole as an Anti-Cancer Agent. *ecancer Med. Sci.* **2014**, *8* (443), 1–16.

(14) Abuhaie, C.-M.; Bîcu, E.; Rigo, B.; Gautret, P.; Belei, D.; Farce, A.; Dubois, J.; Ghinet, A. Letters Synthesis and Anticancer Activity of Analogues of Phenstatin , with a Phenothiazine A-Ring , as a New Class of Microtubule-Targeting Agents. *Bioorg. Med. Chem. Lett.* **2013**, *23* (1), 147–152.

(15) Chan, K. S.; Koh, C. G.; Li, H. Y. Mitosis-Targeted Anti-Cancer Therapies: Where They Stand. *Cell Death Dis.* **2012**, *3*, e411.

(16) Trendowski, M. Recent Advances in the Development of Antineoplastic Agents Derived from Natural Products. *Drugs* **2015**, *75*, 1993–2016.

(17) Pluta, K.; Morak-Młodawska, B.; Jeleń, M. Recent Progress in Biological Activities of Synthesized Phenothiazines. *Eur. J. Med. Chem.* **2011**, *46* (8), 3179–3189.

(18) Michalak, K.; Wesolowska, O.; Motohashi, N.; Molnar, J.; Hendrich, a B. Interactions of Phenothiazines with Lipid Bilayer and Their Role in Multidrug Resistance Reversal. *Curr. Drug Targets* **2006**, *7* (9), 1095–1105.

(19) Belei, D.; Dumea, C.; Samson, A.; Farce, A.; Dubois, J.; Bîcu, E.; Ghinet, A. New Farnesyltransferase Inhibitors in the Phenothiazine Series. *Bioorganic Med. Chem. Lett.* **2012**, *22* (14), 4517–4522.

(20) Qi, L.; Ding, Y. Potential Antitumor Mechanisms of Phenothiazine Drugs. *Sci. China Life Sci.* **2013**, *56* (11), 1020–1027.

(21) Zong D; Haag P; Yakymov. Chemosensitization by Phenothiazines in Human Lung Cancer Cells : Impaired Resolution of c H2AX and Increased Oxidative Stress Elicit Apoptosis Associated with Lysosomal Expansion and Intense Vacuolation. *Cell Death Dis.* **2011**, *2*, 1–12.

(22) Gil-ad, I.; Shtaif, B.; Levkovitz, Y.; Dayag, M.; Zeldich, E.; Weizman, A. Characterization of Phenothiazine-Induced Apoptosis in Neuroblastoma and Glioma Cell Lines. *J. Mol. Neurosci.* **2004**, *22*, 189–198.

(23) Cheng, H.; Liang, Y.; Kuo, Y.; Chuu, C.; Lin, C.; Lee, M.; Wu, A. T. H.; Yeh, C.; Chen, E.; Su, C. Identification of Thioridazine , an Antipsychotic Drug , as an Antiglioblastoma and Anticancer Stem Cell Agent Using Public Gene Expression Data. *Cell Death Dis.* **2015**, *6*, 1–13.

(24) Shin, S. Y.; Lee, K. S.; Choi, Y.; Lim, H. J.; Lee, H. G.; Lim, Y.; Lee, Y. H. The Antipsychotic Agent Chlorpromazine Induces Autophagic Cell Death by Inhibiting the Akt / mTOR Pathway in Human U-87MG Glioma Cells. *Carcinogenesis* **2013**, *00* (00), 1–10.

(25) Motohashi, N.; Sakagami, H.; Kamata, K.; Yamamoto, Y. Cytotoxicity and Differentiation-Inducing Activity of Phenothiazie and Benzo[a]phenothiazine Derivatives. *Anticancer Res.* **1991**, *11*, e1937.

(26) Kumar, M. A.; Nguyen, T.; An, M.; Lee, I. J.; Park, S.; Kumar, M. A.; Nguyen, T.; An, M.; Lee, I. J.; Park, S.; Lee, K. D. Synthesis and Bioactivity of Novel Phenothiazine-Based Thiazole Derivatives. *Phosphorus, Sulfur, and Silicon* **2015**, *190*, 1160–1168.

(27) Kastrinsky, D. B.; Sangodkar, J.; Zawarea, N.; Izadmehr, S.; Dhawanb, N. S.; Goutham, N.; Ohlmeyer, M. Reengineered Tricyclic Anti-Cancer Agents. *Bioorg. Med. Chem.* **2015**, *23* (19), 6528–6534.

(28) Prinz, H.; Schmidt, P.; Böhm, K. J.; Baasner, S.; Müller, K.; Unger, E.; Gerlach, M.; Günther, E. G. 10-(2-Oxo-2-Phenylethylidene)-10H-Anthracen-9-Ones as Highly Active Antimicrotubule Agents: Synthesis, Antiproliferative Activity, and Inhibition of Tubulin Polymerization. *J. Med. Chem.* **2009**, *52* (5), 1284–1294.

(29) Choi, J. H.; Yang, R.; Lee, K.; Kim, S.; Kim, Y.; Cha, J.; Oh, S.; Ha, J.; Ryu, H.; Suh, P. Potential Inhibition of PDK1 / Akt Signaling by Phenothiazines Suppresses Cancer Cell Proliferation and Survival. *Ann. N. Y. Acad. Sci.* **2008**, *1138*, 393–403.

(30) Jaszczyszyn, A.; Gąsiorowski, K.; Świątek, P.; Malinka, W.; Cieślik-Boczula, K.; Petrus, J.; Czarnik-Matusewicz, B. Chemical Structure of Phenothiazines and Their Biological Activity. *Pharmacol. Reports* **2012**, *64* (1), 16–23.

(31) Nagel, D.; Spranger, S.; Vincendeau, M.; Grau, M.; Raffegerst, S.; Kloo, B.; Lenz, P.; Hlahla, D.; Neuenschwander, M.; Kries, J. P. Von; Hadian, K.; Do, B.; Lenz, G.; Schendel, D. J.; Krappmann, D. Article Pharmacologic Inhibition of MALT1 Protease by Phenothiazines as a Therapeutic Approach for the Treatment of Aggressive ABC-DLBCL. *Cancer Cell* **2012**, *22*, 825–837.

(32) Hait, W. N.; Byrne, T. N.; Piepmeier, J.; Durivage, H. J.; Choudhury, S.; Davis, C. A.; Gates, J. A. The Effect of Calmodulin Inhibitors with Bleomycin on the Treatment of Patients with High Grade Gliomas1. *Cancer Res.* **1990**, *50*, 6636–6640.

(33) Azuine, M. A.; Tokuda, H.; Takayasu, J.; Enjyo, F.; Mukainaka, T.; Konoshima, T.; Nishino, H.; Kapadia, G. J. Cancer Chemopreventive Effect of Phenothiazines and Related Tri-Heterocyclic Analogues in the 12-O-Tetradecanoylphorbol-13-Acetate Promoted Epstein-Barr Virus Early Antigen Activation and the Mouse Skin Two-Stage Carcinogenesis Models. *Pharmacol. Res.* **2004**, *49* (2), 161–169.

(34) Jafari, S.; Fernandez-Enright, F.; Huang, X. F. Structural Contributions of Antipsychotic Drugs to Their Therapeutic Profiles and Metabolic Side Effects. *J. Neurochem.* **2012**, *120* (3), 371–384.

(35) Feinberg, A. P.; Snyder, S. H. Phenothiazine Drugs : Structure-Activity Relationships Explained by a Conformation That Mimics Dopamine. *Proc. Nat. Acad. Sci.* **1975**, *72* (5), 1899–1903.

(36) Pollard, S. M.; Yoshikawa, K.; Clarke, I. D.; Danovi, D.; Stricker, S.; Russell, R.; Bayani, J.; Head, R.; Lee, M.; Bernstein, M.; Squire, J. A.; Smith, A.; Dirks, P. Resource Glioma Stem Cell Lines Expanded in Adherent Culture Have Tumor-Specific Phenotypes and Are Suitable for Chemical and Genetic Screens. *Cell Stem Cell* **2009**, *4* (6), 568–580.

(37) Madhusoodanan, S.; Ting, M. B.; Farah, T.; Ugur, U. Psychiatric Aspects of Brain Tumors: A Review. *World J. Psychiatry* **2015**, *5* (3), 273–285.

(38) Cloughesy, T. F.; Cavenee, W. K.; Mischel, P. S. Glioblastoma : From Molecular Pathology to Targeted Treatment. *Annu. Rev. Pathol. Mech. Dis.* **2014**, *9*, 1–25.

(39) Omuro, A.; DeAngelis, L. M. Glioblastoma and Other Malignant Gliomas A Clinical Review. *JAMA* **2013**, *310* (17), 1842–1850.

(40) Bondy, M. L.; Scheurer, M. E.; Malmer, B.; Barnholtz-, J. S.; Davis, F. G.; Il, D.; Kruchko, C.; J, B.; Rajaraman, P.; Schwartzbaum, J. a; Schlehofer, B.; Tihan, T.; Wiemels, J. L. Brain Tumor Epidemiology: Consensus from the Brain Tumor Epidemiology Consortium (BTEC). *Cancer* **2008**, *113*, 1953–1968.

(41) Poteet, E.; Choudhury, G. R.; Winters, A.; Li, W.; Ryou, M.; Liu, R.; Tang, L.; Ghorpade, A.; Wen, Y.; Yuan, F.; Keir, S. T.; Yan, H.; Bigner, D. D.; Simpkins, J. W. Reversing the Warburg Effect as a Treatment for Glioblastoma. *J. Biol. Chem.* **2013**, *288* (13), 9153–9164.

(42) Lee, J.-K.; Nam, D.-H.; Lee, J. Repurposing Antipsychotics as Glioblastoma Therapeutics : Potentials and Challenges (Review). *Oncol. Lett.* **2016**, *11*, 1281–1286.

(43) Mosmann, T. Rapid Colorimetric Assay for Cellular Growth and Survival: Application to Proliferation and Cytotoxicity Assays. *J Immunol. Methods* **1983**, *65*, 55–63.

Chapter 6

Summary, Conclusions and Recommendations

6.1 Overall Summary and Conclusions

The emergence of drug resistance in both communicable and non-communicable diseases threatens the effectiveness of chemotherapy options as pharmaceutical drug pipelines are drying up. Innovative strategies such as drug repurposing, drug repositioning and drug rescue have garnered significant research interest in efforts to rejuvenate drug pipelines. Phenothiazines and related neuroleptic drugs exhibit broad spectrum biological activities including antibacterial, antimalarial, antiemetic, anticancer, antihistaminic and many more (Chapter 1). However, there is resistance to their wider clinical application in non-neuroleptic indications due to potential adverse side effects in addition to inherent neuroleptic effects. Amongst neuroleptic drugs, thioridazine is the only phenothiazine that has been successfully repurposed for the treatment of XDR-TB due to its milder side effects.

The primary objective of this research study was to demonstrate that phenothiazines and related drugs could be structurally remodelled such that their inherent neuroleptic effects are abrogated whilst their antitubercular or anticancer properties are retained. Neuroleptic phenothiazines are native central nervous system (CNS) agents with a well-defined pharmacophore (Figure 6.1). The structural traits associated with their neuroleptic action include conformational resemblance to dopamine, high degree of lipophilicity for blood-brain barrier penetration and presence of a proton accepting distal amine moiety. In full knowledge of the aforementioned structural traits, the remodelling strategies employed in this study were rationally selected to generate new chemical entities (NCEs) with reduced likelihood of neuroleptic effects (Figure 6.1).

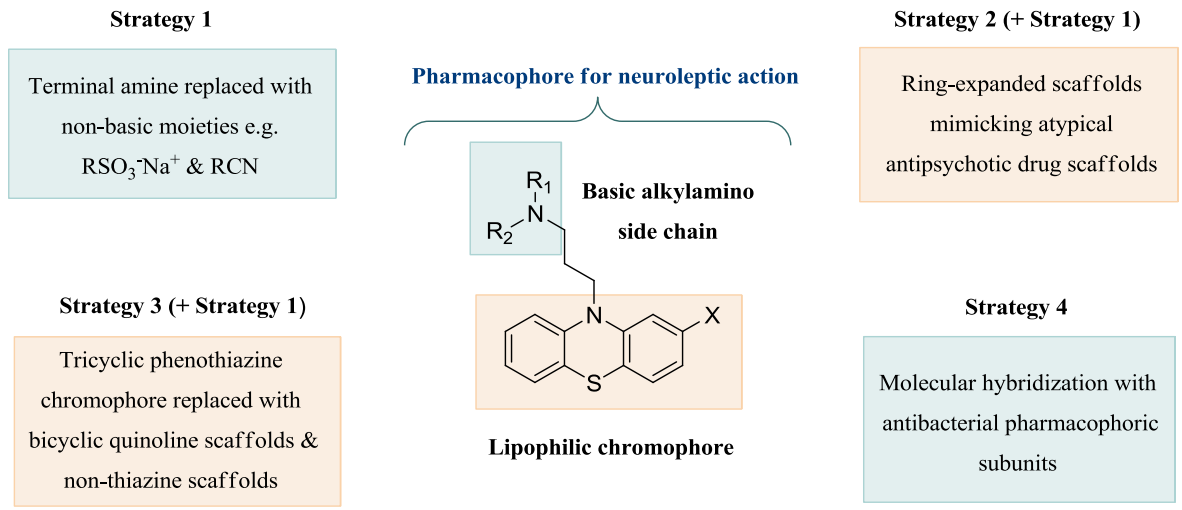

Figure 6.1: Summary of remodelling strategies employed in this research study.

The following aims and objectives were addressed herein:

(i) A diverse focused library of modified phenothiazines and related neuroleptics was generated through rationalized structural remodelling. The library comprised *N*-propylsulfonates of phenothiazines; *N*-butylsulfonates phenothiazines; *N*-propylsulfonates of quinolines; *N*-propylsulfonates of ring-expanded scaffolds & non-thiazine scaffolds; molecular hybrids and *N*-alkyl phenothiazines with other non-basic terminal moieties such as nitriles. *In silico* predictions tools were integrated into the structural remodelling to assess drug-likeness of the NCEs on the basis of Lipinski's rule of five. Moreover, the *in silico* assessment included the prediction of blood-brain partition coefficients and CNS activity to determine their likelihood of exhibiting neuroleptic effects. *In silico* predictions also included ADMET properties such as aqueous solubility, Caco-2 & MDCK cell permeability, number of likely metabolic reactions and hERG inhibition (Chapter 2).

(ii) The remodelled phenothiazines were chemically synthesized *via* adaptation of well-known organic reactions and literature reported synthetic methods. The chemical synthesis mainly involved *N*-alkylations, cross coupling reactions under Buchwald-Hartwig conditions and other mechanistically interesting reactions such as the Ritter reaction and the Michaelis-Arbuzov rearrangement. Several synthetic challenges were encountered, in particular, the assembly of tricyclic scaffolds from functionalized benzenes as highlighted in Chapter 3. Moreover, intricate precautions had to be taken in handling and performing chemical reactions with phenothiazines so as to avoid air oxidation as well as radical reactions under exposure to light. Isolation and purification techniques common in organic synthesis were employed including reversed-phase chromatography. In this study, purification *via* reversed-phase chromatography was advantageous from a commercial and "green" perspective as the mobile phase was primarily aqueous. Spectroscopic techniques such as NMR, IR and LCMS were used for structure elucidation, confirmation and purity analysis (Chapter 3 & 7).

(iii) The focused library of remodelled phenothiazines including commercially available neuroleptic drugs was screened for *in vitro Mycobacterium tuberculosis* (M.*tb)* H37Rv growth inhibition using the Green Fluorescent Protein Microplate Assay (GFPMA) in a GAST/Fe medium or Middlebrook 7H9 medium (Chapter 4). Selected NCEs were further evaluated for intracellular M.*tb*H37Rv growth inhibition using bone marrow-derived macrophages. The observations demonstrated that the antimycobacterial properties were retained post-remodelling. The hits with MIC_{90} (GAST/Fe) less than 25 µM included *N*-butylsulfonate **DS00366** (**3.56**) (23.5 µM), nitrile **DS00396** (**3.82d**) (11.4 µM) and isoniazid hybrid dimer **DS00362** (**3.74a**) **(**10.6 µM). Moreover, the antitubercular activity of the neuroleptics amitriptyline and thiothixene was demonstrated for the first time with MIC_{90} of 75.1 µM and 30.8 µM, respectively. Further evaluation of *N*-propylsulfonates {**DS0031**

(**3.1a**), **DS0032** (**3.1b**), **DS0034** (**3.1d**) & **DS0035** (**3.1e**)} using the GFPMA in a Middlebrook 7H9 medium demonstrated that they also retained their antitubercular properties, with MIC (7H9) of 12.5-25 µg/mL. Furthermore, the *N*-propylsulfonates displayed between 40% and 60% inhibition of intracellular M.*tb*H37Rv thus demonstrating their ability to transverse cell membrane systems and access intracellular bacilli. Moreover, determination of cell viability indicated that in contrast to the parent neuroleptic thioridazine, the *N*-propylsulfonates were not cytotoxic to bone-marrow derived macrophages at higher concentrations (6.25-25 µg/mL).

(iv) The neuroleptic potential of four *N*-propylsulfonates {**DS0031** (**3.1a**), **DS0032** (**3.1b**), **DS0034** (**3.1d**) & **DS0035** (**3.1e**)} was evaluated using dopamine and serotonin receptor radioligand binding assays to corroborate the tentative conclusions drawn from *in silico* CNS activity predictions (Chapter 4). The NCEs were screened for binding to dopaminergic receptor subtypes D_1, D_2 and D_3 as well as serotonergic receptor subtypes 5-HT_{1A}, 5-HT_{2A} and 5-HT_{2C}. All the NCEs displayed no binding to the aforementioned receptor subtypes except for **DS0031** (**3.1a**) which displayed marginal serotonin receptor (5-HT_{1A}) binding. These findings were fundamental to this research study as they demonstrated conclusively that through rationalized structural remodelling, it is possible to abolish inherent neuroleptic effects of phenothiazines whilst their antimycobacterial properties are retained. The replacement of the distal amine moiety of phenothiazines with a sulfonate functionality was one of the key remodelling strategies employed in this study. The rationale behind successfully abolishing neuroleptic properties of the *N*-propylsulfonates involved introducing the polar sulfonate group at a critical post-synaptic receptor recognition site. As mentioned previously, phenothiazines are known to obey a lipophilic chromophore/basic side chain

paradigm, therefore the replacement with a sulfonate moiety is expected to alter the charge of the molecule at physiological pH.

(v) Preclinical studies of the *N*-propylsulfonates {**DS0031** (**3.1a**), **DS0032** (**3.1b**), **DS0034** (**3.1d**) & **DS0035** (**3.1e**)} were carried out to elucidate their pharmacokinetic profiles. The evaluation revealed favourable *in vitro* microsomal metabolic stability, kinetic solubility and *in vivo* toxicity profiles. Preliminary observations indicated that the *in vivo* toxicity profiles of **DS0034** (**3.1d**) and **DS0035** (**3.1e**) were superior to that of the clinically approved neuroleptic drug, thioridazine. These NCEs with promising properties are currently undergoing further preclinical development and are being evaluated for *in vivo* efficacy against M.*tb* in mice.

(vi) The library of remodelled phenothiazines was also subjected to an MTT cell viability screen against the U-251 glioblastoma cell line to evaluate their anticancer potential (Chapter 5). In Chapter 4, the subclass of nitrobenzenesulfonamides displayed poor MIC_{90} against M.*tb*H37Rv. When evaluated against the U-251 glioblastoma cell line, they displayed potent cytotoxic effects i.e. **DS00325** (**3.74a**) (IC_{50} 8.06 µM), **DS00326** (**3.74b**) (IC_{50} 4.51 µM) and **DS00329** (**3.74c**) (IC_{50} 6.63 µM). Furthermore, their cytotoxic effects were more potent than that of the native neuroleptics i.e. thioridazine (IC_{50} 8.32 µM) and thiothixene (IC_{50} 12.43 µM). Also noteworthy was the lack of cytotoxicity of *N*-propylsulfonates **DS0034** (**3.1d**) and **DS0035** (**3.1e**) against the U-251 glioblastoma cell line, which was observed previously using bone-marrow derived macrophages (Chapter 4). These preliminary findings demonstrated that the anticancer properties of phenothiazines could be retained after structural remodelling. It is noteworthy that *in silico* predictions (Chapter 2) revealed that the nitrobenzene-sulfonamides are less likely to exhibit CNS activity or cross the blood-brain barrier. Therefore, further development should address these liabilities whilst still deviating from structural traits that are associated with neuroleptic action.

6.2 Recommendations for future work

Overall, this research study presented subclasses of remodelled phenothiazines that hold great potential for further development as either non-neuroleptic antitubercular or anticancer agents. Iterative standard medicinal chemistry approaches can be applied for their further development into viable drug candidates.

In this study, *N*-alkylsulfonates of phenothiazines have shown great potential as antitubercular agents that are devoid of neuroleptic effects and that have promising toxicity profiles. Further development may include the transformation of the sulfonate group into functionalities such as sulfonamides or sulfonate esters to evaluate the effects on their antimycobacterial efficacy (Figure 6.2).

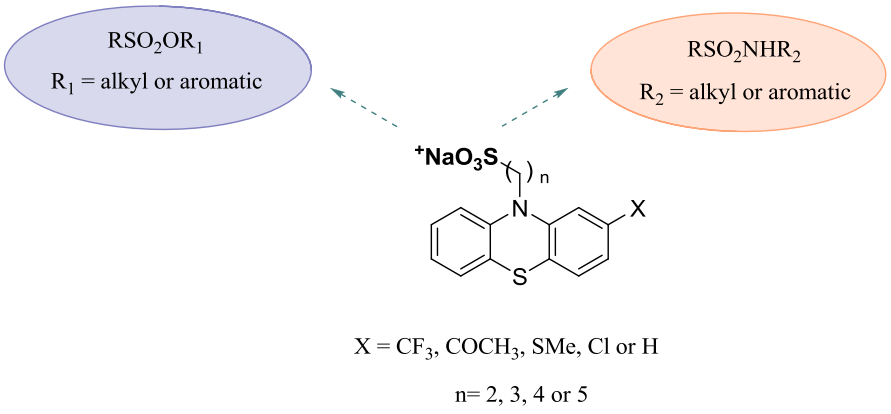

Figure 6.2: Possible structural modifications for further development of *N*-propylsulfonates of phenothiazines.

The rising tide of drug resistance calls for novel drug classes with unexplored modes of action for the treatment of microbial infections. As discussed previously (Chapter 1), native phenothiazines including thioridazine are multi-targeting agents with promising antimicrobial properties. The majority of existing anti-TB drugs target processes such as cell wall

biosynthesis and DNA metabolism which have acquired resistance. Type II NADH: menaquinone odixoreductase in M.*tb* has recently been validated as a biomolecular target of phenothiazines. Moreover, phenothiazines have been reported as efflux pump inhibitors in various pathogens. Herein, the probable mode of action of the remodelled phenothiazines has not been established. Therefore, further studies should include elucidation of plausible mechanisms. In addition to evaluation against drug-susceptible M.*tb*, the remodelled phenothiazines could also be screened against drug-resistant M.*tb* strains. The remodelled phenothiazines reported herein hold great promise for further development as agents in TB adjuvant chemotherapy. This in view of the fact that they have reduced neuroleptic potential as well as promising toxicity profiles relative to native phenothiazine drugs.

In Chapter 5, preliminary results indicated that anticancer properties of phenothiazines could be retained after structural remodelling. The cancer cell type investigated in this study was the U-251 glioblastoma cell line. To potentiate the antiglioblastoma effects of remodelled phenothiazines, liabilities such as blood-brain barrier penetration would have to be addressed. Native neuroleptics have displayed cytotoxic effects against multiple cancer cell types. Further evaluation of the remodelled phenothiazines could be performed against other cancer cell types such as breast cancer, colon cancer, prostate cancer, non-small cell lung cancer and renal cancer. Moreover, the chemosensitizing effect of phenothiazine neuroleptics has been reported to enhance the activity of antineoplastics such as bleomycin and cisplatin. Therefore, further assessment could include screening the remodelled phenothiazines in combination with existing antineoplastics to evaluate their chemosensitizing potential.

6.3 Final remarks

Phenothiazines and related antipsychotics have attracted notable research interest owing to their multiple biological properties. However, at clinically relevant doses, potential adverse side effects in addition to inherent neuroleptic effects preclude their extended clinical use in non-neuroleptic indications. Amongst clinically approved neuroleptics, thioridazine is the only phenothiazine that has been successfully repurposed as therapy for XDR-TB. Although the benefits of repurposing thioridazine seem to outweigh the inherent neuroleptic effects and potential side effects, clinical application of phenothiazines that are non-neuroleptic is also an attractive avenue to explore. The research undertaken herein has demonstrated that it is possible to enhance the selectivity of phenothiazines for non-neuroleptic effects through rational structural remodelling. It is hoped that the findings presented herein would encourage further investigations in terms of clinical application of phenothiazines that are devoid of neuroleptic effects.

Chapter 7

Experimental

7.1 *In silico* profiling

Chemical structures were imported from ChemBioDraw Ultra 11.0 in smiles format and used in either Stardrop 5.5 (http://www.optibrium.com/stardrop/stardrop-features.php)[1] or QikProp (http://www.schrodinger.com/QikProp/)[2] for *in silico* prediction of physicochemical properties and ADMET properties.

7.2 General chemical synthesis information

7.2.1 Chemical Reagents and Solvents

Commercially available chemical reagents, neuroleptic drugs (thioridazine, thiothixene, trimipramine, amitriptyline, clozapine and loxapine), anhydrous solvents and deuterated solvents were purchased from Sigma-Aldrich (United States or Schelldorf, Germany), Merck (South Africa or Darmstadt, Germany) or AK Scientific (United States). AR grade general solvents such as EtOAc, MeOH, and Et_2O were purchased from Kimix (Cape Town, South Africa) or Protea Chemicals (Milnerton, South Africa) and were used without any further distillation. Most of the chemical reactions were performed under an inert atmosphere of nitrogen or argon in oven-dried glassware.

7.2.2 Purification Methods

All reactions were monitored by thin-layer chromatography (TLC) using Merck PF_{254} aluminium-backed pre-coated silica gel plates (with a fluorescent indicator) and viewed under ultraviolet light (UV) at 254 nm and 360 nm. TLC spots were further visualized by spraying with ceric ammonium sulfate solution (CAS) followed by heating, or using iodine vapour. Merck Kieselgel silica gel 60 (0.040-0.063 mm) was used for column

chromatography and appropriate solvent mixtures were used for elution of compounds. Reversed-phase chromatography was carried out using Biotage KP-C-18-HS Sorbent; ultra-filtered water (purified by Millipore Synergy water purification system) and AR grade MeOH were used in appropriate ratios for elution of compounds. All compounds were dried under high vacuum or by lyophilisation before determination of reaction yields or spectroscopic characterization.

7.2.3 Analytical techniques

Melting points were determined on a Reichert-Jung Thermovar hot-stage microscope and are uncorrected. Infrared spectra were recorded on a PerkinElmer Spectrum 100 FT-IR spectrometer in the 4500 - 400 cm^{-1} frequency range, with samples as KBr pellets.

Liquid chromatography-mass spectrometry (LCMS) analyses were carried out using Agilent® UHPLC 1290 Infinity Series and Agilent® 6530 Accurate-Mass Q-TOF system equipped with an Agilent® jet stream ionization source (ESI); or using an Agilent® 1260 Infinity Series and Agilent® 6120 Quadrupole (Single) mass spectrometer equipped with APCI and ESI multimode ionisation source.

One-dimensional (^{1}H and ^{13}C and APT) nuclear magnetic resonance spectra (NMR) were recorded on Varian Mercury 300 MHz (75 MHz for ^{13}C), Varian Unity 400 MHz (101 MHz for ^{13}C) or Bruker Unity 400 MHz (101 MHz for ^{13}C & 162 MHz for ^{31}P) spectrometers. Deuterated solvents of choice were $CDCl_3$, DMSO-d_6, CD_3OD or D_2O. NMR chemical shifts are expressed in parts-per-million (ppm) relative to the internal solvent peak or trimethylsilane (TMS at δ 0 ppm). Coupling constants (*J*) are reported in Hertz (Hz). Spin multiplicities are denoted by the following lower-case letters: s (singlet); d (doublet); dd (doublet of doublets); t (triplet); td (triplet of doublets); q (quartet); qt (quintet); m (unresolved multiplet).

7.3 Chemical synthesis details

General procedure for preparation of *N*-propylsulfonates of phenothiazines {3.1a (DS0031), 3.1b (DS0032), 3.1c (DS0033), 3.1d (DS0034) & 3.1e (DS0035)}

(i) Method A: Synthesis using DMF as the solvent

To a suspension of NaH (60% dispersion in mineral oil, 1.1 eq) in anhydrous DMF (1 mL) under an inert atmosphere of nitrogen, was added a solution of phenothiazine **3.2a-e** (1.0 eq) in anhydrous DMF (2 mL). The mixture was allowed to stir at room temperature for 30 min and then heated at 50 °C for 1 h, during which the colour got darker indicating formation of phenothiazinium anion. After cooling to room temperature, 1,3-propane sultone **3.3** (1.3 eq) in anhydrous DMF (1 mL) was added and the mixture was allowed to stir for 16 h. A few drops of water were added to quench unreacted NaH. Subsequently, toluene was added and the solvents were removed by azeotropic distillation under reduced pressure. The resulting crude material was chromatographed on a C-18 reversed-phase column (H_2O; 9:1 H_2O/MeOH) to afford the desired products **3.1a-e**.

(ii) Method B: Large-scale synthesis using THF as the solvent

To a suspension of NaH (60% dispersion in mineral oil, 1.1 eq) in anhydrous THF (200 mL), was added a solution of phenothiazine (**3.2a**, **3.2b**, **3.2d**, **3.2e**) (8.0 g, 1.0 eq) in anhydrous THF (40 mL) under argon through a cannula. The mixture was allowed to stir under an inert atmosphere of argon for 1 h at room temperature and then for 30 min at 50 °C. The mixture acquired a dark orange colour, following the formation of the phenothiazine anion. After the suspension had cooled to 0°C, a solution of 1,3-propane sultone **3.3** (1.0 eq) in anhydrous THF (40 mL) was added also through a cannula. The colour of the mixture changed almost

immediately to clear yellow. The mixture was allowed to stir at 0°C for thirty minutes after the addition of sultone **3.3** and then at room temperature for another 30 min. Subsequently, the precipitate was filtered, washed with THF and triturated with EtOAc to give the desired product (**3.1a**, **3.1b**, **3.1d** or **3.1e**) in greater than 90% yield.

Sodium 3-(2-(trifluoromethyl)-10*H*-phenothiazin-10-yl)propane-1-sulfonate 3.1a (DS0031)

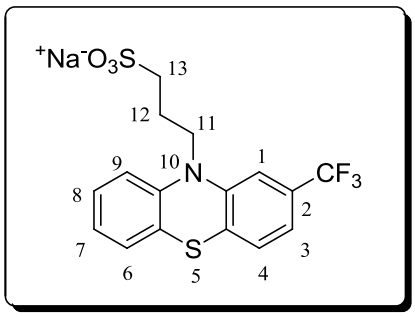

Pale-pink solid (0.62 g, 27%); R_f 0.40 (1.5:8.5 MeOH/ EtOAc); Mp 189-191 °C; ^{1}H NMR (300 MHz, D_2O) δ 7.07 (t, *J* = 6.9 Hz, 1H, H-8), 6.94 (s, 1H, H-1), 6.79 (m, 5H, (H-9. H-6, H-4, H-7 & H-3), 3.73 (t, *J* = 7.2 Hz, 2H, 2 x H-11), 2.87 (t, *J* = 7.2 Hz, 2H, 2 x H-13), 2.06 (qt, *J* = 7.2 Hz, 2H, 2 x H-12); ^{13}C NMR (75 MHz, D_2O) δ 145.31, 143.64, 129.54, 129.25, 128.82, 127.95, 127.43, 126.21, 123.49, 122.60, 119.00, 116.18, 111.97, 48.27, 45.41, 21.85; HRMS (ESI+): *m/z* 412.0265 $[M+H]^+$ calculated for $C_{16}H_{14}F_3NNaO_3S_2$, found 412.0250$[M+H]^+$.

Sodium 3-(2-(methylthio)-10*H*-phenothiazin-10-yl)propane-1-sulfonate 3.1b (DS0032)

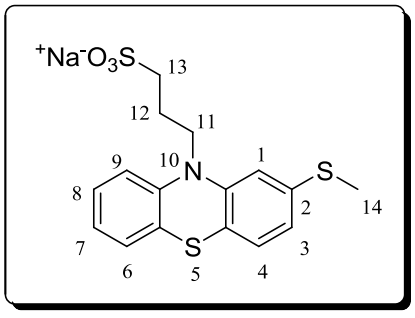

Turquoise solid (0.40 g, 17 %) ; R_f 0.40 (1.5:8.5 MeOH/ EtOAc); Mp 194-196 °C; ^{1}H NMR (300 MHz, D_2O) δ 7.05 (t, *J* = 7.5 Hz, 1H, H-8), 6.89 (d, *J* = 7.5 Hz, 1H, H-9), 6.72 (m, 3H, H-7, H-6 & H-4), 6.62 (s, 1H, H-1), 6.47 (d, *J* = 7.4 Hz, 1H, H-3), 3.68 (t, *J* = 7.5 Hz, 2H, 2 x H-11), 2.88 (t, *J* = 7.5 Hz, 2H, 2 x H-13), 2.28 (s, 3H, 3 X H-14), 2.08 (qt, *J* = 7.5 Hz, 2H, 2 x H-12); ^{13}C NMR (75 MHz, D_2O) δ 145.55, 144.23, 137.52, 127.74, 127.56, 124.67, 122.98, 121.38,

120.66, 120.48, 116.24, 114.08, 48.67, 45.47, 21.94, 15.35 (C-14); HRMS (ESI+): *m/z* 390.0268 $[M+H]^+$ calculated for $C_{16}H_{17}NaNO_3S_3$, found 390.0273 $[M+H]^+$.

Sodium 3-(2-acetyl-10*H*-phenothiazin-10-yl)propane-1-sulfonate <u>3.1c</u> (DS0033)

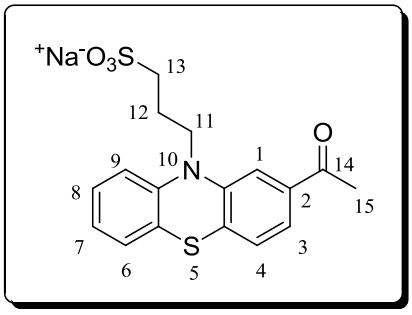

Bright yellow solid (0.55 g, 23%); R_f 0.40 (1.5:8.5 MeOH/ EtOAc); Mp 182-184 °C;^{1}H NMR (300 MHz, D_2O) δ 7.11 (m, 1H, H-3), 7.03 (d, *J* = 7.8 Hz, 1H, H-4), 6.96 (s, 1H, H-1), 6.80 (m, 3H, H-8, H-9 & H-6), 6.57 (d, *J* = 7.7 Hz, 1H, H-7), 3.73 (t, *J* = 7.0 Hz, 2H, 2 X H-11), 2.91 (t, *J* = 7.0 Hz, 2H, 2 x H-13), 2.43 (s, 3H, 3 x H-15), 2.05 (qt, *J* =7.0 Hz, 2H, 2 X H-12); ^{13}C NMR (75 MHz, D_2O) δ 201.88 (C-14), 144.09, 143.65, 135.58, 132.09, 128.25, 127.33, 126.85, 123.33, 123.19, 122.53, 116.07, 113.89, 48.47, 45.35, 26.17, 21.67; HRMS (ESI+): *m/z* 386.0497 $[M+H]^+$ calculated for $C_{17}H_{16}NaNO_4S_2$, found 386.0486 $[M+H]^+$.

Sodium 3-(2-chloro-10*H*-phenothiazin-10-yl)propane-1-sulfonate <u>3.1d</u> (DS0034)

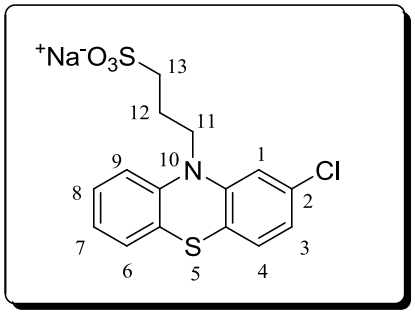

Pale-purple solid (0.98 g, 40 %); R_f 0.40 (1.5:8.5 MeOH/ EtOAc); Mp 192-194 °C; ^{1}H NMR (300 MHz, D_2O) δ 7.06 (t, *J* = 7.4 Hz, 1H, H-8), 6.86 (d, *J* = 7.4 Hz, 1H, H-9), 6.75 (m, 2H, Ar-H, H-6 & H-4), 6.63 (s, 1H, H-1), 6.55 (m, 2H, H-7 & H-3), 3.65 (t, *J* = 6.9 Hz, 2H, 2 x H-11), 2.88 (t, *J* = 6.9 Hz, 2H, 2 x H-13), 2.07 (qt, *J* = 6.9 Hz, 2H, 2 x H-12); ^{13}C NMR (101 MHz, D_2O) δ 146.01, 143.74, 132.83, 127.89, 127.66, 127.50, 124.22, 123.13, 122.98, 122.32, 116.09, 115.61, 48.46, 45.34, 21.85; HRMS (ESI+): *m/z* 378.0001 $[M+H]^+$ calculated for $C_{15}H_{14}ClNaNO_3S_2$, found 377.9996 $[M+H]^+$.

Sodium 3-(10*H*-phenothiazin-10-yl)propane-1-sulfonate 3.1e (DS0035)

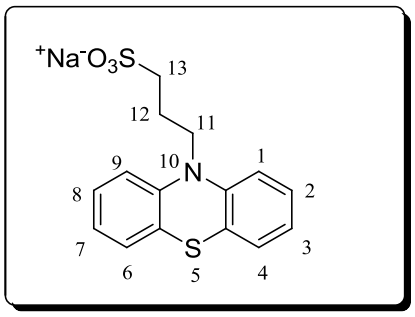

Purple-grey solid (0.99 g, 38 %); R_f 0.40 (1.5:8.5 MeOH/ EtOAc); Mp 287-289 °C; ^{1}H NMR (300 MHz, D_2O) δ 6.98 (t, *J* = 7.6 Hz, 2H, H-2 & H-8), 6.84 (d, *J* = 7.6 Hz, 2H, H-1 & H-9), 6.68 (m, 4H, H-4, H-6, H-3 & H-7), 3.70, (t, *J* = 7.0 Hz, 2H, 2 x H-11), 2.91 (t, *J* = 7.0 Hz, 2H, 2 x H-13), 2.08 (qt, *J* = 7.0 Hz, 2H, 2 x H-12); ^{13}C NMR (101 MHz, D_2O) δ 144.69, 127.63, 127.43, 124.33, 122.74, 115.80, 49.01, 48.54, 45.19, 21.98; HRMS (ESI+): *m/z* 344.0391 $[M+H]^+$ calculated for $C_{15}H_{15}NaNO_3S_2$, found 344.0389 $[M+H]^+$.

General procedure for the preparation *N*-butylsulfonates of phenothiazines {3.5a (DS00369), 3.5b (DS00370) & 3.5c (DS00366)}

To a suspension of NaH (60% dispersion in mineral oil, 1.1 eq) in anhydrous DMF (0.5 mL) under an inert atmosphere of argon, was added a solution of phenothiazine **3.6a-c** (1.0 eq) in anhydrous DMF (1 mL). The mixture was allowed to stir at room temperature for 30 min and then heated at 50 ° C for 1 h, during which the colour got darker indicating formation of phenothiazinium anion. After cooling to room temperature, 1,4-butane sultone **3.8** (1.1 eq) in anhydrous DMF (1 mL) was added and the mixture was allowed to stir for 20 h. A few drops of water were added to quench unreacted NaH. Subsequently, toluene was added and the solvents were removed by azeotropic distillation under reduced pressure. The resulting crude material was chromatographed on a C-18 reversed-phase column (H_2O; 9:1 H_2O/MeOH) to afford the desired products **3.5a-c**.

Sodium 4-(10*H*-phenothiazin-10-yl)butane-1-sulfonate 3.5c (DS00366)

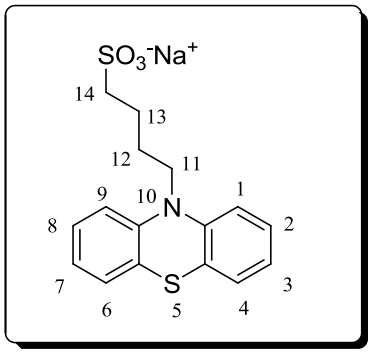

Dark purple solid (0.030 g, 14%); R_f 0.51 (2:8 MeOH/ EtOAc); Mp 184-186 °C; ^{1}H NMR (400 MHz, DMSO-d_6) δ 7.17 (m, 2H, H-2 & H-8), 7.11 (d, *J* = 6.6 Hz, 2H, H-1 & H-9), 7.00 (d, *J* = 7.4 Hz, 2H, H-4 & H-6), 6.91 (t, *J* = 7.3 Hz, 2H, H-3 & H-7), 3.83 (t, *J* = 6.8 Hz, 2H, 2 x H-11), 2.44 (t, *J* = 7.5 Hz, 2H, 2 x H-14), 1.72 (m, 4H, 2 x H-12 & 2 x H-13); ^{13}C NMR (101 MHz, DMSO-d_6) δ 145.24, 128.07, 127.52, 123.88, 122.84, 116.21, 51.41, 46.95, 26.07, 23.15; MS (ESI+): *m/z* 336.0 $[(M-Na) + 2H]^+$, calculated for $C_{16}H_{17}NO_3S_2$, found 336.0 $[(M-Na) + 2H]^+$.

Sodium 4-(2-(methylthio)-10*H*-phenothiazin-10-yl)butane-1-sulfonate 3.5a (DS00369)

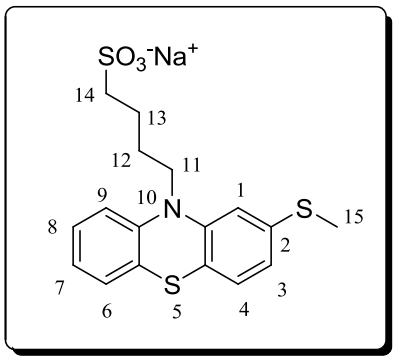

Dark brown solid (0. 040 g, 20%); R_f 0.51 (2:8 MeOH/ EtOAc); Mp 179-181 °C; ^{1}H NMR (400 MHz, DMSO-d_6) δ 7.19 (dd, *J* = 8.1, 1.3 Hz, 1H, H-8), 7.13 (dd, *J* = 7.6, 1.3 Hz, 1H, H-7), 6.99 (m, 4H, H-6, H-4, H-9 & H-1), 6.83 (m, 1H, H-3), 3.87(t, *J* = 6.6 Hz, 2H, 2 x H-11), 2.47 (s, 3H, 3 x H-15), 2.45 (m, 2H, 2 x H-14), 1.74 (m, 4H, 2 x H-12 & 2 x H-13); ^{13}C NMR (101 MHz, DMSO-d_6) δ 145.88, 144.99, 138.22, 128.05, 127.72, 127.53, 124.15, 122.99, 120.61, 120.51, 116.50, 114.02, 51.42, 46.96, 26.13, 23.14, 15.55 (C-15); HRMS (ESI+): *m/z* 381.0527 $[(M-Na) + H]^+$, calculated for $C_{17}H_{19}NO_3S_3$, found 381.0511 $[(M-Na) + H]^+$.

Sodium 4-(2-chloro-10*H*-phenothiazin-10-yl)butane-1-sulfonate 3.5b (DS00370)

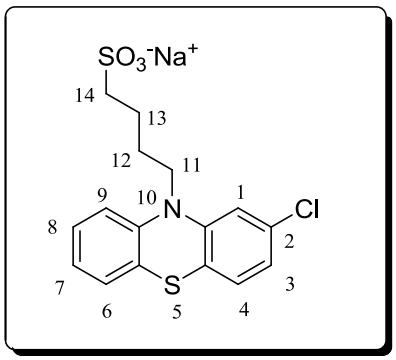

Light brown solid (0.040 g, 19%); R_f 0.51 (2:8 MeOH/ EtOAc); Mp 216-218 °C; ^{1}H NMR (400 MHz, DMSO-d_6) δ 7.21 (t, *J* = 7.7 Hz, 1H, H-8), 7.14 (m, 2H, H-9 & H-6), 7.04 (m, 2H, H-4 & H-7), 6.98 (m, 2H, H-1 & H-7), 3.86 (t, *J* = 6.5 Hz, 2H, 2 x H-11), 2.45 (t, *J* = 7.0 Hz, 2H, 2 x H-14), 1.71 (m, 4H, 2 x H-12 & 2 x H-13); ^{13}C NMR (101 MHz, DMSO-d_6) δ 146.84, 144.51, 132.95, 128.51, 128.26, 127.65, 123.71, 123.39, 122.98, 122.49, 116.71, 116.12, 51.36, 47.01, 25.99, 23.07 ; MS (ESI+): *m/z* 370.0 $[(M-Na) + 2H]^+$, calculated for $C_{16}H_{17}ClNO_3S_2$, found 370.0 $[(M-Na) + 2H]^+$.

General procedure for preparation of *N*-propylsulfonates of quinolines and isoquinolines {3.61 (DS-Q1), 3.60 (DS-Q2), 3.59 (DS-Q3), 3.57 (DS-Q4), 3.62 (DS-Q5) & 3.58 (DS-Q6)}

A mixture of aminoquinoline **3.63a-f** (1.0 eq) and NaH (60% dispersion in mineral oil, 1.1 eq) in anhydrous dioxane (1 mL) was allowed to stir at 40 ° C under an inert atmosphere of nitrogen for 1 h. After cooling to room temperature, 1,3-propane sultone **3.3** (1.1 eq) in anhydrous dioxane (1 mL) was added and then allowed to stir at room temperature for 14 h. A few drops of water were added to quench unreacted NaH. The solvent was removed under reduced pressure and the resulting crude material was chromatographed on a C-18 reversed-phase column using water as the eluent to give the desired products **3.57-3.62**.

Sodium 3-(quinolin-8-ylamino)propane-1-sulfonate 3.61 (DS-Q1)

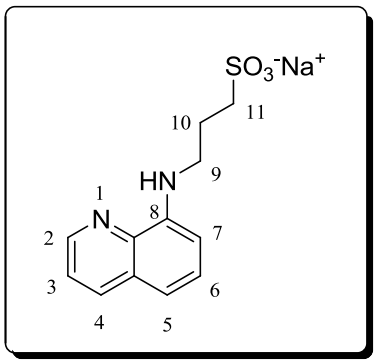

Pale yellow solid (0.080 g, 22%); R_f 0.33 (2:8 MeOH/ EtOAc); Mp 180-182 °C; ^{1}H NMR (300 MHz, D_2O) δ 8.56 (dd, *J* = 4.3, 1.6 Hz, 1H, H-2), 8.05 (dd, *J* = 8.3, 1.6 Hz, 1H, H-7), 7.36 (m, 2H, H-4 & H-3), 7.08 (m, 1H, H-6), 6.74 (d, *J* = 7.7 Hz, 1H, H-5), 3.31 (t, *J* = 7.1 Hz, 2H, 2 x H-9), 3.09 (m, 2H, 2 x H-11), 2.15 (m, 2H, 2 x H-10); ^{13}C NMR (101 MHz, D_2O) δ 147.64, 143.47, 137.29, 137.21, 128.58, 127.71, 121.70, 115.91, 107.39, 48.99, 42.12, 23.89; MS (ESI+): *m/z* 267.1 $[(M-Na) + 2H]^+$, calculated for $C_{12}H_{15}N_2O_3S$, found 267.1 $[(M-Na) + 2H]^+$.

Sodium 3-(isoquinolin-1-ylamino)propane-1-sulfonate 3.60 (DS-Q2)

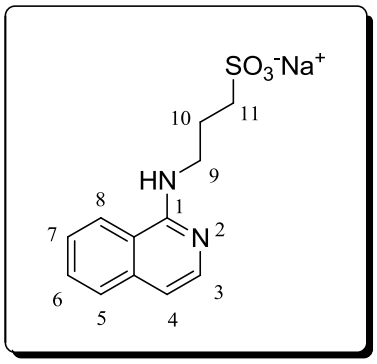

Light yellow solid (0.060 g, 16%); R_f 0.33 (2:8 MeOH/ EtOAc); Mp 219-221 °C; ^{1}H NMR (300 MHz, D_2O) δ 7.80 (d, *J* = 8.5 Hz, 1H, H-3), 7.71 (t, *J* = 7.5 Hz, 1H, H-8), 7.51 (t, *J* = 7.5 Hz, 2H, H-6 & H-7), 7.20 (d, *J* = 7.2 Hz, 1H, H-5), 6.73 (d, *J* = 8.5 Hz, 1H, H-4), 4.09 (t, *J* = 6.6 Hz, 2H, 2 x H-9), 3.04 (t, *J* = 6.6 Hz, 2H, 2 x H-11), 2.20 (qt, *J* = 6.6 Hz, 2H, 2 x H-10); ^{13}C NMR (101 MHz, D_2O) δ 153.61, 135.03, 133.92, 131.43, 128.70, 127.19, 124.07, 118.49, 111.52, 51.15, 47.40, 22.59; MS (ESI+): *m/z* 267.1 $[(M-Na) + 2H]^+$, calculated for $C_{12}H_{15}N_2O_3S$, found 267.1 $[(M-Na) + 2H]^+$.

Sodium 3-(isoquinolin-5-ylamino)propane-1-sulfonate 3.59 (DS-Q3)

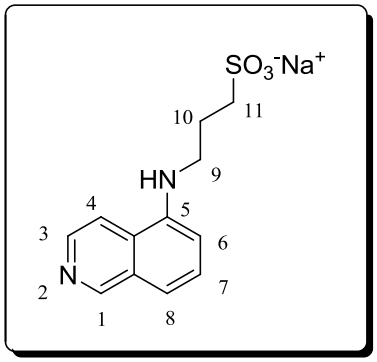

Bright orange solid (0.040 g, 11%); R_f 0.34 (2:8 MeOH/ EtOAc); Mp 281-283 °C; ^{1}H NMR (300 MHz, D_2O) δ 9.41 (s, 1H, H-1), 8.31 (d, *J* = 7.0 Hz, 1H, H-3), 8.20 (dd, *J* = 7.0, 2.8 Hz, 1H, H-4), 7.70 (m, 2H, H-6 & H-8), 7.29 (m, 1H, H-7), 4.78 (t, *J* = 7.0 Hz, 2H, 2 x H-9), 3.01 (t, *J* = 7.0 Hz, 2H, 2 x H-11), 2.49 (qt, *J* = 7.0 Hz, 2H, 2 x H-10); ^{13}C NMR (101 MHz, D_2O) δ 149.23, 143.16, 132.41, 132.06, 128.51, 126.77, 121.29, 119.97, 119.79, 59.44, 47.42, 26.21; MS (ESI+): *m/z* 267.1 $[(M-Na) + 2H]^+$, calculated for $C_{12}H_{15}N_2O_3S$, found 267.1 $[(M-Na) + 2H]^+$.

Sodium 3-(7-chloroquinolin-4-ylamino)propane-1-sulfonate 3.57 (DS-Q4)

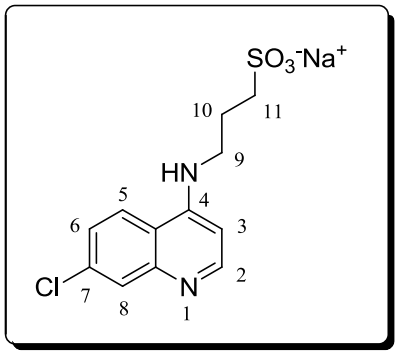

Bright orange solid (0.030 g, 13%); R_f 0.34 (2:8 MeOH/ EtOAc); Mp 256-258 °C; ^{1}H NMR (300 MHz, D_2O) δ 8.28 (dd, *J* = 6.8, 2.1 Hz, 1H, H-3), 8.06 (m, 1H, H-2), 7.68 (m, 1H, H-8), 7.17 (m, 1H, H-6), 6.80 (dd, *J* = 7.3, 3.7 Hz, 1H, H-5), 4.64 (m, 2H, 2 x H-9), 3.06 (t, *J* = 7.2 Hz, 2H, 2 x H-11), 2.37 (m, 2H, 2 x H-10); ^{13}C NMR (101 MHz, D_2O) δ 146.81, 141.39, 135.33, 127.89, 126.17, 124.28, 122.53, 117.75, 103.55, 53.44, 48.07, 24.66; MS (ESI+): *m/z* 301.0 $[(M-Na) + 2H]^+$, calculated for $C_{12}H_{14}ClN_2O_3S$, found 301.0 $[(M-Na) + 2H]^+$.

Sodium 3-(quinolin-6-ylamino)propane-1-sulfonate 3.62 (DS-Q5)

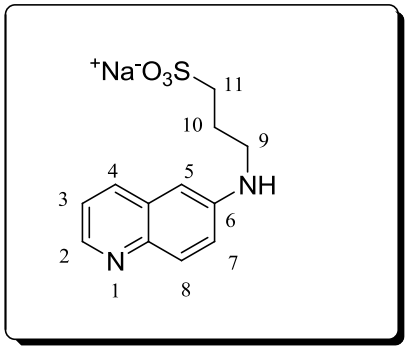

Pale yellow solid (0.040 g, 11 %); R_f 0.31 (2:8 MeOH/ EtOAc); Mp 265-267 °C; ^{1}H NMR (300 MHz, D_2O) δ 8.86 (d, *J* = 6.5 Hz, 1H, H-7), 8.66 (d, *J* = 8.4 Hz, 1H, H-2), 8.16 (d, *J* = 6.0 Hz, 1H, H-4), 7.81 (dd, *J* = 8.4, 6.0 Hz, 1H, H-3), 7.63 (d, *J* = 6.5 Hz, 1H, H-8), 7.22 (s, 1H, H-5), 5.06 (t,

J = 7.2 Hz, 2H, 2 x H-9), 3.12 (t, *J* = 7.2 Hz, 2H, 2 x H-11), 2.52 (qt, *J* = 7.2 Hz, 2H, 2 x H-10); ^{13}C NMR (101 MHz, D_2O) δ 149.10, 144.94, 144.11, 132.95, 128.05, 122.13 (2 x C), 119.74, 109.20, 56.51, 48.03, 25.51; MS (ESI+): *m/z* 267.1 $[(M\text{-}Na) + 2H]^+$, calculated for $C_{12}H_{15}N_2O_3S$, found 267.1 $[(M\text{-}Na) + 2H]^+$.

Sodium 3-(quinolin-5-ylamino)propane-1-sulfonate <u>3.58</u> (DS-Q6)

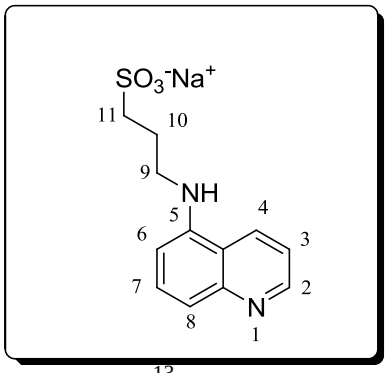

Bright orange solid (0.036 g, 10%); R_f 0.33 (2:8 MeOH/ EtOAc); Mp 295-297 °C; ^{1}H NMR (300 MHz, D_2O) δ 9.02 (m, 2H, H-2 & H-4), 7.76 (m, 2H, H-6 & H-7), 7.47 (d, *J* = 9.0 Hz, 1H, H-3), 7.01 (d, *J* = 8.0 Hz, 1H, H-8), 4.97 (m, 2H, 2 x H-9), 3.05 (t, *J* = 7.2 Hz, 2H, 2 x H-11), 2.44 (m, 2H, 2 x H-10); ^{13}C NMR (101 MHz, D_2O) δ 148.64, 147.70, 142.48, 138.54, 138.03, 119.10, 112.99, 107.57, 106.47, 56.90, 48.05, 25.04; MS (ESI+): *m/z* 267.1 $[(M\text{-}Na) + 2H]^+$, calculated for $C_{12}H_{15}N_2O_3S$, found 267.1 $[(M\text{-}Na) + 2H]^+$.

Preparation of sodium 3-(10,11-dihydro-5*H*-dibenzoazepin-5-yl) propane-1-sulfonate <u>3.12</u> (DS00381)

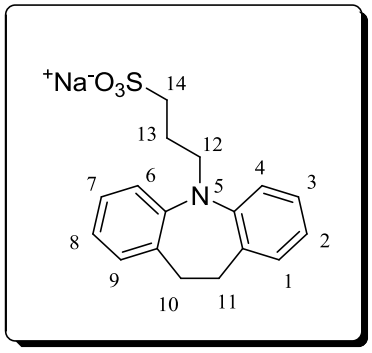

To a suspension of NaH (60% dispersion in mineral oil, 0.034 g, 1.40 mmol) in anhydrous DMF (0.5 mL) under an inert atmosphere of nitrogen, was added dibenzoazepine **3.56** (0.25 g, 1.28 mmol) in anhydrous DMF (1 mL). The mixture was allowed to stir at 0 °C for 30 min and at room temperature for a further 30 min. 1,3-propane sultone **3.3** (0.16 g, 1.28 mmol) in anhydrous DMF (0.5 mL) was then added and the mixture was allowed to stir for 18 h. A few drops of water were added to quench unreacted NaH. Subsequently, toluene was added and the

solvents were removed by azeotropic distillation under reduced pressure. The crude material was chromatographed on a reverse phase C-18 column to afford the desired product **3.12** as a light brown solid (0.080 g, 18%); R_f 0.38 (1:9 MeOH/ EtOAc); Mp 180-182 °C; ^{1}H NMR (300 MHz, D_2O) δ 6.94 (m, 4H, H-9, H-1, H-7 & H-3), 6.76 (m, 4H, H-8, H-2, H-6 & H-4), 3.53 (m, 2H, 2 x H-12), 2.75 (m, 6H, 2 x H-14, 2 x H-10 & 2 x H-11), 1.89 (m, 2H, 2 x H-13); ^{13}C NMR (101 MHz, D_2O) δ 147.95, 134.19, 129.87, 126.58, 122.70, 120.03, 49.15, 48.70, 31.70, 22.86; HRMS (ESI+): *m/z* 317.1086 $[(M-Na)+H]^+$, calculated for $C_{17}H_{19}NO_3S$, found 317.1028 $[(M-Na)+H]^+$.

Preparation of dibenzo-1,4-thiazepine 3.54

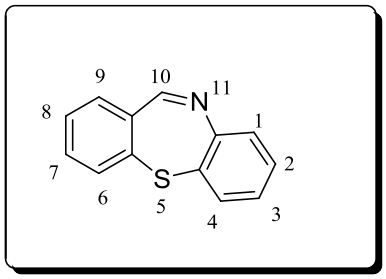

To a mixture of 2-aminothiophenol **3.53** (1.00 g, 8.0 mmol) and K_2CO_3 (0.88 g, 6.40 mmol) in DMF (4 mL), was added 2-fluorobenzaldehyde **3.52** (1.00 g, 8.0 mmol). The mixture was heated at 100 °C and allowed to stir for 20 h. After cooling to room temperature, water was added to the mixture followed by extraction of the product with diethyl ether (3 x 40 mL). The organic extracts were washed with brine and then dried over magnesium sulfate. After removing diethyl ether under reduced pressure, the resulting solid was triturated with hexane and recrystallized from ethyl acetate to afford a light brown solid **3.54** (1.20 g, 53 %); R_f 0.41 (1:9 EtOAc/Hex); Mp 118-120 °C (lit. 124 °C)[3]; ^{1}H NMR (300 MHz, $CDCl_3$) δ 8.92 (s, 1H, H-10), 7.40 (m, 7H, Ar-H), 7.19 (m, 1H, Ar H); ^{13}C NMR (101 MHz, $CDCl_3$) δ 162.22 (C-10), 148.59, 139.44, 137.28, 132.76, 131.62, 131.46, 129.41, 129.26, 128.91, 128.23, 127.21, 126.96.

Preparation of 10,11-dihydrodibenzo-1,4-thiazepine 3.55

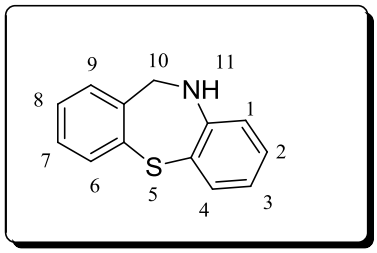

To a solution of dibenzo-1,4-thiazepine **3.54** (1.20 g, 5.66 mmol) in dry MeOH (4 mL), was added $NaBH_4$ (0.21 g 5.60 mmol) portion-wise under an inert atmosphere of nitrogen at 0 °C. The mixture was allowed to stir for 8 h and then quenched with diluted HCl. Water was added to the mixture, followed by extraction of the product with EtOAc (2 x 40 mL). The organic extracts were combined, washed with brine and dried over magnesium sulfate. EtOAc was removed under reduced pressure and the resulting solid was triturated with hexane to give the product **3.55** as a pale brown solid. (1.10 g, 91 %); R_f 0.43 (1:9 EtOAc/Hex); Mp 121-123 °C (lit. 116 °C)[4]; ^{1}H NMR (300 MHz, $CDCl_3$) δ 7.55 (m, 1H, H-6), 7.28 (m, 3H, H-7, H-4 & H-8), 7.19 (m, 1H, H-9), 6.93 (m, 1H, H-2), 6.58 (dd, *J* = 7.3, 1.3 Hz, 1H, H-3), 6.39 (dd, *J* = 8.1, 1.2 Hz, 1H, H-1), 4.85 (s, 2H, 2 x H-10); ^{13}C NMR (101 MHz, $CDCl_3$) δ 146.88, 142.89, 137.18, 132.36, 131.44, 128.59, 128.34, 128.23, 127.92, 118.34, 117.65, 116.26, 48.99.

Preparation of sodium 3-(dibenzo-1,4-thiazepin-10(11*H*)-yl)propane-1-sulfonate 3.11 (DS00380)

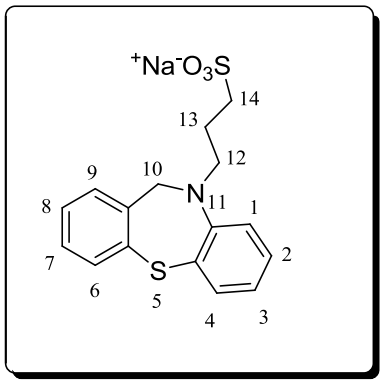

To a suspension of NaH (60% dispersion in mineral oil) (0.072 g, 3.0 mmol) in anhydrous DMF (1.0 mL) under an inert atmosphere of nitrogen, was added dibenzothiazepine **3.55** (0.50 g, 2.3 mmol) in anhydrous DMF (0.5 mL). The mixture was allowed to stir at 0 °C for 30 min, and at room temperature for a further 30 min. 1,3-propane sultone (0.28 g, 2.30 mmol) in anhydrous DMF (0.5 mL) was then added and the mixture was allowed to stir for 16 h. A few drops of water were added to quench unreacted NaH. Subsequently, toluene

was added and the solvents were removed by azeotropic distillation under reduced pressure. The crude material was chromatographed on a reverse phase C-18 column to afford the desired product **3.11** as a light brown crystalline solid. (0.15 g, 18 %); R_f 0.35 (1:9 MeOH/EtOAc); Mp 180-183 °C; ^{1}H NMR (300 MHz, D_2O) δ 7.11 (m, 3H, H-6, H-7 & H-4), 6.96 (m, 3H, H-8, H-9 & H-2), 6.67 (d, *J* = 8.2 Hz, 1H, H-1), 6.49 (m, 1H, H-3), 4.33 (s, 2H, 2 x H-10), 3.01 (t, *J* = 6.5 Hz, 2H, 2 x H-12), 2.77 (t, *J* = 6.5 Hz, 2H, 2 x H-14), 1.93 (m, 2H, 2 x H-13); ^{13}C NMR (101 MHz, D_2O) δ 149.42, 140.14, 135.54, 130.35, 129.43, 128.22, 127.75, 127.49, 127.20, 121.56, 119.66, 119.60, 53.61, 52.42, 48.54, 22.37; HRMS (ESI+): *m/z* 336.0728 $[(M-Na)+2H]^+$, calculated for $C_{16}H_{16}NNaO_3S_2$, found 336.0705 $[M]^+$.

Preparation of 2-aminobenzonitrile <u>3.32</u>

Step (i): Preparation of 3-(hydroxyimino)indolin-2-one **<u>3.31</u>**

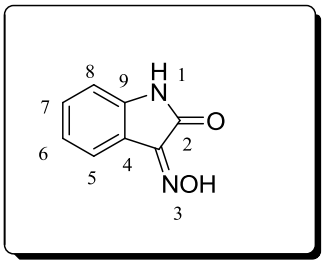

A mixture of isatin **3.30** (4.0 g, 27.0 mmol) and hydroxylamine hydrochloride in water (13.6 mL) was allowed to reflux for an hour. After cooling to room temperature, the precipitate was filtered off, washed with cold water and then dried to give the oxime **3.31** as a bright yellow solid. (4.20 g, 96%); R_f 0.26 (4:6 EtOAc/Hex); Mp 213-215 °C (lit. 215-218 °C)[5].

Step (ii) Preparation of aminobenzonitrile **<u>3.32</u>**

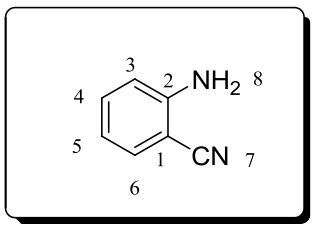

A mixture of the oxime **3.31** (2.00 g, 12.35 mmol) and sodium carbonate (0.1eq) in DMF (4 mL) was heated at 135 °C for 2.5 h and then allowed to cool to room temperature. Water was added to the mixture, followed by extraction of the product with EtOAc (2 x 50 mL). The organic extracts were combined and the solvent was removed under reduced

pressure. The resulting solid was dried to afford aminobenzonitrile **3.32** as a light yellow solid. (1.20 g, 82%); R_f 0.53 (4:6 EtOAc/Hex); Mp 50-52 °C (lit. 47-49 °C)[6]; ^{1}H NMR (300 MHz, DMSO-d_6) δ 7.37 (dd, *J* = 7.8, 6.4 Hz, 1H, H-4), 7.30 (d, *J* = 8.4 Hz, 1H, H-6), 6.79 (dd, *J* = 8.4, 7.8 Hz, 1H, H-5), 6.59 (dd, *J* = 6.4 Hz, 1H, H-3), 5.98 (s, 2H, 2 X NH-8).

Preparation of 2-(4-chloro-2-nitrophenylamino)benzonitrile 3.34[7]

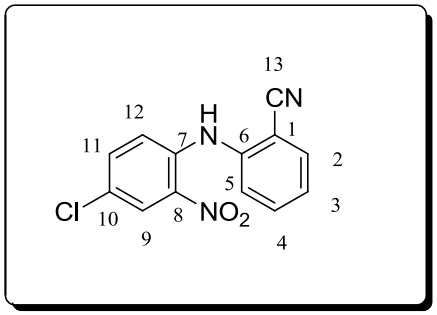

To a mixture of aminobenzonitrile **3.32** (1.09 g, 9.19 mmol) and K_2CO_3 (1.1 eq) in DMF (4 mL), was added 1,4-dichloronitrobenzene **3.33** (1.94 g, 10.11 mmol). The resulting mixture was heated at 120 °C and allowed to stir for 16 h. After cooling to room temperature, water was added the product was extracted with EtOAc (2 x 50 mL). The organic extracts were combined and the solvent was removed under reduced pressure. The resulting crude material was triturated with hexane to afford the desired product **3.34** as a light brown solid (0.50 g, 20%); R_f 0.50 (3:7 EtOAc/Hex); Mp 180-183 °C; ^{1}H NMR (300 MHz, $CDCl_3$) δ 9.53 (s, 1H, NH), 8.27 (d, *J* = 2.5 Hz, 1H, H-9), 7.75 (dd, *J* = 7.8, 1.3 Hz, 1H, H-11), 7.64 (m, 1H, H-4), 7.45 (m, 2H, H-2 & H-3), 7.32 (m, 1H, H-12), 7.20 (m, 1H, H-5); ^{13}C NMR (101 MHz, $CDCl_3$) δ 141.97, 139.08, 135.73, 135.18, 134.06, 134.02, 126.19, 125.42, 124.71, 123.17, 118.19, 116.11, 107.84.

Preparation of 8-chloro-5*H*-dibenzo-1,4-diazepin-11-amine hydrochloride 3.35[7]

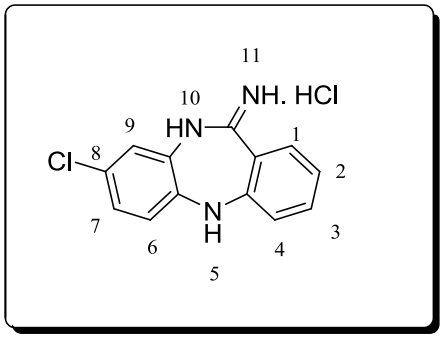

To a solution of 2-(4–chloro-2nitrophenylamino)benzo-nitrile **3.34** (0.40 g, 1.46 mmol) in absolute EtOH, was a solution of stannous chloride dihydrate (0.99 g, 4.38 mmol) in 10 N HCl. The reaction mixture was allowed to stir and reflux for 8 h, thereafter allowed to cool to room

temperature. The mixture was concentrated followed by addition of water to precipitate the product. The precipitate was collected by vacuum filtration, washed with water and dried to give the desired amine hydrochloride **3.35** as a light brown solid (0. 38 g, 93 %); R_f 0.51 (2:8 MeOH/EtOAc); Mp 174-176 °C; ^{1}H NMR (300 MHz, DMSO-d_6) δ 9.67 (s, 1H, NH-5), 9.19 (s, 1H, NH-10), 8.38 (s, 1H, NH-11), 7.61 (m, 2H, Ar-H), 7.19 (m, 5H, Ar-H); ^{13}C NMR (101 MHz, DMSO) δ 166.03, 153.09, 142.53, 136.80, 131.97, 129.72, 127.78, 127.59, 123.18, 122.92, 122.58, 121.23, 117.08.

Preparation of sodium 3-(8-chloro-5*H*-dibenzo-1,4-diazepin-11-ylamino)propane- 1-sulfonate <u>3.9</u> (DS3123)

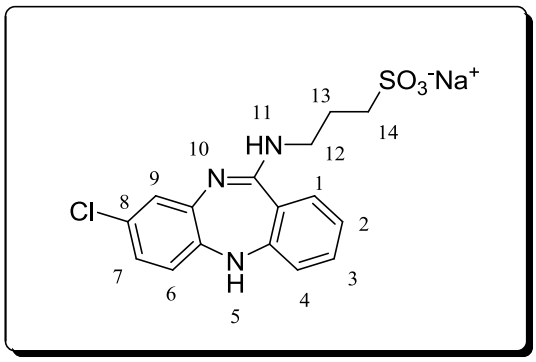

A mixture of 8-chloro-5*H*-dibenzo-1,4-diazepin-11-amine hydrochloride **3.35** (0.10 g, 0.36 mmol) and Na_2CO_3 (0.050 g, 0.47 mmol) in anhydrous DMF (0.5 mL) was allowed to stir at room temperature for 30 min and then at 50 ° C for 1 h. After cooling to room temperature, 1,3-propane-sultone (0.044 g, 0.36 mmol) in anhydrous DMF (0.5 mL) was added and then allowed stirred at room temperature for 12 h. The crude mixture was concentrated under reduced pressure and then chromatographed on a C-18 reversed-phase column using water as the eluent to give the desired product as a brown solid (0.015 g, 11%) ; R_f 0.26 (2:8 MeOH/EtOAc); Mp 284-286 °C; ^{1}H NMR (300 MHz, D_2O) δ 7.57 (m, 2H, Ar-H), 7.03 (m, 5H, Ar-H), 4.19 (m, 2H, 2 x H-12), 2.92 (m, 2H, 2 x H-14), 2.08 (m, 2H, 2 x H-13); HRMS (ESI+): *m/z* 364.0523 $[M\text{-}Na]^+$, calculated for $C_{16}H_{15}ClN_3O_3S_2$, found 364.0522 $[M\text{-}Na]^+$.

Preparation of 1-bromo-2-((2-nitrophenoxy)methyl)benzene 3.42[8]

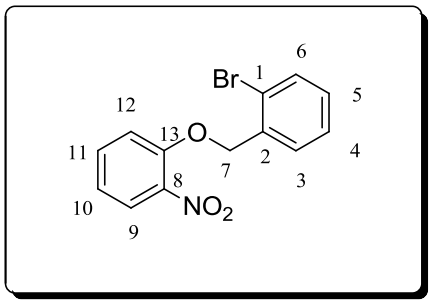

To a mixture of 2-nitrophenol **3.41** (0.53 g, 3.80 mmol and K_2CO_3 (1.31 g, 9.50 mmol) in anhydrous acetonitrile (7.5 mL), was added mixture of 2-bromobenzyl bromide **3.40** (1.00 g, 4.0 mmol). The resulting mixture was heated at 70 ºC and allowed to stir for 3h. After the reaction went to completion, it was quenched with water followed by extraction with EtOAc (2 x 50 mL). The organic extracts were combined, washed with brine and dried over Na_2SO_4. The solvent was removed under reduced pressure and the resulting solid was recrystallized from a mixture of EtOAc/Hex (2:8) to afford product **3.42** faint-yellow crystals (0.84 g, 64 %); R_f 0.42 (1:9 EtOAc/Hex); Mp 91-93 °C; ^{1}H NMR (400 MHz, $CDCl_3$) δ 7.89 (dd, *J* = 8.0, 1.7 Hz, 1H, H-9), 7.69 (dd, *J* = 7.7, 1.1 Hz, 1H, H-11), 7.58 (dd, *J* = 8.0, 1.1 Hz, 1H, H-10), 7.54 (d, *J* = 8.0 Hz, 1H, H-6), 7.38 (dd, *J* = 7.5, 1.7 Hz, 1H, H-4), 7.21 (td, *J* = 8.0, 1.7 Hz, 1H, H-5), 7.15 (d, *J* = 7.5 Hz, 1H, H-3), 7.07 (d, *J* = 7.7 Hz, 1H, H-12), 5.28 (s, 2H, 2 X H-7); ^{13}C NMR (101 MHz, $CDCl_3$) δ 151.68, 140.39, 134.94, 134.21, 132.50, 129.48, 128.60, 127.91, 125.82, 121.52, 120.94, 115.02, 70.46 (C-7).

Preparation of 2-(2-bromobenzyloxy)aniline hydrochloride 3.43[8]

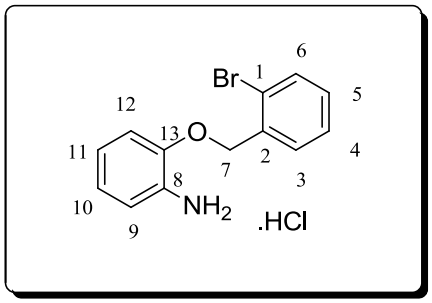

To a solution of 1-bromo-2-((2-nitrophenoxy)methyl) benzene **3.42** (1.10 g, 3.57 mmol) in isopropanol at 60 °C, 10 N HCl was added, followed by Fe filings (4.0 eq). The mixture was allowed to stir for 17 h at 60 °C and then filtered hot through a pad of celite. The filtrate was concentrated, 2 N HCl and diethyl ether were added until a precipitate formed. The resulting off-white solid was recrystallized from a mixture of MeOH and EtOAc to afford **3.43** as a

white solid. (0.72 g, 88%) ; R_f 0.40 (2:8 EtOAc/Hex); Mp 190-192 °C; ^{1}H NMR (400 MHz, CD_3OD) δ 7.66 (m, 2H, H-4 & H-6), 7.43 (m, 3H, H-3, H-5 & H-12), 7.26 (m, 2H, H-10, H-9), 7.11 (dd, *J* = 7.7, 1.2 Hz, 1H, H-11), 5.36 (s, 2H, 2 x H-7); ^{13}C NMR (101 MHz, MeOD) δ 152.90, 136.50, 133.96, 131.60, 131.17, 130.81, 128.95, 125.10, 123.83, 122.79, 120.87, 114.61, 71.50 (C-7).

Preparation of 5,11-dihydrodibenzo-1,4-oxazepine <u>3.44</u>

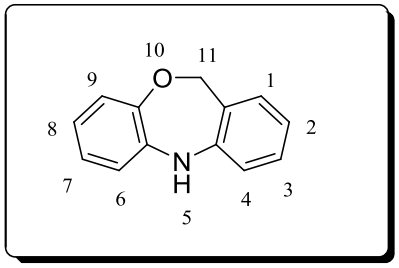

Anhydrous toluene was added to 2-(2-bromobenzyloxy) aniline hydrochloride **3.43** (0.650 g, 2.07 mmol), potassium tert-butoxide (0.46 g, 4.14 mmol), K_2CO_3 (0.57 g, 4.14 mmol) and bis(dibenzylideneacetone)palladium (0) (0.12 g, 0.21 mmol) under an inert atmosphere of nitrogen. This was followed by addition of tri-tert-butyl phosphine (0.020 g, 0.10 mmol) and the mixture was allowed to stir at 95 °C for 10 h. The reaction was cooled to room temperature, concentrated and then chromatographed on a silica gel column (3:7 CH_2Cl_2/Hex) to give **3.44** as a white solid (0.088 g, 22%); R_f 0.43 (2:8 EtOAc/Hex); Mp. 115-117 °C (lit. 119-120 °C)[8]; ^{1}H NMR (400 MHz, $CDCl_3$) δ 7.17 (dd, *J* = 7.7, 1.4 Hz, 1H, H-3), 7.08 (d, *J* = 7.4 Hz, 1H, H-1), 6.96 (dd, *J* = 7.9, 1.1 Hz, 1H, H-9), 6.89 (dd, *J* = 7.4, 1.2 Hz, 1H, H-7), 6.79 (m, 1H, H-2), 6.73 (m, 3H, H-4, H-6 & H-8), 5.94 (s, 1H, NH-5), 5.03 (s, 2H, 2 X H-11); ^{13}C NMR (101 MHz, $CDCl_3$) δ 149.03, 143.36, 134.58, 129.15, 128.81, 125.72, 123.41, 121.57, 119.64, 119.23, 118.44, 116.79, 74.37 (C-11).

Preparation of sodium 3-(dibenzo[1,4]oxazepin-5(11H)-yl)propane-1-sulfonate 3.10 (DS003125)

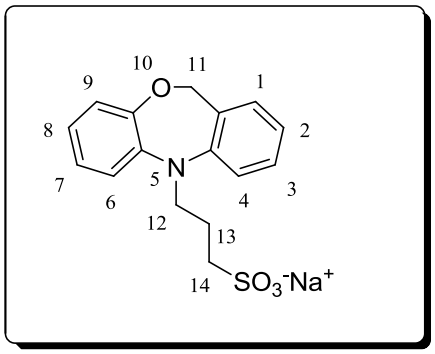

To a suspension of NaH (60% dispersion in mineral oil, 0.014 g, 0.52 mmol) in anhydrous DMF (0.5 mL) under an inert atmosphere of nitrogen, was added dibenzo-1,4-oxapine **3.44** (0.10 g, 0.52 mmol) in anhydrous DMF (1 mL). The mixture was allowed to stir at 0 °C for 30 min and at room temperature for a further 30 min. 1,3-propane sultone (0.090 g, 0.52 mmol) in anhydrous DMF (0.5 mL) was then added and the mixture was allowed to stir for 26 h. A few drops of water were added to quench unreacted NaH. Subsequently, toluene was added and the solvents were removed by azeotropic distillation under reduced pressure. The crude material was chromatographed on a reversed-phase C-18 column to afford the desired product **3.10** as a light brown solid (0.21 g, 12%); R_f 0.36 (1:9 MeOH/EtOAc); Mp 198-200 °C; ^{1}H NMR (300 MHz, D_2O) δ 7.44 (m, 2H, H-3 & H-1), 7.28 (d, *J* = 8.1 Hz, 1H, H-9), 7.19 (m, 2H, H-7 & H-2), 7.01 (t, *J* = 8.1 Hz, 1H, H-8), 6.91 (m, 2H, H-4 & H-6), 5.40 (s, 2H, 2 x H-11), 3.93 (t, *J* = 6.5 Hz, 2H, 2 x H-12), 2.95 (m, 2H, 2 x H-14), 2.10 (m, 2H, 2 x H-13); ^{13}C NMR (101 MHz, D_2O) δ 149.93, 148.29, 136.24, 131.41, 129.94, 128.78, 123.63, 122.86, 122.27, 120.85, 120.25, 119.24, 69.80, 48.73, 48.33, 22.35. HRMS (ESI+): *m/z* 342.0776 $[M+H]^+$, calculated for $C_{16}H_{17}NO_4S$, found 342.0711 $[M+H]^+$.

Preparation of 9*H*-thioxanthene 3.67

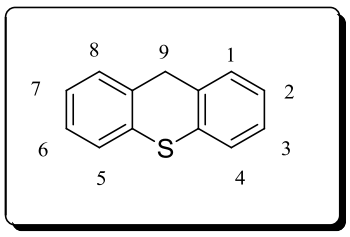

To a solution of thioxanthone **3.66** (0.50 g, 2.36 mmol) in dry THF under nitrogen, was added 1M BH_3.THF complex (2 eq) drop-wise at -10 °C. The mixture was allowed to warm to room temperature and then heated to reflux for 14h. Water was slowly

added to the reaction mixture, followed by extraction with EtOAc (2 x 30 mL). The organic extracts were combined, washed with brine and dried over Na_2SO_4. The resulting solid was recrystallized from DCM (0.24 g, 51%); R_f 0.57 (2:8 EtOAc/Hex); Mp 128-130 °C (lit. 128-130 °C)[9]; ^{1}H NMR (400 MHz, $CDCl_3$) δ 7.47 (m, 2H, H-4 & H-5), 7.34 (m, 2H, H-3 & H-6), 7.22 (m, 4H, H-2, H-7, H-1 & H-8), 3.89 (s, 2H, 2 x H-9); ^{13}C NMR (101 MHz, $CDCl_3$) δ 139.25, 134.71, 127.66, 126.70, 125.87, 114.10, 31.87 (C-9).

General procedure for alkylation with propane sultone using *n*-BuLi as a base

To a solution of acridone **3.69** or thioxanthene **3.67** (1.0 eq) in anhydrous THF (2 mL) under an inert atmosphere of nitrogen at -20 °C, was added *n*-BuLi (1.0 eq) drop-wise. The mixture was allowed to slowly warm to room temperature followed by addition of 1,3-propane sultone **3.3** (1.3 eq) in anhydrous THF (1 mL). The resulting mixture was allowed to stir at room temperature for 16 h, followed by slow addition of water to quench unreacted *n*-BuLi. The crude mixture was concentrated under reduced pressure and then chromatographed on a C-18 reversed phase column (H_2O; 8:2 H_2O/MeOH) to afford the desired products **3.64** and **3.65**.

Lithium 3-(9*H*-thioxanthen-9-yl)propane-1-sulfonate 3.65 (DS00386)

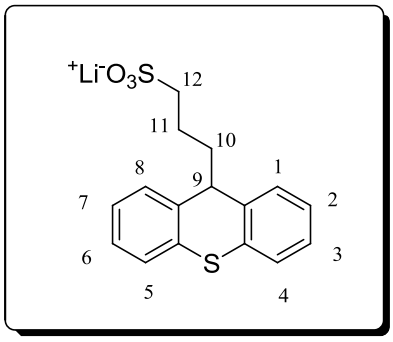

Pale yellow solid (0.030 g, 12%); R_f 0.46 (1.5:8.5 MeOH/ EtOAc); Mp 298-301 °C ; ^{1}H NMR (300 MHz, D_2O) δ 7.22 (d, *J* = 7.7 Hz, 2H, H-4 & H-5), 7.12 (m, 4H, H-3, H-6, H-2 & H-7), 7.03 (m, 2H, H-1 & H-8), 3.85 (t, *J* = 6.9 Hz, 1H, H-9), 2.66 (m, 2H, 2 x H-10), 1.54 (m, 4H , 2 x H-12 & 2 x H-11); ^{13}C NMR (101 MHz, D_2O) δ 137.04, 131.07, 128.60, 128.47, 126.25, 126.01, 50.34, 47.66, 30.18, 21.86; HRMS (ESI+): *m/z* 319.0463 $[M-Li]^+$, calculated for $C_{16}H_{15}O_3S_2$, found 319.0469 $[M-Li]^+$.

Lithium 3-(9-oxoacridin-10(9*H*)-yl)propane-1-sulfonate 3.64 (DS00387)

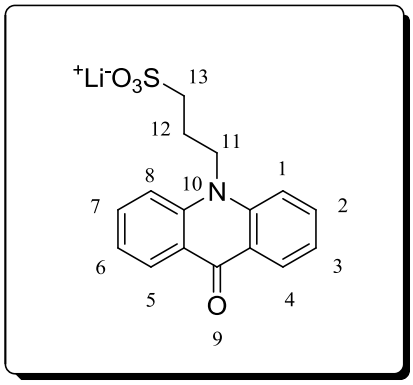

Bright yellow solid (0.050 g, 24 %); R_f 0.42 (1.5:8.5 MeOH/ EtOAc); Mp 270-272 °C; ^{1}H NMR (300 MHz, D_2O) δ 7.97 (dd, *J* = 8.1, 1.2 Hz, 2H, H-4 & H-5), 7.67 (m, 2H, H-2 & H-7), 7.42 (d, *J* = 8.8 Hz, 2H, H-1 & H-8), 7.17 (t, *J* = 7.5 Hz, 2H, H-3 & H-6), 4.13 (m, 2H, 2 x H-11), 3.05 (t, *J* = 7.0 Hz, 2H, 2 x H-13), 2.01 (m, 2H, H-12); ^{13}C NMR (101 MHz, D_2O) δ 178.20 (C-9), 140.57, 134.53, 126.03, 121.50, 120.10, 114.78, 47.68, 44.00, 21.85; HRMS (ESI+): *m/z* 316.0649 $[M-Li]^+$, calculated for $C_{16}H_{14}NO_4S$, found 316.0642 $[M-Li]^+$.

General procedure for preparation of 10-(3-chloropropyl)-10*H*-phenothiazine derivatives 3.71a-c

To a suspension of NaH (60% dispersion in mineral oil, 1.1 eq) in anhydrous DMF (2 mL) under an inert atmosphere of nitrogen, phenothiazine **3.70a-c** (1.0 eq) in anhydrous DMF (2 mL) was added. The mixture was allowed to stir at 0 °C for 30 min, and at room temperature for a further 30 min. 1-bromo-3-chloropropane (1.0 eq) was then added and the mixture was allowed to stir for 21 h. Water was added to quench unreacted sodium hydride. Subsequently, toluene was added and the solvents were removed by azeotropic distillation under reduced pressure. The resulting solid was dissolved in EtOAc and subsequently washed with brine. The organic layer was concentrated and then chromatographed on a silica gel column (100 % Hexane) to afford the desired products **3.71a-c**.

1-(10-(3-chloropropyl)-10*H*-phenothiazin-2-yl)ethanone 3.71a

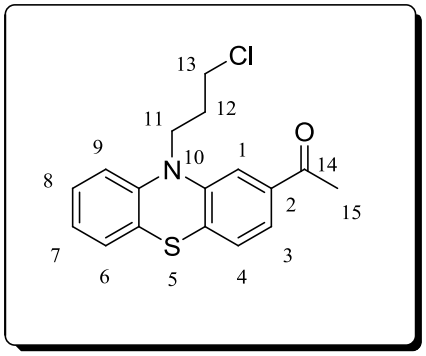

Yellow solid (0.25 g, 38%); R_f 0.51 (2:8 EtOAc/Hex); Mp 53-54 ºC; ^{1}H NMR (400 MHz, $CDCl_3$) δ 7.48 (m, 2H, Ar-H), 7.17 (m, 3H, Ar-H), 6.94 (m, 2H, Ar-H), 4.13 (t, *J* = 6.5 Hz, 2H, 2 x H-11), 3.67 (t, *J* = 6.1 Hz, 2H, 2 x H-13) , 2.57 (s, 3H, 3 x H-15), 2.28 (m, 2H, 2 x H-12). ^{13}C NMR (101 MHz, $CDCl_3$) δ 197.26 (C-14), 145.35, 144.35, 136.43, 132.71, 127.77, 127.65, 127.22, 124.42, 123.31, 123.14, 115.90, 114.14, 45.29, 44.15, 42.21, 26.55.

2-chloro-10-(3-chloropropyl)-10*H*-phenothiazine 3.71b[10]

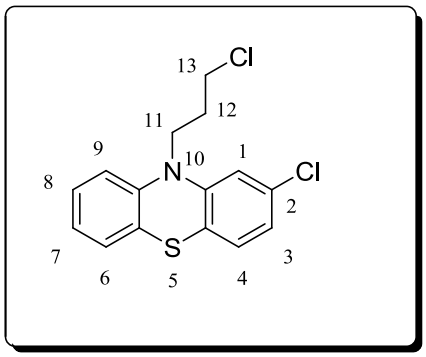

White solid (0.52 g, 79%); R_f 0.51 (2:8 EtOAc/Hex); Mp 51-52 ºC; ^{1}H NMR (400 MHz, $CDCl_3$) δ 7.17 (m, 2H, Ar-H), 7.05 (m,1H, Ar-H), 6.96 (m, 1H, Ar-H), 6.92 (m, 2H, Ar-H), 6.88 (m, 1H, Ar-H), 4.06 (t, *J* = 6.5 Hz, 2H, 2 x H-11), 3.67 (t, *J* = 6.5 Hz, 2H, 2 x H-13), 2.27 (m, 2H, 2 x H-12); ^{13}C NMR (101 MHz, $CDCl_3$) δ 146.42, 144.37, 133.38, 128.11, 127.73, 127.51, 125.52, 124.27, 123.22, 122.63, 115.98, 115.91, 45.27, 44.13, 42.18.

10-(3-chloropropyl)-10*H*-phenothiazine 3.71c[10]

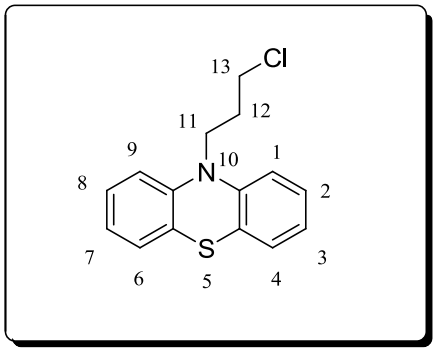

White solid (0.18 g, 26%); R_f 0.51 (2:8 EtOAc/Hex); Mp 58-59 ºC; ^{1}H NMR (400 MHz, $CDCl_3$) δ 7.17 (m, 4H, H-2, H-8, H-1 & H-9), 6.93 (m, 4H, H-4, H-6, H-3 & H-7), 4.09 (t, *J* = 6.5 Hz, 2H, 2 x H-11), 3.63 (m, 2H, 2 x H-13), 2.27 (m, 2H, 2 x H-12); ^{13}C NMR (101 MHz, $CDCl_3$) δ 145.10, 127.65, 127.31, 125.79, 122.75, 115.59, 45.17, 44.03, 42.42.

General procedure for preparation of isoniazid hybrids [monomers 3.72a (DS00362b), 3.72b (DS00364) & 3.72c (DS00365a); dimers 3.73a (DS00362), 3.73b (DS00364) & 3.73c (DS00365)]

To a suspension of NaH (60% dispersion in mineral oil, 1 eq) in anhydrous DMF (1 mL) under an inert atmosphere of nitrogen, was added isoniazid (1 eq) and the resulting mixture was allowed to stir at 0 °C for 30 min. After warming to room temperature, alkylated phenothiazine **3.71a-c** (1 eq) in anhydrous DMF (1 mL) was added and the mixture was allowed to stir at room temperature for 36 h. Water was added to quench unreacted sodium hydride. Subsequently, toluene was added and the solvents were removed by azeotropic distillation under reduced pressure. EtOAc (50 ml) was then added to the crude material, and this was washed with brine. The organic layer was concentrated and then chromatographed on a silica gel column (2:8 EtOAc/Hexane) to afford the desired products (**3.72a-c**; **3.73a-c**).

***N*'-(3-(2-acetyl-10*H*-phenothiazin-10-yl)propyl)isonicotinohydrazide 3.72a (DS00362b)**

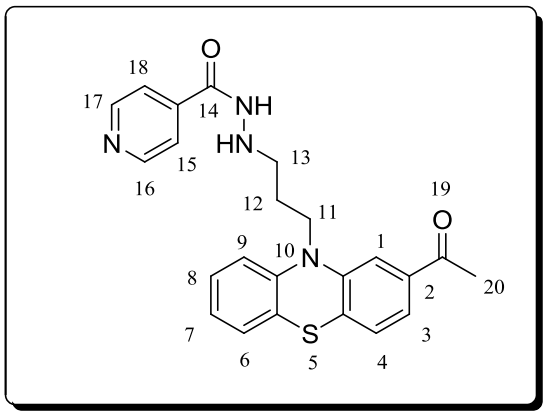

Dark yellow solid (0.028 g, 20%); R_f 0.55 (8:2 EtOAc/Hex); Mp 49-50 °C; ^{1}H NMR (400 MHz, $CDCl_3$) δ 8.72 (d, *J* = 5.9 Hz, 2H, H-16 & H-17), 7.72 (dd, *J* = 5.9, 1.6 Hz , 2H, H-15 & H-18), 7.47 (m, 2H, Ar-H), 7.14 (m, 3H, Ar-H), 6.94 (m, 2H, Ar-H), 4.48 (t, *J* = 6.6 Hz, 2H, 2 x H-11), 4.14 (t, *J* = 6.6 Hz, 2H, 2 x H-13), 2.54 (s, 3H, 3 x H-20), 2.27 (qt, *J* = 6.6 Hz, 2H, 2 x H-12); ^{13}C NMR (101 MHz, $CDCl_3$) δ 197.19, 164.98, 150.55, 145.27, 144.25, 137.23, 136.38, 132.79, 127.74, 127.68, 127.20, 124.45, 123.42, 123.16, 122.78, 115.89, 115.78, 114.19, 113.89, 63.09, 43.89, 26.50, 25.84; HRMS (ESI+): *m/z* 419.1542 $[M+H]^+$, calculated for $C_{23}H_{23}N_4O4S$, found 419.1505 $[M+H]^+$.

***N*'-(3-(2-chloro-10*H*-phenothiazin-10-yl)propyl)isonicotinohydrazide 3.72b (DS00364a)**

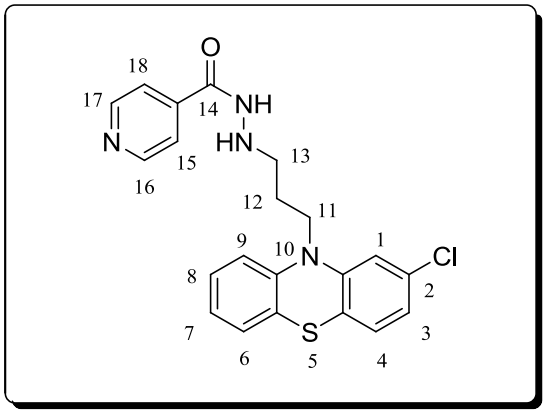

Pale yellow solid (0.034g, 22%); R_f 0.55 (8:2 EtOAc/Hex); Mp 54-56 °C; ^{1}H NMR (400 MHz, $CDCl_3$) δ 8.73 (d, *J* = 6.0 Hz, 2H, H-16 & H-17), 7.71 (d, *J* = 6.0 Hz, 2H, H-15 & H-18), 7.14 (m, 2H, Ar-H), 7.02 (d, *J* = 8.0 Hz, 1H, Ar-H),6.95 (dd, *J* = 7.6, 1.2 Hz, 1H, Ar-H), 6.88 (m, 3H, Ar-H), 4.49 (t, *J* = 6.6 Hz, 2H, 2 x H-11), 4.05 (t, *J* = 6.6 Hz, 2H, 2 x H-13), 2.26 (p, *J* = 6.6 Hz, 2H, 2 x H-12); ^{13}C NMR (101 MHz, $CDCl_3$) δ 164.97, 150.58, 146.28, 144.27, 137.22, 133.32, 128.13, 127.75, 127.49, 125.51, 124.27, 123.25, 122.75, 122.62, 115.87, 115.77, 111.25, 109.76, 63.02, 43.90, 25.95; HRMS (ESI+): *m/z* 411.1046 $[M+H]^+$, calculated for $C_{21}H_{20}ClN_4OS$, found 411.1030 $[M+H]^+$.

***N*'-(3-(10*H*-phenothiazin-10-yl)propyl)isonicotinohydrazide 3.72c (DS00365a)**

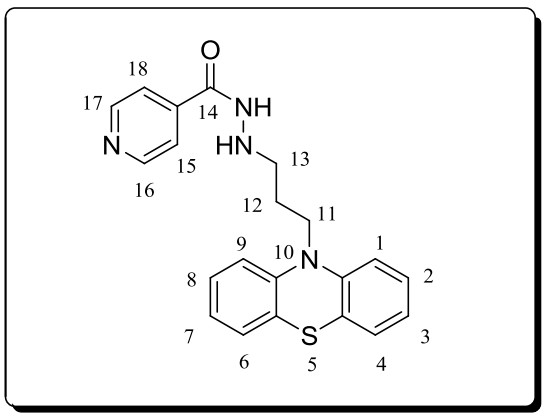

Pale yellow solid (0.024 g, 26%); R_f 0.55 (8:2 EtOAc/Hex); Mp 89-90 °C; ^{1}H NMR (400 MHz, $CDCl_3$) δ 8.71 (d, *J* = 5.9 Hz, 2H, H-17 & H-16), 7.69 (d, *J* = 5.9 Hz, 2H, H-15 & H-18), 7.15 (m, 4H, Ar-H), 6.91 (m, 4H, Ar-H), 4.48 (t, *J* = 6.6 Hz, 2H, 2 x H-15), 4.08 (t, *J* = 6.6 Hz, 2H, 2 x H-17), 2.26 (m, 2H, 2x H-16). ^{13}C NMR (101 MHz, $CDCl_3$) δ 164.99, 150.53, 145.02, 137.34, 127.68, 127.27, 125.86, 122.77, 115.51, 63.25, 43.76, 26.08; HRMS (ESI+): *m/z* 377.1436 $[M+H]^+$, calculated for $C_{22}H_{23}N_4OS_2$, found 377.1428 $[M+H]^+$.

_N'_,_N'_-bis(3-(2-acetyl-10_H_-phenothiazin-10-yl)propyl) isonicotinohydrazide <u>3.73a</u> (DS00362)

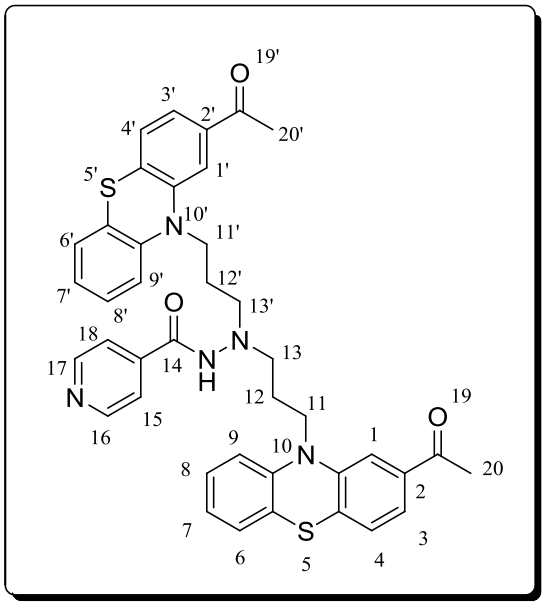

Dark yellow solid (0.022 g, 13%); R_f 0.68 (8:2 EtOAc/Hex); Mp 42-44 °C; ^{1}H NMR (400 MHz, $CDCl_3$) δ 8.64 (d, *J* = 6.1 Hz, 2H, H-16 & H-17), 7.55 (d, *J* = 6.1 Hz, 2H, H-15 & H-18), 7.29 (dd, *J* = 7.9, 1.6 Hz, 2H, Ar-H), 7.23 (d, *J* = 1.7 Hz, 2H, Ar-H), 7.06 (m, 6H, Ar-H), 6.88 (m, 2H, Ar-H), 6.79 (dd, *J* = 8.1, 1.1 Hz, 2H, Ar-H), 3.79 (t, *J* = 6.9 Hz, 4H, 2 x H-11 & 2 x H-11´), 2.43 (s, 6H, 3 x H-20 & 3 x H-20´), 1.91 (m, 4H, 2 x H-13 & 2 x H-13´), 1.26 (m, 4H, 2 x H-12 & 2 x H-12´); ^{13}C NMR (101 MHz, $CDCl_3$) δ 176.88, 165.60, 150.15, 145.12, 143.77, 141.13, 135.77, 131.60, 130.01, 129.77, 127.74, 127.32, 126.59, 123.37, 122.78, 122.61, 121.21, 115.52, 113.34, 52.21, 44.13, 26.34, 23.35; HRMS (ESI+): *m/z* 700.2416 $[M+H]^+$, calculated for $C_{40}H_{38}N_5O_3S_2$, found 700.2459 $[M+H]^+$.

_N'_,_N'_-bis(3-(2-chloro-10_H_-phenothiazin-10-yl)propyl)isonicotinohydrazide <u>3.73b</u> (DS00364)

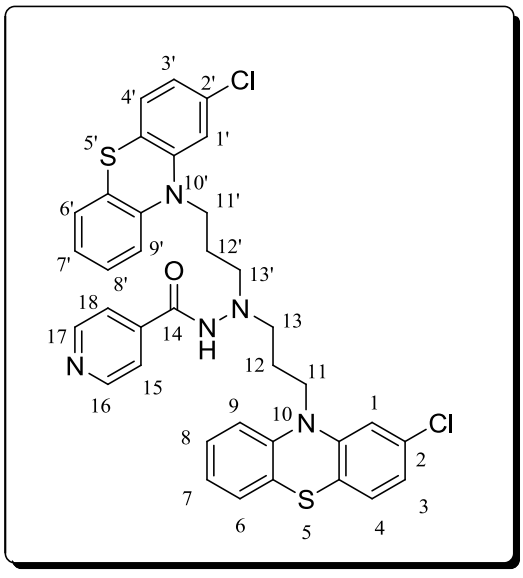

Pale yellow solid (0.028g, 15%); R_f 0.68 (8:2 EtOAc/Hex); Mp 43-45 °C; ^{1}H NMR (400 MHz, $CDCl_3$) δ 8.64 (d, *J* = 5.9 Hz, 2H, H-16 & H-17), 7.32 (d, *J* = 5.9 Hz, 2H, H-15 & H-18), 7.12 (m, 2H, Ar-H), 7.06 (dd, *J* = 7.5, 1.3 Hz, 2H, Ar-H), 6.97 (m, 2H, Ar-H), 6.88 (d, *J* = 7.5 Hz, 2H, Ar-H), 6.84 (m, 4H, Ar-H), 6.79 (d, *J* = 2.0 Hz, 2H, Ar-H), 3.87 (t, *J* = 6.3 Hz, 4H, 2 x H-11 & 2 x H-11´), 2.94

(m, 4H, 2 x H-13 & 2 x H-13´), 1.83 (m, 4H, 2 x H-12 & 2 x H-12´); ^{13}C NMR (101 MHz, $CDCl_3$) δ 165.04, 150.40, 146.44, 144.59, 140.60, 133.38, 127.94, 127.61, 127.50, 124.78, 123.62, 123.05, 122.70, 122.42, 120.84, 116.27, 116.21, 116.13, 55.43, 44.56, 24.53; HRMS (ESI+): *m/z* 684.1425 $[M+H]^+$, calculated for $C_{22}H_{23}N_4OS_2$, found 684.1469 $[M+H]^+$.

***N'*,*N'*-bis(3-(10*H*-phenothiazin-10-yl)propyl)isonicotinohydrazide 3.73c (DS00365)**

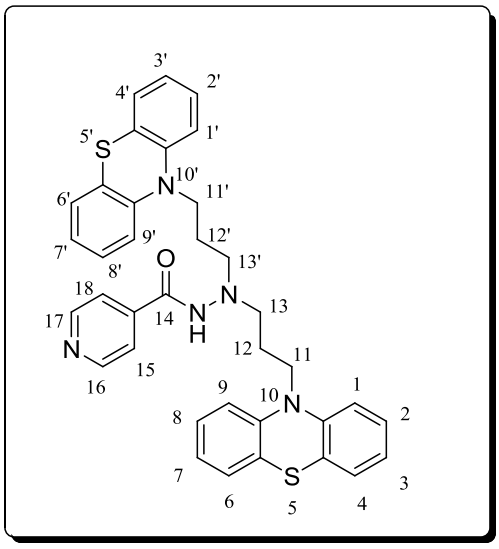

Pale yellow solid (0.016 g, 18%); R_f 0.68 (8:2 EtOAc/Hex); Mp 45-47 °C; ^{1}H NMR (400 MHz, $CDCl_3$) δ 8.61 (dd, *J* = 4.4, 1.6 Hz, 2H, H-16 & H-17), 7.26 (dd, *J* = 4.4, 1.6 Hz, 2H, H-15 & H-18), 7.08 (m, 8H, Ar-H), 6.85 (m, 8H, Ar-H), 3.90 (t, *J* = 6.2 Hz, 4H, 2 x H-11 & 2 x H-11´), 2.92 (m, 4H, 2 x H-13 & 2 x H-13´), 1.84 (m, 4H, 2 x H-12 & 2 x H-12´); ^{13}C NMR (101 MHz, $CDCl_3$) δ 165.07, 150.34, 145.26, 127.45, 127.33, 125.14, 122.55, 120.86, 115.96, 55.62, 44.46, 24.61; HRMS (ESI+): *m/z* 616.2205 $[M+H]^+$, calculated for $C_{22}H_{23}N_4OS_2$, found 616.2290 $[M+H]^+$.

General procedure for preparation of 2-Nitro-benzenesulfonyl-10*H* phenothiazine derivatives [3.74a (DS00325), 3.74b (DS00326) & 3.74c (DS00329)]

To a solution of phenothiazine **3.75** (1 eq) in pyridine (2 mL), was added 2-nitrobenzenesulfonylchloride (1 eq.). The orange-yellow mixture was allowed to stir at 50 °C under an inert atmosphere of nitrogen for 32 h. The reaction mixture formed a brick-red solid precipitate, which was macerated with EtOH. The precipitate was filtered off and washed with diethyl ether (4 x 20 mL) and then recrystallized from MeOH to give desired sulfonamide products **3.74a-c**.

10-(2-Nitro-benzenesulfonyl)-10*H*-phenothiazine 3.74a (DS00325)

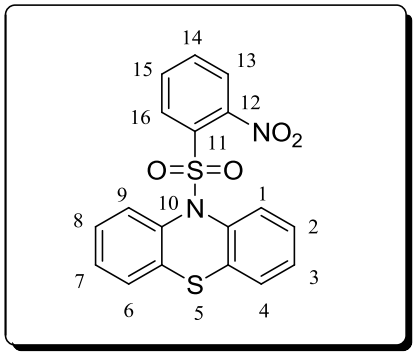

Orange-brown solid (0.94, 49% yield); R_f 0.22 (2:8 MeOH/EtOAc); Mp 233-235 ºC; ^{1}H NMR (400 MHz, DMSO-d_6) δ 9.21 (d, *J* = 5.6 Hz, 1H, H-13), 8.70 (t, *J* = 7.8 Hz, 1H, H-15), 8.23 (m, 1H, H-16), 7.85 (m, 1H, H-14), 7.51 (m, 4H, H-2, H-8, H-1 & H-9), 6.87 (m, 4H, H-4, H-6, H-3 & H-7) ; ^{13}C NMR (101 MHz, DMSO-d_6) δ 146.34, 144.81, 144.62, 140.93, 137.01, 131.10, 130.33, 129.46, 128.60, 128.47, 126.82, 124.41, 123.36, 122.80, 122.77, 118.62, 115.52, 114.84; IR ν_{max} (KBr) cm^{-1} 1531.34 Strong (NO_2), 1471.15 Very Strong (S=O), 1352.92 Medium {-SO_2-N- (S-N)}; HRMS (ESI+): *m/z* 386.0395 [M+2H]$^+$, calculated for $C_{18}H_{14}N_2O_4S_2$, found 386.03849 [M+2H]$^+$.

10-(2-Nitro-benzenesulfonyl)-2-trifluoromethyl-10*H*-phenothiazine 3.74b (DS00326)

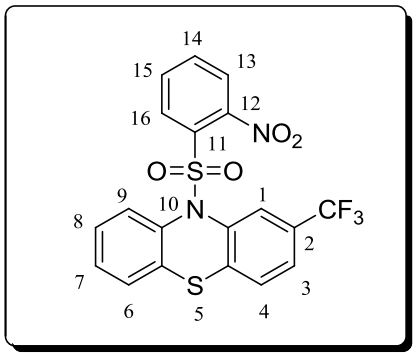

Bright orange solid (0.10 g, 12% yield); R_f 0.20 (2:8 MeOH/EtOAc); Mp 180-182 ºC; ^{1}H NMR (400 MHz, DMSO-d_6) δ 9.22 (d, *J* = 6.8 H, 1H, H-13), 8.71 (t, *J* = 7.8 Hz, 1H, H-15), 8.25 (m, 1H, H-16), 7.86 (m, 1H, H-14), 7.53 (m, 3H, H-8, H-9 & H-6), 7.16 (m, 2H, H-4 & H-3), 6.97 (s, 1H, H-1), 6.85 (dd, *J* = 8.6, 1.1 Hz, 1H, H-7). ^{13}C NMR (101 MHz, DMSO-d_6) δ 146.55, 144.72, 143.68, 141.67, 137.62, 131.10, 130.33, 129.47, 128.49, 127.62, 124.94, 123.11, 122.78, 119.63, 119.59, 117.74, 115.25, 111.18, 111.14; IR ν_{max} (KBr) cm^{-1} 1518.44 Strong (NO_2), 1481.90 Very Strong (S=O), 1350.76 Medium {-SO_2-N- (S-N)}; HRMS (ESI+): *m/z* 454.0269 [M+2H]$^+$, calculated for $C_{19}H_{13}F_3N_2O_4S_2$, found 454.0237 [M+2H]$^+$.

2-Chloro-10-(2-nitro-benzenesulfonyl)-10*H*-phenothiazine 3.74c (DS00329)

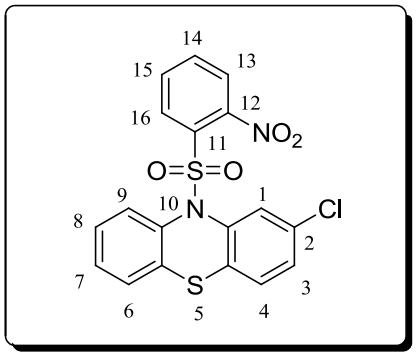

Orange-brown solid (0.39 g, 22% yield); R_f 0.20 (2:8 MeOH/EtOAc); Mp 193-195 ºC; ^{1}H NMR (300 MHz, DMSO-d_6) δ 9.19 (m, 2H, H-13 & H-15), 8.70 (t, *J* = 7.8 Hz, 1H, H-14), 8.23 (m, 2H, H-16 & H-8), 7.51 (m, 3H, H-9, H-6 & H-4), 6.97 (d, *J* = 8.2 Hz, 1H, H-3), 6.86 (m, 1H, H-7), 6.75 (d, *J* = 2.2 Hz, 1H, H-1), ^{13}C NMR (101 MHz, DMSO-d_6) δ 146.50, 144.71, 143.90, 142.46, 137.48, 132.81, 131.11, 130.35, 129.47, 128.49, 128.12, 124.67, 123.01, 122.81, 122.79, 118.43, 115.22, 114.84; IR ν_{max} (KBr) cm^{-1} 1522.74 Strong (NO_2), 1466.85 Very Strong (S=O), 1344.31 Medium {-SO_2-N- (S-N)} HRMS (ESI+): *m/z* 420.0005 $[M+2H]^+$, calculated for $C_{18}H_{13}ClN_2O_4S_2$, found 420.0092 $[M+2H]^+$.

General procedure for preparation of substituted 10-(4-nitrophenylsulfonyl)-10*H*-phenothiazine derivatives [3.76a (DS00342), 3.76b (DS00338) & 3.76c (DS00341)]

To a solution of phenothiazine **3.75** (1.0 eq) in pyridine (2 mL), was added 4-nitrobenzenesulfonylchloride (1.0 eq). The orange yellow mixture was allowed to stir at 50 °C under an inert atmosphere of nitrogen for 26 h. The reaction mixture formed a brick-red solid precipitate, which was macerated with EtOH. The precipitate was filtered off and washed with diethyl ether (4 x 20 mL) and then recrystallized from MeOH to afford desired sulfonamide products **3.76a-c**.

10-(4-nitrophenylsulfonyl)-10*H*-phenothiazine <u>3.76a</u> (DS00342)

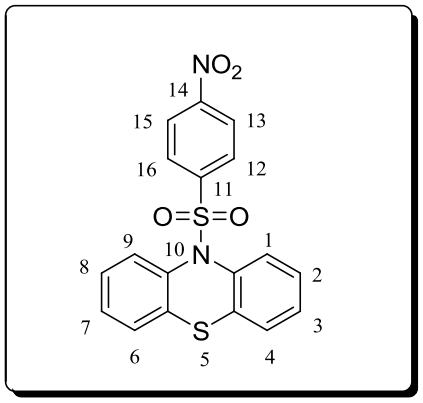

Orange-brown 'diamond-shaped' crystals; (0.10 g, 21% yield); R_f 0.20 (2:8 MeOH/EtOAc); Mp 244-246 ºC; ^{1}H NMR (400 MHz, DMSO-d_6) δ 8.24 (m, 2H, H-13 & H-15), 7.70 (dd, *J* = 8.0, 1.3 Hz, 2H, H-12 & H-16), 7.48 (m, 2H, H-2 & H-8), 7.42 (m, 2H, H-1 7 H-9), 7.37 (m, 4H, H-4, H-6, H-3 & H-7). ^{13}C NMR (101 MHz, DMSO-d_6) δ 151.05, 144.06, 135.01, 132.88, 130.02, 129.30, 129.20, 128.34, 128.04, 124.94; IR ν_{max} (KBr) cm^{-1} 1531.34 Strong (NO_2), 1462.55 Very Strong (S=O), 1357.21 Medium {-SO_2-N-(S-N)}HRMS (ESI+): *m/z* 384.0238 $[M]^+$, calculated for $C_{18}H_{12}N_2O_4S_2$, found 384.0223 $[M]^+$.

10-(4-nitrophenylsulfonyl)-2-(trifluoromethyl)-10*H*-phenothiazine <u>3.76b</u> (DS00338)

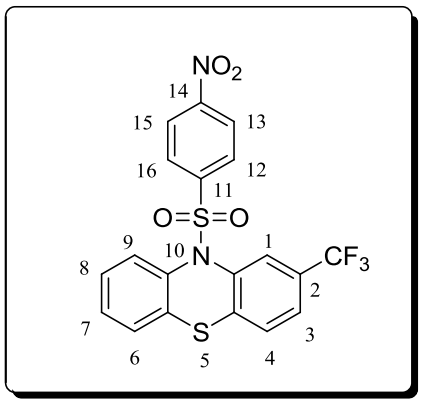

Bright orange solid; (0.16 g, 38%); Mp 158-159 °C ;^{1}H NMR (400 MHz, DMSO- d_6) δ 8.92 (d, *J* = 5.5 Hz, 2H, H-13 & H-15), 8.58 (m, 2H, H-12 & H-16), 8.19 (m, 2H, H-8 & H-9), 8.05 (m, 3H, H-4, H-6 & H-7), 7.84 (m, 2H, H-3 & H-1); ^{13}C NMR (101 MHz, DMSO-d_6) δ 154.82, 147.77, 146.23, 144.72, 143.09, 128.51, 127.62, 127.53, 127.40 (2 x C), 125.03, 124.94, 123.79 (2 X C), 123.09, 115.26; IR ν_{max} (KBr) cm^{-1} 1518.44 Strong (NO_2), 1481.90 Very Strong (S=O), 1350.76 Medium {-SO_2-N- (S-N)}; HRMS (ESI+): *m/z* 454.0269 $[M+2H]^+$, calculated for $C_{19}H_{13}F_3N_2O_4S_4$, found 454.0243 $[M+2H]^+$.

1-(10-(4-nitrophenylsulfonyl)-10*H*-phenothiazin-2-yl)ethanone <u>3.76c</u> (DS00341)

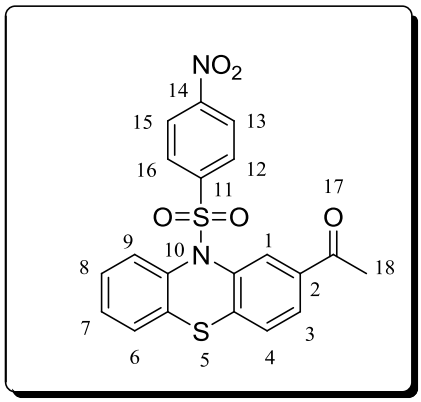

Dark brown solid; (0.20 g, 46%); R_f 0.20 (2:8 MeOH/EtOAc); Mp 233-235 °C; ^{1}H NMR (400 MHz, DMSO-d_6) δ 8.21 (m, 1H, H-13), 8.16 (d, *J* = 1.8 Hz, 1H, H-15), 7.93 (dd, *J* = 8.2, 1.9 Hz, 1H, H-12), 7.71 (dd, *J* = 8.0, 1.0 Hz, 1H, H-16), 7.50 (m, 2H, Ar-H), 7.40 (m, 5H, Ar-H), 2.62 (s, 3H, 3 x H-18); ^{13}C NMR (101 MHz, DMSO-d_6) δ 196.80 (C-17), 150.43, 143.92, 138.81, 136.84, 135.11, 134.63, 131.73, 130.03, 129.40, 129.18, 128.68, 128.64, 128.18, 128.05, 127.40, 124.93, 27.11 (C-18); IR ν_{max} (KBr) cm^{-1} 1632.38 Strong (C=O), 1522.74 Strong (NO_2), 1466.85 Very Strong (S=O), 1344.31 Medium {-SO_2-N- (S-N)}; HRMS (ESI+): *m/z* 427.0422 $[M+H]^+$, calculated for $C_{20}H_{15}N_2O_5S_2$, found 427.0413 $[M+H]^+$.

General procedure for preparation of 3-(10*H*-phenothiazin-10-yl) propanenitrile derivatives [3.82a (DS00394), 3.82b (DS00392) & 3.82c (DS00393)]

A suspension of phenothiazine **3.81a-c** (1 eq) in acrylonitrile (5 mL) was cooled at 0 °C. To this was added Triton B (10 mol%) and the mixture was allowed to stir at 0 °C. Once the reaction subsided, dioxane (1.0 mL- 2.5 mL) was added and the reaction mixture was heated to reflux for 1 h. The mixture was poured into water, the precipitate was filtered and washed several times with diethyl ether (5 x 50 mL). The filtrate was collected and the solvent was removed under reduced pressure to obtain the desired product **3.82a-c**.

3-(10*H*-phenothiazin-10-yl)propanenitrile <u>3.82a</u> (DS00394)

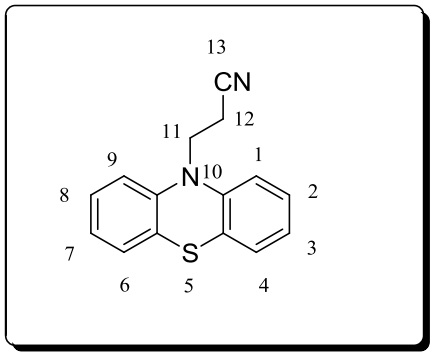

White flakes (1.70 g, 67 %); R_f 0.33 (2:8 EtOAc/Hex); Mp 146-148 °C (lit. 143-144 °C)[11]; ^{1}H NMR (300 MHz, DMSO-d_6) δ 7.23 (m, 4H, H-2, H-8,H-1, H-9), 7.09 (m, 2H, H-4 & H-6), 7.01 (t, *J* = 7.6 Hz, 2H, H-3 & H-7), 4.23 (t, *J* = 6.6 Hz, 2H, 2 x H-11), 2.93 (t, *J* = 6.6 Hz, 2H, 2 X H-12); ^{13}C NMR (101 MHz, DMSO-d_6) δ 144.42, 128.22, 127.83, 124.84, 123.55, 119.28, 116.43, 42.79, 16.46; MS (ESI+): *m/z* 252.1 $[M]^+$, calculated for $C_{15}H_{12}N_2S$, found 252.0 $[M]^+$.

3-(2-chloro-10*H*-phenothiazin-10-yl)propanenitrile <u>3.82c</u> (DS00393)[12]

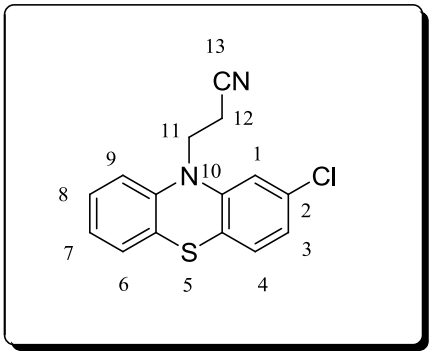

Faint-pink solid (0.37 g, 60 %); R_f 0.33 (2:8 EtOAc/Hex); Mp 165-167 °C; ^{1}H NMR (300 MHz, DMSO-d_6) δ 7.23 (m, 4H, Ar-H), 7.06 (m, 3H, Ar-H), 4.25 (t, *J* = 6.5 Hz, 2H, 2 x H-11), 2.92 (t, *J* = 6.5 Hz, 2H, 2 X H-12); ^{13}C NMR (101 MHz, DMSO-d_6) δ 145.62, 143.15, 132.73, 128.36, 128.01, 127.51, 124.19, 123.61, 123.45, 122.83, 118.75, 116.45, 116.13, 42.51, 16.10; MS (ESI+): *m/z* 286.0 $[M]^+$, calculated for $C_{15}H_{11}ClN_2S$, found 286.1 $[M]^+$.

3-(2-(trifluoromethyl)-10H-phenothiazin-10-yl)propanenitrile <u>3.82b</u> (DS00392)[12]

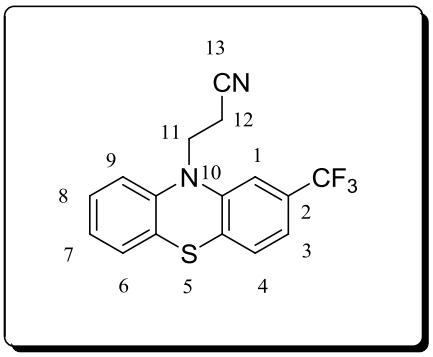

Faint-yellow solid (0.16 g, 54 %); R_f 0.33 (2:8 EtOAc/Hex); Mp 140-142 °C; ^{1}H NMR (300 MHz, DMSO-d_6) δ 7.30 (m, 5H, Ar-H), 7.08 (m, 2H, Ar-H), 4.32 (t, *J* = 6.5 Hz, 2H, 2 x H-11), 2.92 (t, *J* = 6.5 Hz, 2H, 2 x H-12); ^{13}C NMR (101 MHz, DMSO-d_6) δ 144.91,

143.00, 130.12, 128.22, 128.03, 127.60, 123.83, 123.57, 119.71, 119.68, 118.71, 116.61, 112.45, 112.42, 42.58, 16.10; MS (ESI+): *m/z* 320.0 $[M]^+$, calculated for $C_{16}H_{11}N_2S$, found 320.1 $[M]^+$.

Preparation of 3-(3,7-dibromo-10*H*-phenothiazin-10-yl)propanenitrile 3.82d (DS00396)

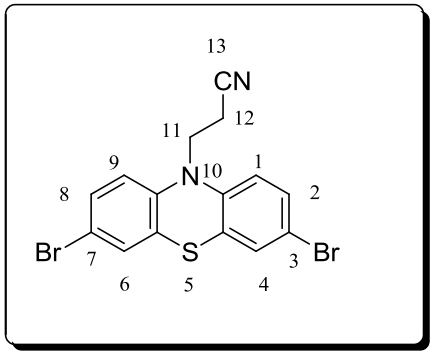

To a solution of alkylated phenothiazine **3.82a** (0.50 g, 1.98 mmol) in dry THF (5 mL), NBS (0.85 g, 4.75 mmol) in dry THF (5 mL) was added dropwise over a period of 1 h at 0 °C. The mixture was stirred at room temperature for 12h. Water was added to the mixture and the product was extracted with DCM (2 x 40 mL). The organic extracts were combined and the solvent was removed under reduced pressure. The resulting solid was recrystallized from a mixture of EtOAc/hexane (1:1) to afford product **3.82d** as a light green solid. (0.53 g, 65 %); R_f 0.36 (3:7 EtOAc/Hex); Mp 108-110 °C; ^{1}H NMR (300 MHz, DMSO-d_6) δ 7.41 (m, 4H, H-2, H-8, H-1 & H-9), 7.04 (d, *J* = 8.5 Hz, 2H, H-4 & H-6), 4.19 (t, *J* = 6.6 Hz, 2H, 2 x H-11), 2.91 (t, *J* = 6.6 Hz, 2H, 2 x H-12); ^{13}C NMR (101 MHz, DMSO-d_6) δ 143.50, 130.96, 129.78, 126.74, 119.03, 118.35, 115.24, 43.05, 16.32. HRMS (ESI+): *m/z* 409.8911 $[M]^+$, calculated for $C_{15}H_{10}Br_2N_2S$, found 409.8909 $[M]^+$.

Preparation of 10-(2-(1*H*-tetrazol-5-yl)ethyl)-10*H*-phenothiazine hydrochloride 3.84 (DS00395)[13]

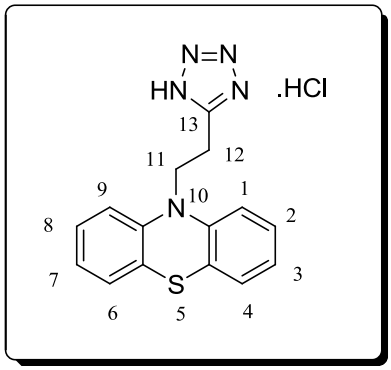

A mixture of alkylated phenothiazine **3.82a** (0.50 g, 1.98 mmol), sodium azide (0.39 g, 5.94 mmol), NH_4Cl (0.32 g, 5.94 mmol) in DMF was heated at 125 °C and allowed to stir for 16 h. Toluene was added to the mixture and the solvents were removed by azeotropic distillation under reduced

pressure. Water was then added to the crude mixture followed by acidification with HCl to pH ~2. The resulting solid was washed with hexane and recrystallized from MeOH to afford the desired product **3.84** as a dark grey solid. (0.29 g, 45 %); R_f 0.28 (0.5:9.5 MeOH/EtOAc); Mp 175-177 °C; ^{1}H NMR (300 MHz, DMSO-d_6) δ 7.22 (m, 4H, H-2, H-8, H-1 & H-9), 7.04 (m, 4H, H-3, H-7 , H-4 & H-6), 4.35 (t, *J* = 6.6 Hz, 2H, 2 x H-11), 3.32 (t, *J* = 6.6 Hz, 2H, 2 x H-12); ^{13}C NMR (101 MHz, DMSO-d_6) δ 153.37, 144.29, 127.80, 127.30, 123.93, 122.90, 115.91, 44.50, 21.45; MS (ESI+): *m/z* 297.1 $[M+2H]^+$, calculated for $C_{15}H_{15}N_5S$, found 297.1 $[M+2H]^+$.

Preparation of *N*-*tert*-butyl-3-(10*H*-phenothiazin-10-yl)propanamide 3.83 (DS00385)

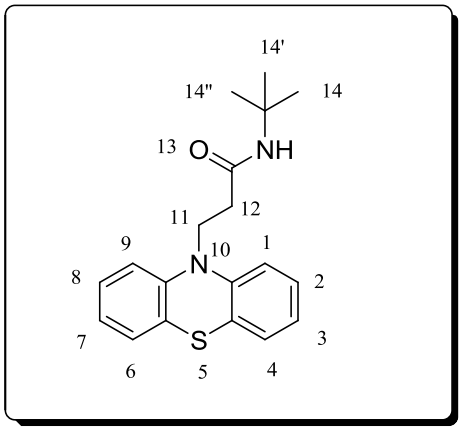

To a solution of nitrile **3.82a** (0.20 g, 0.79 mmol) in *tert*-butyl acetate (1 mL), conc. H_2SO_4 (40 µL) was slowly added at room temperature. The resulting mixture was allowed to stir at 42 °C for 12 h , thereafter poured into ice cold $NaHCO_3$(aq) to neutralize the acid. The product was filtered and purified on a preparative TLC plate (2:8 EtOAc/Hex) to afford propanamide **3.83** as a white solid. (0.051 g, 20 %); R_f 0.33 (2:8 EtOAc/Hex); Mp 109-111 °C; ^{1}H NMR (400 MHz, DMSO-d_6) δ 7.46 (s, 1H, NH), 7.18 (m, 2H, H-2 & H-8), 7.11 (dd, *J* = 7.6, 1.5 Hz, 2H, H-1 & H-9), 7.02 (dd, *J* = 7.3, 1.9 Hz, 2H, H-4 & H-6), 6.92 (t, *J* = 7.5 Hz, 2H, H-3 & H-7), 4.05 (m, 2H, 2 x H-11), 2.48 (m, 2H, 2 x H-12), 1.23 (s, 9H, 2 x H-14, 2 x H-14´, 2 x H-14´´). ^{13}C NMR (101 MHz, DMSO-d_6) δ 169.66 (C-13), 144.48, 127.71, 127.08, 123.07, 122.59, 115.54, 50.13, 43.32, 34.17, 28.61. MS (ESI+): *m/z* 327.1 $[M+H]^+$, calculated for $C_{19}H_{23}N_2OS$, found 327.1 $[M+H]^+$

Preparation of diethyl 3-(10*H*-phenothiazin-10-yl)propylphosphonate 3.87 (DS00390)[14]

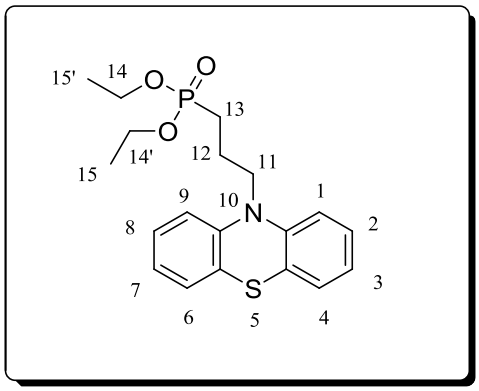

To a solution of 10-(3-chloropropyl)-10H phenothiazine **3.86** (0.10 g, 0.36 mmol) in dry toluene, was added triethyl phosphite (0.31 mL, 1.80 mmol). This was followed by the addition of zinc chloride (1M in DCM) (0.065 mL, 0.40 mmol) and the mixture was stirred at 75 °C under nitrogen for 18 h. The reaction mixture allowed to cool to room temperature and then filtered through a pad of celite. Toluene was removed under reduced pressure and the resulting crude material was triturated with hexane to give the desired product **3.87** as a colourless oil. (0.014 g, 10 %); R_f 0.29 (5:5 EtOAc/Hex); ^{1}H NMR (300 MHz, DMSO) δ 7.20 (m, 4H, H-2, H-8, H-1 & H-9), 7.05 (d, *J* = 7.6 Hz, 2H, H-4 & H-6), 6.96 (dd, *J* = 7.6, 1.1 Hz, 2H, H-3 & H-7), 3.96 (m, 2H, 2 x H-11), 3.89 (m, 4H, 2 x H-14 & 2 x H-14´), 1.84 (m, 4H, 2 x H-13 & 2 x H-12), 1.14 (t, *J* = 7.0 Hz, 6H, 3 x H-15 & 3 x H-15´).; ^{31}P NMR (162 MHz, DMSO-d_6) δ 31.48; ^{13}C NMR (101 MHz, DMSO-d_6) δ 145.11, 128.07, 127.67, 124.50, 123.11, 116.49, 61.31, 46.65, 22.58, 21.19, 16.69. MS (ESI+): *m/z* 378.1 $[M+H]^+$, calculated for $C_{19}H_{25}NO_3PS$, found 378.1 $[M+H]^+$

Preparation of (*E*)-3-(dimethylamino)-1-(10*H*-phenothiazin-2-yl)prop-2-en-1-one 3.78[15]

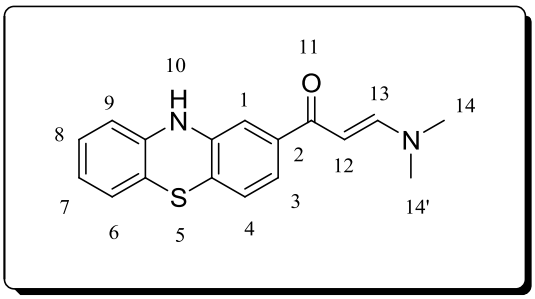

To a solution of 2-acetyl phenothiazine **3.77** (1.20 g, 4.97 mmol) in anhydrous toluene (15 mL), dimethylformamide-dimethylacetal (DMF-DMA) (1.3 mL, 10 mmol) was added. The mixture was allowed to reflux for 20 h under an inert atmosphere of nitrogen, after which the solvent and excess DMF-DMA were removed under

reduced pressure. The resulting solid was washed with diethyl ether and then recrystallized from a mixture of MeOH/EtOAc (1:9) to afford enaminone **3.78** as a bright yellow solid. (0.70 g, 47 %); R_f 0.20 (7:3 EtOAc/Hex); Mp. 243-245 °C; ^{1}H NMR (300 MHz, DMSO-d_6) δ 8.65 (s, 1H, NH-10), 7.69 (d, *J* = 12.3 Hz, 1H, H-13), 7.29 (dd, *J* = 8.0, 1.7 Hz, 1H, H-4), 7.22 (d, *J* = 1.7 Hz, 1H, H-1), 6.99 (m, 1H, H-8), 6.92 (m, 2H, H-9 & H-3) 6.74 (m, 1H, H-7), 6.67 (dd, *J* = 7.9, 1.1 Hz, 1H, H-6), 5.69 (d, *J* = 12.3 Hz, 1H, H-12), 3.14 (s, 3H, 3 X H-14), 2.90 (s, 3H, 3 X H-14´); ^{13}C NMR (101 MHz, DMSO-d_6) δ 185.18 (C-11), 154.64, 142.28, 142.19, 140.14, 128.23, 126.71, 126.15, 122.33, 121.37, 120.42, 115.98, 114.98, 113.26, 91.09 , 44.98 (C-14), 37.81 (C14´).

Preparation of 2-(1*H*-pyrazol-3-yl)-10*H*-phenothiazine 3.79 (DS00398)[15]

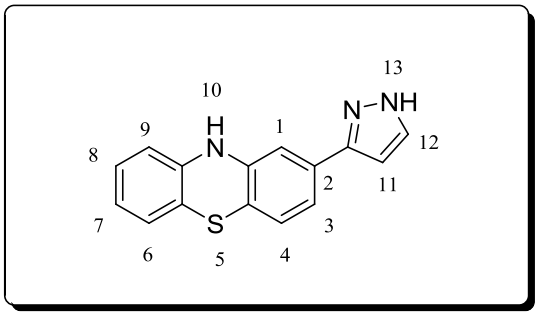

To a solution of enaminone **3.78** (0.20 g, 0.68 mmol) in EtOH (6 mL), was added excess hydrazine hydrate (2 mL). The mixture was allowed to stir at room temperature for 14 h. The precipitate was filtered off, washed with cold EtOH and then dried to afford pyrazole **3.79** as a light yellow solid. (0.15 g, 83%); R_f 0.43 (7:3 EtOAc/Hex); Mp 209-211 °C; ^{1}H NMR (300 MHz, DMSO-d_6) δ 12.88 (s, 1H, NH-13), 8.65 (s, 1H, NH-10), 7.71 (s, 1H, H-1), 7.18 (m, 2H, H-4 & H-12), 7.00 (m, 1H, H-8), 6.93 (m, 2H, H-9 & H-6), 6.74 (m, 2H, H-7 & H-3), 6.56 (d, *J* = 2.2 Hz, 1H, H-11); ^{13}C NMR (101 MHz, DMSO-d_6) δ 142.77, 142.39, 128.04 (2C), 126.86, 126.71, 122.24, 119.35 (2C), 116.80, 115.94 (2C), 115.00, 111.45, 102.11. MS (ESI+): *m/z* 266.1 $[M+H]^+$, calculated for $C_{15}H_{12}N_3S$, found 266.1 $[M+H]^+$

Preparation of 5-(10*H*-phenothiazin-2-yl)isoxazole 3.80 (DS00397)[15]

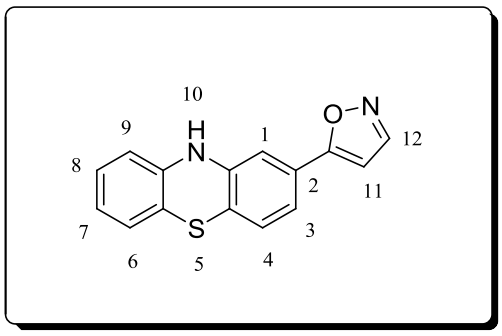

To a solution of enaminone **3.78** (0.20 g, 0.68 mmol) in EtOH (6 mL), was added excess hydroxylamine hydrochloride (3 eq). The yellow solution turned bright orange upon addition of hydroxylamine and the resulting mixture was allowed to stir at room temperature for 14 h. The precipitate was filtered off, washed with cold EtOH and then dried to afford isoxazole **3.80** as a brown solid. (0.15 g, 85%); R_f 0.58 (7:3 EtOAc/Hex); Mp 178-180 °C; ^{1}H NMR (300 MHz, DMSO-d_6) δ 8.80 (s, 1H, NH-10), 8.62 (d, *J* = 1.9 Hz, 1H, H-12), 7.25 (dd, *J* = 8.0 Hz, 1H, H-9), 7.12 (d, *J* = 1.9 Hz, 1H, H-11), 7.06 (d, *J* = 7.6 Hz, H-4), 7.00 (dd, *J* = 8.0 Hz, 1.4 Hz, 1H, H-8), 6.93 (dd, *J* = 7.6 Hz, 1H, H-3), 6.87 (d, *J* = 1.4 Hz, 1H, H-1), 6.78 (dd, *J* = 8.0 Hz, H-6), 6.70 (dd, *J* = 8.0 Hz, 1.4 Hz, 1H, H-7); ^{13}C NMR (101 MHz, DMSO-d_6) δ 168.28, 152.14, 143.07, 141.74, 128.35, 127.37, 126.78, 126.41, 122.68, 119.97, 119.75, 116.17, 115.13, 110.97, 100.05; MS (ESI+): *m/z* 269.1 $[M+3H]^+$, calculated for $C_{15}H_{13}N_2OS$, found 269.1 $[M+3H]^+$.

7.4 Biological assays

The biological assays were conducted by collaborators or service providers as indicated below. Ethical clearance was obtained for the *in vivo* toxicity study.

7.4.1 Green Fluorescent Protein Microplate Assay (GAST/Fe)

The MIC_{90}s and MIC_{99}s determinations were performed at UCT IIDMM. Details of the assay have been reported by van der Westhuyzen *et al*.[16] In brief, the MICs were determined in a GAST/Fe (glycerol-alanine-salts) medium using the standard broth microdilution method[17,18] Test compounds were dissolved in DMSO to make up stock solutions to a final concentration of 128 mM. A two-fold serial dilution of the test compounds was performed across a 96-well microtitre plate from Row 2-11 in GAST/Fe medium with a final DMSO concentration of 5% v/v. The minimum growth control was rifampicin (Row 12) and the maximum growth control was 5% DMSO in GAST/Fe (Row 1). A M.*tb*H37Rv.gfp stock culture was grown to an OD_{600}-0.6, diluted 1:100 and 50 µL was added to each well. The plates were incubated at 37 °C followed by measurement of fluorescence (excitation 485 nM; emission 520 nM) using a plate reader. (FLUOstar, OPTIMA, BMG LABTECH) at day 14. The concentration range tested was 0.244-125 µM. The lowest concentration of drug that inhibits growth of more than 90% and 99% of the bacterial population was considered to be the MIC_{90} and MIC_{99}, respectively.

7.4.2 Green Fluorescent Protein Microplate Assay (Middlebrook 7H9)

The determination of MICs of selected compounds (**DS0031**, **DS0032**, **DS0034** & **DS0035**) was performed at UCT IIDMM. Details of the assay have been reported by Salie, S.; Hsu, N.; Semenya, D.; Jardine, A.; Jacobs, M. Novel Non-Neuroleptic Phenothiazines Inhibit Mycobacterium Tuberculosis Replication. *J. Antimicrob. Chemother.* **2014**, *69* (6), 1551–1558.[19] In brief, direct antibacterial activity screening was performed in black 96-well plates

in a Middlebrook 7H9 medium. Frozen M.*tb*H37Rv.gfp was thawed, spun down and the pellet was resuspended in Middlebrook 7H9 broth with 25 mg/L kanamycin. 100 µL of H37Rv.gfp was added to each experimental well at a concentration of 1×10^6 cfu/mL. Sterile water was added to outer to with sterile water to minimize evaporation. Test compounds and controls were first dissolved in water followed by 2-fold dilutions using 7H9 broth supplemented with 25 mg/L kanamycin. Relative fluorescence readings were measured at various timepoints.

7.4.3 Evaluation against M*tb*.H37Rv infected macrophages (*ex vivo* activity)

Selected compounds (**DS0031**, **DS0032**, **DS0034** & **DS0035**) were screened for intracellular inhibition of M.*tb*H37Rv in bone-marrow derived macrophages (BMDMs) (UCT IIDMM). Details of the assay have been reported by Salie, S.; Hsu, N.; Semenya, D.; Jardine, A.; Jacobs, M. Novel Non-Neuroleptic Phenothiazines Inhibit Mycobacterium Tuberculosis Replication. *J. Antimicrob. Chemother.* **2014**, *69* (6), 1551–1558.[19] Briefly, BMDMs were cultured from the femurs of 6–8-week-old C57Bl/6 mice. The cultures were maintained in RPMI medium supplemented with 20% fetal calf serum (FCS), 30% L929-conditioned medium, 10mM L-glutamine, 100 µg/mL streptomycin and 100 U/mL penicillin for 8–10 days at 37 °C with 5% CO_2. Confluent cells were seeded at a concentration of 1×10^5 cells per well in a 96-well plate. Macrophages were infected with *M. tuberculosis* (H37Rv) at a multiplicity of infection of 5:1 *(M. tuberculosis*:cells) for 4 h. Infected cells were washed with BMDM medium (2 mM L-glutamine, 2% FCS, 10% L929 medium, RPMI) to remove extracellular bacteria, then the initial number of intracellular bacilli was determined by lysing the macrophages and plating the supernatant on Middlebrook 7H10 agar for cfu enumeration. Two sets of cultures were prepared to evaluate intracellular drug activity and cell viability

simultaneously. The infected macrophages were incubated with medium containing isoniazid (1 mg/L), thioridazine (3 mg/L), and test compounds (25 mg/L) in triplicate. After 5 days of treatment, macrophages were either lysed for cfu determination (% inhibition), or incubated with Cell-titer Blue reagent for 4 h then read on a fluorimeter for cell viability. Percentage inhibition was calculated relative to untreated macrophages and percentage viability was calculated relative to uninfected macrophages.

7.5 Dopamine and serotonin receptor radioligand binding assays

Selected compounds were sent to Perkin Elmer (formerly Caliper Life Sciences) (Maryland, USA) to be evaluated in radioligand binding assays in which binding to the dopaminergic receptor subtypes D_1, D_2 and D_3 and the serotonergic receptor subtypes 5-HT_{1A}, 5-HT_{2A} and 5-HT_{2C} was measured. Details of the assays have been reported by Salie, S.; Hsu, N.; Semenya, D.; Jardine, A.; Jacobs, M. Novel Non-Neuroleptic Phenothiazines Inhibit Mycobacterium Tuberculosis Replication. *J. Antimicrob. Chemother.* **2014**, *69* (6), 1551–1558.[19] The radioligand binding assay conditions were in accordance with industry standards as reported by Perkin Elmer (formerly Caliper Life Sciences) (www.perkinelmer.com). Well-established 3_H-labelled reference ligands were utilized as reported in chapter 4 (Figure 4.9). The dopaminergic and serotonergic receptors subtypes were prepared as shown below:

- D_1 receptor (HEK-293 cells expressing human recombinant D_1 subtype receptor)
- D_2 receptor (CHO cells expressing human recombinant D_2 subtype receptor)
- D_3 receptor (SF9 cells expressing rat recombinant D_3 subtype receptor)
- 5-HT_{1A} receptor (bovine hippocampal membrane)
- 5-HT_{2A} receptor (rat cortical membrane)
- 5-HT_{2C} receptor (pig choroid plexus membrane)

The reaction conditions for the radioligand binding of the dopaminergic and serotonergic receptors subtypes are outlined below:

- D_1 receptor (50mM Tris–HCl (pH 7.4), 5mM KCl & 5mM $MgCl_2$ at 25 °C; 1mM EDTA and 1.5 mM $CaCl_2$ also added)
- D_2 receptor (50mM Tris–HCl (pH 7.4), 5mM KCl & 5mM $MgCl_2$ at 25 °C; 1mM EDTA and 120mM NaCl also added)
- D_3 receptor (50mM Tris–HCl (pH 7.4), 5mM KCl & 5mM $MgCl_2$ at 25 °C; 5mM EDTA, 120mM NaCl and 1.5mM $CaCl_2$ also added)
- 5-HT_{1A} receptor (50mM Tris–HCl (pH 7.4) at 25 °C)
- 5-HT_{2A} receptor (50mM Tris–HCl (pH 7.6) at 37 °C)
- 5-HT_{2C} receptor (50mM Tris–HCl (pH 7.7) , 4mM $CaCl_2$ and 0.1% ascorbic acid at 37 °C)

The reactions were terminated by rapid vacuum filtration onto glass fibre filters. Radioactivity trapped onto the filters was measured and compared with control values to evaluate interactions of the modified phenothiazines with the respective receptors. Assays were performed in duplicate. The average bound radioactivity of the reference compound in the presence of the modified phenothiazines was then expressed as a percentage. Interpretation of results was as follows: -20% to + 20% (inactive) standard baseline; 20% to 49% (marginal activity); > 50% (active).

7.6 *In vitro* ADMET assays

7.6.1 Kinetic Solubility

The kinetic solubility assay was carried out using a miniaturised shake flask method (UCT Division of Clinical Pharmacology). Details of the method have been reported by van der Westhuyzen *et al*.[16] Briefly, calibration standards (10-220 µM in DMSO) were prepared from 10 mM stock solutions of the test compounds (**DS0031**, **DS0032**, **DS0034** and **DS0034**). Test compound stock solution were also used to spike (1:50) duplicate aqueous samples of FaSSIF

(bio-relevant buffer that simulates the small intestine juices in fasted state, pH 6.5), with a final DMSO concentration of 2%. The solutions were shaken for 2 hours at 25 °C, filtered and analysed using HPLC-DAD (Agilent 1200 Rapid Resolution HPLC with a diode array detector).

7.6.2 Microsomal metabolic stability

The metabolic stability of selected (**DS0031**, **DS0032**, **DS0034** and **DS0034**) compounds was performed using a single time point microsomal stability assay (UCT Division of Clinical Pharmacology).[16,20] In brief, the test compounds were incubated individually in mouse liver microsomes (0.4 mg/mL) at 37 °C for 30 min (single time point), in the presence and absence of the cofactor NADPH (1mM). Reactions were quenched by adding 300 µL of ice cold acetonitrile containing internal standard (carbamazepine, 0.0236 µg/mL). Test compounds in the supernatant were analysed by means of LC-MS/MS (Agilent Rapid Resolution HPLC AB SCIEX 4000 QTRAP MS) for the disappearance of parent compound.

7.7 *In vivo* toxicity

The toxicity potential of test compounds (**DS0034** and **DS0035**) was evaluated at a dose of 100mg/kg as the maximum starting dose and outcomes were measured against the known in clinically approved phenothiazine drug, thioridazine, or against no treatment (UCT IIDMM). Briefly, initial studies were conducted to evaluate the maximal tolerated dose of thioridazine in mice. 6-8-week-old adult female C57Bl/6 mice (n=10/group) were challenged with 100mg/kg, 40mg/kg, 20mg/kg and 10mg/kg by oral gavage, the animals were monitored for survival and changes in body weight were measured. To evaluate toxicity of single dose (100mg/kg) administration, test compounds were administered by oral gavage in a volume in

200 µL. The animals were monitored for survival and changes in body weight were measured over 14 days. To evaluate toxicity in animals which received therapy on a daily basis, mice (n=10-15/group) were challenged with either thioridazine (10mg/kg or 20mg/kg) or test compounds (100mg/kg) administered in 200 µL water by oral gavage on a daily basis. Changes in body weights were measured and recorded on a daily basis. The experiment was terminated after 14 days when all animals were humanely sacrificed and organs (heart, lung, brain, kidney, liver and spleen) removed and weighed.

7.8 Evaluation against U-251 glioblastoma cell line using an MTT assay

The anticancer effects were determined using an 3-(4,5-dimethylthiazol-2-yl)-2,5 diphenyltetrazolium bromide (MTT) assay as previously described by Mosmann T with slight modifications (University of the Western Cape, Department of Medical Bioscience).[21] The human malignant glioma cell line U-251 (glioblastoma multiforme, World Health Organization grade IV) was generously donated by the Prince Laboratory, Faculty of Health Sciences, UCT. Cells were cultured in monolayer using Dulbeco Modified Eagles Medium (DMEM, Lonza Group Ltd., Verviers, Belgium) with phenol red supplemented with 10% foetal bovine serum (FBS, Gibco, Life Technologies Corporation, Paisley, UK) and 1% 100 U/mL penicillin and 100 µg/mL (Lonza Group Ltd. Verviers, Belgium). All cells were grown at 37°C in a humidified atmosphere consisting of 5% CO2 and 95% air. Media was replaced every two to three days and cells were sub-cultured by splitting with trypsin (Lonza Group Ltd., Verviers, Belgium). Briefly, U251 cells were plated in 96-well cell culture plates at a cell density of 5000 cells per well and incubated overnight for 24 hours. The medium was thereafter replaced with fresh medium containing increasing concentrations of the various phenothiazine derivatives and a vehicle control of untreated cells was included to compare

with the treated cells. All treatment including the vehicle control lasted for 48 hours and was done in triplicate. After the 48 hours incubation, 10 µl of the MTT (Sigma-Aldrich Co Germany) solution (5 mg/ml) was added to each well and the cells were incubated for an additional 4 hours at 37°C. The medium was removed and 100 µL of dimethyl sulfoxide (DMSO) was added to each well to solubilize the MTT formazan. The cell culture plates were then placed on a shaker for 10 minutes and the absorbance was read at 570 nm using a BMG Labtech Omega® POLARStar multimodal plate reader. The percentage cell viability was calculated using the formula below:

$$\%\ \text{Cell Viability} = \frac{\text{Absorbance of treated well}}{\text{Absorbance of Untreated well}}\ \text{X}\ 100$$

The half maximal inhibitory concentration (IC_{50}) was determined *via* a survival curve using GraphPad Prism5 software (GraphPad software, San Diego, CA, USA).

References

(1) Yusof, I.; Shah, F.; Hashimoto, T.; Segall, M. D.; Greene, N. Finding the Rules for Successful Drug Optimisation. *Drug Discov. Today* **2014**, *19* (5), 680–687.

(2) Ntie-Kang, F. An in Silico Evaluation of the ADMET Profile of the StreptomeDB Database. *Springerplus* **2013**, *2* (353), 1–11.

(3) Fujii, T.; Hao, W.; Yoshimura, T. New Method for the Preparation of dibenzo[b,f][1,4]thiazepines. *Heteroat. Chem.* **2004**, *15* (3), 246–250.

(4) Jilek, J. O.; Pelz, K.; Pavlickova, D.; Protiva, M. Neurotropic and Psychotropic Substances IV: About Some New Derivatives of dibenzo[b,f][1,4]thiazepines. *Czechoslov. Chem. Commun.* **1965**, *30* (5), 1676–1683.

(5) Feng, L.-S.; Liu, M.-L.; Zhang, S.; Chai, Y.; Wang, B.; Zhang, Y.-B.; Lv, K.; Guan, Y.; Guo, H.-Y.; Xiao, C.-L. Synthesis and in Vitro Antimycobacterial Activity of 8-OCH3 Ciprofloxacin Methylene and Ethylene Isatin Derivatives. *J. Med. Chem.* **2011**, *46* (1), 341–348.

(6) Munegumi, T.; Kimura, E.; Sodeyama, A.; Sakurai, A. Synthesis of Aminobenzonitrile by Dehydration of Aminobenzamide Using Phenylphosphonic Dichloride in Pyridine. *Asian J. Chem.* **2008**, *20* (4), 3079–3082.

(7) Aicher T; Chen Z; Faul M; Krushinski J; Le Huerou Y; Pineiro-nunez M; Rocco V; Ruley K; Schaus J; Thompson D; TuperD. Piperazine Substituted Aryl Benzodiazepine and Their Use as Dopamine Receptor Antagonists for the Treatment of Psychotic Disorders. WO 03/082877 Al, **2003**.

(8) Margolis, B. J.; Swidorski, J. J.; Rogers, B. N. An Efficient Assembly of Heterobenzazepine Ring Systems Utilizing an Intramolecular Palladium-Catalyzed Cycloamination. *J. Org. Chem.* **2003**, *68*, 644–647.

(9) Gilman, H.; Diehl, J. Novel Reduction of Ketones by Diphenylsilane. *J. Org. Chem.* **1961**, *26*, 4817–4820.

(10) Dunn, E. A.; Roxburgh, M.; Larsen, L.; Smith, R. A. J.; McLellan, A. D.; Heikal, A.; Murphy, M. P.; Cook, G. M. Incorporation of Triphenylphosphonium Functionality Improves the Inhibitory Properties of Phenothiazine Derivatives in Mycobacterium Tuberculosis. *Bioorg. Med. Chem.* **2014**, *22* (19), 5320–5328.

(11) Han, F.; Chi, L.; Wu, W.; Liang, X.; Fu, M,; Zhao, J. Environment Sensitive Phenothiazine Dyes Strongly Fluorescence in Protic Solvents. *J. Photochem. Photobiol.* **2008**, *196* (1), 10-23.

(12) Zhang, Y.; Ballard, C. E; Zheng, S.; Gao, X.; Ko, K.; Yang, H.; Brandt, G.; Lou, X.; Tai, P. C.; Lu C.; Wang B. Design, Synthesis and Evaluation of Efflux Substrate-Metal Chelator Conjugates as Potential Antimicrobial Agents. *Bioorg. Med. Chem. Lett.* **2007**, *17*, 707–71.

(13) Rajasekaran, A.; Thampi, P. P. Synthesis and Analgesic Evaluation of Some 5-[β-(10-Phenothiazinyl) Ethyl]-1-(acyl)-1,2,3,4-Tetrazoles. *Eur. J. Med. Chem.* **2004**, *39* (3), 273–279.

(14) Fitzmaurice, D.; Cummins, D.; Corr, D.; Rao, N. S.; Boschloo, G. Electrochromic Device. WO 2001027690 A2, **2001**.

(15) Mekky, A. E. M.; Saleh, T. S.; Al-Bogami, A. S. Synthesis of Novel Pyrazoles Incorporating a Phenothiazine Moiety: Unambiguous Structural Characterization of the Regioselectivity in the 1,3-Dipolar Cycloaddition Reaction Using 2D HMBC NMR Spectroscopy. *Tetrahedron* **2013**, *69* (33), 6787–6798.

(16) Westhuyzen, R. Van Der; Winks, S.; Wilson, C. R.; Boyle, G. A.; Gessner, R. K.; Melo, C. S. De; Taylor, D.; Kock, C. De; Njoroge, M.; Brunschwig, C.; Lawrence, N.; Rao, S. P. S.; Sirgel, F.; Helden, P. Van; Seldon, R.; Moosa, A.; Warner, D. F.; Arista, L.; Manjunatha, U. H.; Smith, P. W.; Street, L. J.; Chibale, K. Pyrrolo[3,4-C]pyridine-1,3(2H)-Diones: A Novel Antimycobacterial Class Targeting Mycobacterial Respiration. *J. Med. Chem.* **2015**, *58* (23), 9371–9381.

(17) Collins, L.; Franzblau, S. G. Microplate Alamar Blue Assay versus BACTEC 460 System for High-Throughput Screening of Compounds against Mycobacterium Tuberculosis and Mycobacterium Avium. *Antimicrob. Agents Chemother.* **1997**, *41*, 1004–1009.

(18) Franzblau, S. G.; Witzig, R. S.; McLaughlin, J. C.; Torres, P.; Madico, G.; Hernandez, A.; Degnan, M. T.; Cook, M. B.; Quenzer, V. K.; Ferguson, R. M.; Gilman, R. H. Rapid, Low-Technology MIC Determination with Clinical Mycobacterium Tuberculosis Isolates by Using the Microplate Alamar Blue Assay. *J. Clin. Microbiol.* **1998**, *36*, 362–366.

(19) Salie, S.; Hsu, N.; Semenya, D.; Jardine, A.; Jacobs, M. Novel Non-Neuroleptic Phenothiazines Inhibit Mycobacterium Tuberculosis Replication. *J. Antimicrob. Chemother.* **2014**, *69* (6), 1551–1558.

(20) Di, L. I.; Kerns, E. H.; Gao, N.; Li, S. Q.; Huang, Y.; Bourassa, J. I. M. L.; Huryn, D. M.; Al, D. I. E. T. Experimental Design on Single-Time-Point High-Throughput Microsomal Stability Assay. *J. Pharm. Sci.* **2004**, *93* (6), 1537–1544.

(21) Mosmann, T. Rapid Colorimetric Assay for Cellular Growth and Survival: Application to Proliferation and Cytotoxicity Assays. *J Immunol. Methods* **1983**, *65*, 55–63.